Studies of the Radiation Chemistry and Grafting of a Fluoropolymer

A thesis submitted for the fulfillment of the degree of

Doctor of Philosophy

In the Department of Chemistry

The University of Queensland, Australia

by

Tim R. Dargaville, B.Sc. (Hons.)

December 2002

Declaration

The work contained in this thesis was undertaken in the Department of Chemistry at the University of Queensland, the Institute of Polymer Research Dresden (Germany) and Mimotopes Pty Ltd, Melbourne. To the best of my knowledge and belief, all work contained in this thesis is original and my own, except as acknowledged by appropriate references. I declare that I have not submitted this material, either in whole or in part, for a degree at this or any other university.

Tim R. Dargaville

To Mum

Acknowledgements

I would like to thank my principle supervisor Associate Professor Dave Hill for his encouragement, good ideas (the bad ones were mine), support and the knack he had for filling me with enthusiasm whenever I left his office after a meeting. I would also like to thank Associate Professor Andrew Whittaker for his guidance and willingness to offer help whenever things hit a rough patch.

This project would not have been possible without the efforts and vision of Professor Graeme George, Drs Firas Rasoul , Joe Maeji and Senake Perera. Thanks also to Dr Peter Pomery for suggestions at the beginning of the project.

I would also like to thank Drs Ulrich Scheler, Beata Fuchs, Uwe Lappan and Klaus Lunkwitz from the Institute of Polymer Research Dresden for allowing me to work at the IPF, and to the relatives of Francine Kroesen for making travel to Germany possible through the Francine Kroesen Travel Fellowship.

The help from Bob and Ian from the glassblowing workshop for patience and sensational glassblowing skills is greatly acknowledged, as is assistance from Dr Graham Ruhle for use of the Instron, Gavin Gant at ANSTO for irradiation of samples at high temperature, Dr Barry Wood for help with the XPS, and Merrin, Jennifer and Birgit in the office for the gracious handling of my many administrative requests.

Use of the Raman microprobe was provided by Dr Llew Rintoul and Professor Peter Fredricks at QUT, while assistance with the loading tests was from Yen Pham and Fran Ercole at Mimotopes.

My time at UQ would not have been the same without the friendships and help from members of the Polymer Materials and Radiation Group, past and present, who have allowed me to experience a fantastic and memorable 3.5 years at UQ, especially Tri, Chris, Julie, Kris, Liying, Nihal, Shahroo, David and Francisco.

Additional personal financial support and work experience was made possible by Associate Professors John Cotton, Lawrie Gahan and Mary Garson by way of tutoring and casual employment.

Special thanks to Moling Chen for the laughs and helping me quit my job to start a PhD.

The financial support for the project from the Australian Research Council, Mimotopes Pty Ltd and the RACI Polymer Division is gratefully acknowledged.

Finally I would like to pay special thanks to Bronwin for her love and support and help with preparation of this manuscript and to my family—Mum (dec.), Dad, Roger, Toby and Simon.

Abstract

The radiation chemistry and the grafting of a fluoropolymer, poly(tetrafluoroethylene-*co*-perfluoropropyl vinyl ether) (PFA), was investigated with the aim of developing a highly-stable grafted support for use in solid phase organic chemistry (SPOC). A radiation-induced grafting method was used whereby the PFA was exposed to ionizing radiation to form free radicals capable of initiating graft copolymerization of styrene. To fully investigate this process, both the radiation chemistry of PFA and the grafting of styrene to PFA were examined.

Radiation alone was found to have a detrimental effect on PFA when irradiated at 303 K. This was evident from the loss in the mechanical properties due to chain scission reactions. This meant that when radiation was used for the grafting reactions, the total radiation dose needed to be kept as low as possible. The radicals produced when PFA was exposed to radiation were examined using electron spin resonance spectroscopy. Both main-chain ($–CF_2–C^{\bullet}F–CF_2-$) and end-chain ($–CF_2–C^{\bullet}F_2$) radicals were identified. The stability of the majority of the main-chain radicals when the polymer was heated above the glass transition temperature suggested that they were present mainly in the crystalline regions of the polymer, while the end-chain radicals were predominately located in the amorphous regions. The radical yield at 77 K was lower than the radical yield at 303 K suggesting that cage recombination at low temperatures inhibited free radicals from stabilizing.

High-speed MAS ^{19}F NMR was used to identify the non-volatile products after irradiation of PFA over a wide temperature range. The major products observed over the irradiation temperature 303 to 633 K included new saturated chain ends, short fluoromethyl side chains in both the amorphous and crystalline regions, and long branch points. The proportion of the radiolytic products shifted from mainly chain scission products at low irradiation temperatures to extensive branching at higher irradiation temperatures. Calculations of *G* values revealed that net crosslinking only occurred when PFA was irradiated in the melt. Minor products after irradiation at elevated temperatures included internal and terminal double bonds and CF_3 groups adjacent to double bonds. The volatile products after irradiation at 303 K included tetrafluoromethane (CF_4) and oxygen-

containing species from loss of the perfluoropropyl ether side chains of PFA as identified by mass spectrometry and FTIR spectroscopy.

The chemical changes induced by radiation exposure were accompanied by changes in the thermal properties of the polymer. Changes in the crystallinity and thermal stability of PFA after irradiation were examined using DSC and TGA techniques. The equilibrium melting temperature of untreated PFA was 599 K as determined using a method of extrapolation of the melting temperatures of imperfectly formed crystals. After low temperature irradiation, radiation-induced crystallization was prevalent due to scission of strained tie molecules, loss of perfluoropropyl ether side chains, and lowering of the molecular weight which promoted chain alignment and hence higher crystallinity. After irradiation at high temperatures, the presence of short and long branches hindered crystallization, lowering the overall crystallinity. The thermal stability of the PFA decreased with increasing radiation dose and temperature due to the introduction of defect groups.

Styrene was graft copolymerized to PFA using γ-radiation as the initiation source with the aim of preparing a graft copolymer suitable as a support for SPOC. Various grafting conditions were studied, such as the total dose, dose rate, solvent effects and addition of nitroxides to create "living" graft chains. The effect of dose rate was examined when grafting styrene vapour to PFA using the simultaneous grafting method. The initial rate of grafting was found to be independent of the dose rate which implied that the reaction was diffusion controlled. When the styrene was dissolved in various solvents for the grafting reaction, the graft yield was strongly dependent of the type and concentration of the solvent used. The greatest graft yield was observed when the solvent swelled the grafted layers and the substrate. Microprobe Raman spectroscopy was used to map the penetration of the graft into the substrate. The grafted layer was found to contain both poly(styrene) (PS) and PFA and became thicker with increasing radiation dose and graft yield which showed that grafting began at the surface and progressively penetrated the substrate as the grafted layer was swollen. The molecular weight of the grafted PS was estimated by measuring the molecular weight of the non-covalently bonded homopolymer formed in the grafted layers using SEC. The molecular weight of the occluded homopolymer was an order of magnitude greater than the free homopolymer formed in the surrounding solution suggesting that the high viscosity in the grafted regions led to long PS grafts. When a

nitroxide mediated free radical polymerization was used, grafting occurred within the substrate and not on the surface due to diffusion of styrene into the substrate at the high temperatures needed for the reaction to proceed.

Loading tests were used to measure the capacity of the PS graft to be functionialized with aminomethyl groups then further derivatized. These loading tests showed that samples grafted in a solution of styrene and methanol had superior loading capacity over samples graft using other solvents due to the shallow penetration and hence better accessibility of the graft when methanol was used as a solvent.

Publications

Dargaville, T. R., Hill, D. J. T., Whittaker, A. K., "An ESR Study of Irradiated Poly(tetrafluoroethylene-*co*-perfluoropropyl vinyl ether) (PFA)", *Radiat. Phys. Chem.* **62**, 25-31 (2001).

Dargaville, T. R., George, G. A., Hill, D. J. T., Scheler, U., Whittaker, A. K., "High-Speed MAS ^{19}F NMR Analysis of an Irradiated Fluoropolymer", *Macromolecules* **35**, 5544-5549 (2002).

Dargaville, T.; Hill, D., Perera, S., "Grafted Fluoropolymers as Supports for Solid Phase Organic Chemistry: Preparation and Characterization.", *Aust. J. Chem.* **55**, 439-441 (2002), invited paper.

Dargaville, T. R., Hill, D. J. T., "Grafting to Fluoropolymers – A Review", *Prog. Polym. Sci.*, in preparation

Conference Proceedings

Effect Of Ionising Radiation on Poly(tetrafluoroethylene-co-perfluoropropyl vinylether) (PFA), Tim R. Dargaville, David J. T. Hill, Graeme A. George,
Queensland Polymer Symposium 1999 (Poster)

Effect Of Ionising Radiation on Poly(tetrafluoroethylene-co-perfluoropropyl vinylether) (PFA), Tim R. Dargaville, David J. T. Hill, Graeme A. George, 23rd Australian Polymer Symposium (1999) Geelong, Victoria, Australia (Poster)

Radiation Induced Vapour Phase Grafting of Styrene onto a Fluoropolymer, Tim R. Dargaville, David J. T. Hill, Graeme A. George, F. Cardona, Radiation 2000, ANSTO, Sydney, Australia (Poster)

Radiation Induced Vapour Phase Grafting of Styrene onto a Fluoropolymer, Tim R. Dargaville, David J. T. Hill, Graeme A. George, F. Cardona, Pacifichem 2000, Honolulu, USA (Oral)

High Speed MAS NMR Analysis of an Irradiated Fluoropolymer, T.R. Dargaville, D.J.T. Hill, G.A. George, U. Scheler, A.K. Whittaker, 24th Australian Polymer Symposium (2001) Beechworth, Victoria, Australia (Oral)

High Speed ^{19}F MAS NMR Analysis of an Irradiated Fluoropolymer, T.R. Dargaville, D.J.T. Hill, G.A. George, U. Scheler, A.K. Whittaker, World Chemistry Congress 2001, Brisbane, Australia (Poster)

Surface Modification of a Fluoropolymer, T.R. Dargaville, D.J.T. Hill, G.A. George, A.K. Whittaker, 25th Australian Polymer Symposium (2002) Armidale, New South Wales, Australia (Poster) – Awarded Treloar Prize for best poster presentation

Awards

The Francine Kroesen Travel Fellowship 2000

The Treloar Prize for best poster presentation at the 25th Australasian Polymer Symposium

Table of Contents

Chapter 1: Introduction and Review of the Literature

page

Chapter 6: Grafting I – Vapour and Solvent Effects

Chapter 7: Grafting II – Grafting by "Living" Polymerization

Chapter 8: Overall Conclusions and Further Work

List of Figures

Chapter 1

Chapter 2

Chapter 3

Chapter 4

Chapter 5

Chapter 6

Chapter 7

List of Tables

Chapter 1

Page

Chapter 3

Chapter 4

Chapter 6

Chapter 7

List of Schemes

Chapter 1

Page

Chapter 2

Chapter 3

Chapter 4

Chapter 6

Chapter 7

Chapter 8

List of Abbreviations

ATR	Attenuated Total Reflectance
CP	Cross Polarization
DMA	Dynamic Mechanical Analysis
DSC	Differential Scanning Calorimetry
EPR	Ethylene-propylene rubber
ESR	Electron Spin Resonance
ETFE	Ethylene-tetrafluoroethylene copolymer
FEP	Fluorinated ethylene-propylene copolymer
FTIR	Fourier Transform Infrared
G(R)	Radical Yield
LFRP	“Living” Free Radical Polymerization
MAS	Magic Angle Spinning
MS	Mass Spectrometry
MWD	Molecular Weight Distribution
NMR	Nuclear Magnetic Resonance
PCTFE	Poly(chlorotrifluoroethylene)
PFA	Perfluoroalkoxy
PMMA	Poly(methyl methacrylate)
PPVE	Perfluoropropyl vinyl ether
PS	Poly(styrene)
PTFE	Poly(tetrafluoroethylene)
PVDF	Poly(vinylidene fluoride)
PVDF-*co*-HFP	Poly(vinylidene fluoride-*co*-hexafluoropropylene)
PVF	Poly(vinyl fluoride)
SEC	Size Exclusion Chromatography
SEM	Scanning Electron Microscopy
SPOC	Solid Phase Organic Chemistry
TEMPO	2,2,6,6-tetramethyl-1-piperidinyloxy
TEISO	1,1,3,3-tetraethylisoindolin-2-yloxyl
TFE	Tetrafluoroethylene
T_c	Crystallization Temperature
T_m	Melting Temperature

T_g	Glass Transition Temperature
TGA	Thermal Gravimetric Analysis
XPS	X-ray Photoelectron Spectroscopy

Chapter 1

1 Introduction and Review of the Literature

1.1 Overview

Surface modification of polymers by graft copolymerization has afforded a great number of new materials with unique properties. The surface properties of the grafted polymer are often in stark contrast to the properties of the original polymer. Most industrial polymers are hydrophobic in nature, however through introduction of new functional groups to the surface, properties such as hydrophilicity, adhesion, biocompatibility, conductivity, anti-fogging and anti-fouling may be attained.

Fluoropolymers are a class of polymers with excellent chemical and thermal stability, low dielectric constants, and low surface energy. It is quite remarkable, almost iconoclastic, that fluoropolymers can be altered so that the surface behavior displays none of the non-stick, inert properties made famous by this class of polymers.

The chemical stability of fluoropolymers means that extremely harsh conditions are required to modify the surface on the molecular scale. This can be achieved either chemically, by etching, or by using high-energy radiation. Chemical treatment is most commonly performed using sodium-liquid ammonia[1] or sodium naphthalemide.[2] These treatments can improve the bondabilty of the surface, however the environmental concerns as well as the difficulties in controlling the depth profiles of the treatments make these methods unsuitable as a modern industrial process. Cleaner methods are available as fluoropolymers are relatively susceptible to high-energy radiation such as plasma,[3] X-rays,[4] γ-rays,[5] vacuum ultraviolet,[6] excimer or Ar^+ lasers,[7] electron[8] and ion beams.[9,10] Alkyl radicals are usually produced and these can react with air to form oxygen-containing species. Alternatively, the radicals produced may be used to initiate polymerization of a monomer to form a graft copolymer. By using the graft copolymerization method to modify the surface, the properties can be tailored by judicious choice of monomer.

This thesis examines the processes in which the surface of fluoropolymers are modified so they may be used as solid supports for organic synthesis.

1.2 Polymers as Supports for Solid Phase Organic Chemistry

The synthesis of compounds while tethered to an insoluble polymer support was first demonstrated in 1963 by Bruce Merrifield, the recipient of the 1984 Nobel prize in Chemistry.[11] In his pioneering work, Merrifield synthesized a series of peptides in which one terminus of each peptide was covalently bonded to 1 % crosslinked chloromethylated poly(styrene) resin. This method is now the most commonly used tool to synthesize peptides and has become known as solid phase peptide synthesis (SPPS). As can be seen from Figure 1.1, the Merrifield method for peptide synthesis is a series of repeated coupling and deprotecting steps, each separated by washing steps. The advantage of using a functionalized poly(styrene) (PS) resin support is that being insoluble in the solvent used, it acts as a "handle" to which the peptides are attached. This facilitates the synthesis by virtue of the fact that purification after each step becomes trivial: the resin-bound peptide can be filtered and washed free of any excess reagents and non-covalently bonded impurities. The advantages are obvious when compared to traditional solution phase synthesis, where workup may involve evaporation of the solvent, dissolution of the target compound and impurities, some chromatography and further removal of solvent. In addition to the handling advantages of using SPPS, reactions may be driven to completion by addition of excess reagents which are simply washed away after the reaction.

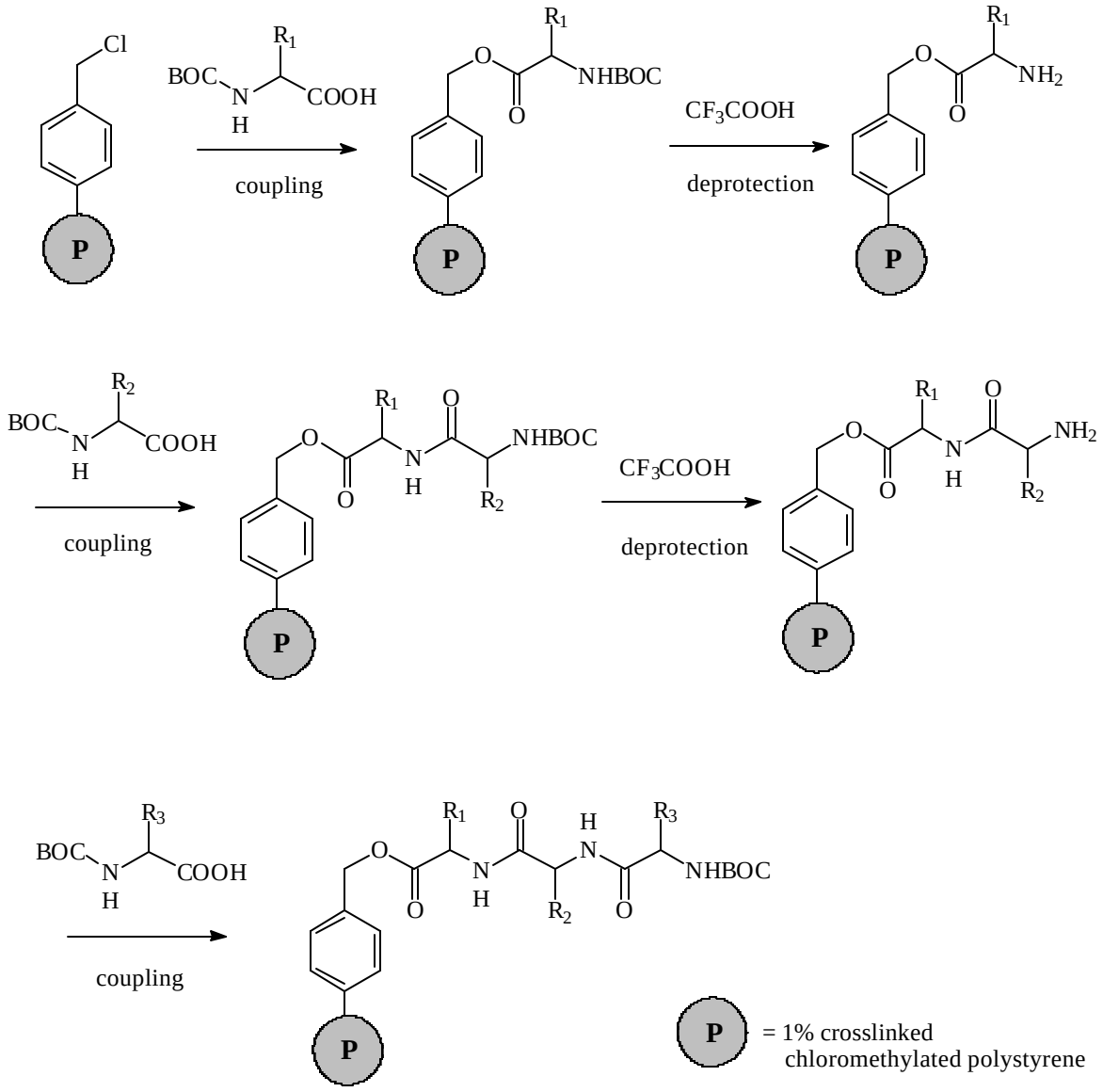

Figure 1.1 Synthesis of a peptide on Merrifield Resin using a series of coupling and deprotecting steps. After each step the excess reagents and non-covalently impurities are washed away with solvent. BOC = *tert*-butyloxycarbonyl.

In the 1970s the same methodology used for SPPS was extended to solid phase synthesis of non-peptidic compounds (called solid phase organic chemistry (SPOC)).[12] However, it was not until some 15 years later that SPOC became popular through the advent of combinatorial chemistry. This relatively new area of chemistry allows large libraries or arrays of compounds to be produced by the random or directed combinations of simple building blocks. For example, in the case of peptide synthesis, the amino acids are the building blocks. Geysen, in 1984, was the first to report the use of a

solid phase / combinatorial chemistry methodology to synthesize a library of several hundred peptides to map an epitope.[13] Unfortunately, peptides are inherently poor drugs as they cannot be taken orally and have short half-lives. It was not until the 1990s when "pharmaceutical type" chemistries were adapted to solid phase chemistry that the realization was made that large arrays of potential drugs could be made using combinatorial chemistry. The growth in this area of chemistry has been driven mainly by advances in high-throughput screening (HTS), in which the capacity to test compounds for biological activity and the types of assays available has increased significantly. This put pressure on the synthetic chemist to produce larger numbers of compounds to keep up with the capacity of the assays. Many large pharmaceutical companies are now using combinatorial solid phase methodologies to synthesize large numbers of compounds in order to improve their chances of discovering new drug leads. Recently these same methods used for drug discovery have been used in a novel way to synthesize libraries of initiators used in the preparation of dendritic nanoscale materials.[14]

To date, many books and journals have been dedicated to exploring the types of chemistry that can be performed on the solid phase. Unfortunately the influence of the solid support is regularly overlooked and more often than not, the polymer phase is depicted as an opaque circle by the synthetic chemist (for example Figure 1.1). Whether it was Merrifield's foresight or the lack of significant development in resins is unclear, but Merrifield resin (first used in 1963) is still the most popular resin.[15] When compared with the chemistry performed on solid phases, the solid support as a separate entity has received little attention in the literature and in the laboratory.

1.2.1 Modern Solid Supports

The term "solid support" may conjure up an image of a rigid, impermeable, static system, whereas in reality a good solid support is none of these things. Reactions commonly occur on mobile, well-solvated, and reagent-accessible polymer strands throughout the interiors of the supports. An ideal support has good swelling ability in a range of solvents; the compounds synthesized have high purity and reactions should proceed at rates similar to solution phase reactions.

The types of commercial solid supports used for SPOC can be crudely categorized into two groups: 1. Resin; and 2. Grafted supports. Resin is made up of particles with diameters typically in the order of hundreds of microns.[16] As mentioned earlier, the first and still the most popular resin is Merrifield resin. Other derivatives include PEG-PS (Tentagel) which contains linear ethylene oxide units designed to improve mobility of the reactive groups, and PEGA, an acrylamide-based resin (Figure 1.2). A more extensive list of resins can be found in papers by Bergbreiter[15] and Barany and Kempe[16] and references cited therein.

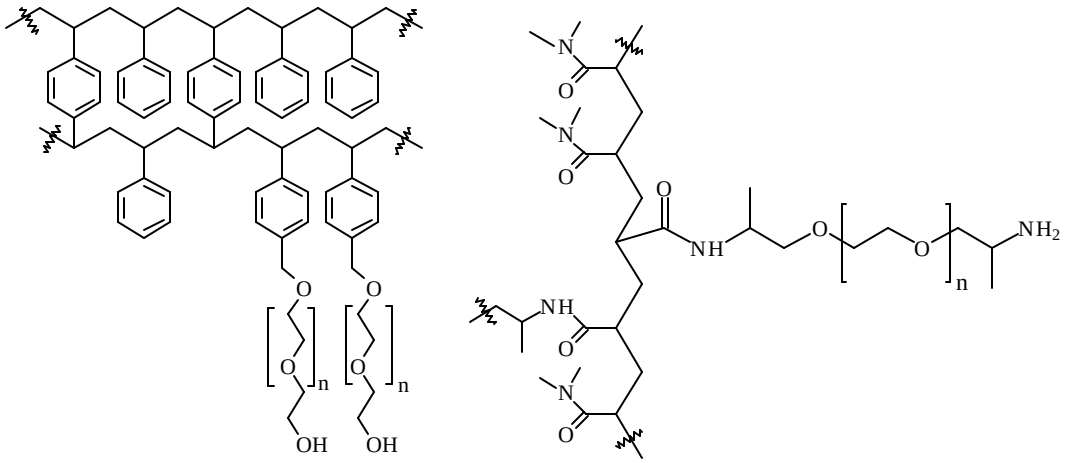

Figure 1.2 Structures of Tentagel (left) and PEGA (right).

Grafted supports have a "resin-like" polymer grafted to an inert polymer substrate and are the subject of this thesis. Some of the first grafted supports were poly(ethylene) substrates grafted with styrene, acrylic acid or 2-hydroxyethyl methacrylate.[17,18] The advantage of these types of supports over resin is that the grafted polymer does not necessarily have to be crosslinked to afford insolubility since the polymer core prevents dissolution. In theory linear polymer chains are more available to reagents than crosslinked ones. There are also handling advantages as the ungrafted polymer substrate may be prefabricated into intricate shapes by injection moulding before the grafting process. The physical form is then retained throughout the grafting and subsequent SPOC steps. When dealing with defined modular moulded shapes compared with powdered resin, the need for weighing is eliminated and handling is made easier. In addition, the shape of the grafted supports can be such that they may be attached to holders facilitating manual and robotic

processes, or have radio-frequency tags inserted to aid identification and sorting. Mimotopes Pty Ltd (Melbourne, Australia) has led the field in grafted supports for SPOC and SPPS. They have coined the term “pins” to describe their product. An example of a pin is the “lantern^{TM}”, shown in Figure 1.3.

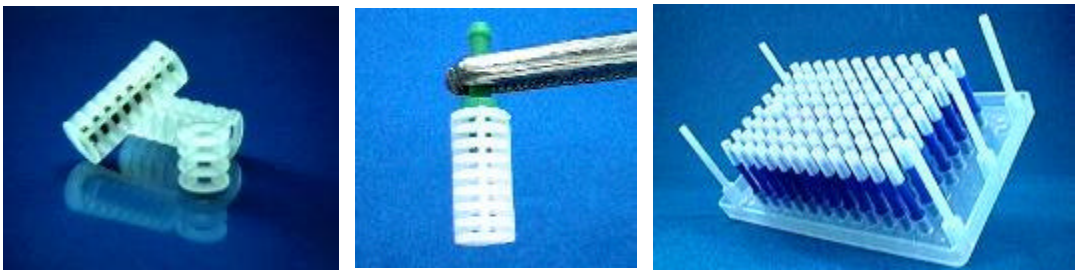

Figure 1.3 Grafted solid supports commercialized by Mimotopes Pty Ltd. Left: injection moulded lanterns; Middle: a lantern on a stem; Right: lanterns on stems in a 8 × 12 array format for multiple handling (pictures courtesy of www.mimotopes.com).

1.3 The Problem

At present the commercially available pins from Mimotopes Pty Ltd are manufactured by grafting various vinylic monomers to a base polymer blend made from poly(propylene), poly(ethylene) and ethylene-propylene rubber using a radiation-grafting method. As the types of chemistry being explored using SPOC widens, so too do the conditions to which the supports are subjected. Poly(propylene)-based or resin supports have relatively low temperature limits and will degrade or dissolve if exposed to certain solvents at high temperatures (for example, toluene heated to reflux temperature) or if exposed to microwaves. By using a more stable base polymer for the pins in terms of temperature and chemical resistance it is hoped that these problems can be overcome.

Another problem occasionally reported with the poly(propylene)-based pins is that while performing multiple step SPOC reactions, impurities from reactions several steps earlier can appear.[19] It is possible that the impurities are being trapped in the poly(propylene) matrix and are released in subsequent synthesis steps. A less penetrable base polymer may solve this problem.

Fluoropolymers are the obvious choice of polymer when high temperature and chemical stability are needed and they swell only slightly in most solvents. These properties stem from the extraordinary C–F bond strength of 481.3 kJ mol^{-1} and orientation of the fluorine atoms about the carbon backbone which shield it against chemical attack.[20] Figure 1.4 illustrates how a fluorinated lantern is resistant to boiling toluene, while a poly(propylene) blend lantern dissolves and becomes unrecognizable after the same treatment. Poly(tetrafluoroethylene) (PTFE) is the most common fluoropolymer and has the highest temperature limit of all the fluoropolymers but it is not melt-processable*, so cannot be injection moulded into lantern shapes. Fortunately, melt-processable fluoropolymers are available which have similar properties to PTFE, and this thesis examines grafting to one of these polymers.

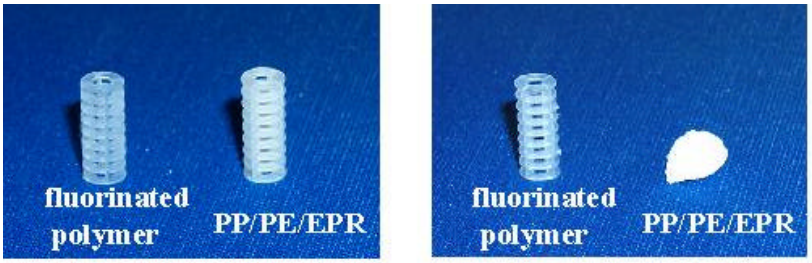

Figure 1.4 The effect of boiling toluene on fluorinated and PP/PE/ERP blend lanterns. Left: a fluorinated lantern and a PP/PE/EPR lantern before treatment; Right: the lanterns after being subjected to boiling toluene for five minutes then cooled. (source: author's experiment).

The use of grafted fluoropolymers for application in solid phase synthesis is not entirely new. Tregear reported the use of a grafted fluoropolymer, poly(trifluorochloroethylene), as a support for SPPS in 1972, however he found that there was no advantage over Merrifield resin for synthesis of a dodecapeptide, although he did admit that the grafted support used had not been fully optimized.[22] Recently, a different approach was reported in preparing a stable solid support, again taking advantage of the strength of the C–F bond but instead of grafting to a fluoropolymer, the fluorine was contained in the backbone of Merrifield resin synthesized from fluorinated-styrene.[23]

Shortly after this project was conceived, Zhao and coworkers published work and filed a patent application describing the use of grafted fluoropolymer tubes for use in a high

* Terwoort *et al.* claimed to have developed melt-processable PTFE made from blending high and low molecular weight PTFE,[21] but this is not a commercial product.

temperature SPOC application.[24,25] Their work is based on creating a rough surface (to increase the surface area) on the fluoropolymer before grafting and is mainly concerned with the application of the product and not the polymer chemistry behind the grafting process.

While grafting to polyolefins using radiation grafting methods is well established, grafting to fluoropolymers is less well understood. In the following sections, the fluoropolymer used for this thesis is introduced and a literature review is presented on the current state-of-the-art of grafting and analysis techniques.

1.4 The Fluoropolymer PFA

This project was carried out in collaboration with Mimotopes Pty Ltd with the aim of developing a thermally-stable fluoropolymer-based solid support for SPOC. The fluoropolymer which has been chosen for this project is poly(tetrafluoroethylene-*co*-perfluoropropyl vinyl ether) (PFA)* (the structure is shown in Figure 1.5). Invented by DuPont and commercialized 1971/2, PFA is a melt-processable fluoropolymer copolymerized from tetrafluoroethylene (TFE) and perfluoropropyl vinyl ether (PPVE) and has similar thermal and chemical properties to PTFE. The bulky perfluoropropoxy side chains in PFA act to disrupt crystallinity of the polymer chains and decrease the melt viscosity. The amount of comonomer incorporated into these resins is typically only 1 – 2 mol. %. The low reactivity of PPVE means that statistically it is very unlikely for the copolymer to contain adjacent PPVE units.[20]

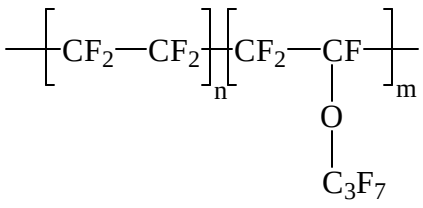

Figure 1.5 The structure of PFA.

* The origin of the name "PFA" is not immediately obvious from the full chemical name and is actually an acronym of **P**er**f**luoro**a**lkoxy resin. Strictly speaking, the name "perfluoroalkoxy resin" can mean any perfluoropolymer with alkoxy side chains; however, to avoid confusion, in this thesis the term "PFA" will refer exclusively to the copolymer of tetrafluoroethylene and perfluoropropyl vinyl ether.

Much of the literature on the behavior of polymers when exposed to radiation was published in the 1950s and 1960s when nuclear technology was first being developed. Polymers such as PTFE received much attention, however as PFA was invented after the peak in the interest in radiation behavior of polymers, it has received little attention in the literature. In recent years radiation modification of fluoropolymers has gained in popularity as methods for crosslinking and new techniques to analyze the polymers have become available. Despite this, PFA is generally considered to be a specialized fluoropolymer, and as such, has not been widely studied.

1.5 Literature Review of Grafting to Fluoropolymers

While there have been many reviews on the topic of grafting to polyolefins (for example references [26-29] and the rather curiously titled review "Radiation-Induced Graft Polymerization in the U.S.S.R."[30]), the only recent review of grafting to fluoropolymers is by Gupta and Scherer[31] from 1994 and is mainly concerned with grafting to FEP (a copolymer of tetrafluoroethylene and hexafluoropropylene) for use as proton exchange membranes. In this literature review, a more up-to-date review is given covering the topic of grafted fluoropolymers, including techniques for optimizing graft yields as well as some of the modern techniques used to analyze graft copolymers. In the following section on radiation-induced grafting there are instances where some non-fluoropolymer examples are given in cases where literature on fluoropolymers is unavailable.

1.5.1 Radiation-Induced Graft Copolymerization

Radiation-induced graft copolymerization is a well established technology dating back almost 50 years. Figure 1.6 illustrates how a substrate "A" can be grafted with monomer "B". If the polymer "A" is exposed to ionizing radiation, (for example: electron beams, γ-rays, X-rays) the active sites produced randomly along they chain can act as macro-initiators, initiating free radical polymerization of the monomer "B". This method is applicable for many polymer / monomer combinations and unlike chemically-initiated grafting, there is no contamination from initiators.

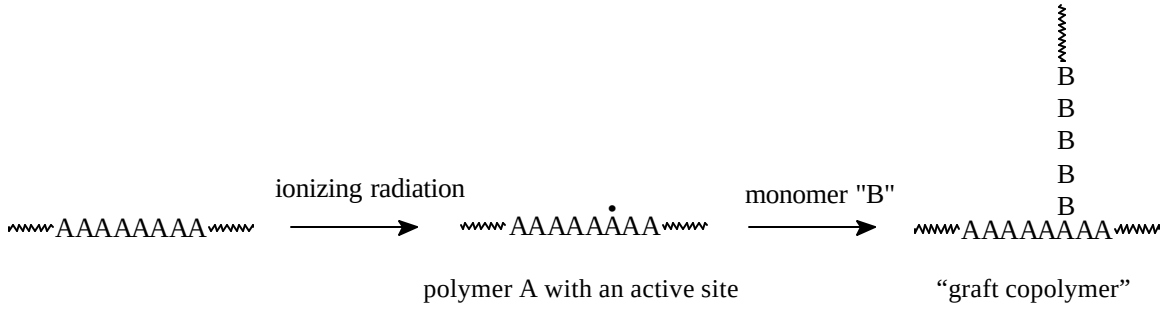

Figure 1.6 The use of ionizing radiation to graft monomer "B" to polymer "A" to form a graft copolymer.

The extent of polymerization of monomer B on substrate A is expressed in terms of the *graft yield* which is also referred to as the *degree of grafting*. This value is simply the mass of the graft polymer as a percentage of the mass of the original polymer substrate. For example, a graft yield of 50 % means that the weight of the graft copolymer is 50 % greater than that of the original substrate.

There are essentially three methods for radiation grafting:[32]

1. *Simultaneous method* – also sometimes called the *mutual method.* The polymer substrate is immersed in the monomer, which may be a liquid, vapour or diluted with solvent and may contain additives, then exposed to ionizing radiation. As well as the formation of the graft polymer, homopolymer will invariably also be formed as both the substrate *and* the monomer are exposed to radiation. Control of homopolymer formation is discussed in Section 1.5.3.1.

2. *Pre-irradiation method (post-irradiation grafting)* – so called because the polymer substrate is first exposed to ionizing radiation in vacuum or under an inert atmosphere to generate radicals before being exposed to a monomer. Homopolymer formation is less of a problem with this method since the monomer is not actually exposed to the radiation.

3. *Peroxy / hydroperoxy method* – similar to the pre-irradiation method, only with this method the polymer is exposed to ionizing radiation in the presence of air. This produces either peroxy radicals or hydroperoxy groups on the polymer substrate which, when heated in the presence of monomer, will decompose and grafting may be initiated. While homopolymer formation is not as serious as with the simultaneous method, there is still some homopolymer formation initiated by the small fragments from the decomposition of the peroxy groups. In addition, oxidative degradation of the polymer may occur during irradiation.

Each of these methods has its advantages and disadvantages. The pre-irradiation and peroxy methods are convenient in that the polymer substrate can be irradiated and stored for some time before the monomer is introduced. This is useful when access to a radiation source is limited. The simultaneous method requires the use of the radiation source during

the entire grafting process, however graft yields are generally higher compared with the pre-irradiation methods due to radical loss through decomposition reactions in the latter method.[33]

1.5.2 Grafting to Fluoropolymers

The unique resistance of fluoropolymers to almost all chemicals has made them suitable for many specialized applications.[34] Despite their chemical stability, fluoropolymers are one of the most sensitive polymers to radiation.[35] This perceived weakness can be exploited to favorably modify the properties of fluoropolymers by either radiation exposure alone, or by radiation-initiated copolymerization.

The seminal works on radiation grafting to PTFE can be found in the 1959 and 1962 publications by Chapiro.[36-38] Given that PTFE is inert to most chemicals and is insoluble in all common solvents, it is quite remarkable that when grafting styrene or methyl methacrylate to PTFE using low radiation dose rates, the films swell and grafting occurs not just on the surface but also homogeneously throughout the film.[36] This result is explained by assuming that grafting occurs initially at the surface of the film then proceeds gradually inwards as the grafting zone is swelled by the monomer. This mechanism is known as the *grafting front mechanism*.

In the last 40 years many fluoropolymers have been developed and made commercially available. The structures of some of these polymers are shown in Table 1.1, each of which has been used as a graft substrate. The grafting front mechanism first proposed by Chapiro has been proven to occur when grafting to PTFE and other fluoropolymers using various analytical techniques, described later in Section 1.5.5 of this chapter. As well as the numerous fluoropolymers used as graft substrates, many different monomers and additives have been used.

Table 1.1 Some of the commercially available fluoropolymers.

Name	Abbreviation	Structure
Poly(tetrafluoroethylene)	PTFE	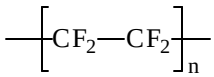
Poly(tetrafluoroethylene-*co*-hexafluoropropylene)	FEP	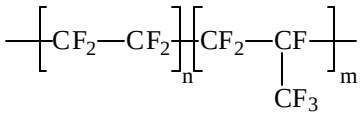
Poly(ethylene-*alt*-tetrafluoroethylene)	ETFE	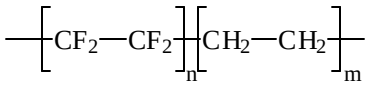
Poly(chlorotrifluoroethylene)	PCTFE	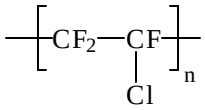
Poly(vinylidene fluoride)	PVDF	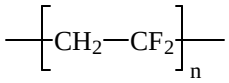
Poly(tetrafluoroethylene-*co*-perfluoropropyl vinyl ether)	PFA	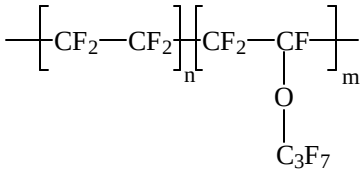
Poly(vinylidene fluoride-*co*-hexafluoropropylene)	PVDF-*co*-HFP	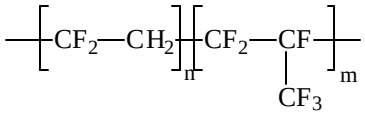
Poly(vinyl fluoride)	PVF	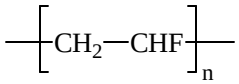

The motivating force behind much of the existing research into grafting to fluoropolymers is the prospect of being able to produce an alternative to the very costly fuel cell membrane Nafion® (Figure 1.7).[31,39-41] By grafting styrene to a fluoropolymer followed by sulfonation, membranes with similar ion-exchange and conductivity to

Nafion® have been synthesized. Grafted fluoropolymers have also been used as charged ultrafiltration membranes,[42] waste treatment membranes,[43] and in biomedical applications.[44,45]

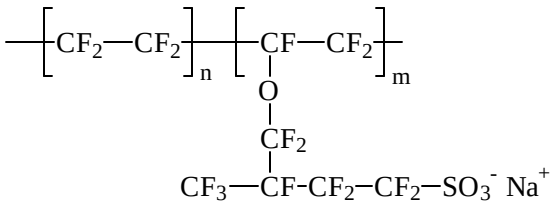

Figure 1.7 The structure of Nafion®.

In the following sections a review of the current literature is given, examining the influence of various solvents, additives and types of fluoropolymers.

1.5.2.1 Influence of Solvent and Monomer Concentration

The addition of solvent to a monomer / substrate combination can enhance grafting and determine the specific nature of the graft copolymer.[46] The penetration of the graft into the substrate is an important factor when preparing grafted surfaces for SPOC and is often dependent on the solvent used and the monomer concentration.

It is common to observe a Trommsdorff phenomenon when grafting styrene to polyolefins[47] and cellulose.[48] This phenomenon was first noticed when polymerizing bulk methyl methacrylate using benzoyl peroxide in which the rate becomes explosively rapid at approximately 20 – 25 % conversion.[49] This is explained by the restricted diffusion of the growing molecular chains, which hinders termination by combination with other growing chains, but does not appreciably disturb diffusion of the monomer. When the polymerization is carried out in a solvent, the explosive rate increase is not observed, however, when a non-solvent for poly(methyl methacrylate) is used the rate increase is even more rapid than the bulk polymerization and there is a higher degree of polymerization.

The Trommsdorff effect has also been observed in grafting reactions as illustrated in Figure 1.8. This figure shows the graft yield versus styrene concentration in methanol for grafting to pre-irradiated poly(propylene) fabric. The plot can be split into two regions. In region 1 the rates of propagation and initiation increase with increasing monomer concentration. Since methanol is a non-solvent for PS, the growing chains became sufficiently immobilized so that termination by combination was inhibited. In Figure 1.8 this effect reaches a maximum at approximately 22 % styrene concentration. At styrene concentrations above the maximum (region 2) the styrene swelled the matrix, increasing mobility and termination was greatly enhanced, lowering the graft yield.[50-52]

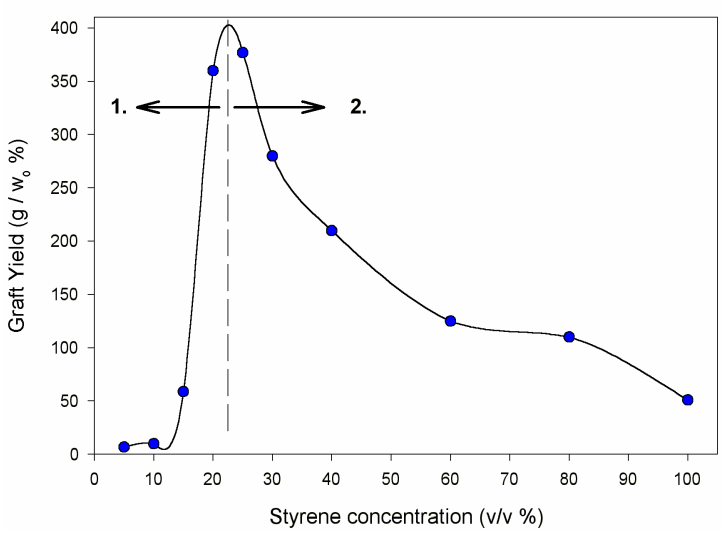

Figure 1.8 Observation of a Trommsdorff effect when grafting styrene to poly(propylene) fabric. Data taken from Nho *et al.*[50]

Maxima in the graft yield with variation in the monomer concentration have been observed when grafting styrene to PTFE,[53] FEP,[54] and PFA,[55] although in these cases dichloromethane was used as a solvent and the greatest graft yield and rates occurred at approximately 60 % styrene concentration. Since dichloromethane is a good solvent for PS, the observed maxima cannot be due to a real Trommsdorff effect. Instead, the behavior has been attributed to an increase in the styrene diffusion and hence concentration in the grafting region, which reached a maximum at approximately 60 % styrene concentration. Above this concentration there was significant homopolymer formation, resulting in hindered monomer diffusion to the grafting region and so lower graft yield.[55] This explanation is a little spurious as it is unlikely that the diffusion of styrene would be hindered enough to prevent propagation unless a glassy state was reached, and if the

viscosity was high enough to prevent styrene diffusion, then termination would also be expected to be hindered due to limited mobility of the growing chains. Similar results were observed when grafting styrene in methanol to ETFE using the pre-irradiation method.[56] In this case the maximum was attributed to an increase in viscosity in the grafted layers at high monomer concentration leading to lower diffusion of monomer to the interiors of the films, and hence less grafting.

The same behavior is generally not observed when grafting hydrophilic monomers to fluoropolymers in aqueous or methanolic / aqueous media. Grafting of methacrylic acid,[57-59] acrylic acid (AAc)[57,60-64] and vinyl acetate[65] to fluoropolymers led to a logarithmic relationship between monomer concentration (typically less than 70 %) and the rate of grafting which increased with increasing monomer concentration. Hegazy *et al.*[61] explained that since poly(acrylic acid) is insoluble in its monomer, the mobility of growing chains decreases with increasing monomer concentration. An exception is the grafting of *N*-vinyl-2-pyrrolidone to PFA using water as the solvent, where a maximum was observed at 50 % v/v monomer concentration.[66]

When a good solvent for PS was used, such as benzene, to graft styrene to FEP at 333 K, there was an almost linear relationship between the final graft yield and monomer concentration.[31] With increasing monomer concentration, diffusion also increased as did the final graft yield.

The penetration rate of the graft front is dependent on the monomer concentration. In preparation of membranes of FEP-*g*-poly(acrylic acid)[67] and PTFE-*g*-poly(acrylic acid)[68] the penetration rate of the graft was low at high acrylic acid concentration in water, while the converse was true at low acrylic acid concentration. This means that grafting throughout the film could be achieved at lower graft yield if the monomer concentration is low.[67] This is especially important for membranes used as ion exchange devices, as complete penetration of the substrate by the graft is required for transport of the ions.

1.5.3 The Use of Additives for Grafting

Generally the graft yield increases with radiation dose for both the simultaneous and pre-irradiation methods – the more radicals produced on the polymer substrate, the more initiation reactions occur, leading to greater amounts of graft. The use of additives can also increase the graft yield so that a particular level of grafting can be reached using a lower total radiation dose. This is of particular interest in cases where the polymer substrate is detrimentally affected by radiation. Lower radiation doses may also decrease the likelihood of crosslinking of the newly-grafted layer, which may be undesirable in some applications.

In 1979 Garnett published a comprehensive review on the role of additives when grafting to poly(ethylene), poly(propylene) and cellulose.[26] Since then some of the theories covering the mechanism in which the additives work have been revised. In the following two sections the literature covering the use of additives to control homopolymerization and to enhance grafting is explored with an emphasis on grafting to fluoropolymers.

1.5.3.1 Additives Used to Control Homopolymerization

As mentioned in Section 1.5.1, the formation of homopolymer can often be detrimental to the grafting reactions, and in many cases the homopolymer can be formed more rapidly than the graft. Homopolymer formation can be predicted from the radical yields (G(R)) of the monomer and polymer substrate. By definition, G(R) is the number of radicals formed for 16 aJ (or 100 eV) of absorbed energy. The larger the G(R) of the monomer compared with that for the polymer substrate, the greater the problem of homopolymer formation.[69] In an ideal case, G(R) for the polymer substrate would be much larger than that of the monomer. Disregarding other factors, this would mean that graft polymerization would be favoured over homopolymerization.

Excessive homopolymer formation may result in a decrease in the graft yield due to increased viscosity, which limits the accessibility of monomer to the polymer substrate. Excessive homopolymer formation can also add to the cost of the grafting process, as the ungrafted polymer is essentially a waste product, and removal of the homopolymer occluded to the grafted layer may require scrupulous washing routines.

Metal salts are commonly used to suppress homopolymerization during grafting reactions, and are almost universal in their application. Ammonium ferrous sulphate (Mohr's salt), ferric chloride and copper chloride have been demonstrated to suppress homopolymer formation in the preparation of grafted fluoropolymers such as PFA-*g*-poly(acrylic acid),[57] PFA-*g*-poly(methacrylic acid),[57,58] and FEP-*g*-poly(acrylic acid).[70]

Typically, the concentration of the metal salt needed to suppress homopolymerization is less than 1 wt %. The suppression of homopolymerization by metal salts is thought to occur by a redox reaction, where the metal cations terminate growing chains.[71] While the formation of both homopolymer and graft are suppressed by metal salts, the homopolymer is suppressed to a greater extent, allowing for reasonable graft yields with little homopolymer formation. For grafted Nylon it is thought that the swollen substrate forms a viscous barrier hindering diffusion of the cations to the growing graft chains.[71] Since fluoropolymers do not swell appreciably in grafting solutions presumably the swollen grafted layer acts as the barrier to the cations.

When fluoropolymers are irradiated in air, the carbon-centred radicals reversibly react with oxygen to form peroxy radicals (Scheme 1.1). The peroxy radicals may then react with small polymer fragments, P' (Scheme 1.2).[72] This differs from hydrogenated systems where chain peroxidation occurs – the $POO^{\bullet}$ radical can abstract a tertiary hydrogen from the polymer chain to form POOH and so form another $P^{\bullet}$ radical which can further react with oxygen.[73,74] Bozzi and Chapiro used Mohr's salt to suppress homopolymerization when grafting acrylic acid to FEP pre-irradiated in air.[70] These workers postulated that $P'O^{\bullet}$ radicals initiated homopolymerization. The effect of the Mohr's salt is to convert the diperoxides, POOP', to $P'O^{-}$ and $PO^{\bullet}$ (Scheme 1.3) and $PO_2^{\bullet}$ to $PO^{\bullet}$ and O^{-} (Scheme 1.4). They also proposed that when grafting to polymers which contain hydrogen, the homopolymer initiating species is $^{\bullet}OH$ which is converted to OH^{-} by Fe^{2+} (Scheme 1.5).

$$P \quad \xrightarrow{\gamma\text{-radiation}} \quad P^{\bullet}$$

$$P^{\bullet} + O_2 \rightleftharpoons POO^{\bullet}$$

Scheme 1.1 Reaction of oxygen with a carbon-centred radical on a polymer.

$$POO^{\bullet} + P' \; ? \; POOP'$$

Scheme 1.2 Reaction of a peroxy radical with a small polymer fragment P'.

$$POOP' + Fe^{2+} \; ? \; PO^{\bullet} + P'O^{-} + Fe^{3+}$$

Scheme 1.3 Decomposition of a diperoxide by Mohr's salt.

$$PO_2^{\bullet} + Fe^{2+} \; ? \; PO^{\bullet} + O^{-} + Fe^{3+}$$

Scheme 1.4 Decomposition of a peroxy radical by Mohr's salt.

$$^{\bullet}OH + Fe^{2+} \; ? \; OH^{-} + Fe^{3+}$$

Scheme 1.5 Conversion of a hydroxy radical to a hydroxy ion using Mohr's salt.

The concentration of the metal salt additive used will affect the graft yield and an optimum concentration must therefore be chosen. If the metal salt concentration is too low homopolymerization will not be completely inhibited, if it is too high the grafting reaction will be suppressed.[59]

1.5.3.2 Acids Used to Enhance Grafting

The use of mineral acids as additives has been studied extensively for the grafting of vinylic monomers to poly(ethylene),[47,75-78] poly(propylene),[47,79] and cellulose.[76-80] An illustration of the enhancing effect of acid in grafting solutions is shown in Figure 1.9.[47] The effect of the inclusion of acid is most pronounced at the Trommsdorff peak, while the effect is lower at concentrations of monomer above and below this point. At some concentrations the acid has no enhancing effect. In cases where there is no Trommsdorff effect in the acid-free solution the addition of acid can actually induce one.[47,80]

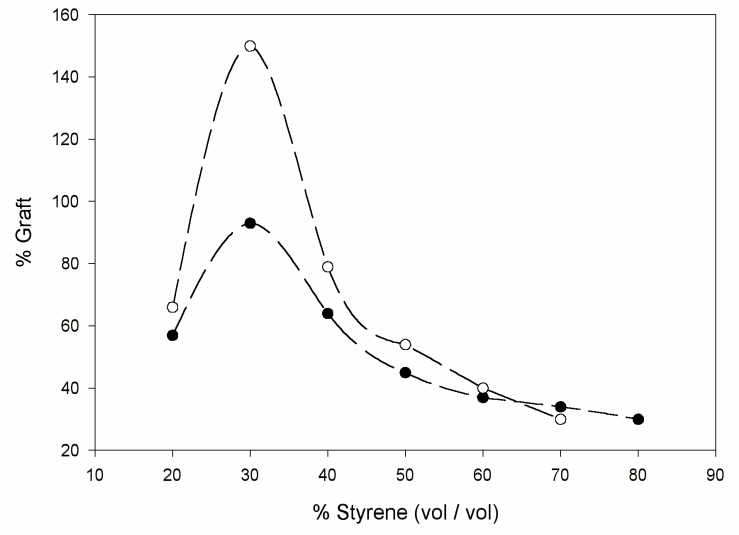

Figure 1.9 Acid effect for radiation-induced grafting of styrene in methanol to poly(propylene). Dose rate: 0.4 kGy hr^{-1}, the total dose was 2 kGy. (-o-) no acid; (-•-) 0.05 M H_2SO_4. Data taken from reference [47].

The use of acids as additives when grafting to fluoropolymers has received relatively little attention in the literature compared to the acid effect when grafting to polyolefins. Dworjanyn *et al.* reported a slight but definite increase in graft yield on addition of an unspecified acid when grafting a mixture of styrene and 2-hydroxyethyl methacrylate (HEMA) in methanol to PTFE using the simultaneous method.[76] In contrast, Nasef found almost no effect on the graft yield upon addition of a series of mineral and organic acids to styrene dissolved in methanol, benzene or dichloromethane when grafting to PTFE, FEP and PFA, also using the simultaneous method.[81]

The mechanism of acid enhancement when grafting to polyolefins and cellulose was initially understood to be a purely radiolytic phenomenon where the irradiation of the solvent increased the hydrogen atom yield (G(H)) (Scheme 1.6).[26,47,77,80] The hydrogen radicals can abstract hydrogen atoms from the polymer substrate creating additional sites for initiation of grafting.[26,47]

$$H^+ + e \; ? \; H^\bullet$$

Scheme 1.6 Conversion of a charged proton to a radical.

As was later revealed, there were some discrepancies with this theory alone.[75,77,78] It was found that acid could have an enhancing effect in situations where there could not possibly be an increase in the yield of hydrogen radicals. The basis for the doubt over this theory was:

1) when ultraviolet light was used as the initiating source acid also had an enhancing effect[77]
2) other neutral inorganic salts had the same effect as acid[77,78]
3) enhancement was also seen when the pre-irradiation grafting method was used[77,78]
4) enhancement was only seen at certain monomer concentrations[78]

In addition, Chappas and Silverman found that when grafting styrene to poly(ethylene), the acid had little effect on the grafting rate below 100 % graft yield.[75] If the effect was due to hydrogen radicals abstracting hydrogen from the polymer substrate and so forming new initiating centres, then it would be expected that the acid would have an effect at all degrees of grafting.

These acid-enhancing phenomena were eventually attributed to a partitioning or "salting-out" effect of the additives. In a grafting system this partitioning increases the rate of diffusion of the monomer, as well as the equilibrium concentration of the monomer within the polymer substrate. The increased monomer supply results in enhanced grafting rates.

The enhancement works best when grafting non-polar monomers to non-polar substrates with methanol as the solvent.[77] The greater polarity of methanol containing the dissolved electrolyte favours the partitioning of the non-polar styrene into the substrate. Conversely, a polar monomer would not be "salted-out", and the same increase in diffusion of the monomer to the grafting sites would not occur.

Considering the success of the partitioning theory by Garnett and coworkers, it is curious that such a small amount of work has been reported on the effect of acid when grafting onto fluoropolymers.

The use of more than one additive can also be useful in grafting reactions. The addition of an acid and a metal salt can have a dramatic affect on the grafting to fluoropolymers and polyolefins when the pre-irradiation peroxy method is used. Gupta and Chapiro were able to double the graft yield across a large monomer concentration range when grafting acrylic acid to pre-irradiated FEP by the addition of acid to a solution containing Mohr's salt.[63] This synergistic effect in the case of grafting to polyolefins is assumed to be due to an accelerated decomposition of the hydroperoxy group in the presence of Fe^{2+} and H_2SO_4 (Scheme 1.7), followed by conversion of OH^- to H_2O by the acid.[82]

$$POOH + Fe^{2+} \; ? \;\; PO^{\bullet} + Fe^{3+} + OH^-$$

Scheme 1.7 Decomposition of a hydroperoxy group Mohr's salt.

1.5.3.3 Crosslinking Agents as Additives

Grafting using the simultaneous grafting method may result in a certain degree of crosslinking of the grafted polymer due to the incidental exposure of the graft to radiation, causing abstraction and crosslinking. In extreme cases, at high doses using the simultaneous method, degradation of the graft can occur resulting in a decrease in the amount of grafted polymer.[83,84] The *G* value for crosslinking of PS is relatively low (0.1),[85] so when grafting styrene to a substrate, addition of a crosslinking agent is a useful way to artificially increase this value.

Polyfunctional crosslinking agents (for example see Figure 1.10) have been shown to either enhance or lower the graft yield depending on the concentration in which they are used. When a high concentration (10 % v/v) of divinylbenzene (DVB) or triallyl cyanurate (TAC) was added to styrene when grafting to FEP using the pre-irradiation peroxy method the graft yield increased with grafting time until it reached a plateau. This final graft yield decreased in the order: no additive > TAC > DVB.[86] Similar results have been reported using the pre-irradiation method where the crosslinking of PS grafted to FEP using DVB (20 % v/v) in benzene led to lower final graft yield compared to the system without any crosslinking agent.[87] Grafting of styrene in methanol to ETFE using the pre-irradiation

peroxy method showed an increase in the final graft yield at low concentrations of DVB, while at higher concentrations the final graft yield dropped.[56] Grafting of styrene to poly(ethylene) with the addition of a small amount of either DVB or trimethylolpropane triacylate (TMPTA) was found to enhance grafting, while when grafting to poly(propylene), addition of DVB had the effect of shifting the Trommsdorff peak to a higher monomer concentration.[88,89]

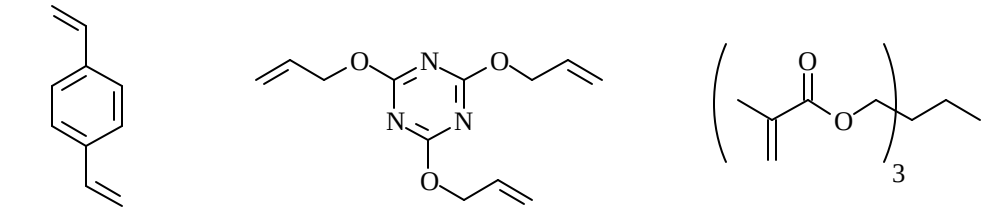

Divinyl benzene Triallyl cyanurate Trimethylolpropane triacylate

Figure 1.10 The structure of several crosslinking agents used in grafting reactions.

The enhancing effect of crosslinking agents at low concentration can be attributed to enhanced branching reactions. When one end of the DVB is immobilized through reaction with a growing PS chain the other vinyl group of the DVB molecules is capable of initiating a new chain through scavenging reactions.[89] At higher concentration of the crosslinking agent there is a significant increase in network formation, which leads to suppression in the swelling of the graft and an increase in viscosity in the surrounding solution, which lowers the diffusion and availability of monomer, leading to lower graft yields. In addition, if the diffusion of monomer to the radicals within the substrate is hindered, there may be decay of the substrate radicals without contribution to the graft reaction.[56,87]

1.5.4 Effect of Fluoropolymer Substrate

The number of commercial fluoropolymers available has expanded greatly since the first fluoropolymers, PCTFE and PTFE were introduced to the market. A wide variety of fluoropolymers are now available with a range of melt viscosities and crystallinities, and there is greater control over the end groups.[90] In this section the literature examining the influence of different fluoropolymer substrates on grafting reactions is presented.

Walsby *et al.* used electron beam irradiation to graft styrene to a range of fluoropolymers and compared the graft yields.[40] The fluoropolymers examined included partially-fluorinated polymers PVF, PVDF, ETFE and PVDF-*co*-HPF (one with 6 % and one with 15 % HPF content), and fully-fluorinated polymers PTFE and FEP. The graft yields ranged from 5 % for PTFE to 76 % for PVF. These workers sited a number of probable influences on the graft yield such as: different radical concentrations produced by irradiation, different structures of the radical centres, variations in crystallinity and glass transition temperature (T_g) of the polymers, and styrene uptake. While they did not measure the first two variables mentioned, they did measure the crystallinity and T_g of each polymer as well as the styrene uptake. In most cases they found reasonable agreement between the styrene uptake of the untreated polymer and the graft yield. This is not surprising as any increase in swelling of the grafting front would facilitate monomer penetration into the bulk of the film. The two PVDF-*co*-HPF polymers were obvious exceptions to this rule. The copolymer with 15 % HPF content had higher styrene uptake than the copolymer with 6 % HPF, however, the graft yield of the former was lower. They attributed this observation to variation in crystallinity between the two copolymers. The effect of the HPF is to disrupt the crystalline packing, hence higher HPF content leads to higher amorphous content.[91] Since the grafting reactions were performed above the T_g of these polymers, the chains in the amorphous regions had a high degree of mobility which favoured the termination of growing PS graft. The low graft yields found for FEP and PTFE were attributed to the low measured crystallinity of 15 % and 14 %, respectively. However it seems quite remarkable that the PTFE used had such low crystallinity considering it is a linear polymer and is generally considered to be highly crystalline.[20] It is of interest to note that the two fully fluorinated polymers studied, PTFE and FEP, showed the two lowest graft yields compared with the partially hydrogenated polymers.

Grafting of styrene to FEP, PVDF and ETFE with crystallinity of 17 %, 41 % and 30-37 %, respectively, has been reported using the peroxy method.[92] The crystallinity of the PVDF samples were similar to that in other reports, however the crystallinity of the ETFE samples was significantly higher than in other reports.[40] In agreement with other reported work the graft yields for PVDF and ETFE were higher than for FEP.[40] It was suggested that because of the higher crystallinity of the PVDF and ETFE, they should have lower graft yields compared with FEP, but the opposite was found. The result was attributed to greater monomer transport and higher radical yields for the two partially fluorinated polymers compared with FEP. This result is in contrast to that of Sakurai *et al.*[93] who showed that PTFE with crystallinity of 62 % and 67 % gave higher graft yields than PTFE with crystallinity of 96 %. In each case the radical yield determined by ESR was the same, regardless of crystallinity. They used a grafting temperature of 273 K, which is below the T_g of PTFE. The monomer used, MMA, was able to diffuse into the amorphous regions, whereas it could not diffuse into the crystallites. In totally-amorphous fluoropolymers, such as the copolymer of tetrafluoroethylene and perfluoromethylvinyl ether, grafting was unsuccessful,[94] presumably due to the lack of stable radicals at the grafting temperature used.

The effect of grafting temperature on the graft yields was reported by Gupta and Chapiro.[63] They found that at grafting temperatures below 313 K, grafting occurred more rapidly in FEP than in poly(ethylene), whereas above 313 K the rates were similar.

1.5.5 Characterization Techniques

Once a grafting reaction is complete it is important to know the answers to several fundamental questions: *has the grafting reaction worked; where on the substrate has the graft formed;* and *what is the nature of the graft?* For soluble graft copolymers an assortment of techniques may be used to analyze the products, however, when grafting to insoluble fluoropolymers, the analysis is somewhat restricted to solid-state methods. The success of a grafting reaction is commonly measured by either the mass increase following thorough washing to remove any non-covalently bonded homopolymer, or by FTIR to identify the new absorption bands of the grafted polymer. To obtain answers to the other questions of "*where has the grafting reaction occurred?* and, *what is the nature of the graft?*" is less straightforward. Following is a review of recently-reported techniques for analyzing grafted fluoropolymers and the information that they provide.

1.5.5.1 Nuclear Magnetic Resonance Spectroscopy

While it is generally accepted that a covalent bond is formed between a graft polymer and the macromolecular substrate (e.g. a polyolefin), this graft point cannot be observed directly by nuclear magnetic resonance (NMR) spectroscopy due to the low concentration of these points.[95] Literature on the characterization of grafted fluoropolymers by NMR spectroscopy is scarce due to the relatively low sensitivity of this technique and the limited information gained. Still, there are several recent additions to the literature which use this technique to analyze fluorinated graft copolymers.

Solid-state broadline ^{1}H NMR has been used by Sakurai *et al.* to locate the position and rotational motion of radiation-induced grafted PTFE-*g*-poly(methyl methacrylate) (PTFE-*g*-PMMA).[96] The solid-state ^{1}H NMR spectrum of fully-protonated PMMA grafted to PTFE was broad and featureless. By using partially-deuterated methyl methacrylate (d_5, with only the OCH_3 undeuterated) as the monomer they were able to greatly narrow the linewidth of the ^{1}H NMR spectra, so the peaks could be resolved into Gaussian and Lorentzian components. These components were assigned by comparison with a graft prepared using a mixture of 100 : 1 d_8 and d_5 methyl methacrylate, enabling them to essentially 'dilute' the OCH_3 groups of the graft. The spectrum of this sample contained

only a Lorentzian component and was assigned to OCH_3 groups in an isolated environment, and as a corollary, the Gaussian component was assigned to aggregated local structures where the OCH_3 groups can magnetically interact. With increasing graft yield in the range 1 – 7 % wt the Lorentzian / Gaussian ratio decreased.

Measurement of the second moments, $<DH^2>$, of the Lorentzian and Gaussian components gave some information regarding the rotational motion of the CH_3 groups of the PMMA. It was found that the diffusion of the CH_3 group attached to the ester of grafted PMMA was lower than that of the CH_3 groups in bulk PMMA, indicating there was a stronger interaction between the PTFE and PMMA chains than between the PMMA chains.

Hietala *et al.* used solid-state ^{13}C cross-polarization magic angle spinning (CP MAS) NMR to measure the miscibility and local heterogeneity of PVDF-*g*-PS membranes.[97] PVDF is a semicrystalline fluoropolymer made up of alternating CF_2 and CH_2 groups. Graft yields of 18 – 73 % were achieved using the post-irradiation method in a styrene / toluene solution.

The size of the phase-separated structures was measured using proton spin-lattice relaxation (T_{1H}) and proton spin-lattice relaxation in the rotating frame ($T_{1\rho H}$) measurements for the PS and PVDF components. Spin relaxation experiments showed that the T_{1H} relaxation time was the same for the two components regardless of the grafting ratio or measurement temperature, suggesting the homogeneity was on a tens of nanometers scale. Conversely, the $T_{1\rho H}$ relaxation measurements showed that while there was no difference for the samples with different graft yields, the $T_{1\rho H}$ was longer for PVDF than for PS when measured at high temperature. This result suggested the phase-separated domains were larger than a few nanometers. Incorporating these two observations they concluded that the phase-separated domains were between a few nanometers and some tens of nanometers in size. A two-dimensional wide-line separation (WISE) experiment showed that the mobility of the amorphous phase of the PVDF was greater than the corresponding phase in PS, which can be attributed to the much higher T_g of PS compared with PVDF (173 K and 313 K, respectively).

1.5.5.2 Graft Molecular Weight by Size-Exclusion Chromatography

The molecular weight and molecular weight distribution of the graft polymer is of great interest, as it can be pivotal in determining the properties and performance of the graft copolymer. The most accurate way to measure the molecular weight of the graft is by cleaving it from the polymer substrate, then use size-exclusion chromatography (SEC) to measure the molecular weight distribution. This method is only possible in cases when the graft point can be selectively cleaved. Garnett *et al.*[77] grafted PS to cellulose using γ-radiation then cleaved the PS graft by acid hydrolysis and measured the number average molecular weight (M_n) by SEC. They observed reasonable agreement in the M_n between the cleaved graft and the homopolymer formed, suggesting that the rates of propagation of the graft polymer and polymer in the bulk were similar.

Miwa *et al.*[98] grafted nitroxide-mediated PS to poly(propylene) using the peroxy method and in doing so introduced an ether bond at the graft point. A small portion of the graft was cleaved by soaking the graft copolymer in trifluoroacetic acid for several days. Comparison of the M_n and polydispersity of the homopolymer formed during grafting with the cleaved PS showed the values were almost the same. No attempt was made to explain why only a small percent of the PS graft could be cleaved.

In many applications the graft copolymer must be resistant to strong acids, therefore any cleavable graft points are undesirable. Molecular weight determination of the graft has been reported by dissolving the grafted polymer and substrate followed by analysis by SEC. While this technique is clearly not possible when the base polymer is an insoluble fluoropolymer, it has been done for partially fluorinated, soluble polymers.

Ducouret *et al.* graft copolymerized styrene to thin (25 μm) poly(vinylidene fluoride) (PVDF) films using the pre-irradiation peroxy method with swift heavy ions, then analyzed the soluble component of the copolymer using SEC.[99] PVDF is one of the few soluble fluoropolymers and will dissolve in solvents such as DMF owing to its dipolar nature from the tendency of the Fs and Hs to align themselves on opposite sides of the carbon backbone.[20] SEC of the grafted copolymer showed that the molecular weight of the PVDF was significantly lower than the grafted PS at high graft yields. The effect of the pre-irradiation dose was also examined. With increasing dose the M_n decreased, which

suggested that with more radicals produced in the substrate, the shorter the graft chains. At high dose there was also an increase in the insoluble component, presumably due to crosslinking.

Aymes-Chodur *et al.* also used the pre-irradiation peroxy method with γ-irradiation as the ionizing source to graft styrene to PVDF-*co*-HFP, then analyzed the resulting graft polymer by SEC.[100] Again the molecular weight of the PS graft was significantly higher than the polymer substrate. The graft yield increased with grafting time, accompanied by an increase in graft chain length which was rapid at first then reached a plateau. Conversely, Safranji *et al.* used the simultaneous radiation grafting method to graft methyl-*a*,ß,ß-trifluoroacrylate to poly(tetrafluoroethylene-propylene) and found that at low doses there was a slow increase in graft yield.[84] Crosslinking of the grafts exposed to higher doses prevented analysis due to solubility problems.

1.5.5.3 X-ray Photoelectron Spectroscopy

Surface characterization of polymers is commonly achieved using X-ray photoelectron spectroscopy (XPS). This technique allows quantitative determination of surface chemical composition and chemical bonding on the surface inferred by the shift in the electron-binding energies of the surface elements. It also provides information about the surface chemical structure with a spatial resolution of a few millimeters and a depth resolution of approximately 5 nm, depending on the take-off angle.[101]

When XPS was used to study the surface of radiation-grafted PTFE-*g*-PS[102] and PFA-*g*-PS[103] films, an increase in the C*1s* peak and a decrease in the F1s peak was observed as the amount of styrene increased with increasing grafting. When PTFE-*g*-PS films were analysed, a C–CF component of the C*1s* peak was identified which was attributed to graft occurring with the loss of fluorine, and although there was no shift in the F*1s* binding energy, there was a decrease in the peak intensity with increasing graft.[102] XPS of the PFA-*g*-PS films before grafting identified perfluoroalkoxy side chains of the perfluoropropylvinyl ether (PPVE) groups partially masked by some oxygen contamination.[103] A larger than predicted F/C ratio for the structure suggested that there

was more fluorine at the surface. The peaks due to CF_3 and CF groups representing the side chain were lost when the film was grafted with PS.

XPS has also been used to examine the distribution of graft on a PTFE film. Inagaki *et al.* treated PTFE with plasma then exposed it to air to introduce peroxy radicals to the surface.[104] The peroxy groups were then decomposed by heating and the resulting radicals reacted with sodium vinyl sulfonate to form a graft layer. The existence of CF_2 in the XPS spectrum of the grafted PTFE led them to propose that either the graft layer was thinner than the sampling depth or the graft gave incomplete coverage. The average thickness of the graft was calculated based on the graft yield and found to be thicker than the sampling depth, thus they concluded that the graft polymer was aggregated in patches on the surface. This aggregation may have occurred after the grafting solvent was removed.

It is also possible to vary the XPS sampling depth by changing the take-off angle. Sakurai *et al.* grafted methyl methacrylate to PTFE samples varying in crystallinity using the post-irradiation method.[93] Using angular-resolved XPS with take-off angles from 5° to 70° a depth somewhere between 45 to 80 Å below the surface was probed. Calculation of the exact probe depth was difficult owing to the different densities of PTFE and PMMA. At low take-off angles they found that the PMMA signal was larger than the CF_2 peak of the PTFE, and vice versa at large take-off angles, for highly crystalline (96 %) PTFE. For PTFE with lower crystallinity (62 %) the grafting occurred more uniformly which was attributed to grafting in the amorphous regions.

XPS analysis of plasma-initiated grafting of acrylamide to PTFE showed that there was migration of the polar graft below the surface because of surface restructuring, resulting in a thin fluorinated surface layer 2-3 nm thick.[105] Similar results have been reported for the grafting of acrylamide, acrylic acid, *N*,*N*-dimethylaminoethyl methacrylate or a salt of 4-styrenesulfonic acid onto hydrocarbon films.[106,107]

1.5.5.4 Microprobe Raman and FTIR-ATR Spectroscopy

The distribution of the graft on or into the substrate is important in many applications. Ion exchange membranes used in fuel cells need to be conducting and require homogeneous bulk grafting of the substrate,[41,64,108] while for SPOC, accessible surface grafting is vital for the performance of the copolymer.

Raman spectroscopy, despite being first discovered in 1928 by C.V. Raman and almost simultaneously by G. Landsbery and L. Mandelstam, only gained popularity years later with the introduction of intense laser sources in the 1960s and then the development of bench-top Raman spectrometers. The Raman microprobe uses an optical microscope coupled to a Raman spectrometer enabling the laser to be focused on a small spot, followed by collection of the scattered light from the illuminated region. Typically the sample spot is in the order of 2 μm.

The homogeneity of PS-grafted PVDF has been measured using microprobe Raman, both on the surface and by cutting a cross-section and recording depth-profile spectra.[109] At low grafting the PS distribution was heterogeneous on the surface and decreased in concentration into the polymer substrate, however at high grafting the surface became homogenous, at least within the resolution of the microprobe Raman. Sulfonation of the PS graft and cross-section map using microprobe Raman showed that the sulfonation reaction was not 100 % efficient at low graft yields, due to the poor swelling of the hydrophobic PVDF polymer. At high graft yields the graft copolymer became easier to swell in the sulfonation reaction solvent and more complete derivatization occurred. This result revealed that it is not correct to assume that the derivatization of a graft is independent of the graft yield.

Extensive microprobe Raman mapping of a plasma-initiated grafted surface of styrene to a blend of poly(propylene), poly(ethylene) and ethylene-propylene rubber (EPR) has been recently reported.[110] A 50 × 50 μm section of the polymer was mapped using resolution of 1 μm before plasma treatment, after plasma treatment and after grafting. From the respective Raman absorption peaks, the concentration and crystallinity of the EPR and the concentration of the PS were mapped. A clear correlation was found between low crystallinity and EPR concentration and also between EPR concentration and high PS graft.

It was concluded that the plasma must introduce a high concentration of reactive species on the EPR particles which are capable of initiating grafting.

FTIR-attenuated total reflectance (ATR) spectroscopy can also be used to perform depth profiles of grafted samples. By varying the angle of incidence, the penetration depth of the evanescent wave changes. Using two types of internal reflection crystals and three angles of incidence, Rouilly *et al.* measured the PS distribution in FEP grafted films. Again homogeneous grafting was found at high graft yields.[41]

Guilmeau *et al.* used FTIR-ATR to determine the surface graft yields and transmission FTIR to determine the bulk graft yields for ETFE-*g*-PS films based on characteristic absorption bands of each component.[111] The penetration depth of the evanescent wave in the ATR experiment was about 3 µm compared with a total film thickness of 30 µm. Comparison of the surface graft yields determined by FTIR-ATR with the volume graft yields by FTIR in transmission mode showed that initially the values were similar, however after longer grafting time the graft yield below the surface exceeded that at the surface. They concluded that the grafting was not diffusion controlled in 30 µm films, although similar measurements for 100 µm films showed that the rate of grafting did depend on the diffusion of monomer.

1.5.5.5 Scanning Electron Microscopy and X-ray Analysis

Like Microprobe Raman and FTIR-ATR Spectroscopy (section 1.5.5.4), scanning electron microscopy (SEM) and X-ray analysis can give information on the distribution of the graft. SEM can be used to view the graft copolymer on a nanometer scale, while elemental analysis can be performed by coupling the SEM to an X-ray spectrometer. The principle of X-ray analysis involves segmenting the X-ray energies dissipated when an electron beam impinges upon a sample into characteristic energies for the elements. In this section a review is given of how scanning electron microscopy and X-ray analysis have been used to analyze fluorinated graft copolymers.

X-ray microscopy has been used to examine the cross-sections of PTFE,[68] FEP,[67] and PFA[108] films grafted with acrylic acid. The X-ray micrograph showed the grafted and non-grafted areas of the cross-section, and hence the penetration depth of the graft can be obtained. At a low graft yield, the poly(acrylic acid) was limited to the surface, but at a higher graft yield it penetrated the entire film. This confirmed the grafting-front mechanism mentioned in Section 1.5.2 where grafting begins at the surface and proceeds into the centre of the films with progressive diffusion. X-ray microscopy has also been used to gain information about the effect of the monomer concentration on the graft penetration. At low monomer concentration homogeneous grafting throughout the entire film was achieved at a lower total graft yield, while the converse was true at high monomer concentration.[67]

Measurement of the fluorine distribution in cross-sections of grafted fluoropolymer films using SEM coupled to an X-ray analyzer can also be used to measure the graft distribution. Walsby *et al.* used this technique to examine the effects of toluene and *n*-propanol when used as solvents in the grafting of styrene to PVDF.[112] Again the grafting-front mechanism was evident from the surface grafting. When toluene was used as the diluent for styrene the penetration depth was greater and the graft was more homogeneous than when *n*-propanol was used where graft was essentially at the edges of the film. SEM analysis of the surfaces of the same grafted films gave some insight into the surface topology. Using toluene, the grafting did not change the surface topology and some of the original surface features of the ungrafted material were visible. When *n*-propanol was used, the surface was very rough and contained large PS domains with cavities up to 10 μm in size. The same observations were made for bulk styrene grafting as for the *n*-propanol case, however there were no cavities. Elemental analysis of the surface showed that there was some fluorine present, suggesting that the surface graft was not pure PS, but included some of the fluoropolymer substrate as well.

SEM has also been used to identify differences between grafting to PVDF and the less crystalline copolymer, PVDF-*co*-HFP.[113] Crystalline domains represented by 1 μm spherulites were identified on the surface of the PVDF virgin polymer. At low concentration of PS graft, small islands of PS could be seen on the surface correlating with the presence of the spherulites. It appeared that the grafting was being initiated by the crystalline zones. Virgin PVDF-*co*-HFP had no crystalline structures on the surface, although small islands of PS did appear at low grafting levels, and these coalesced at high

graft levels. As expected, a higher pre-irradiation dose led to more islands of PS on the surface, consistent with there being more grafting sites. The grafting seemed to be more on the surface for PVDF compared with the PVDF-*co*-HFP, suggesting that the diffusion of styrene in the polymer bulk is faster in the latter matrix, presumably due to the lower crystallinity.

1.6 Conclusions and Thesis Objectives

Despite the stability of fluoropolymers they may be readily modified by radiation-induced graft copolymerization. The number of fluoropolymer substrates and monomer combinations reported in the literature is vast and the conditions employed equally so. Parameters deemed important in predicting the grafting behavior include chemical composition, radical yield, swellability, dose and dose rate, crystallinity, T_g, additives, impurities, substrate thickness, processing, radiation atmosphere and type of radiation. However, in the existing literature the substrate polymers are rarely characterized other than by stating the proprietors responsible for donation or sale of the samples.

Once grafted, the characterization of the resulting graft copolymers is confined to a limited number of techniques. With the exception of one or two fluoropolymers, they are totally insoluble, so that solid-state techniques must be used.

The bulk of research on grafting to fluoropolymers has been focused on producing membranes. In this thesis, the first effort towards understanding the radiation chemistry of PFA and grafting to this fluoropolymer for the application as a solid support for SPOC is presented. The objectives of this thesis are:

- to understand the radiation chemistry of the base fluoropolymer.
- to understand how grafting conditions affect the extent and rate of grafting so that grafted polymer preparation can be carried out in a rapid and reproducible manner.
- to develop a solid support with thermal and chemical stability to a large range of solvents and conditions.

- to develop a solid support with better loading and kinetics than that of existing solid supports.

This thesis has been divided into eight chapters, each written with introduction, experimental, results and discussion, and conclusions sections. Some chapters also include a technical and theoretical aspects section where appropriate. Chapter Two will examine the structure and stability of the radicals produced in PFA when subjected to radiation. In Chapters Three and Four the identity of new structures in PFA irradiated over a range of temperatures is reported. Chapter Five describes the thermal properties of irradiated PFA. In Chapters Six and Seven the grafting of PS to PFA using various solvents and a 'living' polymerization technique are examined. In Chapter Eight conclusions are made and scope for further work is presented.

1.7 References

1. Boittiaux, V., Boucetta, F., Combellas, C., Kanoufi, F., Thiebault, A., Delamar, M., Bertrand, P., *Polymer* **40**, 2011-2026 (1999).

2. Marchesi, J. T., Keith, H. D., Garton, A., *J. Adhes.* **38**, 185-205 (1992).

3. Griesser, H. J., Da, Y., Hughes, A. E., Gengenbach, T. R., Mau, A. W. H., *Langmuir* **7**, 2484-2491 (1991).

4. Rye, R., *J. Polym. Sci. Part B: Polym. Phys.* **31**, 357-364 (1993).

5. Oshima, A., Seguchi, T., Tabata, Y., *Radiat. Phys. Chem.* **55**, 61-71 (1999).

6. Rasoul, F. A., Hill, D. J. T., Forsythe, J. S., O'Donnell, J. H., George, G. A., Pomery, P. J., Young, P. R., Connell, J. W., *J. Appl. Polym. Sci.* **58**, 1857-1864 (1995).

7. Ivanov, B., Popov, C., Lekova, M., Yankova, D., Peev, G., *Appl. Surf. Sci.* **108**, 297-301 (1997).

8. Lappan, U., Haussler, L., Pompe, G., Lunkwitz, K., *J. Appl. Polym. Sci.* **66**, 2287-2291 (1997).

9. Zhang, Y., Huan, A. C. H., Tan, K. L., Kang, E. T., *Nuc. Inst. Meth. Phys. Res. B* **168**, 29-39 (2000).

10. Svorcik, V., Micek, I., Rybka, V., Palmetshofer, L., Hnatowicz, V., *J. Appl. Polym. Sci.* **69**, 1257-1261 (1998).

11. Merrifield, R. B., *J. Am. Chem. Soc.* **85**, 2149-2154 (1963).

12. Moos, W. H. Introduction: Combinatorial Chemistry Approaches the Next Millennium. In: *A Practical Guide to Combinatorial Chemistry;* Czarnik, A. W.; DeWitt, S. H. Eds.; Americal chemical society: Washington, 1997.

13. Geysen, H. M., Meloen, R. H., Barteling, S. J., *Proc. Natl. Acad. Sci. USA* **81**, 3998-4002 (1984).

14. Hawker, C. J., Bosman, A. W., Frechet, M. J., Harth, E., Heumann, A., Ranger, M., Van Horn, B., Klaerner, G., Benoit, D., *Polym. Prep.* **42**, 639-640 (2001).

15. Bergbreiter, D. E., *Med. Res. Rev.* **19**, 439-450 (1999).

16. Barany, G., Kempe, M. The Context of Solid-Phase Synthesis. In: *A Practical Guide to Combinatorial Chemistry;* Czarnik, A. W.; DeWitt, S. H. Eds.; American Chemical Society: Washington, DC, 1997.

17. Valerio, R. M., Bray, A. M., Campbell, R. A., Dipasquale, A., Margellis, C., Rodda, S., Geysen, H. M., Maeji, N. J., *Int. J. Pept. Protein Res.* **42**, 1-9 (1993).

18. Maeji, N. J., Valerio, R. M., Bray, A. M., Campbell, R. A., Geysen, H. M., *React. Polym.* **22**, 203-212 (1994).

19. Rasoul, F. (Mimotopes Pty Ltd), Personal Communication

20. Carlson, D. P., Schmiegel, W. Fluoropolymers, Organic. In: *Ullmann's Encyclopedia of Industrial Chemistry*; VCH Verlag: Weinheim, 1998; Vol. A11.

21. Tervoort, T., Visjager, J., Graf, B., Smith, P., *Macromolecules* **33**, 6460-6465 (2000).

22. Tregear, G. W. "Graft Copolymers as Insoluble Supports in Peptide Synthesis"; Chem. Biol. Pept., Proc. Am. Pept. Symp., 3rd, 1972, Ann Arbor, Mich.

23. Liu, S., Akhtar, M., Gani, D., *Tetrahedron Lett.* **41**, 4493-4497 (2000).

24. Zhao, C., Shi, S., Mir, D., Hurst, D., Li, R., Xiao, X., Lillig, J., Czarnik, A. W., *Comb. Chem.* **1**, 91-95 (2000).

25. Zhao, C., Lillig, J. E., Neeper, R., Hudson, G. W., Czarnik, A. W., Parandoosh, Z., David, G. S., Xiao, X.-Y., *PCT Application WO 98/31732*, (1998).

26. Garnett, J. L., *Radiat. Phys. Chem.* **14**, 79-99 (1979).

27. Stannett, V. T., *Radiat. Phys. Chem.* **35**, 82-87 (1990).

28. Schellekens, M. A. J., Klumperman, B., *J. Macromol. Sci. Rev. Macromol. Chem. Phys.* **C40**, 167-192 (2000).

29. Kang, E. T., Zhang, Y., *Adv. Mater.* **12**, 1481-1494 (2000).

30. Kabanov, V. Y., *Radiat. Phys. Chem.* **33**, 51-60 (1989).

31. Gupta, B., Scherer, G. G., *Chimia* **48**, 127-137 (1994).

32. Chapiro, A. Radiation Chemistry of Polymeric Systems. In: *High Polymers;* Mark, H.; Marwell, C. S.; Melville, H. W. Eds.; Interscience: New York, 1962; Vol. XV.; p. 598.

33. Kamel, I., Machi, S., Silverman, J., *J. Polym. Sci., Part A-1* **10**, 1019-1029 (1972).

34. *Modern Fluoropolymers*; John Wiley and Sons: Chichester, 1997.

35. Clough, R. L., Gillen, K. T. Radiation Resistance of Polymers and Composites. In: *Irradiation Effects on Polymers;* Clegg, D. W.; Collyer, A. A. Eds.; Elservier Applied Science: London, 1991; pp. 79-156.

36. Chapiro, A., *J. Polym. Sci.* **34**, 481-501 (1959).

37. Chapiro, A., Matsumoto, A., *J. Polym. Sci.* **57**, 743-761 (1962).

38. Chapiro, A. Radiation Chemistry of Polymeric Systems. In: *High Polymers;* Mark, H.; Marwell, C. S.; Melville, H. W. Eds.; Interscience: New York, 1962; Vol. XV.; p. 676.

39. Walsby, N., Paronen, M., Juhanoja, J., Sundholm, F., *J. Appl. Polym. Sci.* **81**, 1572-1580 (2001).

40. Walsby, N., Sundholm, F., Kallio, T., Sundholm, G., *J. Polym. Sci., A, Polym. Chem.* **39**, 3008-3017 (2001).

41. Rouilly, M. V., Kotz, E. R., Haas, O., Scherer, G. G., Chapiro, A., *J. Membrane Sci.* **81**, 89-95 (1993).

42. Yamada, K., Gondo, T., Hirata, M., *J. Appl. Polym. Sci.* **81**, 1595-1604 (2001).

43. Hegazy, E. A., Abd, E., Ali, A. M. I., Nowiev, H. G., Aly, H. F., *Nuc. Inst. Meth. Phys. Res. B* **151**, 393-398 (1999).

44. Zou, X. P., Kang, E. T., Neoh, K. G., *Surf. Coat. Tech.* **149**, 119-128 (2002).

45. Wang, P., Tan, K. L., Kang, E. T., Neoh, K. G., *J. Adhes. Sci. Tech.* **16**, 111-127 (2002).

46. Chapiro, A. Radiation Chemistry of Polymeric Systems. In: *High Polymers;* Mark, H.; Marwell, C. S.; Melville, H. W. Eds.; Interscience: New York, 1962; Vol. XV.; p. 679.

47. Garnett, J. L., Yen, N. T., *Polym. Lett.* **12**, 225-229 (1974).

48. Dilli, S., Garnett, J. L., Martin, E. C., Phuoc, D. H., *J. Polym. Sci., C* **37**, 57-118 (1972).

49. Trommsdorff, E., Kohle, H., Lagally, P., *Makromol. Chem.* **1**, 169-198 (1948).

50. Nho, Y. C., Chen, J., Jin, J. H., *Radiat. Phys. Chem.* **54**, 317-322 (1999).

51. Li, Y., Desimone, J. M., Poon, C.-D., Samulski, E. T., *J. Appl. Polym. Sci.* **64**, 883-889 (1997).

52. Beenen, W., Wal, D. J., Janssen, L. P. B. M., *Macromol. Symp.* **102**, 255-263 (1996).

53. Nasef, M. M., Saidi, H., Dessouki, A. M., El-Nesr, E. M., *Polym. Int.* **49**, 399-406 (2000).

54. Nasef, M. M., Saidi, H., Nor, H. M., *J. Appl. Polym. Sci.* **76**, 220-227 (2000).

55. Nasef, M. M., Saidi, H., Nor, H. M., Dahlan, K. Z. M., Hashim, K., *J. Appl. Polym. Sci.* **73**, 2095-2102 (1999).

56. Elmidaoui, A., Cherif, A. T, Brunea, J., Duclert, F., Cohen, T., Gavach, C., *J. Membrane Sci.* **67**, 263-271 (1992).

57. Taher, N. H., Dessouki, A. M., Khalil, F. H., El-Arnaouty, M. B., *Polym. Int.* **41**, 383-389 (1996).

58. Hegazy, E. A., Taher, N. H., Ebaid, A. R., *J. Appl. Polym. Sci.* **41**, 2637-2647 (1990).

59. Hegazy, E. A., Taher, N. H., Kamal, H., *J. Appl. Polym. Sci.* **38**, 1229-1242 (1989).

60. Hegazy, E. A., El-Assy, N. B., Rabie, A. M., Ishigaki, I., Okamoto, J., *J. Polym. Sci.* **22**, 597-604 (1984).

61. Hegazy, E. A., Ishigaki, I., Okamoto, J., *J. Appl. Polym. Sci.* **26**, 3117-3124 (1981).

62. Hegazy, E. A., Ishigaki, I., Dessouki, A. M., Rabie, A.-G. M., Okamoto, J., *J. Appl. Polym. Sci.* **27**, 535-543 (1982).

63. Gupta, B. D., Chapiro, A., *Eur. Polym. J.* **25**, 1145-1148 (1989).

64. Hegazy, E. A., Dessouki, A. M., El-Assy, N. B., El-Sawy, N. M., El-Ghaffar, M. A. A., *J. Polym. Sci., A, Polym. Chem.* **30**, 1969-1976 (1992).

65. El-Sawy, N. M., Hegazy, E. A., Rabie, A. M., Hamed, A., Miligy, G. A., *Polym. Int.* **33**, 285-291 (1994).

66. Hegazy, E. A., Osman, M. B. S., Mokhtar, S. M., Mostafa, A. E. B., *Polymer* **33**, 4230-4235 (1992).

67. Hegazy, E. A., Ishigaki, I., Rabie, A.-G. M., Dessouki, A. M., Okamoto, J., *J. Appl. Polym. Sci.* **28**, 1465-1479 (1983).

68. Hegazy, E. A., Ishigaki, I., Rabie, A.-G. M., Dessouki, A. M., Okamoto, J., *J. Appl. Polym. Sci.* **26**, 3871-3883 (1981).

69. Chapiro, A. Radiation Chemistry of Polymeric Systems. In: *High Polymers;* Mark, H.; Marwell, C. S.; Melville, H. W. Eds.; Interscience: New York, 1962; Vol. XV.; p. 605.

70. Bozzi, A., Chapiro, A., *Radiat. Phys. Chem.* **32**, 193-196 (1988).

71. Huglin, M. B., Johnson, B. L., *J. Polym. Sci., A-1* **7**, 1379-1384 (1969).

72. Bozzi, A., Chapiro, A., *Eur. Polym. J.* **23**, 255-257 (1987).

73. Wilson, J. E. *Radiation Chemisty of Monomers, Polymers and Plastics*; Marcel Dekker, Inc.: New York.

74. Gupta, B. D., Chapiro, A., *Eur. Polym. J.* **25**, 1137-1143 (1989).

75. Chappas, W. J., Silverman, J., *Radiat. Phys. Chem.* **14**, 847-852 (1979).

76. Dworjanyn, P. A., Garnett, J. L., Khan, M. A., Maojun, X., Meng-Ping, Q., Nho, Y. C., *Radiat. Phys. Chem.* **42**, 31-40 (1993).

77. Garnett, J. L., Jankiewicz, S. V., Sangster, D. F., *Radiat. Phys. Chem.* **36**, 571-579 (1990).

78. Garnett, J. L., Jankiewicz, S. V., Levot, R., Sangster, D. F., *Radiat. Phys. Chem.* **25**, 509-516 (1985).

79. Chaplin, R. P., Dworjanyn, P. A., Gamage, N. J. W., Garnett, J. L., Jankiewicz, S. V., Khan, M. A., Sangster, D. F., *Radiat. Phys. Chem.* **47**, 435-437 (1996).

80. Dilli, S., Garnett, J. L., Phuoc, D. H., *J. Polym. Sci., Polym. Letts. Edn.* **11**, 711-715 (1973).

81. Nasef, M. M., *Polym. Int.* **50**, 338-346 (2001).

82. Kwon, O. H., Nho, Y. C., Lee, Y. M., *J. Mat. Sci., Mat. Med.* **11**, 593-600 (2000).

83. Shiraishi, N., Williams, J. L., Stannett, V., *Radiat. Phys. Chem.* **19**, 73-78 (1982).

84. Safranj, A., Omichi, H., Okamoto, J., *Radiat. Phys. Chem.* **27**, 447-453 (1986).

85. Charlesby, A. The Effects of Ionising Radiation on Polymers. In: *Irradiation Effects on Polymers;* Clegg, D. W.; Collyer, A. A. Eds.; Elsevier Science Publishers Ltd: Essex, 1991; p. 44.

86. Gupta, B., Buchi, F., Scherer, G. G., *J. Polym. Sci., A, Polym. Chem.* **32**, 1931-1938 (1994).

87. Xu, Z., Wang, G., Wang, H., Cian, G., Ni, M., *Radiat. Phys. Chem.* **22**, 939-945 (1983).

88. Ang, C. H., Garnett, J. L., Levot, R., Long, M. A., *J. Appl. Polym. Sci.* **27**, 4893-4895 (1982).

89. Dworjanyn, P. A., Garnett, J. L., *Radiat. Phys. Chem.* **33**, 429-436 (1989).

90. Hintzer, K., Lohr, G. Melt Processable Tetrafluoroethylene - Perfluoropropylvinyl Ether Copolymers (PFA). In: *Modern Fluoropolymers;* Scheirs, J. Ed.; John Wiley & Sons, 1997; pp. 223-237.

91. Pucciariello, R., Villani, V., Mancusi, C., *J. Appl. Polym. Sci.* **74**, 1607-1613 (1999).

92. Brack, H., Buhrer, H. G., Bonorand, L., Scherer, G. G., *J. Mater. Chem*. **10**, 1795-1803 (2000).

93. Sakurai, H., Shiotani, M., Yahiro, H., *Radiat. Phys. Chem.* **56**, 309-313 (1999).

94. Uschold, R. E., *J. Appl. Polym. Sci.* **29**, 1335-1344 (1984).

95. Dokolas, P., Looney, M. G., Musgrave, S., Poon, S., Solomon, D. H., *Polymer* **41**, 3137-3145 (2000).

96. Sakurai, H., Shiotani, M., Yahiro, H., *J. Appl. Polym. Sci.* **74**, 1386-1394 (1999).

97. Hietala, S., Maunu, S. L., Sundholm, F., *Macromolecules* **32**, 788-791 (1999).

98. Miwa, Y., Yamamoto, K., Sakaguchi, M., Shimada, S., *Macromolecules* **34**, 2089-2094 (2001).

99. Ducouret, C., Betz, N., Le Moel, A., *J. Chim. Phys.* **93**, 70-77 (1996).

100. Aymes-Chodur, C., Yagoubi, N., Betz, N., Le Moel, A., Ferrier, D., *Chromatographia* **51**, 269-276 (2000).

101. Munro, H. S., Singh, S. In: *Polymer Characterization;* Hunt, B. J.; James, M. I. Eds.; Chapman & Hall: London, 1993.

102. Nasef, M. M., Saidi, H., Nor, H. M., Yarmo, M. A., *J. Appl. Polym. Sci.* **76**, 336-349 (2000).

103. Nasef, M. M., Saidi, H., Yarmo, M. A., *J. Appl. Polym. Sci.* **77**, 2455-2463 (2000).

104. Inagaki, N., Tasaka, S., Goto, T., *J. Appl. Polym. Sci.* **66**, 77-84 (1997).

105. Tan, K. L., Woon, L. L., Wong, H. K., Kang, E. T., Neoh, K. G., *Macromolecules* **26**, 2832-2836 (1993).

106. Loh, F. C., Tan, K. L., Kang, E. T., Uyama, Y., Ikada, Y., *Polymer* **36**, 21-27 (1995).

107. Loh, F. C., Tan, K. L., Kang, E. T., Neoh, K. G., Pun, M. Y., *J. Vac. Sci. Technol. A* **12**, 2705-2710 (1994).

108. Hegazy, E. A., Dessouki, A. M., Rabie, A. M., Ishigaki, I., *J. Polym. Sci. Polym. Chem. Ed.* **22**, 3673-3685 (1984).

109. Hietala, S., Paronen, M., Holmberg, S., Nasman, J., Juhanoja, J., Karjalainen, M., Serimaa, R., Toivola, M., Lehtinen, T., Parovuori, K., Sundholm, G., Ericson, H., Mattsson, B., Torell, L., Sundholm, F., *J. Polym. Sci., A, Polym. Chem.* **37**, 1741-1753 (1999).

110. Keen, I., Rintoul, L., Fredericks, P. M., *Appl. Spec.* **55**, 984-991 (2001).

111. Giulmeau, I., Esnouf, S., Betz, N., Le Moel, A., *Nuc. Inst. Meth. Phys. Res. B* **131**, 270-275 (1997).

112. Walsby, N., Paronen, M., Juhanoja, J., Sundholm, F., *J. Polym. Sci., A, Polym. Chem.* **38**, 1512-1519 (2000).

113. Aymes-Chodur, C., Betz, N., M.-C., P.-D., Baquey, C., Le Moel, A., *Nuc. Inst. Meth. Phys. Res. B* **151**, 377-385 (1999).

Chapter 2

2 Radical Formation in PFA

2.1 Introduction

The nature of the initiating species in any free radical polymerization plays a pivotal role in determining the success or failure of the reaction. A radiation-induced grafting reaction to a pre-existing polymer is a specific type of free radical polymerization where a monomer is polymerized to a polymer backbone. In this situation, the initiating species is in the form of a free radical macro-initiator. The stability and accessibility of this initiator must be such that the monomer is able to react with it. The stability will depend on the chemical structure as well as the temperature at which the graft copolymerization reaction is performed. When radiation is used to create the initiating species on the polymer substrate, the radical yield will also influence the amount of graft.[1]

Radiation-induced grafting reactions of a monomer to a polymer substrate involves firstly creating radicals on or in the polymer substrate followed by either immediate reaction with the monomer (as is the case for the simultaneous grafting method), or by reaction with the monomer some time in the future (the pre-irradiation grafting method). For both the simultaneous and pre-irradiation grafting methods, the chemical environment, stability and accessibility of the radicals produced on the substrate are important factors in predicting the outcome of the grafting reaction.

The structure of PFA is relatively simple and there are only three types of bonds which may be cleaved by radiation, namely C–C, C–F, and a small amount of C–O bonds from the comonomer units. The possible radicals are thus limited to C, F and O-centred radicals. The morphological environment in which these radicals may be formed in PFA is more complex as PFA is semicrystalline. This, in conjunction with the insolubility of PFA, means that the graft copolymer will undoubtedly be heterogeneous.

In addition to initiating grafting reactions, the radicals formed in PFA may also act as precursors to chemical changes within PFA such as branches or double bond formation. By using ESR spectroscopy to identify the radicals produced in PFA when exposed to γ-radiation it may be possible to predict the mechanism of the grafting reaction and offer an understanding of the pathways to possible new chemical structures formed in PFA.

The radiolysis of PFA has been studied by several workers. Like PTFE, it is considered to be a radiation-degradable polymer. γ-Irradiation to low doses in vacuum or in air at ambient temperature results in a loss of mechanical properties and an increase in the crystallinity, suggesting that chain scission is the main radiolytic process.[2-4] Hegazy *et al.*[5] observed an initial slight increase in the tensile strength and elongation of PFA irradiated to low dose, followed by a decrease in these properties with increasing radiation dose. When irradiated to high doses with accelerated electrons in air, a drop in the melting point and the introduction of chain scission products as well as some unsaturation was observed.[6] Sun *et al.* claimed that under special conditions it is possible to radiation-crosslink PFA, based on an observed increase in the zero-strength-temperature after treatment.[7] Although the conditions were not specified, it might be assumed that irradiation was performed at a temperature where the chain mobility was high enough for radicals to recombine as branched and eventually crosslinked structures.

The structure of PFA is very similar to PTFE in that it contains mostly $–CF_2–CF_2–$ chains. The difference between the structure of PFA and PTFE is that PFA contains a small amount of perfluoroalkoxy pendant groups. PTFE is by far the most studied fluoropolymer, so it is of interest to review what is known about the radicals formed in PTFE. The first report of the radicals formed in irradiated PTFE was in 1955 by Schneider,[8] although his findings were widely rejected and it was not until several years later, in work by Tamura[9] and by Siegel and Hedgpeth,[10] that any consensus was agreed upon as to the components making up the ESR spectrum of PTFE irradiated and measured in vacuum at room temperature. Siegel and Hedgpeth[10] observed a spectrum comprising of a double quintet due to the main-chain radical (I) (Figure 2.1) (splitting ~ 3.3 mT ß-F and ~ 9.2 mT a-F) and a triplet due to the end-chain radical (II) (splitting 1.6 mT ß-F, wing peaks ~ 8.5 mT for the a-F). The yield of the end-chain radical was reportedly ten times greater than that of the main-chain radical.

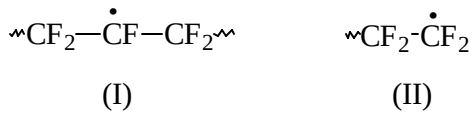

(I) (II)

Figure 2.1 Main-chain (I) and end-chain (II) radicals.

In fluorinated copolymers such as FEP (a copolymer of TFE and hexafluoropropylene (HFP)), the comonomer is known to have an effect on the radiation behavior due to the changes in chain mobility, radical reactivity and steric hindrance.[11] The perfluoropropyl vinyl ether (PPVE) comonomer in PFA might be expected to have a similar effect.

There is just one report in the literature examining the radical formation in irradiated PFA. Momose *et al.* used ESR spectroscopy to examine the peroxy radicals formed in PFA when subjected to an argon plasma and then exposed to air.[12] After the admission of oxygen to the sample, the spectrum contained a signal assigned to peroxy radicals in the crosslinked structures at the surface which was superimposed with a peroxy signal from oxygen reaction with radicals in the bulk.

In this chapter the radicals produced when PFA was exposed to γ-radiation in vacuum are examined. Their identity, stability and number will be examined with the aim of determining the initiating species for grafting reactions and the precursors to chemical changes within PFA.

2.1.1 Theory and Technical Aspects

In this section a brief review of ESR theory is given. Many books have been published on ESR theory and the reader is directed to Ranby and Rabek,[13] Weil and Bolton,[14] Ingram[15] or Ayscough[16] if a more detailed discussion of this technique is sought.

Electron Spin Resonance (ESR) (also often referred to as Electron Paramagnetic Resonance (EPR)) spectroscopy is used to study chemical species with an odd number of unpaired electrons. Radiation-induced cleavage of a chemical bond (an electron pair) will often result in formation of a type of unpaired electron called a free radical. Unpaired

electrons are found in other forms including stable organic compounds, transition metal ions and biradical species, however, in this chapter only free radicals will be considered.

An unpaired electron has an intrinsic angular momentum (spin vector) and a magnetic moment which is proportional, but opposite in sign, to the spin vector. In the most simple case, if a magnetic field (*H*) is applied to a paramagnetic sample with spin of ½, the magnetic moment will have two possible orientations relative to the magnetic field. The energy difference between the two orientations is such that transitions between the two energy levels may be induced with an external electromagnetic field with frequency in the microwave region (*E*) (Figure 2.2). *E* has an energy *h?*, where *?* is the frequency of the electromagnetic field and *h* is Planck's constant. This energy difference is equal to *gßH*, where *H* is the magnetic field, *ß* is the Bohr magnetron and *g* is a constant called the "Lande *g*-factor". When the population in the lower energy level is less than the population in the higher energy level, there is an absorption of microwave frequency which is detected, giving rise to an ESR absorbance. The electrons in the upper energy level repopulate the lower level via relaxation processes. In practice, the microwave frequency (and hence, *E*) is kept constant while the magnetic field (*H*) is scanned so that the equation *h?=gßH* is satisfied. Typically, a microwave frequency of the order of 9 GHz will require a magnetic field of approximately 0.3 T.

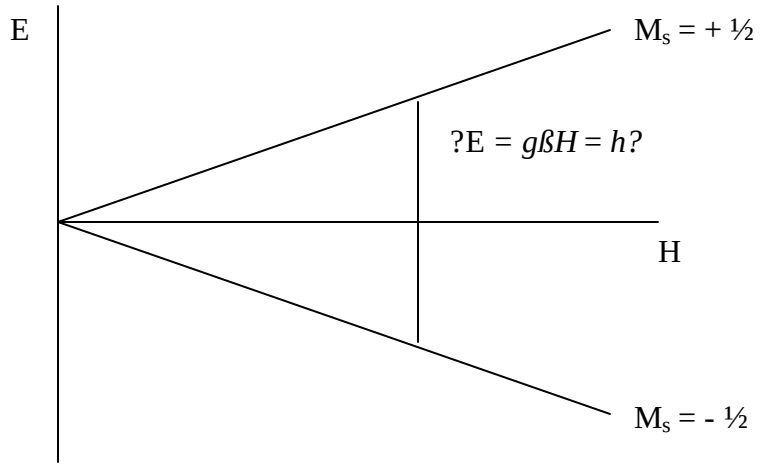

Figure 2.2 Possible energy levels for a single unpaired electron as a function of magnetic field.[16]

The line position of an ESR signal is expressed as a *g*-value (not to be confused with *G* values in Section 2.3.5). The *g*-value is a function of the microwave frequency and

the external magnetic field at resonance, that is, when the microwave energy is equal to the difference in the energy levels. Different types of radicals have different *g*-values, and they may be used to aid in the identification of the radicals.

Magnetic interactions between the radicals and surrounding nuclei can lead to hyperfine couplings in the ESR signal due to small additional splitting of the energy levels. The number of hyperfine couplings in conjunction with their magnitude and intensity can be used to determine the structure of the group containing the free radical. The rule governing the splitting of the electron magnetic levels is $2I + 1$, where I is the spin of the nucleus. ^{19}F is the only non-zero spin nucleus (ignoring the isotopically rare ^{13}C nucleus) in perfluoropolymers. ^{19}F has 100 % natural abundance and has I equal to ½ so that each ^{19}F atom will add to the hyperfine coupling by: $(2 \times ½) + 1 = 2$.

2.2 Experimental

PFA (code TE 7132) with PPVE comonomer content of 1.7 ± 0.2 mol. % as determined by NMR analysis was supplied by DuPont in pellet form. The crystallinity of the polymer by DSC was 34 ± 3 % based on the heat of fusion of 100 % crystalline PTFE of 82 J g^{-1}.[17] Pellets were freezer milled into powder and packed into ESR tubes, evacuated at 1×10^{-2} Pa for 48 hours and then sealed. All samples were checked for the absence of radicals by ESR spectroscopy prior to any irradiation. Irradiation was performed using a 220 Nordian ^{60}Co Gammacell facility either at 303 K or at 77 K using a liquid nitrogen dewar. Dose rates were 6.2 and 5.4 kGy hr^{-1} for 303 K and for 77 K irradiations, respectively.

The ESR spectrometer used was a Bruker ER200D operating in the X-band microwave frequency range and fitted with variable temperature and 77 K dewar inserts. All spectra were acquired using a modulation amplitude of 0.2 mT, a centre field of 330 mT, and a sweep width of 50 mT. By rotating the ESR tube in the ESR cavity it was confirmed that the ESR signals were isotropic and that the sample orientation did not affect the shape or intensity of the ESR spectrum.

Annealing of the sample irradiated at 303 K was performed by heating the sample at the desired temperature for five minutes, then cooling back to 298 K to record the ESR spectrum. Annealing of the sample irradiated at 77 K was performed by warming the sample to a predetermined temperature (in 10 K increments) for five minutes before recording the spectrum at this temperature.

The software used for acquiring and processing data and performing simulations was SIMOPR written by Wayne Garrett (The University of Queensland). Radical concentrations (spins g^{-1}) were calculated from the area of the absorption spectra determined from the double integration of the first derivative spectra, and by calibration of the instrument with a Varian Strong Pitch Standard (4×10^{15} spins g^{-1}). Microwave powers of 0.063 mW at 77 K and 0.63 mW at 298 K were used to avoid power saturation. Powerplots are shown in Figure 2.3. At 77 K and 298 K power saturation, as represented by deviation from linearity, occurred at approximately 0.13 mW and 6.3 mW, respectively.

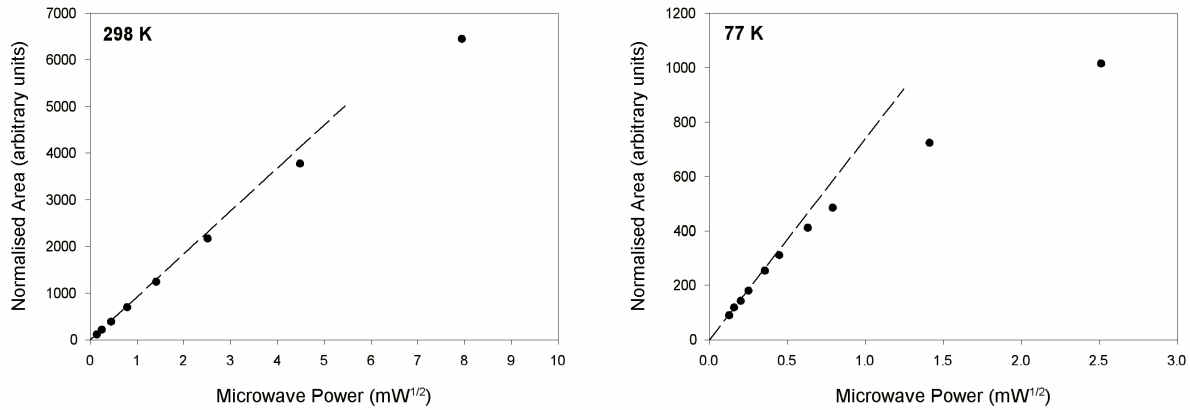

Figure 2.3 Powerplots of PFA irradiated at 303 K and measured at 298 K (left) and PFA irradiated and measured at 77K (right). The total dose was 500 kGy. The dashed line is an aid to illustrate where the microwave power deviates from linearity (power saturation).

The *G* values reported herein are based upon the number of events per 16×10^{-18} J (16 aJ or 100 eV) of absorbed energy.

2.3 Results and Discussion

2.3.1 303 K Radiolysis

The ESR spectra of PFA irradiated at 303 K in the dose range 5 to 100 kGy and recorded at 298 K are shown in Figure 2.4. The spectra can be described as a double quintet (splitting 3.4 and 8.9 mT; centred at g = 2.0021) superimposed with a triplet (splitting 1.7 mT; centred at g = 2.0029) and a broad signal just beyond the double quintet separated by 27.2 mT. Similar spectra have been observed for irradiated PTFE.[9,18] The sharp signal in the centre of the spectra denoted by "gs" was due to colour centres in the quartz ESR tube. The double quintet was assigned to the main-chain radical (I in Figure 2.1). The four ß-fluorines gave rise to a quintet with splitting of 3.4 mT, which were split by 8.9 mT by the *a*-fluorine. The central triplet was assigned to the end-chain radical (II in Figure 2.1), with a splitting of 1.7 mT from the ß-fluorine.

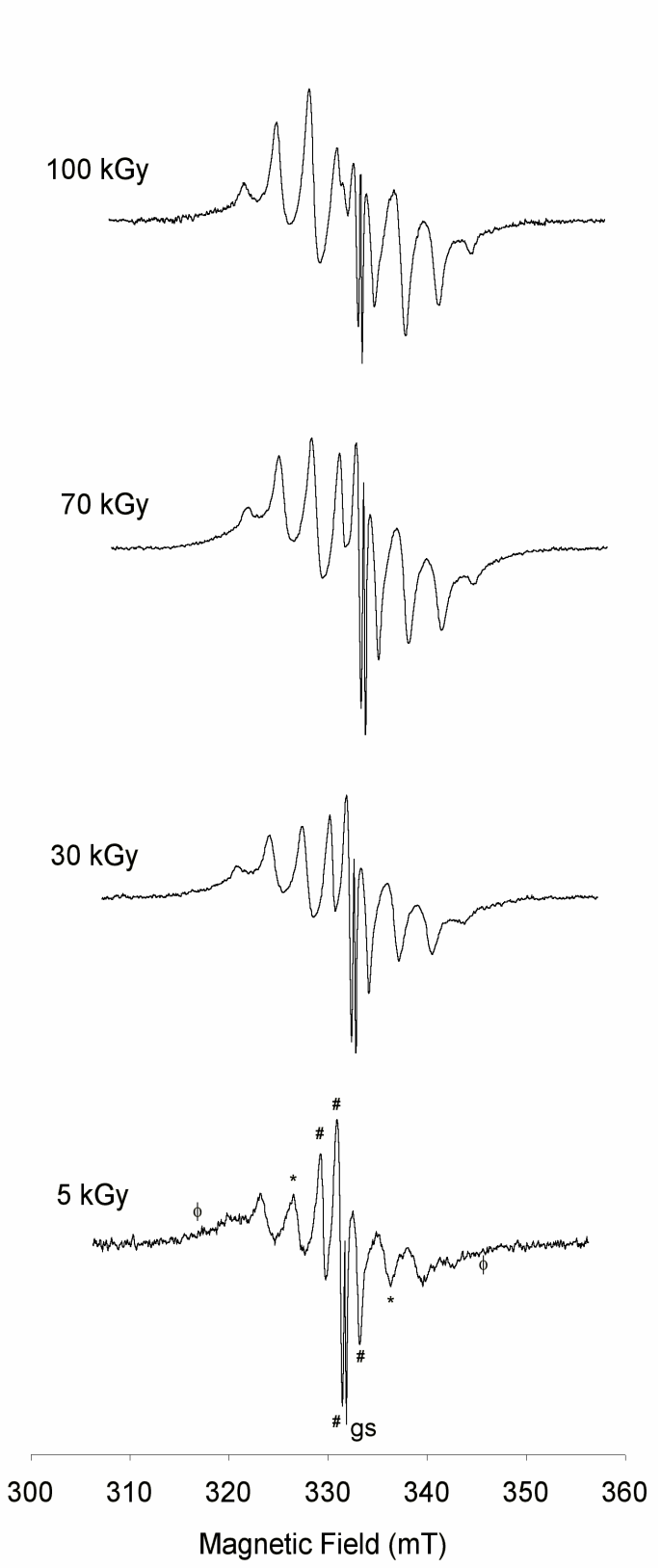

Figure 2.4 ESR spectra of PFA irradiated at 303 K in vacuum. Doses: 5, 30, 70, 100 kGy. Features of the spectra are indicated by: # - the triplet; * - the central line of the double quintet; ϕ - outer wing of the broad component. The glass signal is indicated by "gs".

The splitting effect of the *a*-fluorine in the end-chain radical (II) has been studied by Toriyama and Iwasaki using orientated PTFE.[19] By irradiating stretched PTFE then exposing it to air, the peroxy radicals at the main-chain and end-chain positions were formed. Photolysis and re-evacuation of the sample at 77 K led to exclusive production of the end-chain radical (II). Toriyama and Iwasaki showed that at room temperature the signal due to this radical was comprised of a central triplet and outer wing peaks ascribed to splitting by the ß- and *a*-fluorines, respectively.[19] The *a*-fluorine was found to have a splitting between 11.0 mT (parallel to the magnetic field) and 7.4 mT (perpendicular to the field). The separation between the tails of these wing peaks was measured and found that they approximately match the broad overlapping signals seen in the spectra in Figure 2.4. Thus, the broad component in Figure 2.4 was tentatively assigned to the *a*-fluorine coupling of the end-chain radical.

A simulation of the main-chain radical (I) and ß-fluorine coupling of the end-chain radical (II) of the spectra for PFA is shown in Figure 2.5. The simulated spectrum shows reasonable agreement with the splitting pattern of the experimental spectrum, although any anisotropic interactions could not be accounted for by the simulation software which assumes an isotropic tensor.

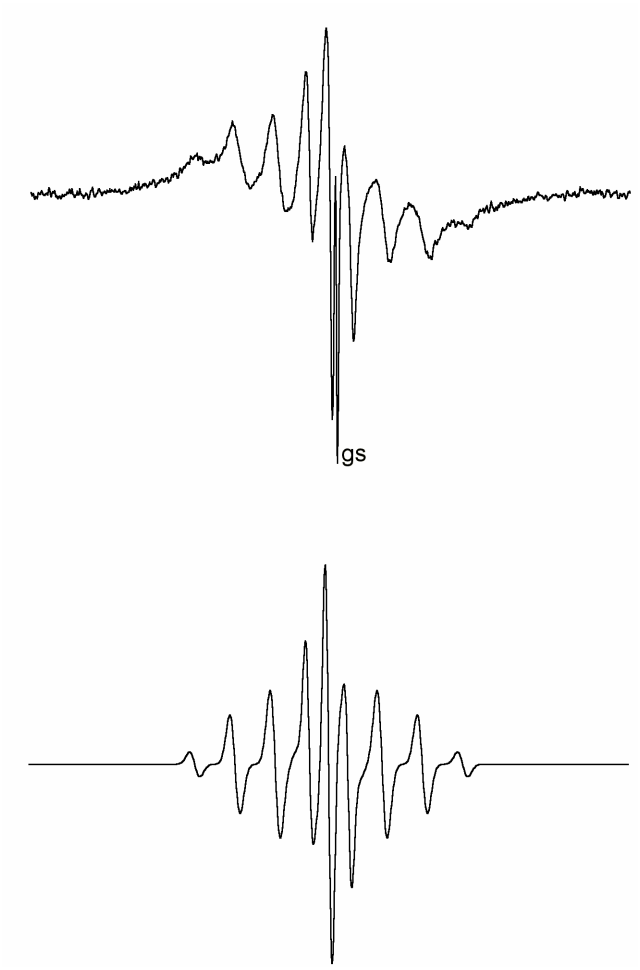

Figure 2.5 Top: ESR spectrum of PFA irradiated to 10 kGy at 303 K in vacuum, Bottom: simulation of the double quintet and triplet.

As the dose was increased, the ratio of the end-chain radical to main-chain radical decreased based on visual inspection of Figure 2.4. With increasing radical density the likelihood of radical recombination also increases, especially for any end-chain radicals in the amorphous regions. This dose effect was accompanied by a deviation from linearity in the radical yield plot at 298 K (Figure 2.6).

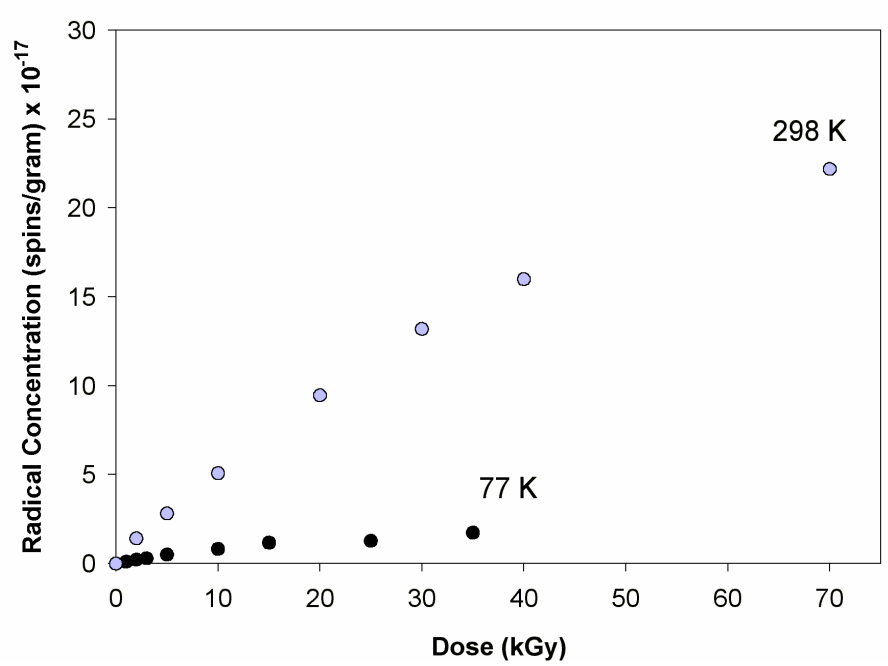

Figure 2.6 Radical concentration of PFA as a function of dose. 298 K (irradiated at 303 K and acquired at 298 K); 77 K (irradiated and acquired at 77 K).

There were significant differences in the proportion of the central triplet attributed to the end-chain radical in PFA, FEP and PTFE for samples irradiated to similar doses. Siegel and Hedgepeth and Oshima *et al.* reported that the triplet for irradiated PTFE was only a minor component,[10,18] while Hill *et al.* and Kim and Liang reported that for FEP it was the major feature.[20,21] For PFA the triplet constituted approximately half of the total signal, although it did vary depending on the dose. These observations may relate to the morphology of these fluoropolymers. Oshima *et al.*[18] used PTFE with crystallinity of 50 %, which was significantly higher than that of the PFA used here (34 ± 3 %) and presumably higher than that of the FEP used by Hill *et al.*[20] and Kim and Liang.[21] Although neither Hill *et al.* or Kim and Liang reported the crystallinity of the FEP they used, it is known that the HFP comonomer in FEP significantly disrupts chain packing, leading to a higher amorphous content when compared with PTFE.[22] At room temperature it might be expected that C–C bond scission in the crystalline regions would more likely result in recombination compared with C–C scission in the amorphous regions where the radicals may be able to move apart and stabilize due to the greater mobility in the amorphous regions. The end-chain radicals in PTFE are known to decay when warmed above the T_g [9] which has been exploited by Siegel and Hedgpeth to isolate the main-chain radical.[10] The same

observation was made for PFA irradiated at 303 K and then annealed (see Section 2.3.2), which also suggested that the end-chain radical is present in the amorphous regions when the polymer is irradiated at 303 K. Hence the greater amorphous content in PFA and FEP led to more end-chain radicals in the copolymers compared with PTFE. End-chain formation may also be aided in the copolymers by cleavage of the PPVE and HFP units in PFA and FEP, respectively.

The PPVE units in PFA might be expected to be radiolytically labile, however no component in the spectra of irradiated PFA could be assigned to any of the possible radicals formed from cleavage at this group (Scheme 2.1). Any main-chain and end-chain radicals formed from the PPVE units will be indistinguishable from those formed from the TFE units. The oxy radical (IV in Scheme 2.1), if present, would give rise to an asymmetric spectrum since it would have a higher *g*-value than either of the alkyl radicals.[13] While Iwasaki *et al.*[23] and Matsugashita and Shirohara[24] have claimed to have identified $R–CF_2–O^{\bullet}$ oxy radicals formed from degradation of peroxy radicals ($R–O–O^{\bullet}$), subsequent studies have thrown doubt onto this assignment. Rasoul *et al.*[25] and Schlick *et al.*[26] found that the peroxy radical was stable at room temperature and that the oxy radical would give rise to a singlet, not a triplet. Olivier *et al.*[27] also disputed the assignment of the oxy radical from experiments using isotopically-labeled oxygen when they did not observe the six hyperfine lines expected for $R–CF_2–^{17}O^{\bullet}$, instead assigning the signal as a superimposition of the end-chain radical and main-chain peroxy radical. On the other hand, the *g*-value of the carbon centred radical (III) may not be as easily distinguishable.

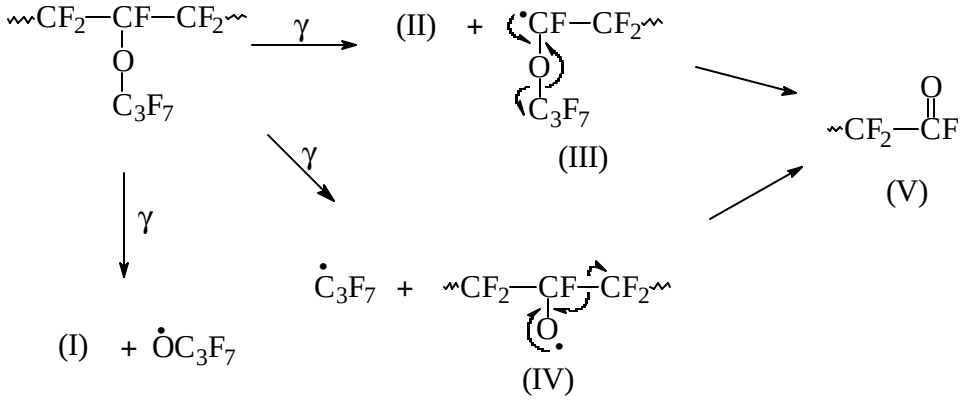

Scheme 2.1 Possible radicals formed from scission at the PPVE units and the ß-rearrangement to form acyl fluoride (V).

There are several possible reasons why none of the radicals attributed to scission at the PPVE units were observed in the ESR spectra. The first reason may simply be that the concentration of PPVE units in the polymer is so small that the signals due to the radicals produced were swamped by the signals due to cleavage at the TFE groups. Another reason may be that the products are not detectable by ESR spectroscopy. The products from cleavage of the CF–O bond will be radical (I) which is already present from the cleavage of C–F bonds, and the small fragment $^{\bullet}OC_3F_7$ which would quickly combine with another radical or possibly rearrange to form a non-radical species. The other possible pathways in Scheme 2.1 lead to radicals capable of rearrangement at 303 K, again resulting in a non-radical species, in this case the acyl fluoride group (V).

2.3.2 Annealing of PFA Irradiated at 303 K

The thermal stabilities of each of the radicals observed were examined by annealing the irradiated PFA over a range of temperatures. The radical concentration as a percentage of the original concentration is presented in Figure 2.7 which shows the radical concentration decreasing to almost zero with increasing annealing temperature up to 513 K. A selection of the spectra from the annealing experiments are shown in Figure 2.8. It is clear from Figure 2.8 that the species assigned to the central triplet and the outer wing peaks decayed preferentially to the double quintet. At 503 K the triplet and broad component disappeared completely, leaving the double quintet with diminished intensity. The T_g of non-irradiated PFA is 363 K as measured by dynamic mechanical analysis (Chapter 5, Section 5.3.1), although the onset of the transition begins at approximately room temperature. The preferential loss of the end-chain radicals in the temperature range 300 to 503 K again suggested they were present either in the amorphous regions or at the surface of the crystallites.

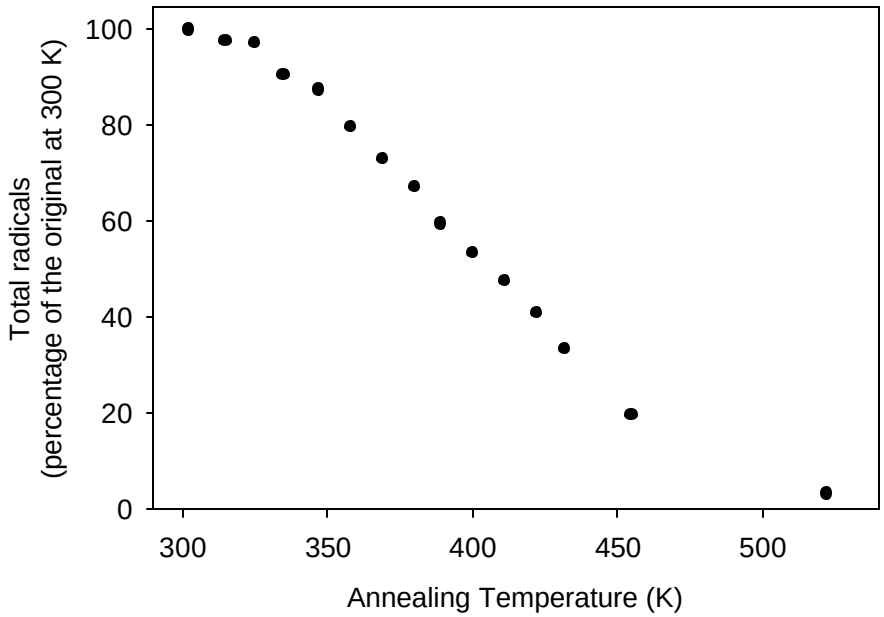

Figure 2.7 Decay curve for the total number of free radicals in PFA irradiated (100 kGy) at 303 K then annealed.

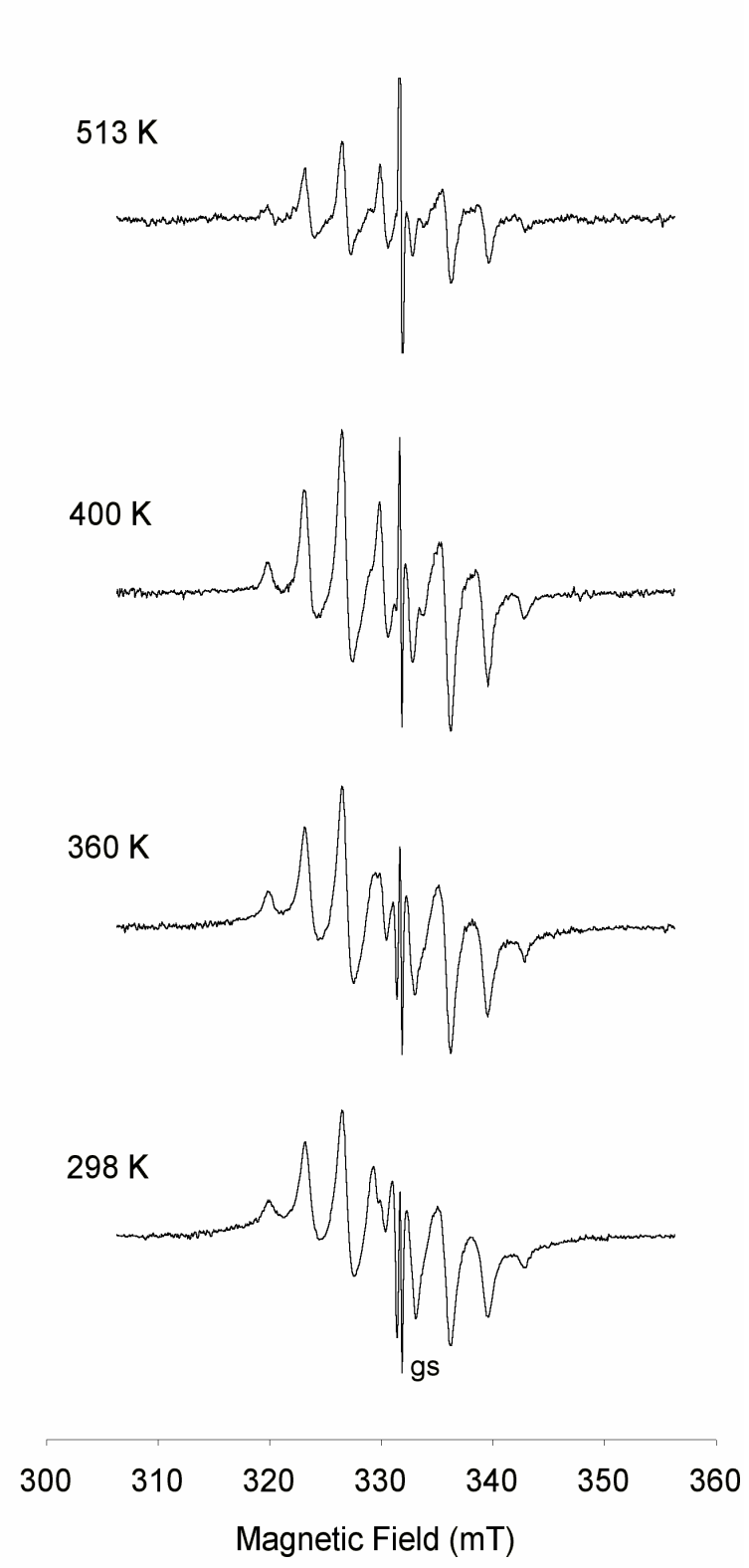

Figure 2.8 ESR spectra of PFA irradiated (100 kGy) at 303 K then annealed. The glass signal is indicated by "gs".

2.3.3 Life-times of Radicals at Ambient Temperature

The stability of radicals in PFA at ambient temperature is important for the success of grafting reactions. This is especially true when using the pre-irradiation grafting method where the substrate polymer is irradiated prior to introduction of any monomer for grafting.

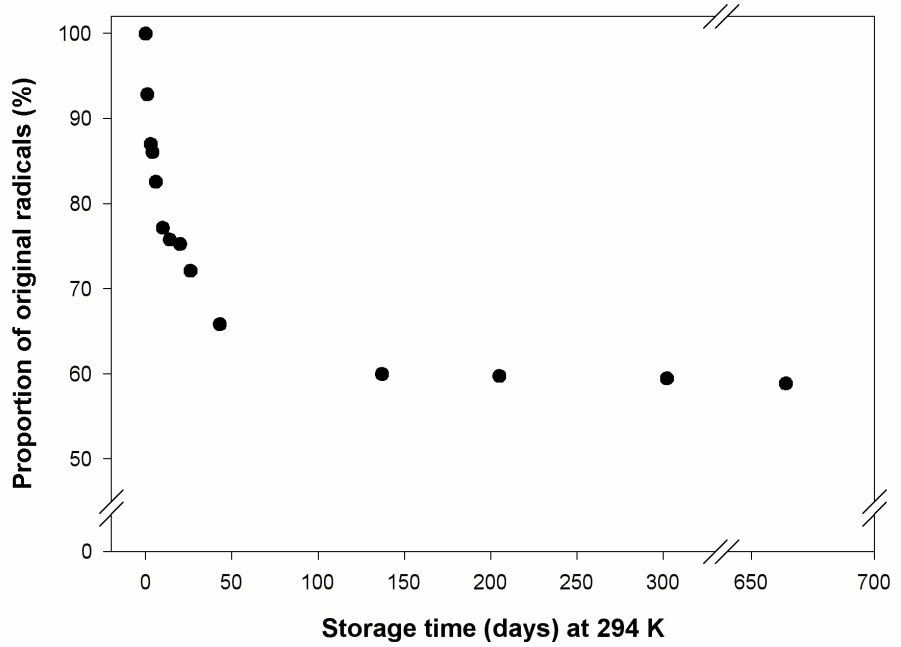

Figure 2.9 Stability of the radicals created in PFA when irradiated at 303 K and stored at 294 K in vacuum.

The decay of radicals in a sample of PFA irradiated to 60 kGy at 303 K in vacuum and stored at 294 K in the dark was measured using the peak area under the first derivative of the ESR spectra and is shown in Figure 2.9. There was relatively rapid decomposition of radicals during the first 50 days, after which the radical concentration reached approximately 60 % of the original and remained constant, even after 664 days. The initial rapid decomposition was due to loss of end-chain radicals, presumably by recombination. This is evident from the ESR spectra recorded over the period 0 to 664 days (Figure 2.10) which show that the central triplet due to end-chain radicals is greatly diminished after 10 days and completely absent after 664 days. As with the annealing studies, evidence suggested the end-chain radicals were present in the amorphous regions or at the surfaces of the crystallites while the main-chain radicals were predominantly in the crystallites. The

longevity of radicals in PFA was similar to PTFE where radicals are stable over long periods owing to the rigid chains in the crystallites.[18]

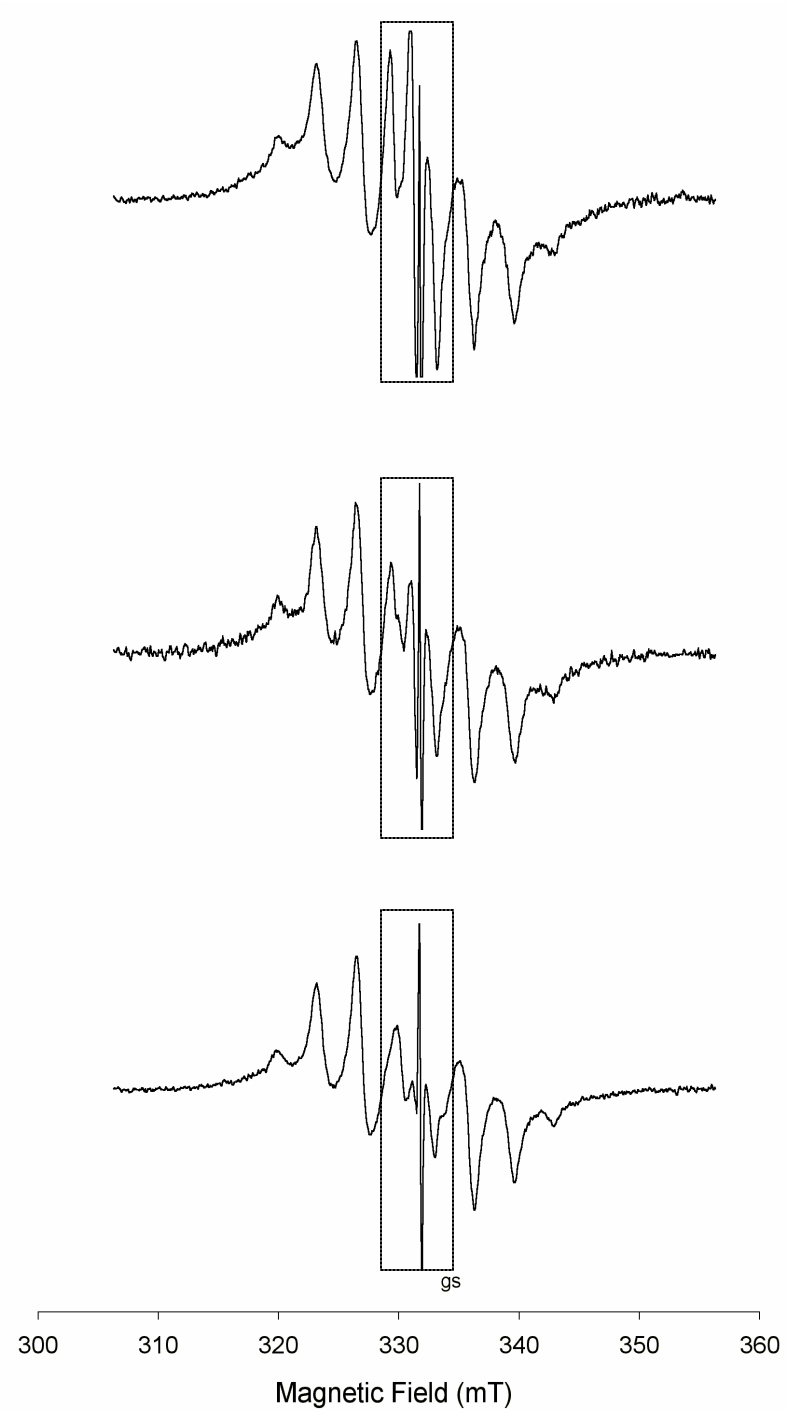

Figure 2.10 ESR spectra of PFA irradiated to 60 kGy. Top: immediately after irradiation; Middle: 10 days after irradiation; Bottom: 664 days after irradiation. The dotted box highlights the decay of the central triplet. The glass signal is indicated by "gs".

2.3.4 77 K Irradiation and Annealing Study

The spectrum of PFA irradiated to 395 kGy and measured at 77 K is shown in Figure 2.11 A. The anisotropic hyperfine couplings were not averaged at low temperature resulting in a broad spectrum. The spectrum may be considered to consist of a broad outer component, with width ~ 40 mT, as well as a sharp central line with peak to peak width ($?H_{pp}$) ~ 1.5 mT and shoulders of width ~ 15 mT. The spectrum is centred at g = 2.0061.

When the sample irradiated at 77 K was warmed to 170 K (Figure 2.11 B) the sharp central line seen in the 77 K spectrum was missing, in its place was a signal beginning to resemble the triplet of the end-chain radical (II) seen at 298 K. The double quintet did not become resolved until 292 K (Figure 2.11 C) where the spectra resembled that of the sample irradiated at 303 K and measured at 298 K. The total radical signal at 292 K was reduced to 25 % of the original 77 K spectrum. Subsequent cooling of the sample back to 77 K (Figure 2.11 D) resulted in a broad spectrum similar to the spectrum of the unannealed sample, but with the relative proportions of the inner and outer regions changed compared with the spectrum in Figure 2.11 A.

Allayarov *et al.*[28] and Tamura[9] have examined the main-chain radical spectrum at 77 K. Allayarov *et al.* studied PTFE irradiated at 77 K to very high doses (0.8 and 19 MGy) and then annealed to 300 K to isolate the main-chain radical.[28] When cooled back to 77 K and the spectrum acquired, they found a doublet of triplets of triplets due to non-equivalent ß-fluorines ($a_{Fß1} = a_{Fß3}$ = 7.2 mT; $a_{Fß2} = a_{Fß4}$ = 1.8 mT; a_{Fa} = 23.8 mT). Tamura, on the other hand, described the spectrum at 77 K as the same double quintet seen at room temperature, only the triplet splitting had widened to 6.1 mT from 3.2 mT at room temperature with fine structure in each line.[9]

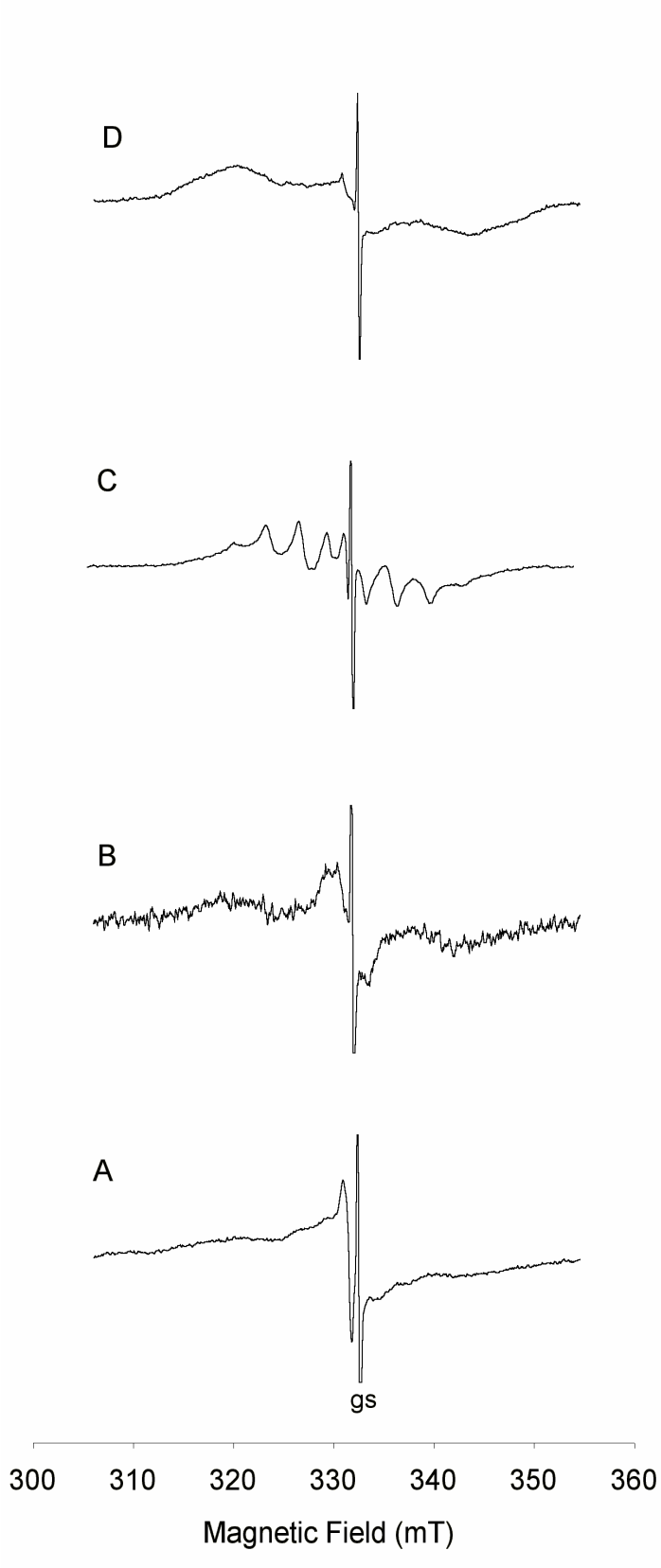

Figure 2.11 ESR spectra of PFA irradiated and acquired at (A) 77 K; (B) annealed and acquired at 170 K; (C) annealed and acquired at 292 K; (D) cooled back to 77 K and acquired at 77 K. The glass signal is indicated by "gs".

Toriyama and Iwasaki[19] examined the end-chain radical at 77 K in orientated PTFE. They observed a sharp central peak with $?H_{pp}$ ~ 1.6 mT parallel to the magnetic field, and a multiplet with width ~ 12 mT perpendicular to the field, as well as minor wing peaks separated by ~ 32 mT. The spectrum in Figure 2.11 A measured at 77 K may be considered to be comprised of a mixture of the signal seen when PTFE was orientated parallel and perpendicular to the field.

The inner sharp component and the shoulders in the spectra in Figure 2.11 of irradiated PFA have been assigned to the end-chain radical (II), which is partially overlapping with the outer broad component which has been assigned to the main-chain radical (I). These assignments were based on the observations made by warming PFA to 292 K after irradiation at 77 K and subsequent cooling back to 77 K, and from the results of Allayrov *et al.*,[28] Tamura,[9] and Toriyama and Iwasaki[19] for radicals in PTFE.

Although no radicals due to scission of bonds at the PPVE units were observed at 298 K, they may be stabilized at 77 K. However, due to the loss of resolution at low temperature, it was difficult to ascertain whether these radicals were present.

During the annealing from 77 K to 292 K the polymer undergoes both relaxation of the side chain (tan *d* maximum at 94 K) as well as a ?-relaxation (tan *d* maximum at 200 K) due to the short chain motion as reported by Starkweather *et al.*[29] In the annealing experiments there was a rapid decrease in the radical concentration above approximately 200 K, presumably due to radical recombination as a result of the short-chain motion.

2.3.5 Radical Yields

Radical yields, $G(R^{\cdot})$, for PFA were calculated from the initial slopes of the plots of radical concentration against dose as shown in Figure 2.6 in Section 2.3.1. $G(R^{\cdot})$ values of 0.93 and 0.16 were calculated for 298 K and 77 K, respectively. The deviation from linearity of the radical yield at higher doses in Figure 2.6 was due to radical recombination as the radical density increased. These values are similar to the corresponding values for FEP of $2.0 \pm 0.1_{(\text{room temperature})}$ and $0.22 \pm 0.1_{(77\ \text{K})}$,[20] but in contrast to the values reported for PTFE where the $G(R^{\cdot})$ at room temperature (0.14) was lower than at 77 K (0.4).[18] This suggested that like FEP, the comonomer in PFA has a dramatic effect on the radical formation especially at ambient temperature.

As is the case with FEP, PFA exhibits three motional transitions below room temperature as measured by dielectric spectroscopy, compared with just one transition for PTFE.[29] The higher chain mobility and lower crystallinity in PFA when compared with PTFE limits the cage recombination at room temperature, resulting in higher radical formation. This was also reflected in the ratio of the end-chain radical (II) to other radicals formed in these fluoropolymers where FEP > PFA > PTFE for comparable doses.

2.4 Conclusions

The radicals identified in irradiated PFA were the same as those found in PTFE, although the end-chain radical was more evident in PFA. While the comonomer in PFA did not cause a large variation in the radical yield when compared with PTFE at 77 K, after irradiation at 303 K the radical yield of PFA was significantly higher. This has been attributed to the greater amount of amorphous content in PFA which helped to limit the cage effect while scission at the PPVE units may also directly contribute to the increased radical yield when compared with PTFE.

2.5 References

1. Battaerd, H. A. J., Tregear, G. W. *Graft Copolymers*; Interscience Publishers: New York, 1967.

2. Zhong, X., Yu, W., Zhang, Y., Sun, J., *Polym. Degrad. Stab.* **40**, 115-116 (1993).

3. Rosenberg, Y., Siegmann, A., Narkis, M., Shkolnik, S., *J. Appl. Polym. Sci.* **45**, 783-795 (1992).

4. Nasef, M. M., Saidi, H., Nor, H. M., Dahlan, K. Z. M., Hashim, K., *J. Appl. Polym. Sci.* **73**, 2095-2102 (1999).

5. Hegazy, E. A., Dessouki, A. M., Rabie, A. M., Ishigaki, I., *J. Polym. Sci. Polymer Chem Ed.* **22**, 3673-3685 (1984).

6. Burger, W., Lunkwitz, K., Pompe, G., Petr, A., Jehnichen, D., *J. Appl. Polym. Sci.* **48**, 1973-1985 (1993).

7. Sun, J., Zhang, Y., Zhong, X., Zhang, W., *Radiat. Phys. Chem.* **42**, 139-142 (1993).

8. Schneider, E. E., *J. Chem. Phys.* **23**, 978 (1955).

9. Tamura, N., *J. Chem. Phys.* **37**, 479-484 (1962).

10. Siegel, S., Hedgpeth, H., *J. Chem. Phys.* **46**, 3904-3912 (1967).

11. Lovejoy, E. R., Bro, M. I., Bowers, G. H., *J. Appl. Polym. Sci.* **9**, 401-440 (1965).

12. Momose, Y., Tamura, Y., Ogino, M., Okazaki, S., Hirayama, M., *J. Vac. Sci. Technol.* **A 10**, 229-238 (1992).

13. Ranby, B., Rabek, J. F. *ESR Spectroscopy in Polymer Research*; Springer-Verlag: Berlin, 1977.

14. Weil, J. A., Bolton, J. R., Wertz, J. E. *Electron Paramagnetic Resonance: Elementary Theory and Practical Applications*; Wiley-Interscience: New York, 1994.

15. Ingram, D. J. E. *Free Radicals as Studied by Electron Spin Resonance*; Butterworths scientific publications: London, 1958.

16. Ayscough, P. B. *Electron Spin Resonance in Chemistry*; Methuen: London, 1967.

17. Lau, S. F., Suzuki, H., Wunderlich, B., *J. Polym. Sci., Polym. Phys. Ed.* **22**, 379-405 (1984).

18. Oshima, A., Seguchi, T., Tabata, Y., *Radiat. Phys. Chem.* **50**, 601-606 (1997).

19. Toriyama, K., Iwasaki, M., *J. Phys. Chem.* **79**, 2919-2924 (1969).

20. Hill, D. J. T., Mohajerani, S., Pomery, P. J., Whittaker, A. K., *Radiat. Phys. Chem.* **59**, 295-302 (2000).

21. Kim, S. S., Liang, R. H. Effects of Ultraviolet and Vacuum Ultraviolet Irradiation on Fluorinated Ethylene-propylene Copolymers. In: *Radiation Effects on Polymers;* Clough, R. L.; Shalaby, S. W. Eds.; American Chemical Society: Washington, 1991; pp. 135-145.

22. Carlson, D. P., Schmiegel, W. Fluoropolymers, Organic. In: *Ullmann's Encyclopedia of Industrial Chemistry*; VCH Verlag: Weinheim, 1998; Vol. A11.

23. Iwasaki, M., Toriyama, K., Sawaki, T., Inoue, M., *J. Chem. Phys.* **47**, 554-559 (1967).

24. Matsugashita, T., Shinohara, K., *J. Chem. Phys.* **35**, 1652-1656 (1961).

25. Rasoul, F. A., Hill, D. J. T., George, G. A., O'Donnell, J. H., *Polym. Adv. Tech.* **9**, 24-30 (1998).

26. Schlick, S., Chamulitrat, W., Kevan, L., *J. Phys. Chem.* **89**, 4278-4282 (1985).

27. Olivier, D., Marachi, C., Che, M., *J. Chem. Phys.* **75**, 3348-3353 (1980).

28. Allayarov, S. R., Mikhailov, A. I., Barkalov, I. M., *High Energy Chem.* **34**, 141-144 (2000).

29. Starkweather, H. W., Avakian, P., Matheson, R. R., Fontanella, J. J., Wintersgill, M. C., *Macromolecules* **24**, 3853-3856 (1991).

Chapter 3

3 Structural Changes in γ-Irradiated PFA: High-Speed MAS ^{19}F NMR

3.1 Introduction

When a polymer substrate is grafted to using the radiation-induced grafting method excess radicals will invariably be formed in the substrate. If a deeply-penetrating form of radiation is used, such as γ-radiation, radicals may be produced in regions below the surface which may be inaccessible to the monomer. Instead of these radicals participating in grafting reactions, they may act as precursors to formation of new structures. The identification of new structures in radiation-treated polymers can be determined using non-destructive techniques such as nuclear magnetic resonance (NMR) spectroscopy and fourier transform infrared (FTIR) spectroscopy.

High-resolution NMR spectroscopy has become a prerequisite for microstructural investigations of polymers. Unfortunately, not all polymers are easily analyzed by NMR spectroscopy. Apart from those which are either soluble or have low viscosity at low temperature, solid-state NMR must be used. In polycrystalline polymers where the molecules have restricted mobility, tensorial NMR interactions such as chemical shift anisotropy (CSA) and dipolar couplings are manifested in broadening of the resonance lines. Advances in solid-state NMR spectroscopy, such as magic angle spinning (MAS) where the sample is spun at high speed along an axis inclined at the magic angle (54.74°) from the direction of the external magnetic field $\boldsymbol{B}_o$, have overcome problems such as chemical shift anisotropy and weak dipole–dipole interactions which permits obtaining a "liquid-like" spectrum for polycrystalline solids. However, fluoropolymers pose the additional problem of strong dipole–dipole interactions from the abundant ^{19}F nuclei leading to severe line-broadening when the experiment is run under standard MAS conditions.

Of the two NMR-active nuclei present in perfluoropolymers, namely ^{13}C and ^{19}F, ^{19}F is the most attractive to study given its 100 % natural isotropic abundance, large magnetogyric ratio and large chemical shift range of about 400 ppm. Observation of the ^{13}C nucleus in fluoropolymers poses difficulties due the small chemical shift range and low natural abundance. Poly(tetrafluoroethylene-*co*-perfluoromethyl vinyl ether) (TFE/PMVE) has been studied by ^{13}C NMR spectroscopy using MAS and cross-polarization (transfer of magnetization from one nuclei to another to improve signal to noise) although the linewidths were broad due to ^{13}C–^{19}F dipolar couplings.[1] Recently, high-resolution ^{13}C NMR spectra of PTFE were reported using rotation-synchronized ^{19}F 180° pulses which refocuses the ^{19}F–^{13}C *J*-couplings but not the dipolar interactions.[2]

The first high-resolution NMR spectrum of a semicrystalline fluoropolymer was reported in 1979 and was not a solid-state spectrum but rather a molten-state spectrum. English and Gaza demonstrated this technique by acquiring well resolved spectra, with linewidths of ~ 300 Hz, for PTFE, FEP and ETFE while in the melt.[3] This method failed to gain popularity due to the specialised equipment necessary to heat samples in the NMR probe to such extreme temperatures and the possibility of thermal degradation of the samples. In addition, since fluoropolymers have the greatest application while in the solid-state, it is desirable to be able to analyse the polymer as a solid and not in the molten form.

In 1986, Maciel and coworkers used a combination of MAS and fast spinning speeds (up to 23 kHz) to average the CSA and dipole–dipole interactions to obtain high-resolution spectra of poly(chlorotrifluoroethylene) (PCTFE).[4] This technique has since gained popularity for the study of other fluoropolymers. Recently, solid-state high-speed MAS ^{19}F NMR has been used to characterize PTFE irradiated at room temperature,[5] PTFE irradiated in the melt,[5,6] and FEP irradiated below and above the T_g.[7]

The effect of temperature and molecular motion in PTFE on the radiation products have received much attention in recent years after the discovery that PTFE could be crosslinked if irradiated in the melt in an inert atmosphere.[8-10] When PTFE is irradiated below the melting temperature, it does not crosslink, either in the amorphous or crystalline regions, presumably due to the lack of mobility of the macro-radicals. During irradiation at low temperature the polymer degrades and the molecular weight decreases to $^{1}/_{10}$ of the

original after just 2 kGy at room temperature or 8 kGy at 77 K. In the molten state crosslinks are able to form in the polymer by combination reactions between the freely moving macro-radicals.[11]

In this chapter high-speed MAS NMR has been used for the first time to investigate the new structures formed in the non-volatile component of PFA after exposure to γ-radiation over the temperature range 303 to 573 K in vacuum, as well as in air at 303 K. The volatile component has been studied using FTIR spectroscopy and mass spectrometry (MS).

3.2 Theory and Technical Aspects

^{19}F NMR spectroscopy of solid, semicrystalline fluoropolymers suffers from severe line broadening effects from two sources under normal conditions, namely dipole–dipole interactions, and chemical shift anisotropy (CSA). Both of these effects can be averaged using a combination of magic angle spinning (MAS) and high-speed spinning.

Of the two sources of line broadening, the most influential are the dipole–dipole interactions. Fluoropolymers have a high concentration of spins due to the 100 % natural abundance of spin ½ ^{19}F nuclei. Perfluorinated polymers do not contain protons and the only other spin ½ nucleus is the isotopically rare ^{13}C nucleus so that almost all of the dipolar interactions are homonuclear between ^{19}F nuclei. In solid samples, unlike liquids or solutions, the dipole–dipole interactions do not average to zero due to the restricted motion. Since the resonance frequency of a particular nucleus depends on the magnetic field at its site, and since the local field due to neighbouring spins varies appreciably from place to place throughout the sample owing to a variation in the orientation of the neighbouring spins, there will be a significant spread in the resonance frequencies. This results in a line broader by several orders of magnitude than a typical line from a liquid sample.

CSA is similar to dipole–dipole line broadening in that it is a result of variation in orientation in polycrystalline samples. Since the chemical shift may depend on the orientation of the molecule with respect to the external magnetic field, the variation in

molecular orientation from crystal to crystal results in a continuous spread in the shifted lines.

The dipole–dipole interactions and CSA can be averaged under MAS orientation when the spinning speeds exceed the strength of the interactions measured in units of frequency. The static linewidth of CF_2 of fluoropolymers is in the order of 20 kHz[12,13] so that a spinning speed in excess of this value is required to achieve full line narrowing. Recent hardware developments by probe manufactures has allowed these speeds to be routinely achieved.

3.3 Experimental

3.3.1 NMR Spectroscopy

PFA (DuPont, code TE 7132 pellets) samples were exposed to γ-radiation at either the Australian Nuclear Science and Technology Organisation (ANSTO) in a pond facility or at the University of Queensland using a 220 Nordian Gammacell. Irradiation at 303 K was performed using a dose rate of 5.9 kGy hr^{-1}, while irradiation at higher temperature was performed using a dose rate of 1.5 kGy hr^{-1}. Samples to be irradiated in vacuum were evacuated at 1×10^{-2} Pa in glass tubes for 24 hours before being sealed. All samples with the exception of the samples irradiated in the presence of air were heated at 473 K after irradiation for 2 hours to remove the majority of the radicals before being opened to the atmosphere. Samples irradiated in the presence of air were not thermally treated after irradiation. All samples were cryogenically milled into powders for NMR analysis.

Single-pulse NMR experiments were performed using a Bruker 300 MHz NMR spectrometer with a H/F-X BL 2.5 probe with the high-frequency channel tuned to ^{19}F, operating at a ^{19}F resonance frequency of 282 MHz. Samples were spun at a frequency of 32 kHz at the magic angle using a 2.5 mm outer diameter rotor. The recycle time used (10 seconds) was long enough to obtain quantitative integrated peak intensities. Spectra were acquired using a p/2 pulse duration of 3 μs. The ^{19}F chemical shifts were reported relative to the CF_2 signal of PTFE at –122 ppm which was externally referenced to $CFCl_3$.

The broad signal due to static fluorine in probe materials was removed using a spline baseline correction algorithm.

Hahn echo experiments were performed using a MSL 300 spectrometer operating at 282 MHz with a Doty Scientific triple-resonance MAS probe. Samples were spun at a frequency of 20.5 kHz at the magic angle using a 4 mm outer diameter rotor. The spin-echo experiment is described by the pulse sequence:

$$p/2 - \tau_D - p - \tau_D - \text{echo}$$

Spectra were acquired using a p/2 pulse duration of 6 μs and a total echo time of 10 ms. The method of referencing and removal of the static fluorine signal was the same as for the single-pulse experiments.

FTIR spectra of the non-volatile component were recorded on a Bio-Rad FTS-155 spectrometer. Samples were prepared by pressing PFA pellets under 4 tonnes of pressure at room temperature. Intensities in the spectra were normalized to the CF_2 backbone overtone at 2365 cm^{-1}.

3.3.2 Analysis of Volatile Products

3.3.2.1 Irradiation

Gaseous products evolved from PFA (DuPont, milled TE 7132 pellets) and PTFE (Aldrich, beads) after irradiation to 350 kGy in vacuum at 303 K were analyzed using FTIR spectroscopy and MS. For both FTIR and MS analysis, the samples (100 mg for each experiment) were evacuated at 1×10^{-2} Pa for 24 hours before being sealed and irradiated. For FTIR spectroscopy analysis, the samples were in small thin-walled ampoules, while for MS analysis, the samples were in Pyrex tubes each fitted with a break seal connected to a B10 adaptor.

3.3.2.2 FTIR Spectroscopy

FTIR spectra were recorded using a Perkin Elmer 1600 series FTIR with a sample cell of dimensions: 150 mm length × 10 mm ID, fitted with KBr discs at each end. Teflon tubing was used to connect the sample cell to a cylinder of argon gas. A small ampoule containing irradiated PFA or PTFE was placed in the tubing as close to the sample cell as possible. The sample cell was flushed with argon gas for 20 minutes before the sample cell and the tubing containing the ampoule was isolated by sealing the tubing using clamps. After acquiring a background spectrum, the ampoule was crushed, allowing the gases produced during irradiation to diffuse into the sample cell. Spectra were acquired at regular intervals after the ampoule was crushed. 32 scans were recorded for each spectrum at a resolution of 4 cm^{-1}.

3.3.2.3 Mass Spectrometry

Mass spectra were recorded using a Balzers ThermoCube MSC200 MS-Cube. Irradiated samples were connected to the MS through a B10 adaptor and a break seal opened using a metal slug inside a glass casing. A secondary electron multiplier detector was used at a voltage of 1000 V. A background spectrum was recorded before opening the break seal and subtracted from the spectra after introduction of the gases to the MS.

3.4 Results and Discussion

3.4.1 Effect of Spinning Speed

High-speed MAS NMR spectroscopy is a relatively new technique. The effect of spinning speed on the NMR spectrum is demonstrated in Figure 3.1 for a sample of irradiated PFA. The narrowing of the lines and spacing of the spinning sidebands of the CF_2 peak at –122 ppm, separated by the spinning speed, can be observed as the dipole–dipole interactions and CSA are averaged. Full assignments of the peaks will be made in Section 3.4.3.1.

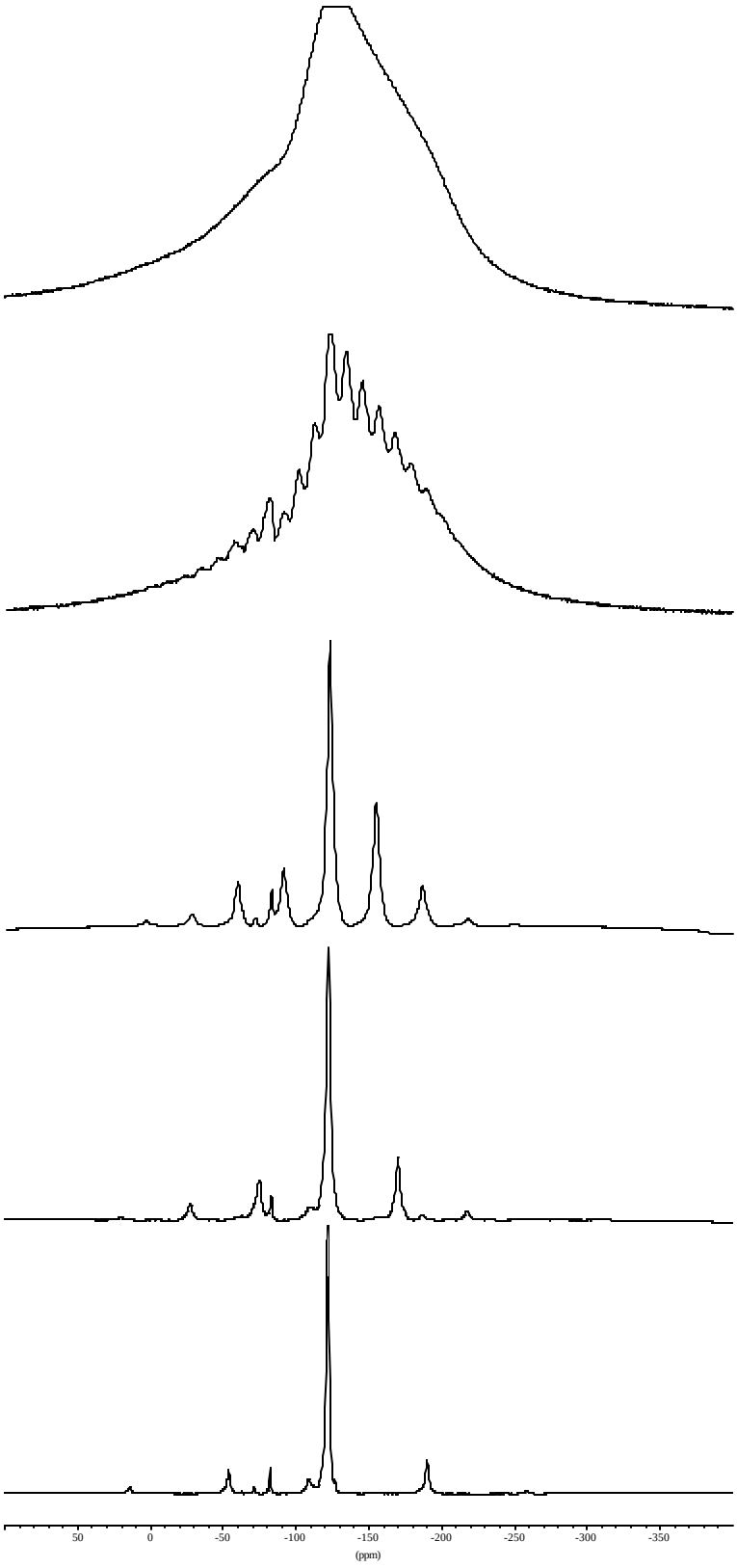

Figure 3.1 Effect of spinning speed. From top to bottom: static; 3 kHz; 9 kHz; 13.5 kHz; 19.5 kHz.

3.4.2 Untreated PFA

The ^{19}F NMR spectrum of untreated PFA shown in Figure 3.2 is dominated by the CF_2 peak at –122 ppm. An expansion of the region between –50 and –210 ppm reveals a number of small peaks due to the comonomer units. Assignments are shown in Table 3.1 which were made according to tables of chemical shifts[14a,b] and on the expected peak area ratios. The perfluoroalkoxy comonomer was identified as perfluoropropyl vinyl ether (PPVE). The fraction of this comonomer was determined from the relative peak area of the PPVE groups to TFE groups. The mole percent of the comonomer in untreated PFA was 1.7 ± 0.2 %.

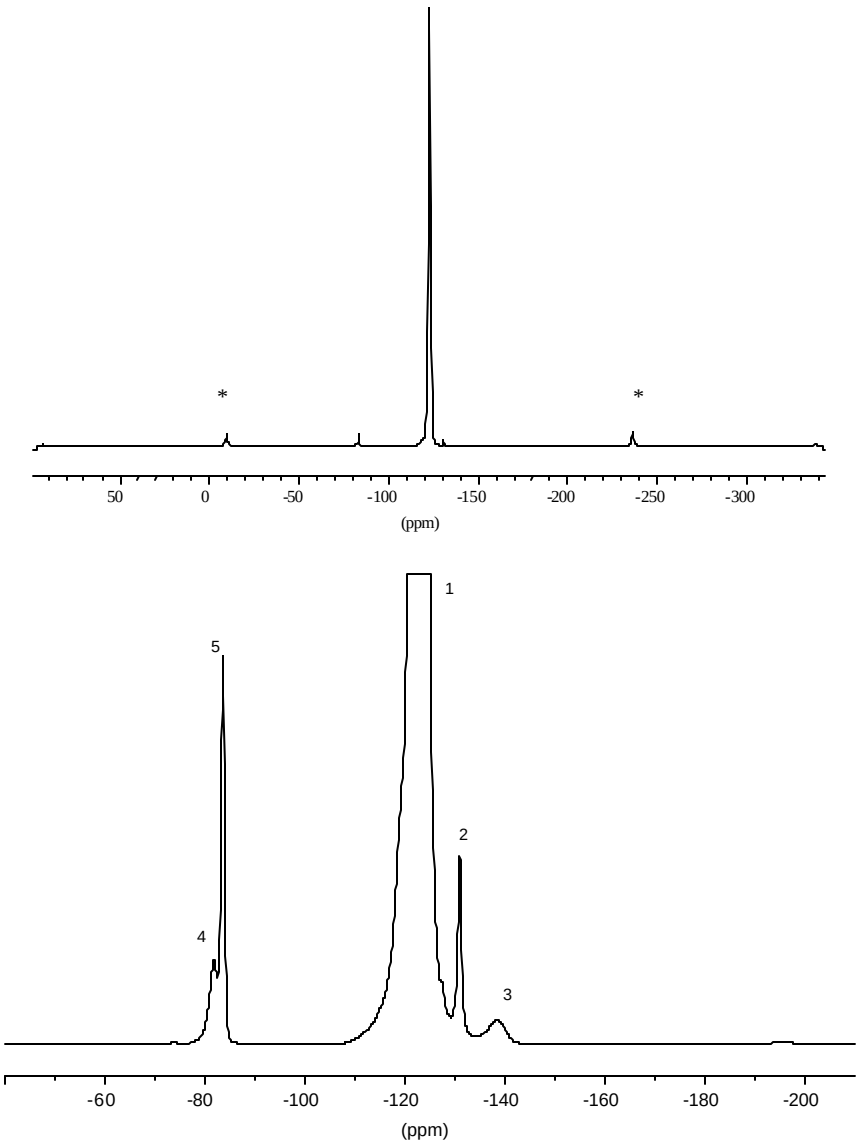

Figure 3.2 High-speed ^{19}F MAS NMR spectrum of PFA. Top: full spectrum; spinning sidebands denoted with an asterisk, Bottom: expansion of –50 to –210 ppm region with 10 times vertical expansion.

Table 3.1 Peak assignments for untreated PFA.

Peak Number	Structure	Chemical shift (ppm)
1	—CF_2–C**F**$_2$–CF_2—	–110 to –129 (centre at –122)
2	~~CF_2–CF(O–CF_2–C**F**$_2$–CF_3)–CF_2~~	–130.9
3	~~CF_2–C**F**(O–CF_2–CF_2–CF_3)–CF_2~~	–138.5
4	~~CF_2–CF(O–C**F**$_2$–CF_2–CF_3)–CF_2~~	–81.8
5	~~CF_2–C**F**$_3$	–83.6

The peak due to perfluoromethyl chain ends would be expected to appear at approximately –83 to –84 ppm,[14c] which would overlap with the peak due to the CF_3 of the PPVE side chains, making them indistinguishable. By comparing the area of the peak at –83.6 ppm with that due to the OC**F**$_2$ group, and taking into account the different number of fluorine nuclei, it was determined whether a portion of this peak was due to perfluoromethyl chain ends. It was found that there was no excess peak area under the peak at –83.6 ppm, therefore, the molecular weight of the untreated material must exceed the uncertainty in the measurement of the CF_3 peak area. This was estimated to be ± 5 % so that the minimum molecular weight of the untreated PFA would be at least 1.2×10^5 g mol^{-1}.

3.4.3 Irradiated PFA

3.4.3.1 Radiolytic Products From TFE Groups

Due to the low probability of addition of PPVE monomer units during synthesis of PFA, it would be expected that the PPVE units would be isolated in the copolymer.[15] Indeed, the NMR spectrum of the untreated material suggests this is the case with no evidence of

sequence effects. Given that the PFA used was composed of 98.3 ± 0.2 mol. % tetrafluoroethylene (TFE) units, the majority of the radiolytic products would be expected to be the same as for PTFE, although the different morphology, glass transition, and crystalline melting temperatures of PFA may be expected to affect the temperature at which various products are formed. Fuchs and Scheler[5] and Katoh *et al.*[6] have both reported the high-speed ^{19}F MAS NMR of irradiated PTFE. Katoh *et al.* used spinning speeds of 12 and 15 kHz, and while at these speeds the spinning sidebands overlapped with the peaks of interest, by using two spinning speeds the spinning sidebands were shifted so that between the two spectra recorded at different speeds most of the isotropic peaks could be observed. Fuchs and Scheler used higher spinning speeds of 35 kHz to remove the spinning sidebands altogether from the region of interest.

When PTFE was irradiated at room temperature, Fuchs and Scheler observed just two new peaks at approximately –82 and –126 ppm, which were attributed to new –C**F$_2$**C**F$_3$** chain ends. For PTFE irradiated in the melt, Fuchs and Scheler[5] and Katoh *et al.*[6] observed a number of new structures which were consistent with branching, including CF_3 side groups and Y-branching points. Chain end structures included CF_3 groups on saturated chain ends, COF end groups, and CF_3 groups adjacent to double bonds. Fuchs and Scheler concluded that PTFE undergoes net crosslinking when irradiated in the melt based on the excess of branch points over chain ends. Katoh *et al.* measured the crosslinking density and *G* values of crosslinking based only on the intensity of the tertiary CF peak, which does not distinguish between crosslinks and long-chain branches.

Figure 3.3 A-D shows the ^{19}F NMR spectra of the non-volatile products of PFA irradiated with γ-radiation to 1 MGy at 303, 473 and 573 K, all in vacuum. The peak assignments are shown in Table 3.2 as well as a comparison with the assignments made by Katoh *et al.* and Fuchs and Scheler for PTFE irradiated in the melt. The major products formed from radiolysis are the same as in PTFE irradiated in the melt, although in different proportions depending on the radiation temperature. Spectra of samples irradiated to other doses (not shown) indicate the same structures, only in different proportions for each respective temperature. The lowest dose used was 0.5 MGy, below which the sensitivity and dynamic range of the NMR experiment were not sufficient to observe any new peaks.

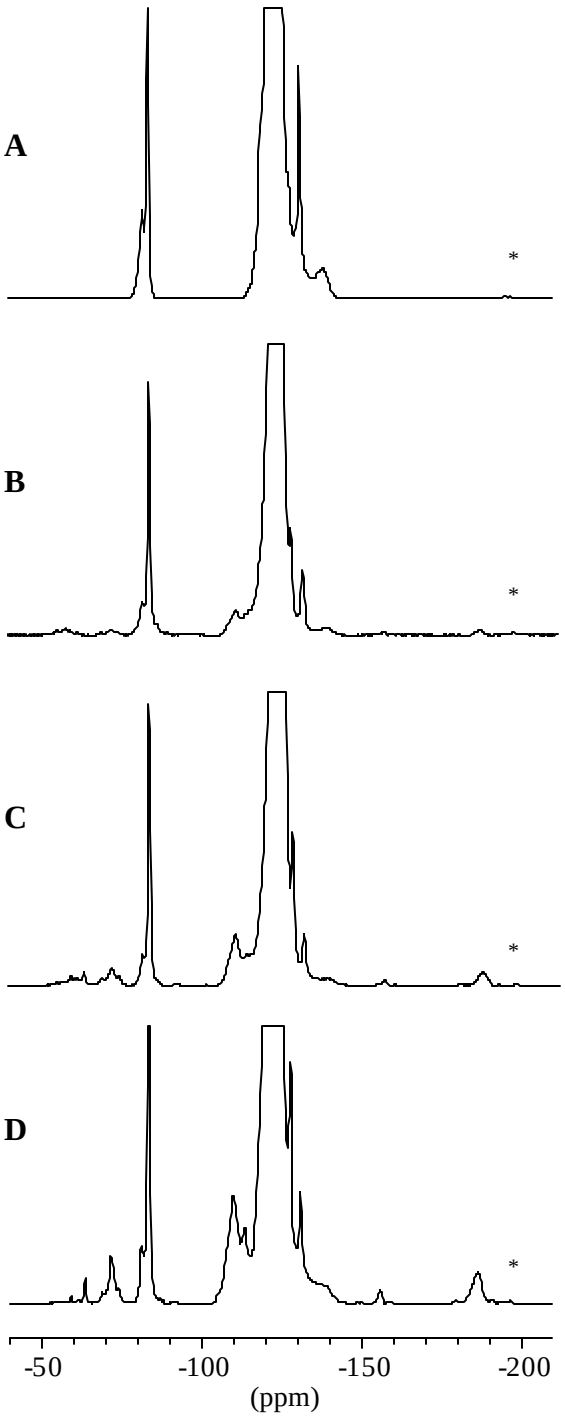

Figure 3.3 ^{19}F MAS NMR of PFA: (A) untreated PFA, (B) irradiated to 1 MGy at 303 K, (C) irradiated to 1 MGy at 473 K, (D) irradiated to 1 MGy at 573 K. Spinning sidebands from the peak assigned to CF_3 groups at –83.6 ppm are denoted by an asterisk.

Table 3.2 Peak assignments for PTFE irradiated in the melt by Katoh *et al.*[11] and Fuchs and Scheler[10] and assignments for new peaks in irradiated PFA.

Structure	Katoh *et al.* PTFE irradiated in melt	Fuchs and Scheler PTFE irradiated in melt	Assignments for PFA irradiated at 303, 473, 573 K
~~CF_2-CF_3	–84	–82	–83.6
~~CF_2-CF_3	–128	–126	–127.6
$-\underset{\vert}{CF}-$	–190	–185	–186.4
$R_f-CF_2-R_f$	–124, –110, –120	–122	–122
$-CF_2-\underset{\vert}{\overset{\vert}{CF}}-CF_2-$ CF_2	not specifically assigned	–108	–109.8
$-CF_2-\underset{\vert}{\overset{\vert}{CF}}-CF_2-$ CF_3	not specifically assigned	–111	–113.3
$-CF_2-\underset{\vert}{\overset{\vert}{CF}}-CF_2-$ CF_3	–72	–72	–68.6 (crystalline) –71.7 (amorphous)
$>CF-CF<$	not resolved	–154	-
R_f R_f $>C=C<$ CF_3 R_f	–59, –60, –62	not assigned	not assigned
$CF_2=CF-CF_2-$	not observed	not observed	–91.6, 108.6
$CF_2=CF-CF_2-$	"	"	–190.9
$CF_3-CF=CF-$ or $(CF_3)_2-CF-$	"	"	–73.5
$R_f-CF=CF-R_f$	"	"	–150.3, –155.7, –158.9

Two new peaks at –71.7 and –68.6 ppm were observed in the spectra in Figure 3.3 B-D. These were assigned to CF_3 side chains in different morphological environments based on their different T_2 relaxation times implied from the Hahn echo experiment shown in Figure 3.4. In the Hahn echo experiment the peaks decreased in intensity compared with the single pulse experiment due to the spin-spin or T_2 relaxation times of the nuclei. More mobile groups, for example chain ends, have longer T_2 times and their respective peaks will decrease in intensity less than peaks attributed to less mobile (shorter T_2 relaxation times) species in the Hahn echo experiment. The peaks over the range –108 to –128 ppm associated with the in-chain methylene CF_2 groups were significantly attenuated relative to the more mobile fluoromethyl peaks. The peak at –68.6 ppm had a shorter T_2 relaxation time than the peak at –71.9 ppm, suggesting that the CF_3 side chain due to the former is less mobile and perhaps incorporated into the crystalline lattices, whereas the latter are due to CF_3 side chains in the more mobile amorphous regions. It has been shown by several authors that CF_3 groups can be incorporated into the crystalline lattice as point defects in FEP.[16-18] The same two peaks have been observed in untreated FEP and the different $T_{1?}$ times measured supporting this assignment.[19]

It is known that the crystallinity of PTFE irradiated in the melt decreases with increasing dose,[10] and as a result of this the appearance changes from opaque to transparent.[20] Although unassigned by Fuchs and Scheler, the spectra of PTFE irradiated in the melt includes a peak at –68 ppm, which decreases in intensity compared to the peak at –72 ppm with increasing dose and crosslinking, supporting the assignment of the peak at –68.6 ppm as being due to CF_3 side chains within the crystal lattices. The same peak was not resolved in the spectra of Katoh *et al.* due to incomplete averaging of dipole-dipole couplings at the lower spinning speeds used. Adjacent to the two CF_3 side chain peaks in the spectra in Figure 3.3 B-D is a peak at –73.5 ppm with very long T_2, suggesting it is due to a structure on the end of a chain – possibly due to either CF_3– groups adjacent to a double bond[14c] or $–CF(CF_3)_2$ groups.[14d]

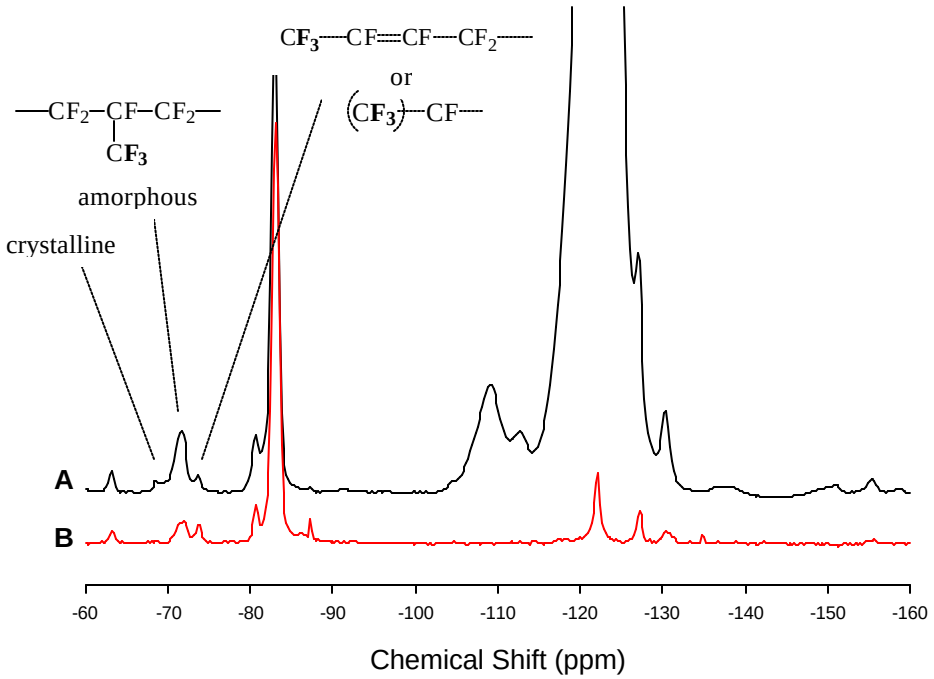

Figure 3.4 Hahn echo experiment of PFA irradiated to 1 MGy at 573 K. (A) Single-pulse experiment; (B) Hahn echo experiment. The spectra were normalized to the peak at –83.6 ppm.

The formation of unsaturated groups in PFA samples irradiated at 473 and 573 K has been confirmed using FTIR spectroscopy (Figure 3.5). The band at 1785 cm^{-1} was attributed to terminal double bonds while bands at 1730 and 1717 cm^{-1} were attributed to internal double bonds.[21,22] Previously, Fisher and Correlli[23] postulated that similar bands between 1735 and 1715 cm^{-1} observed in the IR spectra of irradiated PTFE were due to branching points. However, in this case the assignment by Lappan *et al.*[22] and Lunkwitz *et al.*[21] of these bands as being due to internal double bonds was favoured and is supported by NMR evidence. In addition, it was also observed that the samples irradiated at 573 K changed from translucent to black, suggesting some conjugation of double bonds. Similar observations were made by Tutiya[24] for PFA irradiated under analogous conditions to that used here. To prove that the colour change was due to radiation *and* heat, a control sample was heated at 573 K for a time corresponding to the radiation time and it was found that it did not discolour or reveal any new peaks by NMR spectroscopy.

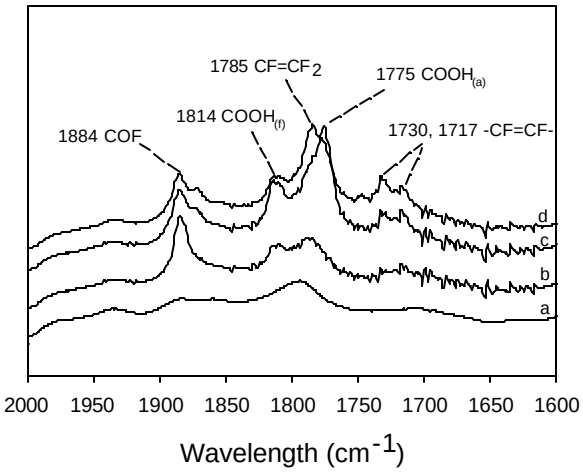

Figure 3.5 FTIR spectra of PFA: (a) untreated, (b) irradiated to 0.5 MGy at 303 K, (c) irradiated to 0.5 MGy at 473 K, (d) irradiated to 0.5 MGy at 573 K. Assignments were made according to Lappan *et al*.,[22] Lunkwitz *et al*.,[21] and Carlson.[25]

In the ^{19}F MAS NMR spectra of PTFE irradiated in the melt, Fuchs and Scheler assigned the peak at –154 ppm to >C**F**–C**F**<, while this peak was not resolved in the spectra of Katoh *et al.* This type of structure seems doubtful due to the unlikelihood of combination of alkyl radicals,[11,26] therefore this peak, as well as peaks at –150.3 and –158.9 ppm in Figure 3.5 B-D, have been assigned to either –C**F**=C**F**–CF_3 or –C**F**=C**F**– groups on the basis of tabulated chemical shifts in the literature.[14c] Observation of the terminal unsaturated group peaks was less ambiguous; the peaks at –91.6 and –108.6 ppm were assigned to the fluoromethylene group, and the peak at –190.9 ppm was assigned to the fluoromethine group of the unsaturated group –C**F**=C**F_2**.[14a]

A number of relatively small peaks in the region –54 to –64 ppm appeared in the NMR spectra of PFA samples irradiated across the temperature range studied. An expansion of this region is shown in Figure 3.6. The most prominent peak in the spectrum of PFA irradiated in air (Figure 3.6 A) in this region is the peak at –57.8 ppm. This was assigned to an oxygenated species, –OC**F_3** on a chain end,[27] which was also seen as a small peak when PFA was irradiated at 303 K under vacuum (Figure 3.6 B). As the irradiation temperature was increased, the proportions of these peaks changed and new peaks at –59.1,

–61.4 and –63.4 ppm became significant. Peaks in this region have also been observed in the spectra of Katoh *et al.* and Fuchs and Scheler for PTFE irradiated in the melt and in FEP irradiated at 300 and 363 K.[7] Attempts to assign these peaks have not been made except by Katoh *et al.* who postulated that the peaks at –59, –60 and –62 ppm are due to a CF_3 group adjacent to a double bond at a branch point.[6] However, in earlier work with fluoro-oligomers Katoh *et al.* assigned peaks with similar chemical shifts to >C=C**F₂** and –C(C**F₃**)$_3$.[28] In this work these peaks cannot be unequivocally assigned at this stage without further data.

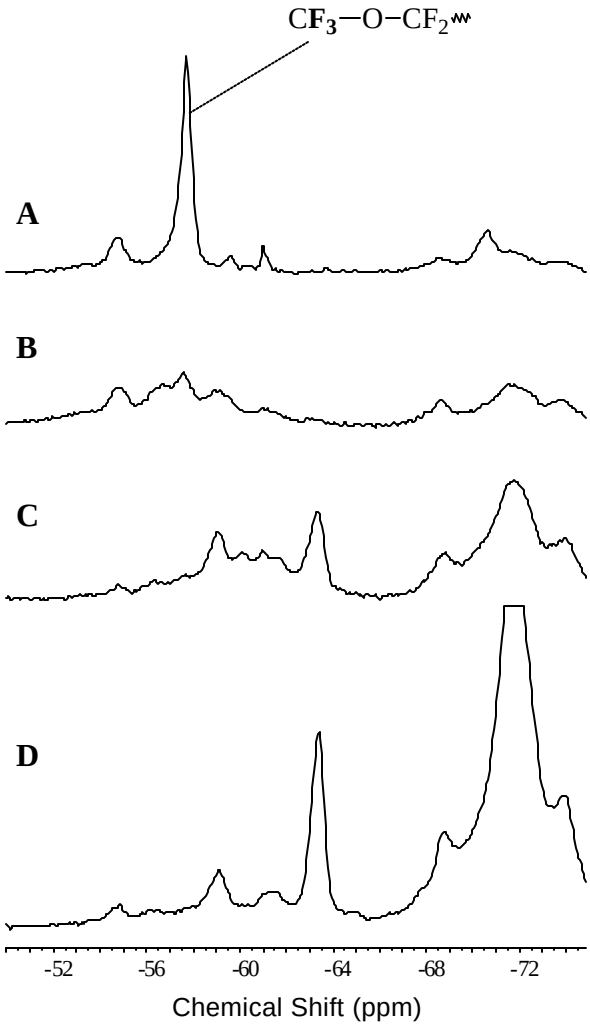

Figure 3.6 ^{19}F MAS NMR of PFA: expansion of the region from –50 to –75 ppm: (A) PFA irradiated to 1 MGy at 303 K in air, (B) PFA irradiated to 1 MGy at 303 K in vacuum, (C) irradiated to 1 MGy at 473 K in vacuum, (D) irradiated to 1 MGy at 573 K in vacuum.

The peak at –186.4 ppm was assigned to C**F** branch points. These will be associated with both the fluoromethyl short branches and longer branches. In Chapter 2 both the main-chain (–CF_2–C$^{\bullet}$F–CF_2–) and end-chain radicals (–CF_2–C$^{\bullet}F_2$) were identified in PFA irradiated in vacuum. Formation of long branches may occur when these two radicals combine. To form short CF_3 side chains, it is postulated that $^{\bullet}CF_3$ radicals or difluorocarbene radicals (**:**CF_2) directly combine with the main-chain radical. The difluorocarbene radical has been postulated as the product of "unzippering" during thermal degradation of PTFE[29] and FEP.[30]

3.4.3.2 Radiolytic Products From PPVE Groups

The products formed from the perfluoropropyl vinyl ether (PPVE) groups in PFA are not as evident as the products from extended sequences of TFE units due to the low amount of PPVE present in the untreated material. The relative peak area of peaks at –138.5, –81.8, and –130.9 ppm decreased with increasing dose at all the temperatures studied, implying that alkoxy side chains were being consumed. Scheme 3.1 shows all the possible products from bond scission at the PPVE units. Peaks due to acyl fluoride groups (pathways 1 and 3) were observed at +23 ppm (not shown) in samples irradiated at 303 K and decreased in intensity with increasing irradiation temperature. Further reaction of the acyl fluoride with atmospheric moisture would form a carboxylic acid group. Due to overlapping signals, no peak due to the –C**F$_2$**COOH group was resolved in the NMR spectra (expected –118 ppm[31]), although –COOH (1775 cm^{-1} (hydrogen-bonded form) and 1814 cm^{-1} (free form)) as well as –COF (1884 cm^{-1}) were observed in the FTIR spectra (Figure 3.5).

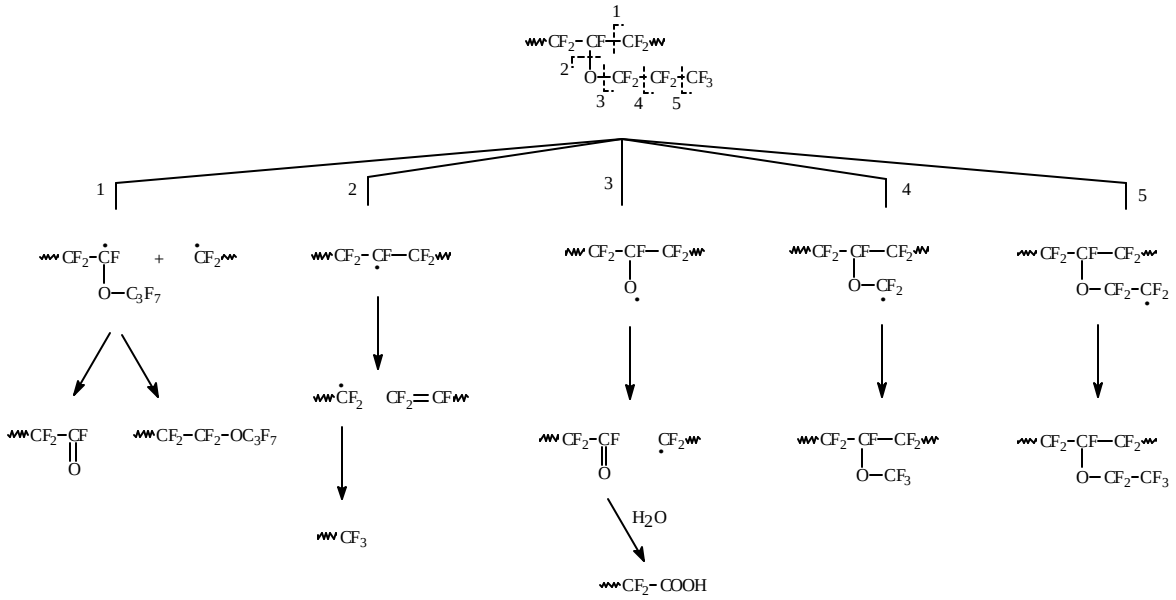

Scheme 3.1 Possible pathways of the PPVE units during radiation treatment of PFA.

Pathways 4 and 5 in Scheme 3.1 would yield methyl ether and ethyl ether side chains, respectively. The expected chemical shift for the methyl ether (–OC**F$_3$**) is –52.4 ppm,[1] while the expect chemical shifts for the ethyl ether are –87.6 and –86.0 ppm[14b,e] for the OCF$_2$C**F$_3$** and OC**F$_2$**CF$_3$ groups, respectively. It was difficult to identify peaks at these chemical shifts above the noise in the single-pulse experiments. In the Hahn echo experiment (Figure 3.4) enhancement of peaks at –87.6 and –86.0 ppm was observed allowing identification of the ethyl ether in small amounts. The enhancement of the ethyl ether peaks in the Hahn echo experiment is indicative of their location in the amorphous regions, as would be expected. Curiously, no –OC**F$_3$** side chain of the methyl ether was seen at –52.4 ppm, suggesting that either pathway 4 is not important or that the methyl ether is not the end product.

3.4.4 *G* Values

The radiation chemical yields for the formation of the new chemical structures were expressed as *G* values, which are the number of new structures formed on the deposition of 16×10^{-18} J (16 aJ or 100 eV) of energy. The *G* values were calculated from plots of the number of new functional groups against dose for PPVE units, short CF_3 side chains, long

branches and CF_3 chains ends (Figure 3.7). Due to overlap of the CF_3 of the alkoxy side chains and new CF_3 chain ends, the fraction of the peak at –83.6 ppm due to new CF_3 end groups was calculated by deconvolution. Fortunately, the peak at –81.8 ppm assigned to OCF_2 groups of the alkoxy side chains was resolved and could be used to calculate how much of the alkoxy CF_3 groups were present based on the 1 : 1 ratio of alkoxy OCF_2 groups to alkoxy CF_3 groups. The peak area due to alkoxy CF_3 groups was calculated from the peak area of the OCF_2 peak at –81.8 ppm, taking into account the different number of fluorine nuclei, then subtracted from the area of the peak at –83.6 ppm. The excess peak area was taken as a measure of the amount of new CF_3 chain ends. The *G* values derived from the initial slopes of the plots in Figure 3.7 are shown in Figure 3.8.

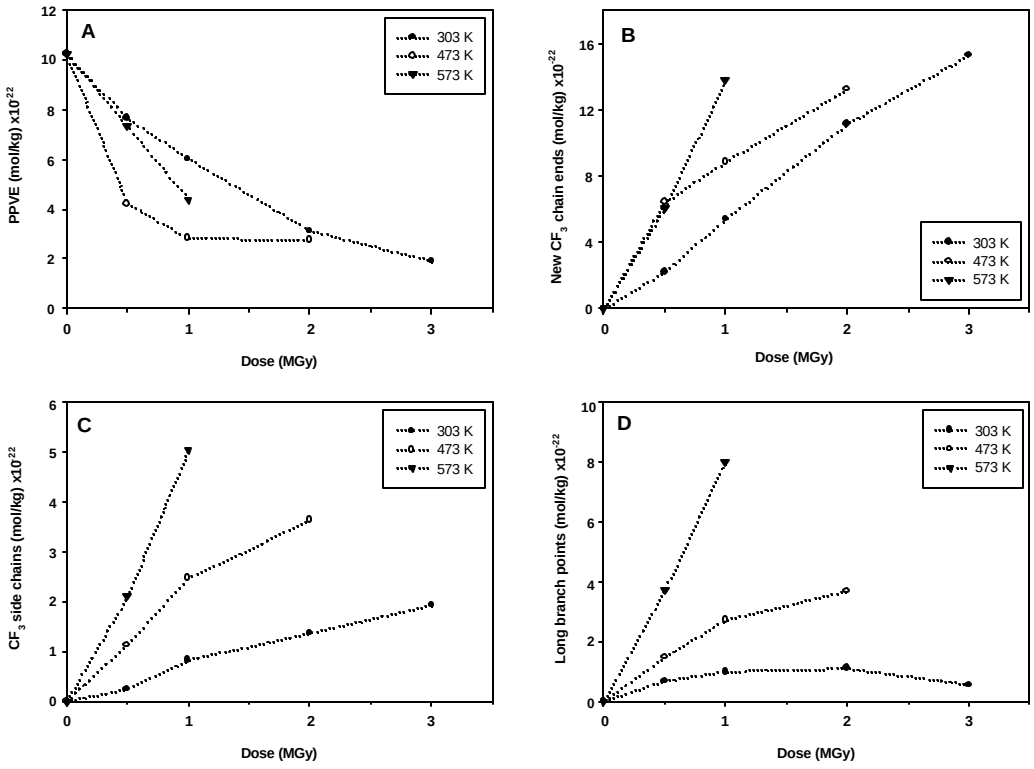

Figure 3.7 New functional groups as a function of radiation dose: (A) PPVE units; (B) new CF_3 chain ends; (C) CF_3 side chains; (D) long branch points. The dotted lines are an aid to the eye only.

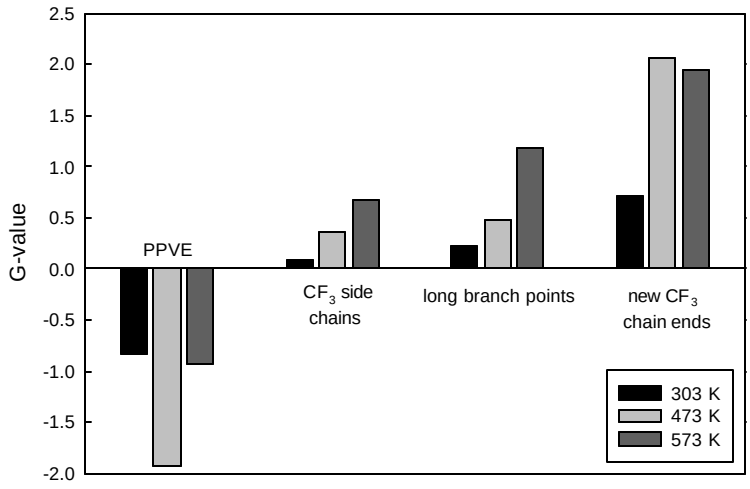

Figure 3.8 *G* values for PPVE, CF_3 side chains, long branch points and new chain ends for irradiation temperatures of 303, 473 and 573 K.

From Figure 3.8 it is clear that the number of branch points increased with irradiation temperature. The relationship between molecular mobility and formation of branches in PTFE has been reported by Tabata *et al.*[11] who postulate that branched structures can only occur when the end-chain and main-chain radicals have sufficient mobility to move freely and combine. In PTFE this only occurs when it is in the molten form. The only new structures identified in PTFE irradiated at room temperature were $–CF_2CF_3$ chain ends,[5] whereas in PFA irradiated at 303 K a small number of structures associated with branching as well as chain ends were observed. The T_g of PFA is 363 K as measured by dynamic mechanical analysis (DMA), although it is a broad transition with the onset at approximately 300 K. The small amount of branched structures identified in the sample irradiated at 303 K was presumably due to an increase in mobility of the amorphous regions at this temperature. At 473 K the PFA is well above the T_g so that the radicals in the amorphous regions could move freely and form branched structures in an analogous manner to the formation of branches in PTFE in the molten state. At 573 K the PFA was at the onset of the crystalline melting transition, permitting additional chain mobility within the crystallites, which led to more branching.

While the NMR spectra showed the existence of branching, it was not clear whether a crosslinked network had been formed or simply a highly branched system. The *G* values

for new CF_3 chain ends were greater than the *G* values for long branch points at each of the temperatures studied. Given the excess of CF_3 chain ends over long branch points, in theory each long branch point could be terminated with a CF_3 chain end at each temperature, resulting in a highly branched, but not crosslinked, system. Between the irradiation temperatures of 473 – 573 K the *G* values for the long branch points increased while the *G* values for new chain ends remained approximately constant. It might be expected that if the irradiation temperature was increased to above the crystalline melting point of 578 K, then the number of long branch points might have exceeded the number of new chain ends. Fuchs and Scheler showed that PTFE irradiated in the melt exhibited an excess of branch points over chain ends, suggesting that not all branches were terminated with CF_3, but some must react with other chains, forming crosslinks.[5]

The system was complicated by the existence of crystalline and amorphous regions and the probable differences in radiation sensitivity between the two phases. It may be that crosslinking predominated in the amorphous regions whereas chain scission dominated in the crystalline regions. However, the probability for cage recombination would be expected to be higher in the crystalline regions than the amorphous regions, due to the facile nature of radical-radical reactions and the lower mobility of the fragments of scission reactions in the crystalline phases. While it was possible to distinguish between some of the peaks in different morphological environments (for example, the peaks due to CF_3 side chains), the chemical shifts of the remaining peaks gave little or no information as to the morphological environments of their assigned structures. One conclusion that can be made is that after irradiation more short branches are formed in the amorphous regions based on more intense $CF_{3(amorphous)}$ side chain peaks at –71.7 ppm compared with the $CF_{3(crystalline)}$ side chain peak at –68.6 ppm.

Figure 3.8 showed a large negative *G* value for PPVE units at all temperatures studied. *G* values for loss of side groups in low density polyethylene with similar branch frequency as for PFA measured using gas chromatography of the volatile products[32] are 2 – 3 orders of magnitude lower than that observed for the PPVE units here. It may be concluded that much of the radiation damage in PFA occurs at the comonomer units, possibly due to the larger free volume and lower cage effect at these units compared with the TFE units.

3.4.5 Analysis of the Volatile Products from Irradiation of PFA

To further investigate the radiation damage to PFA, the volatile products evolved after irradiation of PFA in vacuum at 303 K were measured using FTIR spectroscopy and MS. The identity of the volatile products was of interest for determining the mechanism of decomposition of PFA when exposed to radiation.

The FTIR spectra of the volatile products when PFA and PTFE were irradiated to 350 kGy in vacuum are shown in Figure 3.9. The spectra of the gases evolved from the two polymers after irradiation are significantly different, with the spectra of the PFA gases approximately five times more intense than the spectrum of PTFE, indicating that more volatile compounds are being evolved from the PFA compared with PTFE for the same mass and dose for each polymer. The spectra of the gases evolved from irradiated PFA one minute after admission of the gases from the ampoule into the sample cell, and PTFE gases fifteen minutes after admission were very weak and have been expanded vertically by a factor of two in Figure 3.9. The major band in the spectrum of PTFE gases at 1282 cm^{-1} was due to CF_4 which has also been observed in the FTIR spectrum of the volatile component of irradiated TFE/PFMVE[33] and polyperfluroinated ether liquids[34] formed by cleavage of $^{\bullet}CF_3$ followed by reaction with a fluorine radical. Since PTFE does not contain any side groups, the origin of the $^{\bullet}CF_3$ is most likely to be from the chain ends.

The spectra of PFA gases, like that of PTFE gases, contain a band due to CF_4, but also include a number of other bands in the 1350 to 1000 cm^{-1} region and a band at 1889 cm^{-1}. The spectra observed for PFA and PTFE gases were repeated several times and showed excellent reproducibility. Given the reproducibility and the difference between the PTFE and PFA spectra, it was concluded that the additional peaks observed in the PFA spectra were a product of decomposition of the PPVE units in PFA and not from any other source, such as leakage of air into the system or from oxygen trapped in the polymer.

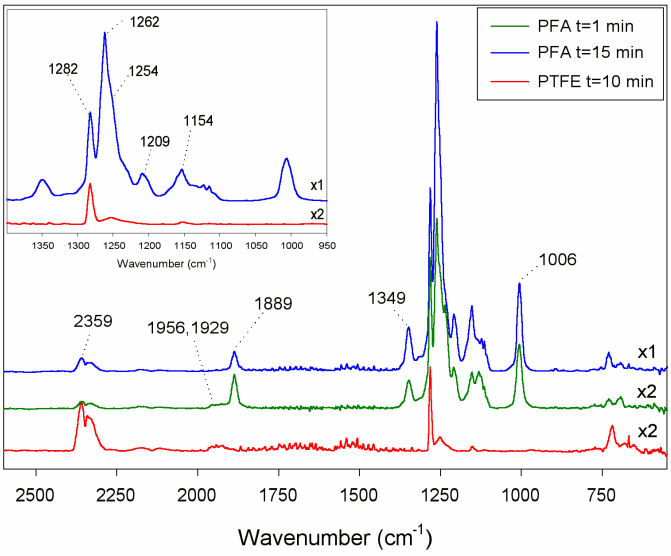

Figure 3.9 FTIR spectra of the volatile products from irradiated PFA and PTFE over the range 2600 to 550 cm^{-1}. The spectra of the volatile products from irradiation of PTFE and PFA after 15 minutes are expanded by ×2. Inset: expansion of the region from 1400 to 950 cm^{-1}.

Possible pathways of the volatile products following cleavage of the alkoxy side chain in PFA are shown in Scheme 3.2. Pacansky found that one of the major products from radiolysis of poly(TFE-*co*-PFMVE) was COF_2 (carbonyl fluoride) formed from loss of $^{\bullet}F$ by $^{\bullet}OCF_3$ fragments of the side chain.[33] The spectra of PTFE and PFA one and 10 minutes after introduction of the gases show some of the bands observed by Pacansky assigned to carbonyl fluoride at 1956, 1929 and 774 cm^{-1}, although in Figure 3.9 the bands are barely above the baseline. The other characteristic carbonyl fluoride bands reported by Pacansky at 1256 and 976 cm^{-1} were indistinguishable from the other intense bands between 1300 and 1100 cm^{-1}. Scheme 3.2 shows how carbonyl fluoride might be formed from decomposition of $C_2F_5CF_2O^{\bullet}$. Fifteen minutes after the gases were introduced from irradiated PFA the identified bands due to carbonyl fluoride were no longer present. Extinction coefficients were not available so a quantitative measurement could not be made.

The other decomposition pathway from $C_2F_5CF_2O^{\bullet}$ in Scheme 3.2 affords the product C_2F_5COF which has carbonyl stretching at 1889 cm^{-1}.[35] The boiling point of C_2F_5COF is approximately 243 K, well below the temperature at which the FTIR measurements were made.[36] The bands at 1254, 1209 and 1154 cm^{-1} are typical of

perfluoroalkane structures,[34] possibly part of C_2F_5COF, $^{\bullet}C_3F_7$ or $^{\bullet}C_2F_5$ (Scheme 3.2), although without authentic samples for comparison, it is difficult to make definitive assignments of these bands. The band at 1006 cm^{-1} is typical of an ether, possibly $C_3F_7OCF_3$ formed from reaction of the radical $C_2F_5CF_2O^{\bullet}$ with a $^{\bullet}CF_3$ radical or with a difluorocarbene radical ($:CF_2$) which was proposed as an intermediate during the thermal decomposition of PTFE,[30] followed by further reaction with a fluorine radical.

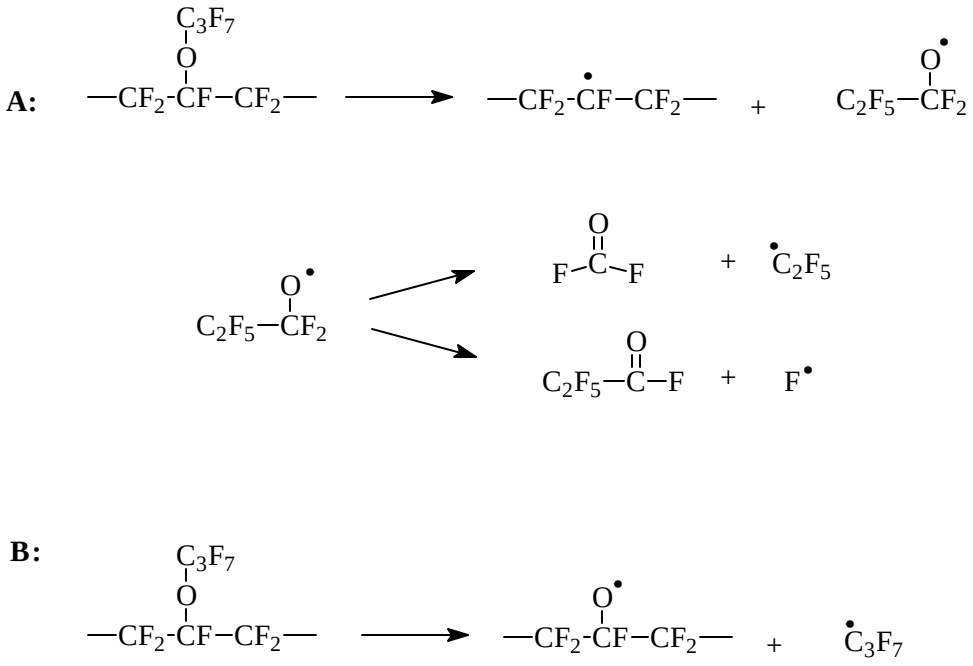

Scheme 3.2 Possible volatile products formed from decomposition of the ether side chain.

The minor band present in all the spectra at 2357 cm^{-1} was supposedly mainly due to CO_2 from the air gap between the sample cell and the laser beam of the spectrometer, however, CO_2 was also identified in the MS which was performed in vacuum. It is possible that CO_2 is formed in the sample from radiolytic decomposition of R–CFO or carbonyl fluoride.[33]

The mass spectrum on the volatile component is shown in Figure 3.10 with possible assignments shown in Table 3.3. Carbonyl fluoride has a cracking pattern which includes ions with masses of 66 (minor) and 47 (major).[37] Both these peaks are present in the mass

spectrum of the volatile products from PFA and are supported by the FTIR data after one minute after opening of the tube. The conditions used for the MS and FTIR spectroscopy were different in that the MS was performed under high vacuum while for the FTIR spectroscopy the sample was introduced at atmospheric pressure, therefore it was not surprising that some compounds clearly present based on the MS data are less apparent in the FTIR spectra, and vice versa.

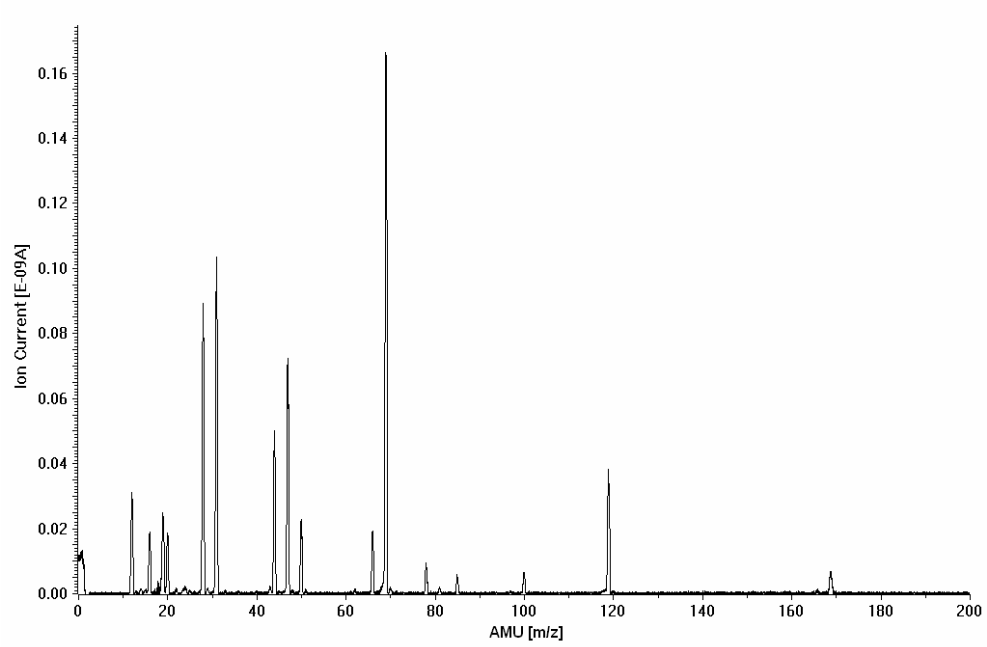

Figure 3.10 Mass spectrum of the gases evolved from PFA irradiated at 303 K to 60 kGy.

Table 3.3 Assignment of the MS.

Peak (in order of intensity)	Assignment
69	CF_3^+
31	CF^+
28	N_2^+
47	OCF^+
44	CO_2^+
119	$C_2F_5^+$
50	CF_2^+
66	OCF_2^+
78	$OC_2F_2^+$
100	$C_2F_4^+$
169	$C_3F_7^+$
85	SiF_3^+ or OCF_3^+
81	$C_2F_3^+$

Other peaks in the MS include fragments from perfluoroalkane structures and oxygen-containing species. It should be noted that many of the volatile products are extremely dangerous and additional care should be taken when handling grafting reactions after being removed from the radiation source.

In summary, the oxygen content of the gas-phase products indicated that scission of the side chain is the major radiolytic reaction leading to volatile products after irradiation of PFA in vacuum at 303 K.

3.5 Conclusions

High-speed MAS ^{19}F NMR has been used to identify non-volatile products in semi-crystalline PFA following γ-irradiation. When PFA was irradiated at 303 K the main process was chain scission, while at higher temperatures formation of short and long branches becomes more prominent as did double bond formation. Perfluoromethyl side chains were identified in two different morphological environments after γ-radiation. The large negative *G* value for the PPVE comonomer suggested that it is highly sensitive to radiation which was confirmed by MS and FTIR spectroscopy of the volatile products after irradiation.

3.6 References

1. Forsythe, J. S., Hill, D. J. T., Logothetis, A. L., Seguchi, T., Whittaker, A. K., *Macromolecules* **30**, 8101-8108 (1997).

2. Liu, S.-F., Schmidt-Rohr, K., *Macromolecules* **34**, 8416-8418 (2001).

3. English, A. D., Garza, O. T., *Macromolecules* **12**, 351-353 (1979).

4. Dec, S. F., Wind, R. A., Maciel, G. E., Anthonio, F. E., *J. Magn. Reson.* **70**, 355-359 (1986).

5. Fuchs, B., Scheler, U., *Macromolecules* **33**, 120-124 (2000).

6. Katoh, E., Sugishwa, H., Oshima, A., Tabata, Y., Seguchi, T., Yamazaki, T., *Radiat. Phys. Chem.* **54**, 165-171 (1999).

7. Forsythe, J. S., Hill, D. J. T., Mohajerani, S., Whittaker, A. K., *Radiat. Phys. Chem.* **60**, 439-444 (2001).

8. Sun, J., Zhang, Y., Zhong, X., *Polymer* **35**, 2881-2883 (1994).

9. Sun, J., Zhang, Y., Zhong, X., Zhu, X., *Radiat. Phys. Chem.* **44**, 655-659 (1994).

10. Oshima, A., Tabata, Y., Kudoh, H., Seguchi, T., *Radiat. Phys. Chem.* **45**, 269-273 (1995).

11. Tabata, Y., Oshima, A., Takashika, K., Seguchi, T., *Radiat. Phys. Chem.* **48**, 563-586 (1996).

12. Dec, S. F., Wind, R. A., Maciel, G. E., *Macromolecules* **20**, 2754-2761 (1987).

13. Scheler, U., *Solid State NMR* **12**, 9-13 (1998).

14. Wray, V. Annual Reports on NMR Spectroscopy*;* Webb, G. Ed.; Academic Press: London, 1980; Vol. 10B; (a) p. 28; (b) p. 93; (c) p. 53; (d) p. 54; (e) p. 22.

15. Hintzer, K., Lohr, G. Melt Processable Tetrafluoroethylene - Perfluoropropylvinyl Ether Copolymers (PFA). In: *Modern Fluoropolymers;* Scheirs, J. Ed.; John Wiley & Sons, 1997; pp. 223-237.

16. Weeks, J. J., Eby, R. K., Clark, E. S., *Polymer* **22**, 1496-1499 (1981).

17. Starkweather, H. W., Zoller, P., Jones, G. A., *J. Polym. Sci., Polym. Phys. Ed.* **22**, 1431-1437 (1984).

18. White, M. L., Waddon, A. J., Atkins, E. D. T., Farris, R. J., *J. Polym. Sci., Polym. Phys. Ed.* **36**, 2811-2819 (1998).

19. Whittaker, A. K., *unpublished results.*

20. Oshima, A., Seguchi, T., Tabata, Y., *Polym. Int.* **48**, 996-1003 (1999).

21. Lunkwitz, K., Lappan, U., Lehmann, D., *Radiat. Phys. Chem.* **57**, 373-376 (2000).

22. Lappan, U., Geissler, U., Lunkwitz, K., *Nuc. Inst. Meth. Phys. Res. B* **151**, 222-226 (1999).

23. Fisher, W. K., Correlli, J. C., *J. Polym. Sci., Polym. Chem.* **19**, 2465-2493 (1981).

24. Tutiya, M., *Jap. J. Appl. Phys.* **11**, 1542-1546 (1972).

25. Carlson, D. P., *US Pat. 3,642,742*, (1972).

26. Tsuda, M., Oikawa, S., *J. Polym. Sci. (Chem.)* **17**, 3759 (1979).

27. Wray, V. Annual Reports on NMR Spectroscopy; Academic Press: London, 1983; Vol. 14; p.22.

28. Katoh, E., Sugimoto, H., Kita, Y., Ando, I., *J. Mol. Struct.* **355**, 21-26 (1995).

29. Errede, L. A., *J. Org. Chem.* **27**, 3425-3430 (1962).

30. Morisaki, S., *Thermochimica Acta* **25**, 171-183 (1978).

31. Ciampelli, F., Venturi, M. T., Sianesi, D., *Organic Mag. Res.* **1**, 281-293 (1969).

32. Bowmer, T. N., Ho, S.-Y., O'Donnell, J. H., *Polym. Degrad. Stab.* **5**, 449-456 (1983).

33. Pacansky, J., Waltman, R. J., Jebens, D., *Macromolecules* **29**, 7699-7704 (1996).

34. Pacansky, J., Waltman, R. J., Jebens, D., Heery, O., *J. Fluorine Chem.* **82**, 85-90 (1997).

35. Carre, D. H., Markowitz, J. A., *Am. Soc. Lubr. Eng. Trans.* **27**, 40-46 (1985).

36. Lappan, U., Fuchs, B., Geissler, U., Scheler, U., Lunkwitz, K., *Polymer* **43**, 4325-4330 (2002).

37. Kupel, R. E., Nolan, M., Keenan, R. G., Hite, M., Scheel, L. D., *Anal. Chem.* **36**, 386-389 (1964).

4 Crosslinking of PFA by High Temperature Electron Beam Irradiation

4.1 Introduction

An implication of the polarity and strength of the C–F bond is that during synthesis of fully-fluorinated polymers, F atom abstraction or disproportionation and branch formation is improbable. PTFE is therefore an inherently linear polymer, although, fluoropolymers containing a small percentage of short-branches have been prepared by incorporation of comonomers with pendant groups to form copolymers such as FEP and PFA. While these copolymers are melt-processable, they essentially still have the properties of linear polymers. Producing fluoropolymers with crosslinked networks offers the possibility of improving the strength, dimensional stability, and resistance to solvents at elevated temperatures of these polymers.[1] In the previous chapter it was shown that branched structures were formed when PFA was treated with γ-radiation at high temperature, although it was not conclusive whether crosslinking occurred. In this chapter the effect of electron beam irradiation on PFA is examined with the aim of forming a crosslinked network.

Since chemical crosslinking of fluoropolymers is not feasible, radiation processing offers the only pathway to formation of a crosslinked network in these polymers and has attracted much attention in the literature. One of the first fully-fluorinated polymers to be crosslinked by high-temperature irradiation was FEP.[1,2] Bowers and Lovejoy observed an increase in the melt viscosity of FEP after it was irradiated under a nitrogen atmosphere at a temperature above the T_g of 353 K. They proposed that the changes observed were caused by an excess of crosslinking reactions over chain scission reactions. When FEP was irradiated above the crystalline melting temperature the melt viscosity decreased, suggesting that the polymer was degrading. These workers also attempted to crosslink PTFE by subjecting it to irradiation above the T_g but below the melting temperature but found that the polymer only degraded. Forsythe *et al.* cast doubt over the conclusions

reported by Bowers and Lovejoy for the observations made when FEP was irradiated. Instead of crosslinking causing the observed increase in melt viscosity, Forsythe *et al.* suggested that perhaps an increase in crystallinity and presence of in-chain double bonds could lead to chain rigidity which would be responsible for the observations.[3]

Other workers have since reported the successful crosslinking of PTFE by irradiation above the crystalline melting point in the absence of oxygen. Using the NMR linewidth as a measure of the crystallinity of irradiated PTFE, Tutiya noticed a correlation between the crystallinity and irradiation temperature. When PTFE was irradiated with γ-radiation below 593 K the crystallinity dropped with increasing temperature, while when the irradiation temperature was above 593 K the crystallinity increased.[4] The same trend of decreasing crystallinity with increasing irradiation temperature was later reported based on DSC measurements.[5] Increases in yield strength and modulus have also been observed when PTFE was irradiated at approx 613 K.[6-8] More recently, with improvements in NMR spinning speeds, solid-state NMR spectroscopy has been used to characterize PTFE crosslinked by electron beam irradiation.[9-11]

No details of the experimental conditions necessary to crosslink PFA could be found in the literature. Sun *et al.* reported in 1993 that they had crosslinked PFA but did not disclose the conditions they used.[12] In the previous chapter it was determined that PFA undergoes net chain scission when irradiated at or below 573 K. Unfortunately, due to limitations in the equipment used, the upper temperature allowable for the irradiation was 573 K so it was not possible to irradiate PFA in the melt with γ-radiation. However, using different heating equipment and electron beam irradiation, higher irradiation temperatures were feasible. In this chapter, PFA is examined using spectroscopic methods after irradiation with electron beams in the melt at 633 K.

4.2 Experimental

4.2.1 Electron Beam Irradiation

PFA pellets (DuPont, code TE 7132) were irradiated using an electron beam accelerator (ELV-2, Budker Institute of Nuclear Physics, Novosibirsk, Russia). The electron energy was 1.5 MeV with a beam current of 2 mA. A transport system was used with conveyor speed of 0.6 m min^{-1} with the irradiation done in steps with a dose of 50 kGy for each pass. The average dose rate was 14.7 kGy min^{-1} and samples were irradiated with total doses of 0.5, 1 and 2 MGy.

Irradiation was performed by placing the PFA pellets in a vacuum vessel and evacuating to a pressure of 4×10^{-2} Pa. The vessel was fitted with a thin metal foil window for electron beam penetration and contained an electric heating device. The vacuum vessel mounted on the conveyor system of the irradiation facility was passed under the electron beam at a speed such that the specimens received a dose calculated to be 50 kGy per pass. Irradiation experiments were carried out at a temperature of 633 ± 2 K measured with a resistance thermocouple in the sample holder. After irradiation the temperature was held at 633 ± 2 K for 20 min then the vessel was filled with nitrogen gas to atmospheric pressure before cooling. The real temperature of the specimens was probably different to the temperature measured with the resistance thermocouple in the sample holder. In order to estimate the temperature difference, a second, non-permanent resistance thermocouple was used for measuring the temperature of the surface of the sample holder at atmospheric pressure in air (open vessel). At 633 K the temperature of the surface measured was approximately 593 K. The real temperature of the surface in vacuum was probably slightly higher because of the decreased heat dissipation to the surrounding atmosphere (reduced pressure).

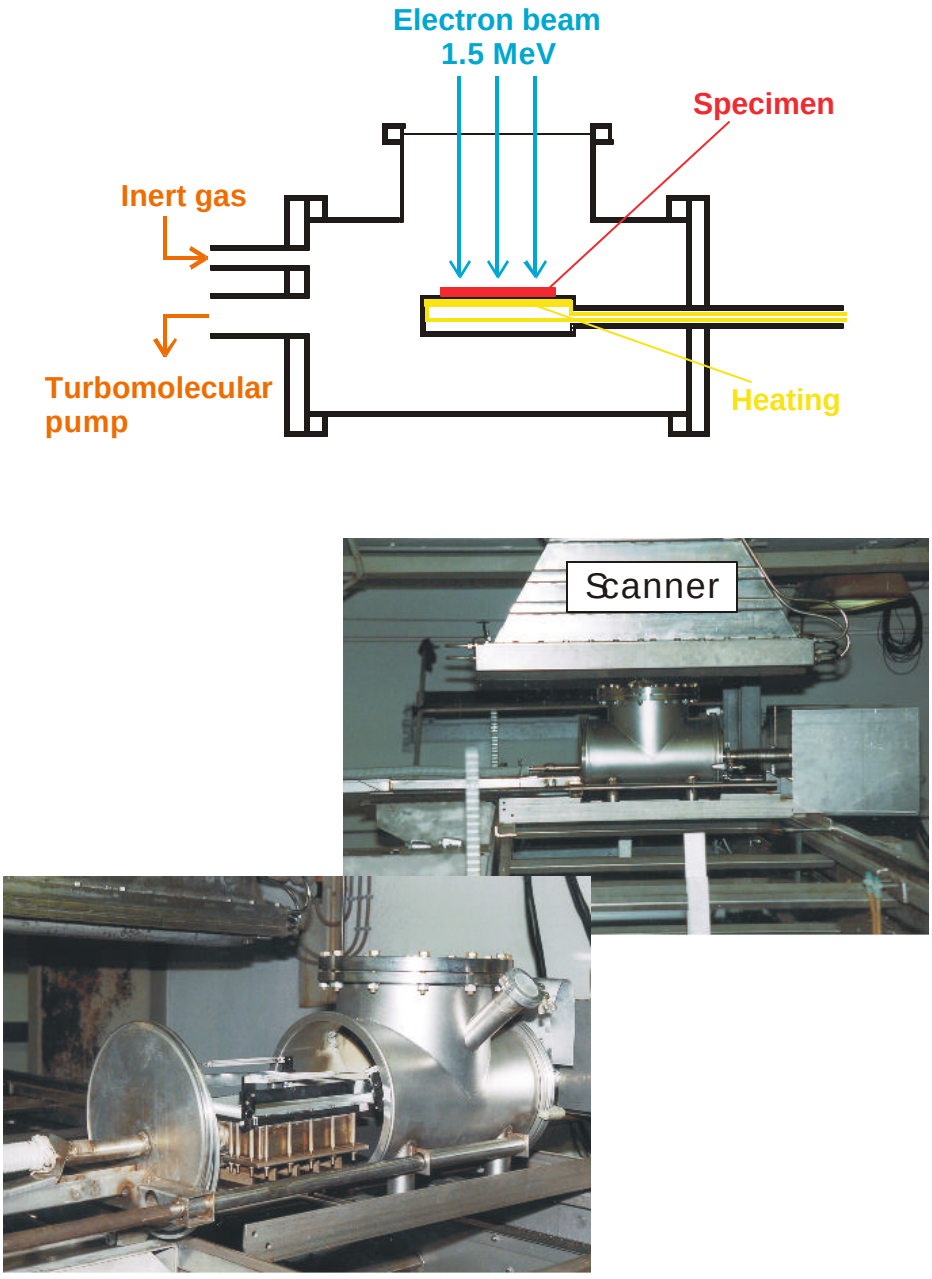

Figure 4.1 Top: Diagram of the chamber used for electron beam irradiation; Middle and Bottom: photographs of the scanner and vacuum chamber (courtesy of Dr Uwe Lappan, IPF).

4.2.2 NMR Spectroscopy

NMR spectroscopy was performed using a Doty probe using the same conditions in Chapter 3, Section 3.1.1.

4.2.3 FTIR Spectroscopy

FTIR spectroscopy was performed using the same conditions in Chapter 3, Section 3.1.1.

4.3 Results and Discussion

4.3.1 NMR Spectroscopy

The untreated PFA used had a crystallinity of 34 ± 3 % and was semi-opaque. After irradiation with electron beams in vacuum at 633 K, the PFA changed in appearance compared to the untreated material. At the doses examined (0.5, 1 and 2 MGy) the samples became progressively less opaque and more transparent with increasing dose. Accompanying the change in appearance was a significant weight loss. At the highest dose examined (2 MGy) the weight loss was 41 % (Figure 4.2). These observations are evidence of dramatic chemical and structural changes of the PFA.

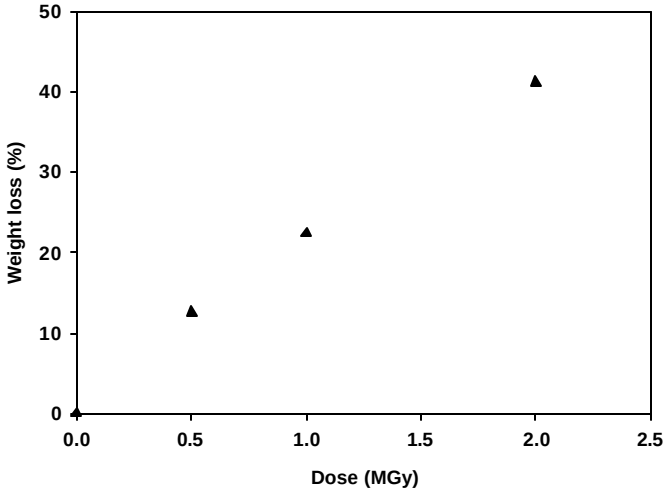

Figure 4.2 Weight loss (measured gravimetrically) of PFA samples irradiated at 633 K with electron beams.

To investigate the chemical changes in electron beam irradiated PFA, high-speed MAS ^{19}F NMR spectroscopy was used. The NMR rotor used had an outer diameter of 2.9 mm and could be spun at a maximum spinning speed of approximately 20 kHz using the equipment available. At this speed the chemical shift anisotropy and dipole interactions were sufficiently averaged so that the linewidths were narrow enough to identify individual peaks, however, the spectra were partially obscured by spinning sidebands. At speeds between 17 and 19.5 kHz there were spinning sidebands overlapping with the >C**F**– region (–180 to –190 ppm). To observe the full spectral range of interest, a second set of spectra were recorded using a slower spinning speed of 13.5 kHz to shift the spinning sideband from the –180 to –190 ppm region.

Examination of the spectra in Figure 4.3 A-F acquired of PFA irradiated to 0.5, 1 and 2 MGy at 633 K, reveals that chain scission and branching reactions are occurring simultaneously at this irradiation temperature. Chain scission is evident from the growth in the peaks at –83 and –127 ppm due to –C**F**$_2$C**F**$_3$ chain ends, while the peak assigned to branch-point fluorine groups (>C**F**–) at –187 ppm also increases in intensity with increasing dose.

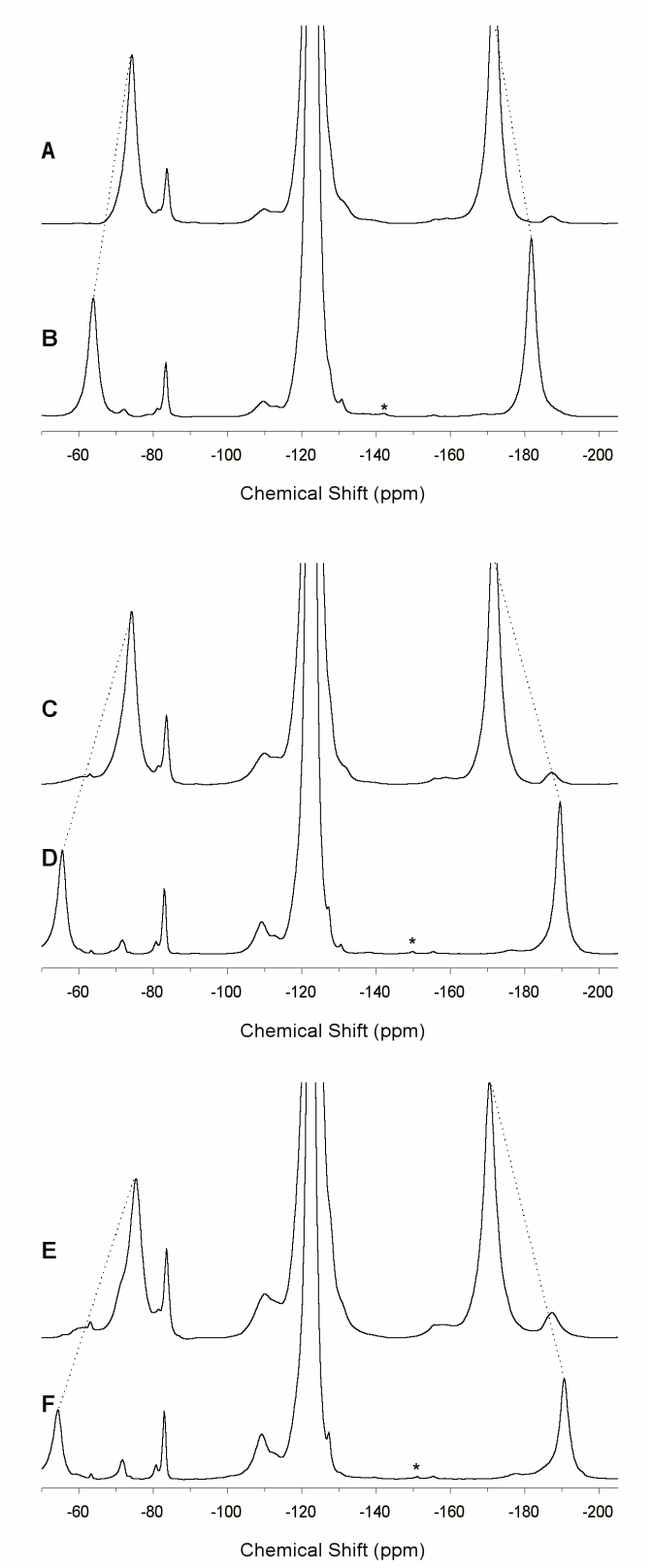

Figure 4.3 HS MAS ^{19}F NMR of PFA irradiated at 633 K in vacuum. (A) 0.5 MGy,13.5 kHz; (B) 0.5 MGy, 17 kHz; (C) 1 MGy, 13.5 kHz; (D) 1 MGy, 19 kHz; (E) 2 MGy, 13.5 kHz; (F) 2 MGy, 19.5 kHz. The movement of the spinning sidebands due to the C**F**$_2$ peak at –122 ppm is indicated by the dashed lines. The asterisk on the peak at –150 ppm denotes the spinning sideband from the peak at –83 ppm.

When PFA was irradiated below the melting temperature, the ^{19}F NMR spectra contained two new peaks due to CF_3 side chains in two different morphological environments (Chapter 3, Section 3.3.5.1). In the spectra of PFA irradiated to 1 and 2 MGy at 633 K, the intensity of the peak at –68 ppm (assigned to CF_3 side chains in the crystalline regions) is negligible (Figure 4.3 D,F). In the spectra of PFA irradiated to 0.5 MGy, this region of the spectra is partially obscured by a spinning sideband at both of the spinning speeds used. The diminishing intensity of the peak at –68 ppm due to CF_3 side chains incorporated into the crystallites can be related back to the changing crystallinity of the samples after irradiation (of course during the irradiation the samples are totally amorphous as they are in molten form). Formation of long branches can hinder crystal formation and lower the overall crystallinity. In Chapter 5, it is shown that when PFA is irradiated at 633 K, the overall crystallinity dropped significantly after irradiation. After a dose of 2 MGy, the crystallinity was just 18 %, almost half the crystallinity of the untreated material, so that there were fewer crystalline regions in which the CF_3 side chains can be incorporated.

Less intense peaks in the spectra in Figure 4.3 A-F not obscured by spinning sidebands include one at –155 and one at –73 ppm. These peaks were also observed in similar intensity in the spectra of PFA irradiated at 473 and 573 K (Chapter 3) and can be assigned to either C**F**$_3$–CF=CF– or (C**F**$_3$)$_2$–CF– for the peak at –73 ppm, and –C**F**=C**F**– for the peak at –155 ppm. All assignments for the spectra acquired on PFA samples irradiated at 633 K are presented in Table 4.1.

Table 4.1 Assignments of new peaks observed in the ^{19}F NMR spectra of PFA after irradiation at 633 K.

Structure	Chemical shift (ppm)
~~CF_2–$\mathbf{CF_3}$	–83
~~$\mathbf{CF_2}$–CF_3	–127
—CF_2–$\underset{\underset{\mathbf{CF_3}}{\vert}}{CF}$–$CF_2$—	–71 (crystalline), –68 (amorphous)
—$\mathbf{CF_2}$–$\underset{\underset{CF_3}{\vert}}{CF}$–$\mathbf{CF_2}$—	–113
—$\mathbf{CF_2}$–$\underset{\underset{\mathbf{CF_2}}{\vert}}{CF}$–$\mathbf{CF_2}$—	–109
—$\underset{\vert}{\mathbf{CF}}$—	–187
R_f—$\mathbf{CF}$=$\mathbf{CF}$—R_f	–155
$\mathbf{CF_3}$—CF=CF— or $(\mathbf{CF_3})_2$—CF—	–73

4.3.2 FTIR Spectroscopy

The FTIR spectra of PFA, irradiated at 633 K (Figure 4.4), and PTFE irradiated in the melt[13-16] showed many of the same structures. Bands include internal and terminal double bonds (1785, 1730 and 1717 cm^{-1}), double bonds at branch points (–CF=C<) (1671 cm^{-1}) (only seen at 2 MGy), as well as oxygen-containing end groups such as –COF and –COOH (1884, 1814, 1775 and 3557 cm^{-1} (not shown)). A list of the assignments is shown in Table 4.2. The oxygen-containing species were initially thought to originate from the cleavage of the ether group of the alkoxy side chain since no oxygen would have been available as the irradiation was carried out in vacuum. After irradiation, the samples were checked for residual radicals which may have reacted with oxygen in the air, but it was found that no

radicals were present. This suggested that the oxygen-containing species must originate from the ether group of the side chain. However, when PTFE was irradiated under almost identical conditions by Lappan and coworkers, –COF and –COOH end groups were also observed in the FTIR spectra.[14,16] This was attributed to either trace amounts of oxygen in the vacuum or oxygen dissolved in the polymer. If –COF and –COOH groups can form in PTFE, which does not contain any bonded oxygen, when irradiated under almost identical conditions to those used here, then it may be possible that the source of the oxygen in PFA is not exclusively the oxygen of the ether group in the alkoxy side chain.

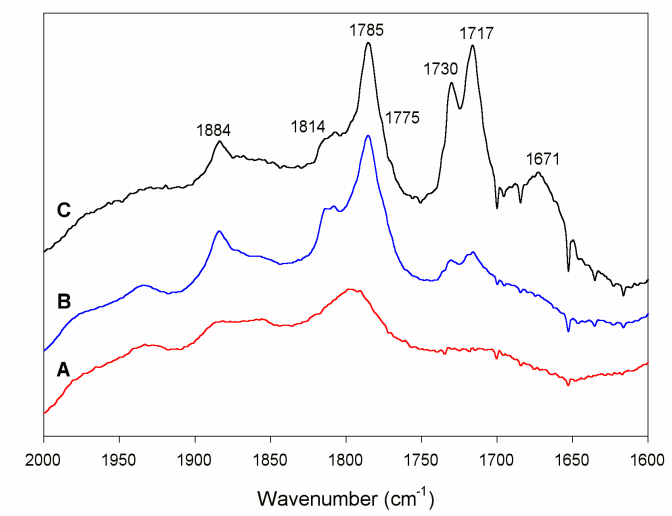

Figure 4.4 FTIR spectra of (A) untreated PFA; (B) PFA irradiated to 0.5 MGy at 633K; (C) PFA irradiated to 2 MGy at 633K.

Table 4.2 Assignments of bands in the FTIR spectra of PFA irradiated in vacuum at 633 K.

Band (cm^{-1})	Assignment	Reference
1671	-CF=C<	13-17
1730, 1717	-CF=CF-	"
1785	$-CF=CF_2$	"
1814	-**CO**OH (free)	16-18
1884	-**CO**F	"
1775 (shoulder)	-**CO**OH (associated)	18,19
3100 (not shown)	-CO**OH** (associated)	18
3557 (not shown)	-CO**OH** (free)	18

4.3.3 *G* Values of Crosslinking

The proportion of crosslinks in PTFE irradiated in the melt have been reported by Katoh *et al.* and also by Scheler and coworkers.[9-11] Unfortunately, the results cannot be directly compared as each group of workers have different definitions of what constitutes a crosslink. Scheler and coworkers define a crosslink as a long branch which meets with another main chain. This type of crosslink may be considered to be a "pseudo" H-type crosslink. A "real" H-type crosslink is formed when two main-chain radicals on adjacent molecules react to form a single-bond crosslink between the two chains.[20] H-type crosslinks are generally observed in polyolefins, but have a low probability of being formed in crosslinked PTFE and FEP due to the difficulty in alkyl radicals combining.[21-23] The crosslinks Scheler and coworkers describe are H-type in shape but are formed through many bonds ($–CF_2–CF_2–CF_2–$ chains) between the main chains. They calculated the proportion of crosslinks as the difference between the number of long branch points and chain ends and stated that it was an estimate of the lower bound of crosslinking. At low dose, they reported that short and long branches were formed, while at high dose the long branches reacted with radicals formed on neighbouring chains to form a crosslink between the two chains.[11]

Katoh *et al.* define a crosslink as any type of branch point or Y-type crosslink, perhaps erroneously including CF_3 side chains as crosslinks. They reported the crosslink density as simply the number of tertiary CF groups as a fraction of the total number of CF, CF_2 and CF_3 groups. The *G* value of crosslinking was then calculated by converting the crosslink density to moles then expressing this as the number of crosslinks per 100 eV of energy input into the polymer. In this way they report a *G* value for crosslinking ($G(X)$) for each dose from 0 to 10 MGy. $G(X)$ passes through a maximum at 2 MGy indicating that at this dose the increase in crosslinking density was at its greatest. Above this dose, the crosslinking may be expected to hinder chain mobility and limit any subsequent crosslinking.

Fuchs and Scheler[10] reported the relative content of crosslinks, branches and CF_3 side chains over the dose range 0.5 to 3 MGy. While they did not report the relative content of the chain ends, it could be calculated from the difference between long branches and

crosslinks. The calculated *G* values for crosslinking, chain ends, and short and long branches are compared with the results obtained for PFA in Table 4.3.

Table 4.3 Comparison of the *G* values for formation of functional groups in irradiated PFA (633 K) and PTFE (638 K).

	PFA	PTFE (Fuchs and Scheler[10])
PPVE	–6.0	n.a.
New chain ends	1.4	2.0
CF_3 side chains	0.4	1.2
Long branch points	1.6	2.4
Crosslinks	0.2	0.4

The large negative *G* value for the PPVE groups indicated that the perfluoropropyl ether side chains were being cleaved very efficiently during the irradiation of PFA. Possible non-volatile products from cleavage of the CF–O–C bonds of the perfluoroalkoxy side chains are shown in Scheme 4.1. If the PPVE groups were cleaved according to the mechanism shown in pathway A, then a main chain radical and a small fragment would be formed. The latter would have been lost since the irradiation was performed under high vacuum. The alternative mechanism shown in pathway B results in an oxy radical being formed which would likely undergo rearrangement to form an acyl fluoride and a new chain end.[24,25] If the main pathway was pathway B, then the *G* value for new chain ends would be expected to be at least as large as the *G* value for loss of PPVE units. Since the *G* value for new chain ends (1.5) is much less than the *G* value for loss of PPVE groups (6.0), it suggests that pathway A is more likely than pathway B for the loss of PPVE groups. In support of this, the *G* value for new chain ends in irradiated PFA (1.5) is not significantly different than for irradiated PTFE (2.0) which does not contain any alkoxy side chains.

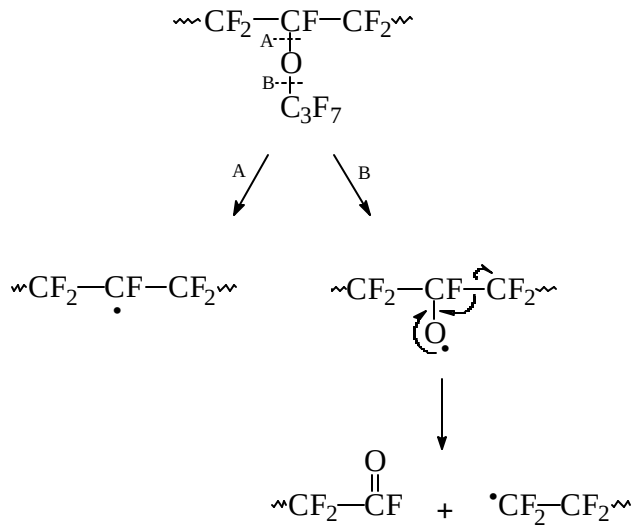

Scheme 4.1 Possible non-volatile products from cleavage of the C–O bonds of the alkoxy group of PFA.

The amount of branching, both long and short side chains, was less in PFA than in PTFE as indicated by the higher *G* values for CF_3 side chains and long branch points for PTFE compared with PFA (Table 4.3). It should be noted that in their measurement of CF_3 side chains, Fuchs and Scheler[10] included structures such as >C=C(C**F**$_3$)– which were assigned to a number of small peaks in the region –55 to –65 ppm. In the spectra of PFA this region was obscured by spinning sidebands so it could not be measured. Interference from the spinning sidebands with other peaks was also problematic in the measurement of peak areas. The peaks at –71 ppm and –187 ppm (Figure 4.3 B,D,F) assigned to C**F**$_3$ side chains and >C**F**– groups, respectively, were partially obscured by spinning sidebands. This led to a certain degree of error in the measurements of the peak areas making it difficult to compare the absolute *G* values of branching for PFA with PTFE. In addition to this, Fuchs and Scheler used an irradiation temperature 5 K higher than what was used for PFA. This temperature difference may also explain the differences in the amount of branching in the two polymers. Despite the small discrepancies between the experimental conditions and measurement of the peak areas used to derived the *G* values, it is clear that these *G* values for branching in PFA and PTFE are of the same order of magnitude.

The *G* value for crosslink formation in PFA in Table 4.3 was calculated by subtracting the number of chain ends from the number of long branch points. The value

obtained, 0.2, is less than that of PTFE reported by Fuchs and Scheler but is still a positive value, indicating that crosslinking was the net process.

4.4 Conclusions

PFA has been crosslinked using electron beam irradiation at 633 K in vacuum. This conclusion is based on the observation that the polymer lost most of its crystallinity based on the change in appearance from opaque to transparent after irradiation, and on NMR spectroscopy data showing an excess of branch points over chain ends, implying net crosslinking. The results in this chapter are complementary to the results in Chapter 3, proving that, under the correct choice of conditions, net crosslinking of PFA can be achieved.

4.5 References

1. Bowers, G. H., *US Pat. 3116226*, (1963).

2. Bowers, G. H., Lovejoy, E. R., *I&EC Product Research and Development* **1**, 89-92 (1962).

3. Forsythe, J. S., Hill, D. J. T., Mohajerani, S., Whittaker, A. K., *Radiat. Phys. Chem.* **60**, 439-444 (2001).

4. Tutiya, M., *Jap. J. Appl. Phys.* **11**, 1542-1546 (1972).

5. Oshima, A., Ikeda, S., Kudoh, H., Seguchi, T., Tabata, Y., *Radiat. Phys. Chem.* **50**, 611-615 (1997).

6. Oshima, A., Tabata, Y., Kudoh, H., Seguchi, T., *Radiat. Phys. Chem.* **45**, 269-273 (1995).

7. Sun, J., Zhang, Y., Zhong, X., *Polymer* **35**, 2881-2883 (1994).

8. Sun, J., Zhang, Y., Zhong, X., Zhu, X., *Radiat. Phys. Chem.* **44**, 655-659 (1994).

9. Katoh, E., Sugishwa, H., Oshima, A., Tabata, Y., Seguchi, T., Yamazaki, T., *Radiat. Phys. Chem.* **54**, 165-171 (1999).

10. Fuchs, B., Scheler, U., *Macromolecules* **33**, 120-124 (2000).

11. Fuchs, B., Lappan, U., Lunkwitz, K., Scheler, U., *Macromolecules* **35**, 9079-9082 (2002).

12. Sun, J., Zhang, Y., Zhong, X., Zhang, W., *Radiat. Phys. Chem.* **42**, 139-142 (1993).

13. Oshima, A., Ikeda, S., Katoh, E., Tabata, Y., *Radiat. Phys. Chem.* **62**, 39-45 (2001).

14. Lappan, U., Geissler, U., Lunkwitz, K., *J. Appl. Polym. Sci.* **74**, 1571-1576 (1999).

15. Lappan, U., Geissler, U., Lunkwitz, K., *Radiat. Phys. Chem.* **59**, 317-322 (2000).

16. Lappan, U., Geissler, U., Lunkwitz, K., *Nuc. Inst. Meth. Phys. Res. B* **151**, 222-226 (1999).

17. Lunkwitz, K., Lappan, U., Lehmann, D., *Radiat. Phys. Chem.* **57**, 373-376 (2000).

18. Fischer, D., Lappan, U., Hopfe, I., Eichhorn, K.-J., Lunkwitz, K., *Polymer* **39**, 573-582 (1998).

19. Fisher, W. K., Correlli, J. C., *J. Polym. Sci., Polym. Chem.* **19**, 2465-2493 (1981).

20. Hill, D. J. T., Lewis, D. A., O'Donnell, J. H., Whittaker, A. K., *Polym. Adv. Tech.* **9**, 45-51 (1998).

21. Tsuda, M., Oikawa, S., *J. Polym. Sci. (Chem.)* **17**, 3759 (1979).

22. Tabata, Y., Oshima, A., Takashika, K., Seguchi, T., *Radiat. Phys. Chem.* **48**, 563-586 (1996).

23. Zhong, X., Sun, J., Wang, F., Sun, Y., *J. Appl. Polym. Sci.* **44**, 639 (1992).

24. Pacansky, J., Waltman, R. J., Jebens, D., *Macromolecules* **29**, 7699-7704 (1996).

25. Forsythe, J. S., Hill, D. J. T., Logothetis, A. L., Seguchi, T., Whittaker, A. K., *Radiat. Phys. Chem.* **53**, 657-667 (1998).

Chapter 5

5 The Thermal Properties of Irradiated PFA

5.1 Introduction

The thermal properties of PTFE indicate that it is a linear, non-branched, non-crosslinked polymer.[1] When polymerized, PTFE has a high degree of crystallinity and melts at high temperature over a narrow temperature range. The polymer is stable up to 723 K but when heated further a single step weight-loss profile is observed by thermal gravimetric analysis.[2] If PTFE is crosslinked by exposure to radiation while in the molten form, the melting temperature and crystallinity drop due to hindrance of chain packing in the network structure.[3] The polymer is also less thermally stable after crosslinking and decomposes in two steps as a result of the low molecular weight component which is a product of radiation-induced scission.[4]

When TFE is copolymerized with HFP to form FEP, or with PPVE to form PFA, the melting temperatures and crystallinity of the resulting copolymers are lower than for PTFE. FEP with 12 % HFP incorporated melts at 535 K while PFA has a slightly higher melting temperature due to the lower concentration of the comonomer used.[5]

At temperatures close to room temperature PTFE undergoes two crystal-crystal transitions, corresponding to the triclinic-hexagonal and hexagonal-pseudohexagonal transitions. FEP and PFA exhibit just one transition in this low temperature region, although in the case of FEP the transition becomes broad and difficult to detect if the comonomer concentration is high.[5,6]

Thermal analysis of FEP and tetrafluoroethylene-*co*-perfluorovinyl ethers has been used to examine the incorporation of comonomer side-chains into the crystallites. Pucciariello and coworkers observed that the melting temperatures of FEP copolymers quenched from the melt were higher than the melting temperatures of perfluorovinyl ether copolymers with similar amount of comonomer. They considered this as evidence for the

incorporation of perfluoromethyl side chains into the homopolymer crystal lattice as point defects and exclusion of larger perfluoroalkoxy side chains.[7-11] X-ray diffraction studies also support these finding.[12-15]

While the thermal properties, particularly the melting transitions, of PTFE and crosslinked PTFE have been widely studied, however the same is not true for PFA. In this chapter the thermal properties of untreated PFA and PFA irradiated over a wide temperature range are examined. The mechanical properties of PFA irradiated at 303 K are also examined with the view of determining the maximum allowable limits of radiation exposure for subsequent grafting reactions.

5.2 Experimental

5.2.1 Radiolysis

The samples used were the same as in Chapters 3 and 4.

5.2.2 Thermal Analysis

Dynamic mechanical analysis (DMA) was performed using a Perkin Elmer DMA 7 over the temperature range 303 to 473 K. The sample used was a ring from a Mimotopes lantern injection moulded from PFA pellets (DuPont, code TE 7132) and had a thickness of 0.486 mm. Parallel plates were used with a static force of 100 mN and a dynamic force of 83 mN at a frequency of 1 Hz.

Differential scanning calorimetry (DSC) was performed using a Perkin Elmer DSC 7. All runs were performed on 10 ± 0.5 mg samples in a nitrogen atmosphere. Samples were weighed both before and after analysis to check for weight-loss due to decomposition during the DSC runs. It was found that in all cases the difference in weight before and after analysis was less than 2 % and was ignored for the calculation of the heat of fusion. The apparatus was calibrated using the onset of melting of indium (429.6 K) and zinc (692.47 K) and the heat of fusion of indium (28.45 J g^{-1}). Before each run the baseline

was optimized in the range of interest and later subtracted from the corresponding calorimetric curve.

Samples crystallized by uniform cooling were first heated to 613 K and held at this temperature for 10 minutes. Subsequent cooling and heating scans were performed at 40 K min^{-1}. Isothermal crystallizations were carried out in the DSC instrument in a nitrogen atmosphere by holding the sample at 613 K, then rapidly cooling using the maximum cooling rate of the instrument (approximately 400 K min^{-1}) to the selected crystallization temperature and holding at that temperature for 30 minutes. The samples were then cooled to 323 K at 20 K min^{-1} then heated to 613 K at 20 K min^{-1} to measure the melting endotherm. Melting temperatures were taken from the maxima of the peaks

Thermal gravimetric analysis (TGA) was performed using a Perkin Elmer TGA 7. Samples with weight 10 ± 0.5 mg were heated from 373 to 1246 K at a rate of 10 K min^{-1} in a nitrogen atmosphere.

5.2.3 Preparation of Films for Tensile Measurements

Films were prepared by compression moulding of PFA pellets (DuPont code TE 7132, washed with acetone) in a nitrogen atmosphere between polished Monel® 400 plates (Pinch Alloys Australia) heated to 613 K (Monel is a nickel-copper alloy resistant to hydrofluoric acid). Minimal pressure was applied for 10 minutes while the polymer melted, then the pressure was increased to 2 tonne for 2 minutes to form a film. The thickness of the films was controlled using metal windows (0.5 mm thick) placed between the plates. The heating plates were then cooled using a stream of cool water, and the pressure released once the plates had cooled to room temperature. Dogbones were cut using a die with gauge length of 15 mm.

5.2.4 Radiolysis of Dogbones for Tensile Measurements

Dogbones were placed in Pyrex tubes and evacuated at 1×10^{-2} Pa for 24 hours. The tubes were sealed by melting a narrow neck in the glass, then the samples were irradiated in a 220

Nordian Gammacell at ambient temperature (303 K) at a dose rate of 5.7 kGy hr^{-1}. After irradiation, the tubes containing the dogbones were opened in a glove box in a nitrogen atmosphere and the tensile measurements immediately after each dogbone was removed from the glove box. This was done to minimize any reaction of the irradiated PFA with air.

5.2.5 Tensile Measurements

Tensile measurements were conducted on an Instron 4505 operated with an Instron 4500 controller and Series IX Method Editor. Wedge grips (5 kN) were used hold the dogbones in place. A crosshead speed of 50 mm min^{-1} was used at a temperature of 296 K.

5.3 Results and Discussion

5.3.1 Glass Transition Temperature of Untreated PFA

The glass transition temperature (T_g) of untreated PFA was taken from the maximum in tan d (Figure 5.1) measured using DMA. The transition is a broad one ranging from approximately 310 to 460 K with a maximum at 376 K. This value is in good agreement with the literature value of 363 K.[16] As expected, this is lower than the T_g of PTFE of 399 K.[17]

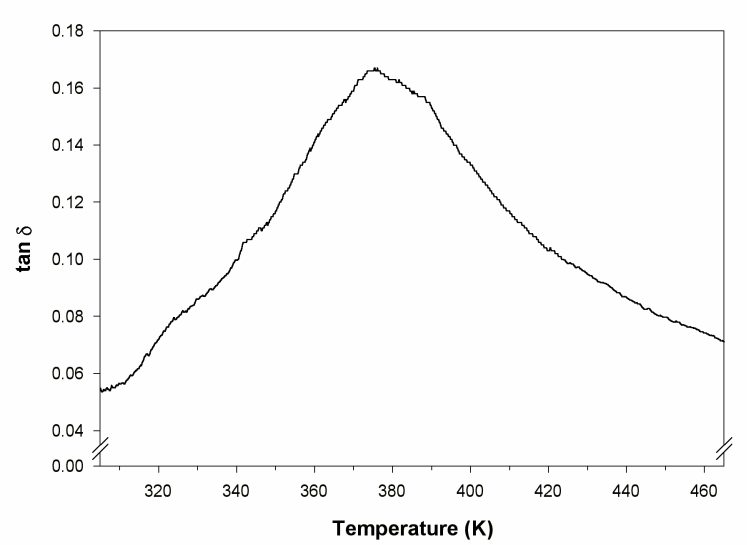

Figure 5.1 DMA of untreated PFA. Tan δ as a function of temperature.

5.3.2 Melting Behavior of Untreated PFA

Superheating is an often sited problem when measuring the melting temperature of fluoropolymers.[5-7,18,19] The most obvious symptom of superheating is that the melting rate of the crystals is lower than the heating rate. This can be detected by a change in the melting temperature with variations in the heating rate. The intrinsic melting temperature can be defined by the equilibrium melting temperature which is the temperature at which a perfectly formed polymer crystallite melts.

Several methods have been reported in the literature to overcome the shortcomings of superheating of fluoropolymers. Wunderlich and coworkers estimated the equilibrium melting temperature of PTFE by annealing samples for 12 hours at a predetermined temperature in the melting range then quickly cooling the samples to a temperature which was too high to induce crystallization but was significantly below the melting temperature. The annealing temperature at which no melting endotherm was observed on subsequent heating was taken as the equilibrium melting temperature.[5] Hoffman and Weeks determined the equilibrium melting temperature of PCTFE using a different method where the polymer was isothermally crystallized at a temperature T_c. They then plotted the melting temperature (T_m) of the crystals against the crystallization temperature for a range of T_c values. The intercept of the line fitted to the data with the line $T_m = T_c$ was taken as the equilibrium melting temperature.[20] This method is less cumbersome and time consuming than the method of Wunderlich and coworkers and has also been used by Pucciariello and coworkers to determine the equilibrium melting temperature for FEP and TFE/PMVE polymers.[9,11]

To determine the equilibrium melting temperature of PFA the isothermal crystallization method of Hoffman and Weeks was used. Untreated* PFA was cooled from the melt at the maximum rate the instrument would allow then held at a predetermined temperature between 553 and 565 K for one hour, cooled to 323 K then heated to 613 K at 20 K min^{-1}. If the crystallization temperature (T_c) was above 565 K an exotherm was observed on subsequent cooling which suggested there was incomplete crystallization at

* "untreated" refers to the polymer before exposure to radiation, regardless of heat treatment. The term "untreated" will be used only to describe the non-irradiated polymer. To distinguish between melted and non-melted PFA, the thermal history will be referred to in the text.

this temperature. For this reason, the highest value of T_c used was 565 K. The DSC traces of the first run of PFA and runs after crystallization are shown Figure 5.2. The first run was used to determine the initial crystallinity of PFA before any irradiation or heat treatment. The heat of fusion from the area under the melting endotherm was converted to crystallinity based on the figure of 82 J g^{-1} reported for the melting of a perfect crystal of PTFE.[5] This gave a measure of the crystallinity of untreated pellets of PFA of 34 ± 3 %.

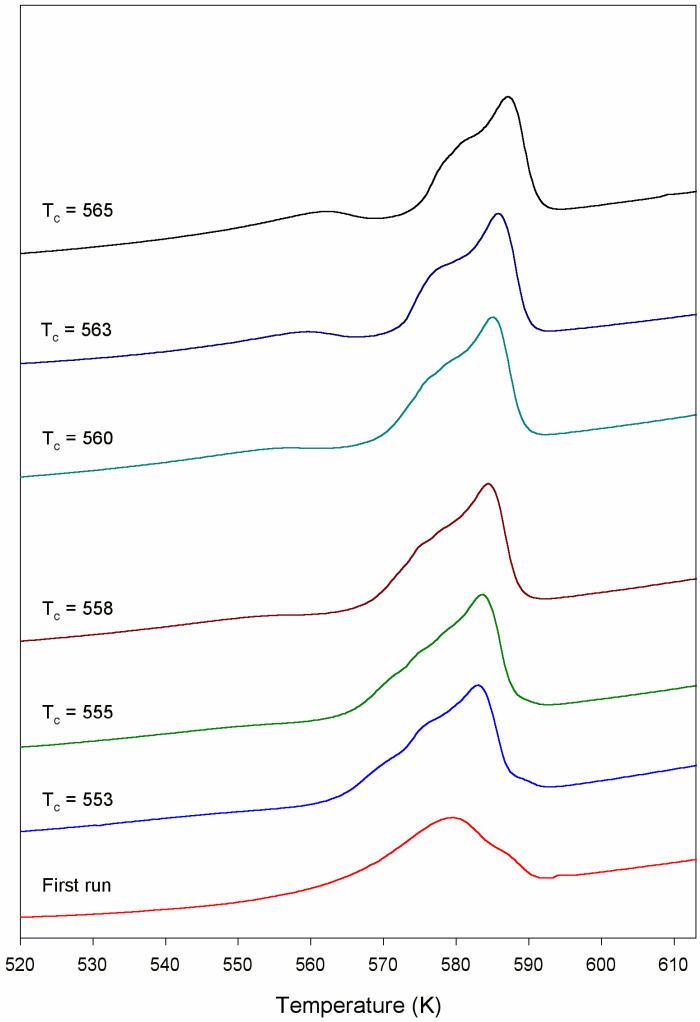

Figure 5.2 Melting endotherms (positive direction) of as received PFA and after crystallization at temperatures T_c. The heating rate was 20 K min^{-1}.

The multi-modal nature of the endotherms in Figure 5.2 was due to formation of less perfect crystals (lower melting temperature) amongst the more perfect ones (higher melting temperature). As T_c was decreased there is less chance for well ordered crystals to form and the melting temperatures were shifted to lower values and the peaks broadened.

When a T_c of 565 K was used, there is a broad endotherm at approximately 561 K and a shoulder at 580 K which can be attributed to melting of less perfect crystals. As T_c was decreased, the broad peak at 561 K shifted to lower temperature and became broader. At T_c less than 555 K this peak became so broad it is almost indistinguishable from the baseline. The shoulder which was at 580 K when T_c was 565 K also shifted to lower melting temperature as T_c was decreased. Similar observations have been made for isothermal crystallization experiments with TFE/PMVE.[8] It is possible for the less perfect crystals to recrystallize after melting to form more ordered crystals, however, the area under each trace for each value of T_c in Figure 5.2 did not vary by more than 2 % suggesting that this effect, if present, can be ignored for the purpose of this experiment.

The equilibrium melting temperature was estimated from the plot of T_c verses T_m in Figure 5.3. Extrapolation of the line of best fit of the data intercepts the line $T_c = T_m$ at 599 K. This value is only marginally below the value found for PTFE of 605 K using the method of Wunderlich[5] and would suggest that the perfluoropropyl ether side chains are excluded from the crystallites. If they were included in the crystallites the T_m° would be expected to me much lower than for PTFE. This is in agreement with work by Pucciariello and coworkers who found that small CF_3 side chains in FEP were partially included in the homopolymer crystal lattice while larger perfluoroalkoxy side chains in TFE/PMVE copolymers were excluded.[9-11]

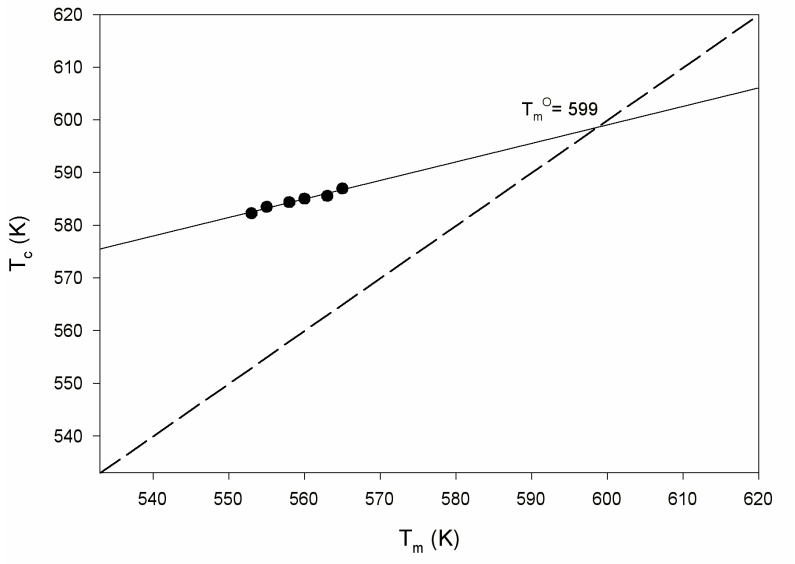

Figure 5.3 Melting temperature (T_m) plotted as a function of crystallization temperature (T_c). The dashed line satisfies the equation $T_c = T_m$.

5.3.3 Thermal Properties of Irradiated PFA

Determination of the equilibrium melting temperature of PFA samples after irradiation was not possible due to the chemical changes within the polymer. ^{19}F NMR spectroscopy studies (Chapters 3 and 4) revealed the formation of CF_3 side chains which may be incorporated or excluded from the crystallites. While the equilibrium melting temperature of FEP has been reported using the method by Hoffman and Weeks,[11] Centore *et al.* postulated that when FEP is crystallized isothermally, the CF_3 side chain concentration incorporated into the crystallites may change with crystallization temperature, hence it is not strictly correct to use this method for polymers containing HFP groups.[6] Instead, to compare the effects of radiation and radiation temperature on the melting temperature and melting endotherms on PFA, samples were crystallized from the melt at a constant cooling rate then heated through the melting transition at the same rate. Since a range of irradiation temperatures were used, it was important to erase the thermal history of the polymers before the melting transition was measured, thus the first DSC runs after irradiation were ignored.

The effect of irradiation temperature on the melting behavior of PFA is compared in Figure 5.4 for samples irradiated to 1 MGy and for untreated PFA. No transitions were observed below 450 K and this region has been omitted for clarity. The melting temperatures (taken from the maxima in the melting endotherms) and crystallinity (calculated from the area under the endotherms) over the entire dose range examined are plotted in Figure 5.5 and Figure 5.6, respectively. The irradiation temperatures used can be split into three groups: below the T_g maximum (irradiation at 303 K), above the T_g, but below the T_m (irradiation at 423 K and 473 K), and at or above the T_m (irradiation at 573 K and 633 K). When PFA was irradiated at 303 K there was little change in the melting temperature while the crystallinity increased significantly. The increase in crystallinity may be attributed to loss of alkoxy side chains, cleavage of chains in the amorphous regions interconnecting the crystallites (tie molecules), and overall lowering of the molecular weight allowing better packing of the chains and hence an increase in crystallinity. In support of this argument the melting endotherm of samples irradiated to 1 MGy at 303 K was sharper than the endotherm of the untreated sample. The lowering of the molecular weight is supported by the solid-state ^{19}F NMR spectra (Chapter 3) which showed that the

major non-volatile products resulting from irradiation at 303 K were new saturated chain ends.

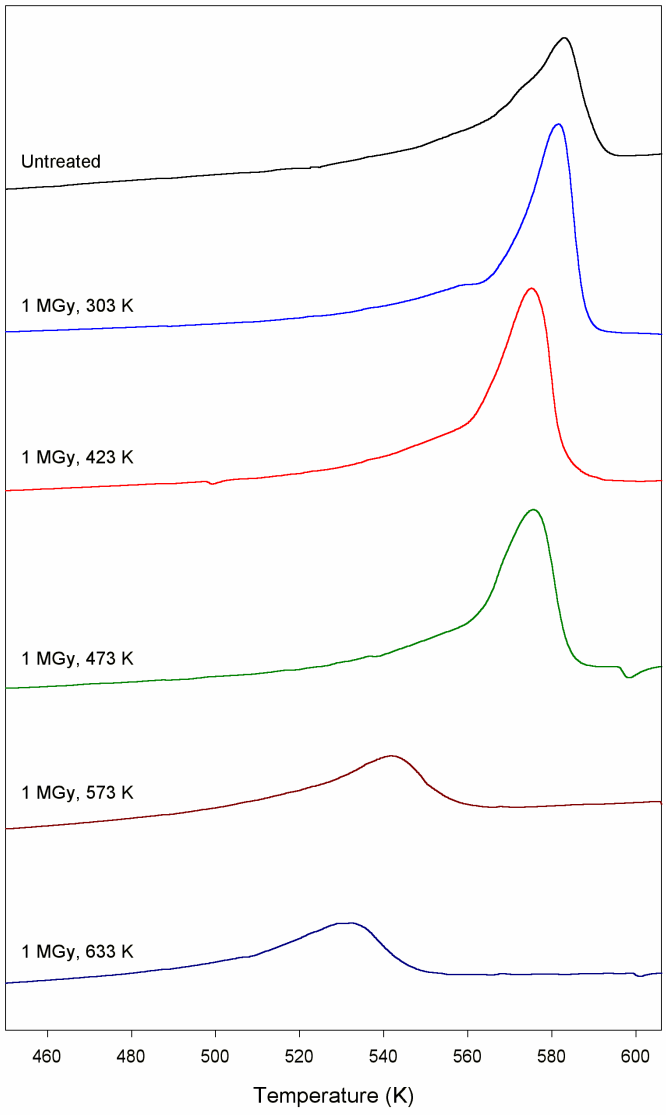

Figure 5.4 DSC traces of non-irradiated PFA and PFA irradiated to 1 MGy over a range of temperatures. Samples were crystallized from the melt by cooling at 40 K min^{-1} followed by subsequent heating at 40 K min^{-1} to measure the melting endotherms (positive direction).

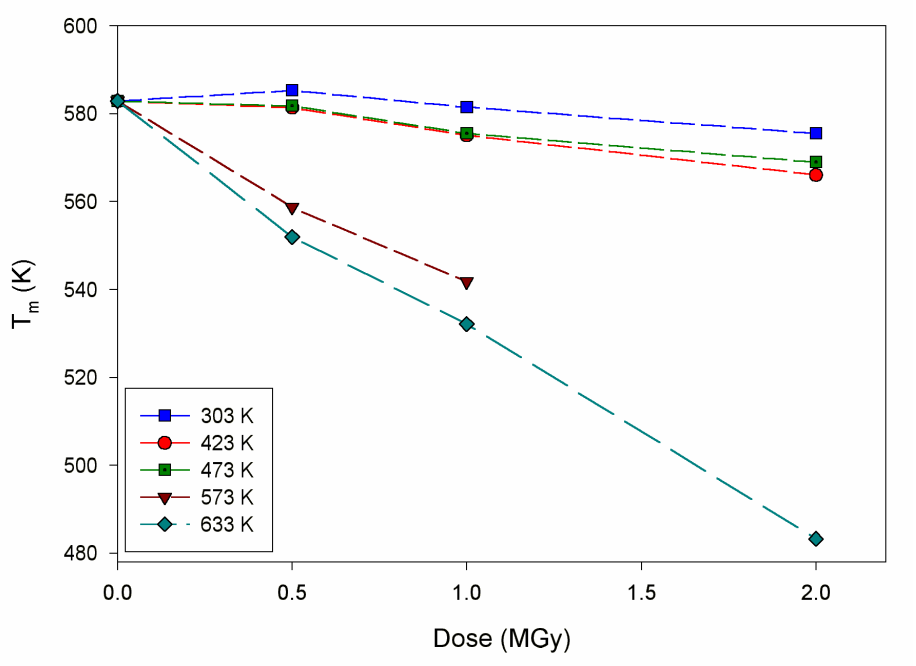

Figure 5.5 Melting temperature as a function of dose for samples irradiated at 303, 423, 473, 573 and 633 K.

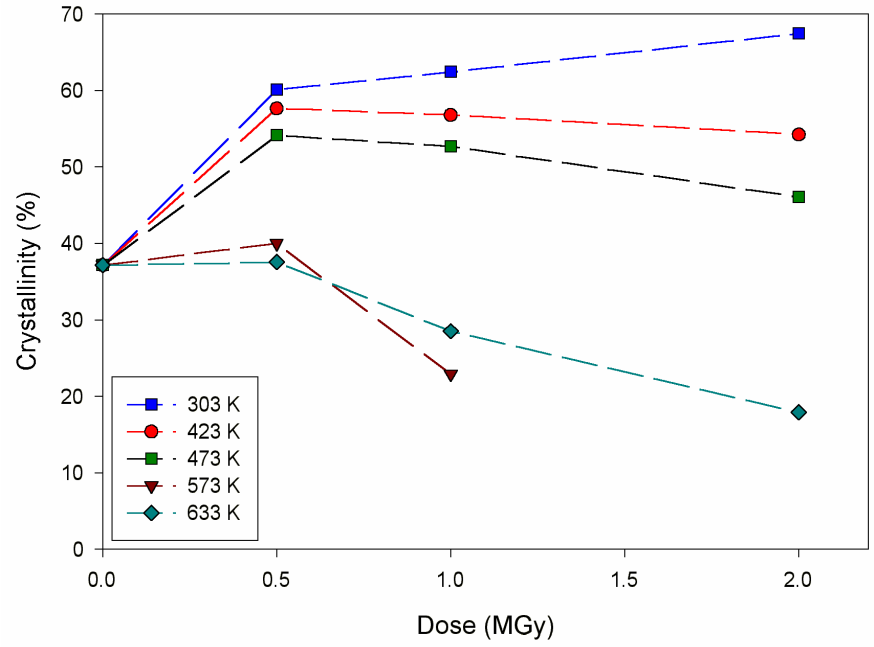

Figure 5.6 Crystallinity as a function of dose for samples irradiated at 303, 423, 473, 573 and 633 K.

Samples irradiated at 423 K and 473 K had similar thermal characteristics to one another, namely slightly lower T_m and higher crystallinity than untreated PFA. The large increase in crystallinity between 0 and 0.5 MGy may again be attributed to cleavage of tie

molecules and alkoxy side chains, however above this dose the crystallinity decreased due to fewer tie molecules and alkoxy side chains remaining and the formation of long and short branches capable of disrupting the chain packing. The short branches (CF_3) may be able to be included in the crystallites, giving rise to less perfect crystal growth which may explain the low temperature shoulder in the DSC traces (Figure 5.4) and the lower T_m maximum. Analogous behavior was reported for FEP which found that increasing the comonomer concentration decreased the T_m.[11]

Samples irradiated at or above the T_m of untreated PFA (573 K, 633 K) had dramatically different DSC traces to the other samples, indicating major structural changes within the polymer. The melting endotherms were broad and shifted to significantly lower temperature when compared with the untreated PFA. The crystallinity marginally increased after a dose of 0.5 MGy and may be considered to be a combination of release of strain through cleavage of tie molecules as well as formation of short and long branches. Above 0.5 MGy the crystallinity dropped dramatically — the sample irradiated to 2 MGy at 633 K had crystallinity of 18 % and a melting temperature of 530 K (note that the 2 MGy / 573 K sample was lost due to excessive pressure build-up which led to an explosion of the glass tube containing the sample during irradiation). Oshima *et al.* found that PTFE irradiated in the melt to a dose of 2 MGy became almost completely amorphous.[21]

5.3.4 Thermal Gravimetric Analysis (TGA)

The thermal stabilities of PFA with and without radiation treatment were examined by thermal gravimetric analysis (TGA). Figure 5.7 and Figure 5.8 show the weight-loss as a function of temperature for the various irradiated PFA samples measured by TGA ranging from 373 K to 1246 K with a heating rate of 10 K min^{-1}. Below 450 K and above 950 K there was no weight change so these regions have been omitted from the plots for clarity. Decomposition of untreated PFA was a one step process beginning at approximately 725 K, most likely to be via depolymerization and production of predominantly TFE units as is the case for thermal decomposition of PTFE.[22] The alkoxy side chains may be expected to decompose at lower temperature due to the ether bond, however this is not obvious from the TGA curve.

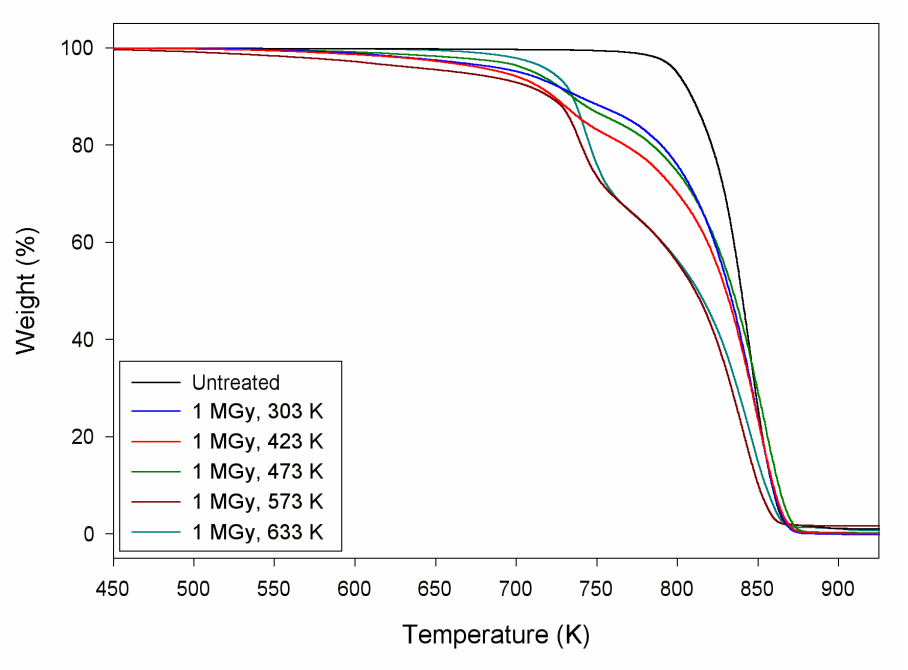

Figure 5.7 TGA traces of untreated PFA and PFA irradiated to a dose of 1 MGy at 303, 423, 473, 573 and 633 K.

The onset of decomposition was shifted to lower temperature by radiation treatment at all temperatures. At all irradiation temperatures with the exception of 633 K, the initial lower temperature decomposition may be attributed to loss of low molecular weight fragments. The absence of these fragments in the samples irradiated at 633 K was due to the experimental conditions used. At this temperature electron beams were used instead of γ-radiation and the samples were under continual vacuum, thus any low molecular weight fragments formed would have been removed by the vacuum during the radiation treatment.

Aside from loss of low molecular weight material below 700 K, all the irradiated samples had essentially a two step weight-loss profile. The relative proportion of these two steps gives some insight into their possible origins. Examination of Figure 5.8 D (irradiation at 633 K) shows that the low temperature decomposition step increased with increasing dose while the converse was true for the higher temperature step. ^{19}F NMR spectra showed that in these samples branching and crosslinking increased with dose. Therefore, as a corollary it may be concluded that the first step between approximately 700 K and 775 K was due to decomposition of branched or crosslinked PFA while the second

step between 775 K and 850 K was due to decomposition of non-crosslinked PFA. In support of this argument, Oshima *et al.* reported the TGA of PTFE crosslinked at 610 K in an argon atmosphere and found that the crosslinked material was less thermally stable than the untreated PTFE.[4] The lower stability of the branched / crosslinked material over the linear material may originate from weak points and defects in the structure. FEP, which contains CF_3 branches introduced by copolymerization of TFE with HFP, decomposes in two steps when heated in a nitrogen atmosphere.[23] The first step is due to the lower stability of the branched structures, while the second step is due to decomposition of TFE units. This supports the observation that branched structures in PFA after irradiation decompose at a lower temperature than non-branched structures.

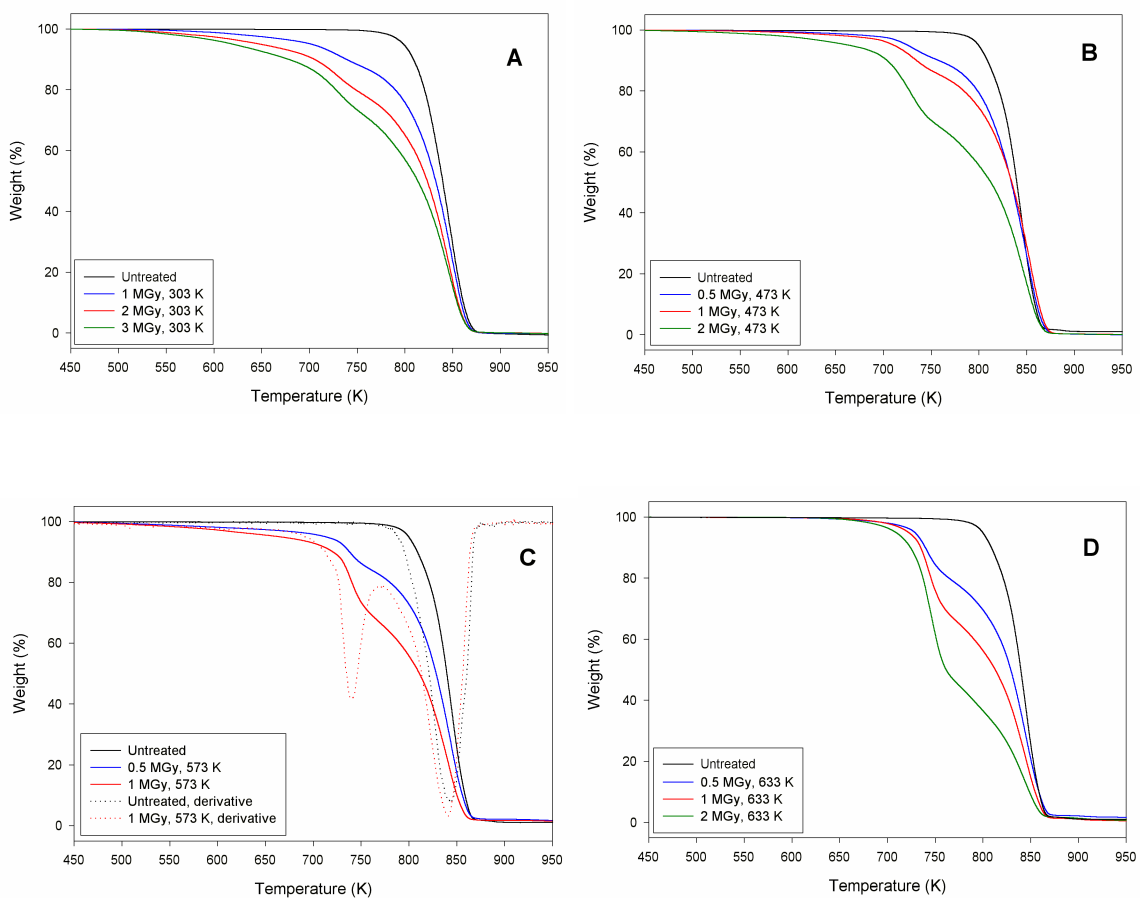

Figure 5.8 TGA traces. (A) irradiated at 303 K; (B) irradiated at 473 K; (C) irradiated at 573 K (derivative curves are included to highlight the predominately two-step decomposition); (D) irradiated at 633 K.

5.3.5 Tensile Measurements of Low-Dose PFA

It is known that perfluoropolymers degrade when exposed to radiation.[24] When irradiataed in vacuum, PFA has slightly better radiation resistance when compared with FEP and PTFE at low doses (< 30 kGy), but at high doses (> 100 kGy) all three polymers become embrittled.[25] In fact, a common method of recycling PTFE is to expose it to radiation to break the polymer down into a free-flowing micropowder which can then be used as a lubricant.[26] One of the aims of this project was to graft styrene to PFA using γ-irradiation to produce a graft copolymer with excellent chemical and thermal stability and reasonable mechanical properties. To determine what maximum recommended total dose can be used for the grafting reactions, the mechanical properties of PFA before and after irradiation in vacuum were examined using an Instron tester.

Figure 5.9 shows a selection of stress-strain curves for PFA before and after irradiation. The untreated material initially displayed Hookean elastic type behaviour at low strain where the stress/stain curve is almost linear before reaching a point where there is ductile flow. Upon further strain there was necking and strain-hardening of the polymer before it finally broke. Similar profiles are observed up to 5 kGy dose, above which, the samples broke without strain hardening. Above 10 kGy, the samples underwent brittle fracture.

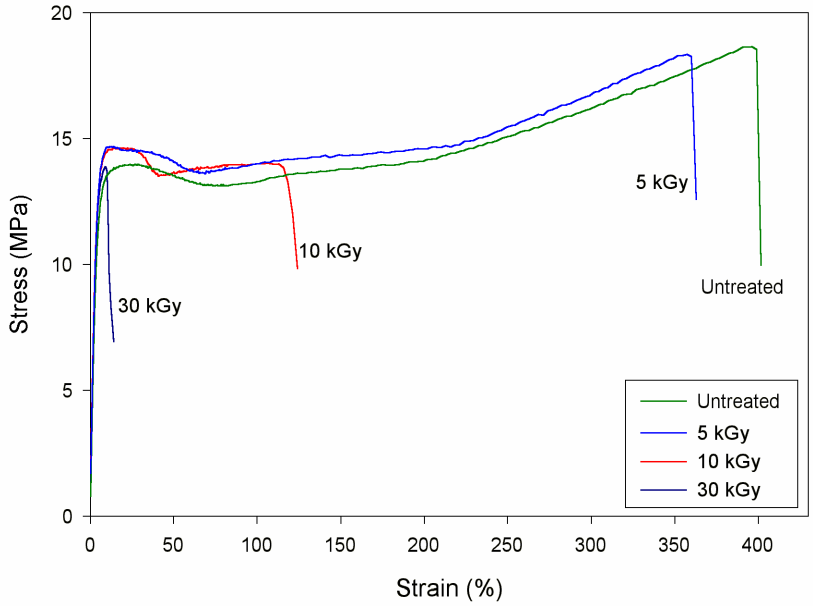

Figure 5.9 Typical stress-strain plots for untreated PFA and PFA irradiated to 5, 10 and 30 kGy, all in vacuum at 303 K. Measurements were made at 296 K.

In Figure 5.10 the tensile strength, Young's modulus, elongation and energy to break are plotted as a function of radiation dose. These figures show that the mechanical properties of PFA were dramatically altered after relatively low radiation doses. The loss in tensile strength, elongation and energy to break together with the increase in rigidity as indicated by the increase in the Young's modulus are consistent with chain scission. Other workers have observed similar trends in the tensile strength and elongation of irradiated PFA.[25,27] This is in agreement with the NMR results for PFA irradiated at 303 K in Chapter 3 which showed that chain scission was the main reaction at this irradiation temperature.

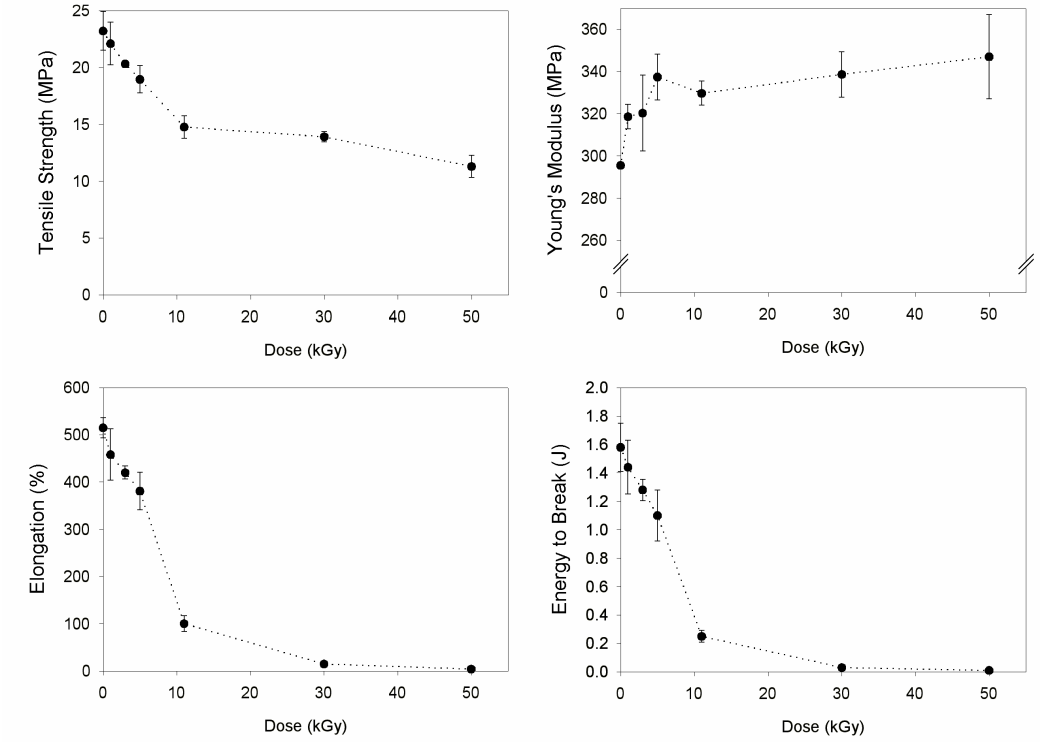

Figure 5.10 Tensile strength, Young's modulus, elongation and energy to break of irradiated PFA as a function of irradiation dose. The dotted line is an aid to the eye only.

The results presented in Figure 5.10 suggested that when grafting to PFA, the radiation dose should be kept as low as possible to avoid degradation of the polymer. The actual mechanical properties of the graft copolymer will be different to the results here as the graft may be expected to add to the properties. El-Sawy *et al.* found that when PFA was grafted with vinyl acetate there was an improvement in the tensile strength at low graft yields possibly due to crosslinking of the graft.[28] Another consideration is that grafted

supports for SPOC would more likely undergo compressive stresses rather than tensile stresses during handling of the support. It is known that fluoropolymers perform better under compression than elongation.[29] Based on this information, it is recommended that the total dose used for grafting preferably be kept below 10 kGy, and definitely not allowed to exceed 30 kGy.

5.4 Conclusions

In this chapter the thermal properties of PFA before and after irradiation have been examined. The equilibrium melting temperature of untreated PFA was estimated to be 599 K, slightly below the corresponding value for PTFE. When PFA was irradiated over a temperature range from below the T_g to above the melting point, the thermal properties of the polymer changed significantly. Low-temperature irradiation resulted in a decrease in thermal stability and an increase in the crystallinity with little change in the melting temperature. This was explained by the lowering of molecular weight and improved chain packing accompanied by formation of a small amount of short branch structures. When PFA was irradiated at or above the melting temperature the crystallinity, melting temperature and thermal stability of the resulting polymer decreased which was attributed to long and short branch formation and formation of low molecular weight fragments. At irradiation temperatures above the T_g but below the melting temperature the properties were intermediate between the higher and lower irradiation temperatures.

Tensile measurements of PFA irradiated at 303 K showed that the polymer experienced a dramatic loss in the mechanical properties even at low dose. A recommended upper limit of the total allowable dose to be used for grafting reactions of approximately 30 kGy was suggested in order for the graft copolymer to retain any useful mechanical properties.

5.5 References

1. Fisher, W. K., Correlli, J. C., *J. Polym. Sci., Polym. Chem.* **19**, 2465-2493 (1981).

2. Lappan, U., Haussler, L., Pompe, G., Lunkwitz, K., *J. Appl. Polym. Sci.* **66**, 2287-2291 (1997).

3. Oshima, A., Ikeda, S., Kudoh, H., Seguchi, T., Tabata, Y., *Radiat. Phys. Chem.* **50**, 611-615 (1997).

4. Oshima, A., Ikeda, S., Katoh, E., Tabata, Y., *Radiat. Phys. Chem.* **62**, 39-45 (2001).

5. Lau, S. F., Suzuki, H., Wunderlich, B., *J. Polym. Sci., Polym. Phys. Ed.* **22**, 379-405 (1984).

6. Centore, R., De Rosa, C., Guerra, G., Petracocone, V., Corradini, P., Villani, V., *Eur. Polym. J.* **24**, 445-448 (1988).

7. Pucciariello, R., *J. Polym. Sci.: Part B: Polym. Phys.* **32**, 1771-1776 (1994).

8. Pucciariello, R., *J. Polym. Sci. Part B: Polym. Phys.* **34**, 1751-1759 (1996).

9. Pucciariello, R., *J. Appl. Polym. Sci.* **64**, 407-409 (1997).

10. Pucciariello, R., Villani, V., Mancusi, C., *J. Appl. Polym. Sci.* **74**, 1607-1613 (1999).

11. Pucciariello, R., Mancusi, C., *J. Appl. Polym. Sci.* **73**, 919-925 (1999).

12. Starkweather, H. W., Zoller, P., Jones, G. A., *J. Polym. Sci., Polym. Phys. Ed.* **22**, 1431-1437 (1984).

13. Weeks, J. J., Eby, R. K., Clark, E. S., *Polymer* **22**, 1496-1499 (1981).

14. White, M. L., Waddon, A. J., Atkins, E. D. T., Farris, R. J., *J. Polym. Sci., Polym. Phys. Ed.* **36**, 2811-2819 (1998).

15. Marigo, A., Marega, C., Zannetti, R., Ajroldi, G., *Macromolecules* **29**, 2197-2200 (1996).

16. DuPont. Teflon PFA Properties Handbook, 1997.

17. Brankdrup, J., Immergut, E. H. Polymer Handbook; John Wiley and Sons: New York, 1999.

18. Starkweather, H. W., *J. Polym. Sci., Polym. Phys. Ed.* **23**, 1177-1185 (1985).

19. Hellmuth, E., Wunderlich, B., Rankin, J. M., *Appl. Polym. Sym.* **2**, 101-109 (1966).

20. Hoffman, J. D., Weeks, J. J., *J. Res. Natl. Bur. Stand. A* **66A**, 13-28 (1962).

21. Oshima, A., Tabata, Y., Kudoh, H., Seguchi, T., *Radiat. Phys. Chem.* **45**, 269-273 (1995).

22. Morisaki, S., *Thermochimica Acta* **25**, 171-183 (1978).

23. Mohajerani, S. *PhD Thesis*, The University of Queensland (2002).

24. Florin, R. E., Wall, L. A., *J. Res. Natl. Bur. Stand. A* **65A**, 375-387 (1961).

25. Gangal, S. V. Tetrafluoroethylene-Perfluorovinyl Ether Copolymers. In: *Encyclopedia of Chemical Technology;* Kirk-Othmer Ed.; John Wiley & Sons: New York, 1994; Vol. 11; pp. 671-683.

26. Lyons, B. J. The Radiation Crosslinking of Fluoropolymers. In: *Modern Fluoropolymers;* Scheirs, J. Ed.; John Wiley & Sons Ltd: Chichester, 1997; pp. 335-347.

27. Taher, N. H., Dessouki, A. M., Khalil, F. H., El-Arnaouty, M. B., *Polym. Int.* **41**, 383-389 (1996).

28. El-Sawy, N. M., Hegazy, E. A., Rabie, A. M., Hamed, A., Miligy, G. A., *Polym. Int.* **33**, 285-291 (1994).

29. Scheirs, J. Structure/Property Considerations for Fluoropolymers and Fluoroelastomers to Avoid In-service Failure. In: *Modern Fluoropolymers;* Scheirs, J. Ed.; John Wiley & Sons Ltd: Chichester, 1997; pp. 1-69.

Chapter 6

6 Grafting I – Vapour and Solvent Effects

6.1 Introduction

The pioneering work on radiation-induced grafting to PTFE was reported by Chapiro in the late 1950s and early 1960s.[1,2] Examining the process of simultaneous radiation-induced grafting of styrene and methyl methacrylate to PTFE, Chapiro found that at low dose rates the rate of polymerization was slow and grafting was diffusion controlled. Conversely, at higher dose rates the higher rate of polymerization exceeded the rate of diffusion and grafting was limited to the surface of the film. When the irradiation temperature was raised, the dose rate required for the rate of polymerization to exceed the rate of diffusion also increased. Since PTFE swells only slightly in styrene, Chapiro concluded that the diffusion of monomer occurred not into the pure PTFE, but into the partially grafted layers.

Much of the recent interest in grafted fluoropolymers has stemmed from the need to develop membranes for fuel-cells. Fluoropolymers are thought to be a good substrate for this application due to their excellent chemical and thermal stability and reasonable mechanical properties.[3] In order to prepare a conducting fuel-cell membrane from a fluoropolymer, the graft must penetrate the entire substrate. Much of the literature on this subject has been dedicated to studying the effects of dose, dose rate, temperature, chemical structure of the fluoropolymer, additives, graft monomer and to a lesser extent, solvents, with the aim of obtaining an homogeneous graft throughout the substrate.[4-16] One of the aims of the work contained in this thesis was to prepare a graft copolymer suitable for high temperature SPOC. For this application an accessible surface graft is desired, and while the knowledge in the literature is useful for understanding the grafting process, few publications have been aimed at achieving a surface graft with properties suitable for SPOC.

Until recently, there were few publications covering the grafting of monomers to PFA. Shortly after this project was conceived, Nasef *et al.* reported for the first time the

effect of solvents on the grafting of styrene to PFA.[12] Later, Nasef reported similar work examining the effects of solvents when grafting to PFA, FEP and PTFE.[13] The solvents Nasef and coworkers employed were dichloromethane, benzene and methanol. They found that the graft yield, when grafting styrene to thin films of PFA, was strongly dependent on the solvent used to dilute the monomer and the concentration employed. Like Chapiro,[1,2] Nasef and coworkers found that at low dose rates diffusion of the monomer was enhanced, leading to high graft yields while at high dose rates the rate of termination was fast, leading to lower graft yields compared with lower dose rates for the same total dose. The papers of Nasef and coworkers contain some spurious explanations of some of their findings. Firstly, they reported that the reason a higher graft yield was observed when dichloromethane or benzene was used compared with methanol was because of an increase in the number of radicals produced in the grafting system, particularly in the polymer substrate, when the former two solvents were used. No further explanation was given as to why the number of radicals produced would be different. It is highly unlikely that merely changing the solvent would affect the number of radicals produced within the polymer substrate to any significant degree. Secondly, they claimed that no homopolymer was formed when dichloromethane was used as a solvent. They made no attempt to isolate the homopolymer formed in their grafting reactions and it can only be concluded that the reason they did not observe any homopolymer in dichloromethane was that it was soluble and hence the solution did not become cloudy. Finally, while differences in graft yields between the various solvents are argued in terms of diffusion of the monomer, no attempts were made to measure the diffusion or penetration of the graft into the substrate. To clarify some of these anomalies, the effect of solvents on the grafting of styrene to PFA is revisited in this chapter.

Also in this chapter, grafting of styrene vapour to PFA is investigated. In liquid-phase grafting, the grafting rates have been shown to be approximately 70 % higher than in the vapour-phase for grafting of styrene to polyethylene. This has been accounted for by the high diffusion resistance at the polymer-vapour interface.[17] Put another way, using monomer vapour instead of monomer liquid, the graft can supposedly be limited to the surface. No reports could be found where grafting to fluoropolymers had been conducted using monomers in the vapour-phase. Vapour-phase grafting has advantages over liquid- or

solution-phase grafting in that no solvent is required and it is a very efficient use of monomer as there is low parasitic loss of monomer by homopolymerization.

To characterize the grafted PFA copolymers both weight increase and Raman microprobe spectroscopy (a brief overview of this technique is given in the next section) have been used. In the final section of this chapter, a comparison is made of the suitability of a selection of the graft copolymers prepared for use as supports for rudimentary SPOC using loading tests.

6.2 Theory and Technical Aspects

6.2.1 Microprobe Raman Spectroscopy

The Raman effect was first predicted in the early 1920s by Smekal[18] and later demonstrated almost simultaneously by C.V. Raman and G. Landsberg and L. Mandelstam in 1928.[19,20] This effect relates to the inelastic scattering of photons by matter.

When light illuminates a sample a small fraction of the light is scattered. This scattered light is composed of two parts, namely Rayleigh scattering and Raman scattering. Rayleigh scattering makes up the majority of the scattered light and originates from elastic scattering, that is, it has the same energy as the incident light. The Raman scattering has intensity equal to approximately one millionth of the Rayleigh scattering and is due to inelastic scattering. In the Raman spectrum on either side of the Rayleigh line are Raman lines of lower frequency (Stokes lines) and of higher frequency (anti-Stokes lines). The more intense Stoke lines arise from interaction of incoming light with molecules in the ground state energy level, while the less intense anti-Stokes lines are from interaction with molecules already in a high energy state. Raman spectrometers use filters to remove the Rayleigh scattering to measure the Raman scattering. The shift in frequency of the Stokes and anti-Stokes Raman scatter lines from the exciting line form the Raman spectrum which correspond to frequencies of molecular vibrations.

Unlike infrared spectroscopy, which requires a dipole moment to observe an absorption band, Raman spectroscopy relies on a change in the polarisability of the

molecule during the vibration. Polarisability can be considered as a measure of the ease with which the electron cloud surrounding a molecule can change shape. Thus, the information which can be gained from a Raman spectrum is different but complementary to the infrared spectrum. Raman spectroscopy is particularly informative about groups such as C–C and C=C, while infrared spectroscopy can be used to characterize groups such as OH and C=O.

Microprobe Raman spectroscopy involves focusing of the incident light onto a small point on the sample so that the Raman spectrum *at that point* may be measured. This spot illumination is achieved using a Raman spectrometer coupled to a confocal microscope. The spatial resolution of this technique depends on the equipment used. If the laser is focused with a $50\times$ objective, the spot size is of the order of 1 μm^2 although it does depend on the wavelength of the laser used. With proper focusing the depth into the sample from which the Raman signal is generated is 3 – 4 μm from the surface.[21] If the sample under the microscope is on a movable stage, preferably automated, spot spectra can be acquired over a relatively large area allowing a map of Raman spectra to be generated of the surface. If a grafted sample is cut perpendicular to the surface such that the cross-section is exposed, a map of the penetration of the graft into the substrate can be obtained. Later in this chapter the results using this technique to map the penetration of polystyrene graft into PFA are discussed.

6.3 Experimental

6.3.1 Materials

All substrates were prepared from PFA pellets (DuPont, code TE 7132). Vapour-phase grafting was performed on PFA films prepared in the same way as dogbones used for tensile measurement (Chapter 5, Section 5.2.3) but cut into rectangles $1.9\times0.8\times0.05$ cm instead of dogbones. Mimotopes lanterns were used as the graft substrate for solution-phase grafting. A photograph of one of these lanterns is shown in Figure 6.1. The dimensions of the ungrafted lanterns are: length 13 mm; width 5 mm; ring and strut thickness 0.5 mm. The lanterns had been injection moulded from PFA pellets. Both the films and lanterns were

washed in acetone overnight in a Soxhlet-extractor, dried under vacuum and weighed before use. Styrene (Fluka) was purified immediately before use by passing through a column of aluminium oxide to remove the 4-*tert*-butylcatechol inhibitor then distilled under reduced pressure. All solvents were of HPLC purity except for the methanol used to precipitate the polystyrene which was AR grade.

Figure 6.1 A photograph of a Mimotopes lantern made from PFA before grafting. Injection moulding has left injection points on the third and seventh rings indicated by the arrows.

6.3.2 Vapour-Phase Grafting

PFA films were placed into the bottom of a long tube designed to fit into the hole passing through the top of the 220 Nordian Gammacell (Figure 6.2). Styrene feed monomer was put into the reservoir in the top of the tube outside the gamma-cell and degassed by three freeze-pump-thaw cycles then sealed at a pressure of approximately 1×10^{-2} Pa. The tube containing the PFA film was placed into the gamma-cell at 303 K with lead attenuation used to vary the dose rate. After irradiation the tube was removed from the gamma-cell and opened so the film could be removed and washed for two days with dichloromethane in a Soxhlet-extractor before being dried to constant weight under a vacuum. The graft yield was calculated as a function of the surface area of the films:

$$\text{Graft Yield } (\%) = \frac{W_f - W_i}{S.A.} \times 100$$

where W_i is the initial weight of the ungrafted film, W_f is the weight of the film after grafting, and *S.A.* is the surface area of the film.

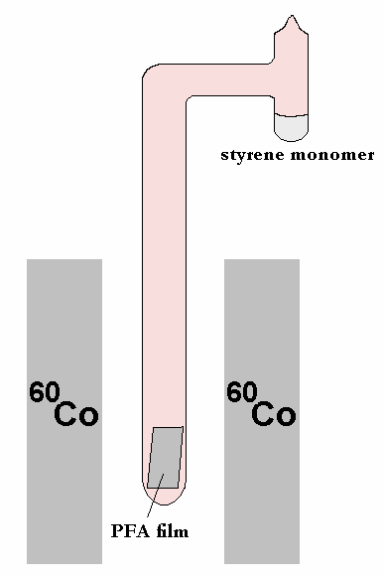

Figure 6.2 Glassware used for vapour-phase grafting. The PFA film was in the radiation source, while the styrene feed monomer was outside the s ource.

6.3.3 Solution Grafting

Grafting reactions were performed by placing one lantern in each tube containing styrene dissolved in the solvent made up to the desired concentration (total volume 2 mL). The tubes were sealed with Subaseal brand rubber seals and degassed for 5 minutes by passing a steady stream of nitrogen gas through a pair of needles passing through the Subaseals. The samples were then irradiated at 298 K in a 200 Gammacell from the Atomic Energy of Canada Limited at dose rate of 0.69 kGy hr^{-1}. After irradiation the graft copolymers were immediately removed from the grafting solutions to minimize any post-irradiation grafting and washed in the same manner as for the vapour-phase grafted samples. The graft yield was calculated from the weight increase after grafting:

$$\text{Graft Yield } (\%) = \frac{W_f - W_i}{W_i} \times 100$$

where W_i is the initial weight of the ungrafted lantern, and W_f is the weight of the lantern after grafting.

6.3.4 Microprobe Raman Spectroscopy

Microprobe Raman spectroscopy was performed using a Renishaw System 1000 Raman spectrometer (Renishaw plc. Wotton-under-Edge, UK) equipped with Renishaw laser diode emitting at 785 nm. An Olympus MD Plan microscope with a $50\times$ objective lens was used to focus the laser to a spot size of approximately 1 μm. Each spectrum was collected in the static mode for 20 seconds in the range 700 – 1200 cm^{-1}. Graft copolymer samples to be analyzed were mounted on a microscope slide and held in place with a generic putty. Maps were made by acquiring spectra over the sample using an automated movable stage.

6.3.5 Size-Exclusion Chromatography (SEC)

Free homopolymer from the surrounding solutions of the solution-phase grafting reactions was isolated by precipitation into methanol (500 mL), filtration, and drying under vacuum and then dissolved in tetrahydrofuran (THF) for SEC analysis. Occluded homopolymer was isolated by removing the grafted lanterns from the grafting solution, then briefly washing the grafted lanterns in methanol to remove most of the residual styrene. The lanterns were then soaked in THF for 48 hours to extract the occluded homopolymer. To check that the THF washing effectively removed all the occluded homopolymer, the lanterns were then further washed in dichloromethane in a Soxhlet-extractor overnight after which no weight difference was observed.

SEC was performed using a Waters 2690 Alliance system equipped with two Waters Ultrastyragel linear columns of dimensions 7.8 × 300 mm coupled in series to a Waters 410 differential refractometer detector. THF (HPLC grade, EM Science) was used as the solvent at a flow rate of 1.0 mL min^{-1}. Each sample was prepared to a concentration of approximately 1 mg mL^{-1} and 100 μL injections made.

A calibration curve was constructed using narrow molecular weight polystyrene standards (Pressure Chemical Company, Pittsburgh) of molecular weight: 1.2×10^{6}, 9.5×10^{5}, 6.7×10^{5}, 4.11×10^{5}, 1.10×10^{5}, 2.33×10^{5}, 3.7×10^{4}, 1.98×10^{4}, 1.03×10^{4}, 4.8×10^{3}, 2.1×10^{3} and 9.0×10^{2} g $mol.^{-1}$. From the calibration curve the molecular weight distributions of the free and occluded homopolymer were calculated.

6.3.6 Loading Tests

6.3.6.1 Aminomethylation

To PFA-*g*-PS (19 grafted lanterns) and a PP-*g*-PS control lantern (Mimotopes Pty Ltd) was added a solution of *N*-(hydroxymethyl phthalimide) (Lancaster) (0.6 g) and methanesulfonic acid (Fluka) (2 mL) dissolved in a trifluoroacetic acid / dichloromethane 1:4 solution (40 mL). The grafted lanterns and the aminomethylation solution was shaken gently at 298 K for 23 hours before the supernatant solution was removed and the lanterns washed in trifluoroacetic acid / dichloromethane (1:4 ratio, ca. 50 mL) for 10 minutes followed by washing with dichloromethane (ca. 2 × 50 mL) for 10 and 45 minutes then methanol
(ca. 50 mL) for 15 minutes. The lanterns were then heated to reflux overnight in a 5 % solution of hydrazine hydrate (Lancaster) (25 mL) in methanol (500 mL). The lanterns were then washed in hot methanol (4 × 50 mL for 25 minutes) followed by washing in dichloromethane (50 mL for 5 minutes), 1 % trifluoroacetic acid / dichloromethane (50 mL for 15 minutes) then again with dichloromethane (50 mL, 5 minutes) to convert any free amine to the more stable trifluoroacetic acid salt.

Conversion of the trifluoroacetic acid salt back to the free amine was performed by reacting the lanterns with a 5 % v/v triethylamine in a 1:1 dimethyl formamide / dichloromethane mixture (50 mL for 15 minutes), removing the supernatant and adding another aliquot (50 mL) of the 5 % triethylamine / dimethyl formamide / dichloromethane solution and leaving for a further 15 minutes. The lanterns were then washed with 1:1 dimethyl formamide / dichloromethane (50 mL, 5 minutes), dichloromethane (50 mL, 5 minutes), 1:1 dimethyl formamide / dichloromethane (50 mL, 5 minutes) and dichloromethane (50 mL, 5 minutes).

6.3.6.2 Fmoc-Rink Coupling

Fmoc-Rink (1.94 g), 1-hydroxybenzotriazole hydrate (Albatross Chemicals Inc.) (0.66 g) and *N*, *N*'-diisopropyl-carbodiimide (Aldrich) (0.564 mL) were dissolved in a 1:4 dimethyl formamide / dichloromethane solution (30 mL) and allowed to sit for 5 minutes to activate.

Portions (1.5 mL) of the Fmoc-Rink solution were added to individual vials containing one lantern each and gently agitated at 298 K overnight. After Fmoc-Rink coupling the solution was removed, the lanterns washed with 1:1 dimethyl formamide / dichloromethane mixture (ca. 10 mL) then each lantern was acetylated by immersing in a solution of acetic anhydride (0.25 mL) and diisopropylethylamine (0.05 mL) in 1:1 dimethyl formamide / dichloromethane (2.5 mL) for one hour. The acetylating solution was then removed and the lanterns washed using the same dichloromethane, dimethyl formamide / dichloromethane procedure as above. The Fmoc-Rink was cleaved from each of the lanterns by adding a 20 % piperidine / dimethyl formamide solution (10 mL) to each of the individual lanterns in tubes and allowed to react for two hours. A portion (1 mL) was taken from each vial and diluted to 1 in 110 with 20 % piperidine / dimethyl formamide solution or 1 in 210 for the PP-*g*-PS controls and the UV absorbance measured at 301 nm. The loading of the Fmoc-Rink groups was calculated from the equation:

$$\text{Loading} = \left[A_{301\text{nm}} / e \times \text{volume in mL} \right] \ \mu\text{m lantern}^{-1}$$

where A_{301} is the UV absorbance of the solution at 301 nm and e = 7800 M^{-1} cm^{-1}.

6.4 Results and Discussion

6.4.1 Vapour-Phase Grafting

Vapour-phase grafting in the absence of additives represents possibly the most simple grafting system, free of solvents and significant homopolymer formation. Previous workers have shown that when monomer vapour is used to graft to polyolefins, the diffusion of the monomer at the polymer–vapour interface is hindered, resulting in predominately surface grafting.[17,22-25] In this section, the effect of dose and dose rate when grafting of styrene vapour to films of PFA is examined using the simultaneous grafting method.

The PFA substrate used was in the form of a film 0.5 mm thick. While strictly speaking a “film” usually refers to a thin object, for simplicity these thick pieces of PFA

will be referred to as films. The reason 0.5 mm was chosen was to resemble the Mimotopes lanterns which have rings and struts approximately 0.5 mm thick. To introduce styrene vapour experiments were performed using long tubes designed so that the monomer feed solution was outside the radiation source and the PFA film inside the source, surrounded by the styrene vapour as depicted in Figure 6.2 in the experimental section. This design was developed after initial experiments with both the styrene and PFA film inside the gamma-cell failed due to homopolymerization of the feed styrene which led to a drop in the vapour pressure. The long tube with the monomer liquid outside of the radiation source did not completely solve this problem as some homopolymerization could be detected at high doses due to radiation leakage through the top of the gamma-cell. It is unlikely that reaction with volatile radical fragments from degradation of the PFA would be able to travel the distance of the tube to the monomer to cause initiation. While it was not done, it is possible that the addition of a large amount of inhibitor to the feed monomer may prevent homopolymerization.

Graft yields when PFA films were grafted using styrene vapour for four different dose rates are shown in Figure 6.3. Since films were used, the graft yield has been expressed as mass per unit surface area rather than mass increase as a percentage of the original mass. The reason for this was that each film had slightly different thickness due to problems with reproducibility and uniformity during film pressing. Since the graft did not penetrate the entire film, the thickness would not affect the graft yield so this was considered to be a reasonable measure of the graft yield. In Figure 6.3 it is evident that the graft yield is independent of dose rate at times less than approximately 10 hours. The exception is for the highest dose rate examined, 6.2 kGy hr^{-1}, which deviates slightly from this trend.

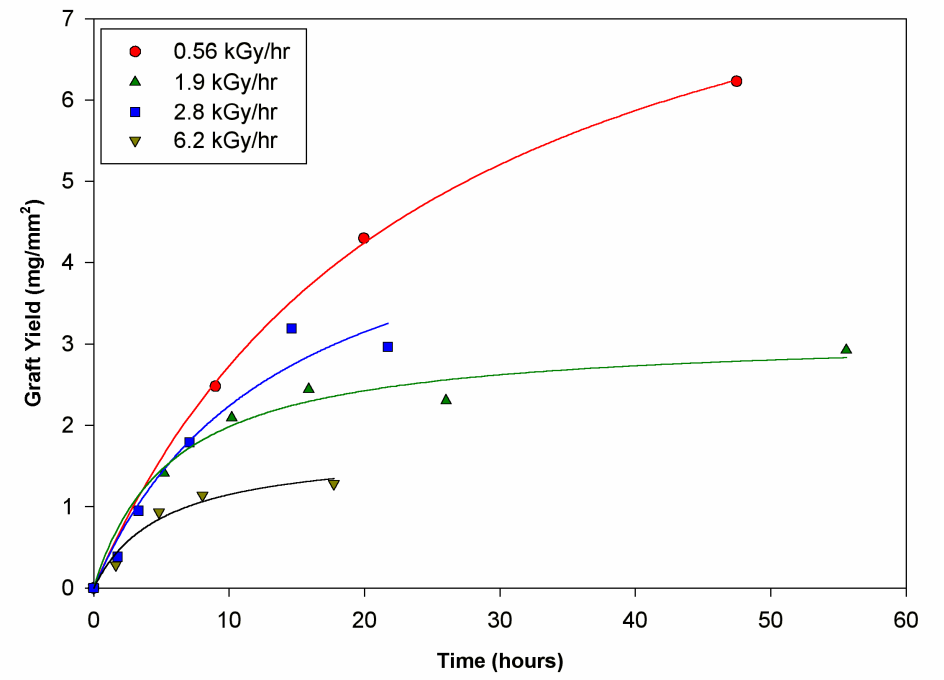

Figure 6.3 Graft yield as a function of time for the grafting of styrene vapour to PFA films using the simultaneous grafting method.

The initial independence of the graft yield on the dose rate suggested that in the early stages of the reaction the grafting was diffusion controlled. The same observation has been made when grafting to PTFE using bulk monomer solutions,[1,2,4] although in other cases the rate of grafting has been observed as being dependent on the dose rate which has been attributed to radiation-induced crystallization of the substrate and increased homopolymer formation at high dose rates.[12,26,27]

At higher grafting times and doses, the plots deviate from being diffusion dependent and begin to plateau. For example, after 20 hours the graft yield was highest for the low dose rates while the opposite was true for the highest dose rates. This was due to several possible reasons. At low dose rates, the grafted chains will be longer as the rate of termination is low compared with higher dose rates. Longer chains will lead to higher graft yields for the same number of initiation reactions. In the radical yield plots based on ESR measurements (Chapter 2, Section 2.3.1), the number of stable radicals present per unit of radiation reached a plateau at high total dose as combination reactions became important due to high radical density. This same effect would also lead to a plateau in the graft yield at high doses. Using high dose rates would result in higher radiation-induced crystallization

which may lead to lower grafting as styrene cannot penetrate the crystallites. In addition, the homopolymerization of the monomer may be more of a problem at high dose rates where there was less lead attenuation allowing for a higher dose rate at the top of the gamma-cell where the monomer was located.

The distribution of the graft into the substrate is important not only in examining the mechanism of the grafting process, but also in determining the applicability of the graft copolymer for use in SPOC. To investigate the penetration depth, microprobe Raman spectroscopy was used.

6.4.2 Raman Microprobe Mapping of Vapour-Phase Grafted Films

Raman microspectroscopic mapping of grafted polymer surfaces has been demonstrated recently as a powerful tool in measuring the distribution of poly(styrene) (PS) in a poly(propylene-*g*-styrene) copolymer.[21,28] In order for this method to be useful, the Raman spectra of the graft and substrate polymers should be easily distinguishable from one another. Fortunately, PFA has a rather simple Raman spectrum (Figure 6.4), identical to PTFE. Peaks include: symmetrical CF_2 stretching (1382, 1301 cm^{-1}), asymmetric CF_2 stretching (1217 cm^{-1}), C–C stretching (734 cm^{-1}), CF_2 rocking and wagging (600, 575 cm^{-1}), CF_2 bending (386 cm^{-1}), and CF_2 stretching (292 cm^{-1}).[29,30] No peaks were identified which could be used to distinguish between chains in the amorphous and crystalline regions.

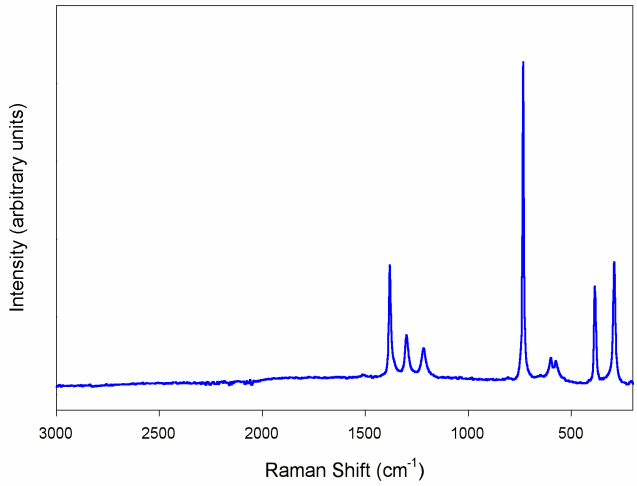

Figure 6.4 Raman spectrum of untreated PFA in the region 3000 - 200 cm^{-1}.

The Raman spectrum of PS is dominated by a peak at 999 cm^{-1} in the 1250 to 700 cm^{-1} region. Comparison of the Raman spectra of PFA and PS over this range is shown Figure 6.5. The most intense peak in the spectrum of PS at 999 cm^{-1} has no overlap with the PFA spectrum and was used as a measure of the PS content in the maps. Likewise, the characteristic PFA peak at 734 cm^{-1} was used as a measure of the PFA content.

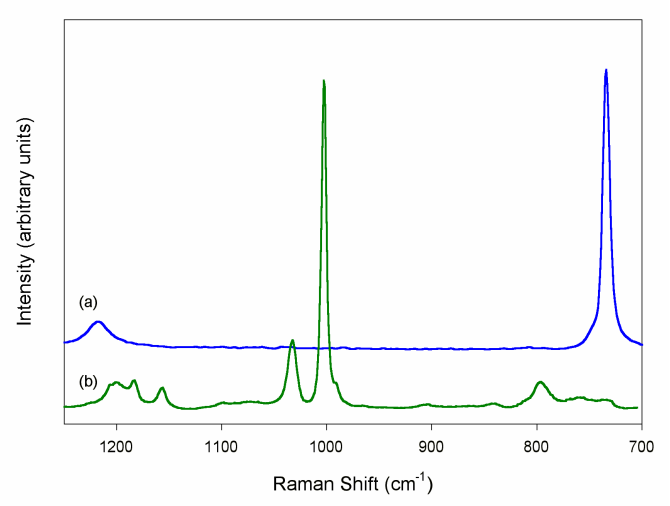

Figure 6.5 Raman spectra of (a) untreated PFA, and (b) pure PS in the region 1250 – 700 cm^{-1}.

Microprobe Raman spectroscopy was used to map the penetration depth of the graft into PFA after grafting with styrene vapour at different dose rates. To do this, cross-sections of the graft copolymer were exposed by physically cutting the grafted films. A microphotograph of one of these cross-sections is shown in Figure 6.6. The dark regions are due to the graft while the lighter internal region is due to the PFA substrate. From this photograph it would appear that there is a layer of PS on the PFA substrate and that there is a reasonably sharp boundary between the graft and the substrate. To investigate this further, microprobe Raman spectroscopy was used to construct a radial line map across the grafted region of the cross-section. Spectra were recorded at 2 μm intervals over the cross-section with the aid of an automated stage controller. An example of a stack plot constructed from the Raman spectra of a vapour-phase grafted PFA film is shown in Figure 6.7.

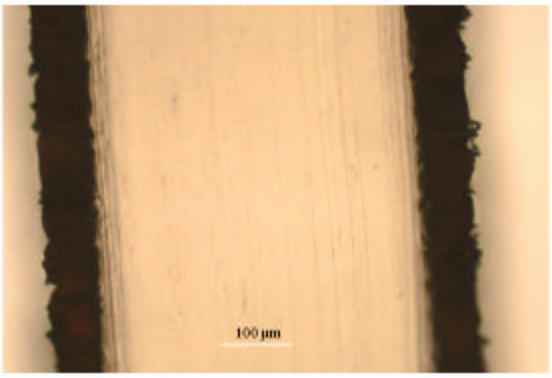

Figure 6.6 Microscope photograph of a cross-section of a PFA film grafted using styrene vapour.

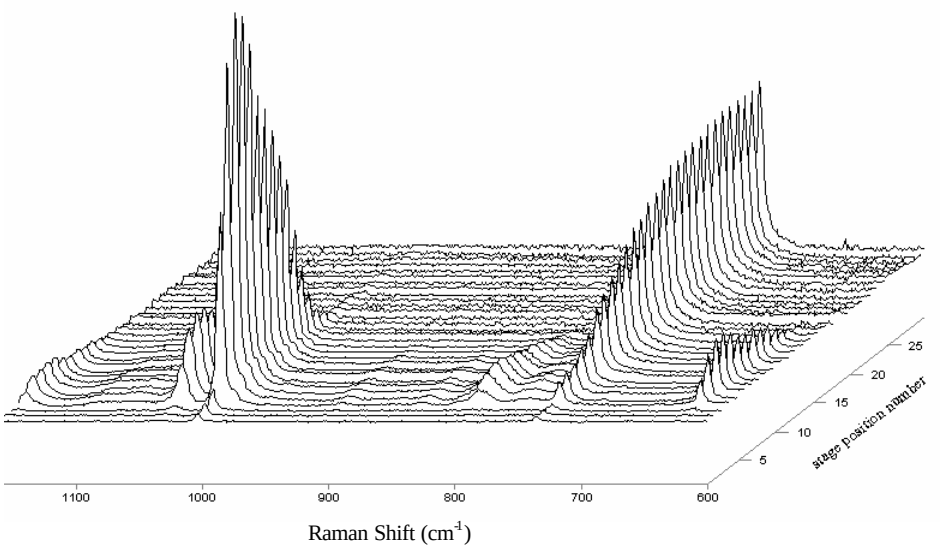

Figure 6.7 Stack plot of vapour-phase grafted PFA. The total dose was 19.6 kGy at a dose rate of 1.9 kGy hr^{-1}.

In Figure 6.7 the first three spectra at the front of the stack plots are weak due to the map being started at the very edge of the cross-section. For these spectra the illumination spot was only partially incident with the sample. The next several spectra are from the edge of the cross-sections and was assigned to mostly PS from the intensity of the peak at 999 cm^{-1}, while the spectra at the rear of the plots were recorded from the interiors of the cross-sections which were composed of mostly PFA (734 cm^{-1}). What was interesting to note was that the graft was a mixture of both PS and PFA and not just PS and that the boundary between the graft and the substrate was not sharp but was graded.

To further quantify these results, a method used Keen *et al.* was adopted.[28] The mole fraction of PS was calculated from the areas under the peaks at 999 cm^{-1} and 734 cm^{-1} then expressed as a fraction of the two signals using the equation:

$$\text{Mole fraction of PS} = \frac{\mathbf{A}_{\text{PS (999 cm}^{-1})} / s_{\text{PS (999 cm}^{-1})}}{(\mathbf{A}_{\text{PS (999 cm}^{-1})} / s_{\text{PS (999 cm}^{-1})}) + (\mathbf{A}_{\text{PFA (734 cm}^{-1})} / s_{\text{PFA (734 cm}^{-1})})}$$

where $\mathbf{A}_{\text{PS(999 cm}^{-1})}$ is the area under the peak at 999 cm^{-1}, $\mathbf{A}_{\text{PFA (734 cm}^{-1})}$ is the area under the peak at 734 cm^{-1}, and $s_{\text{PS(999 cm}^{-1})}$ and $s_{\text{PFA(734 cm}^{-1})}$ are the relative Raman scattering cross-sections. $s_{\text{PS(999 cm}^{-1})}$ and $s_{\text{PFA(734 cm}^{-1})}$ were measured by acquiring spectra of pure PS and PFA, respectively.

Figure 6.8 shows the calculated mole fraction of PS as a function of the distance from the edge of the cross-sections for PFA films grafted with styrene vapour to various total doses over a range of dose rates. It should be noted that the edges of the samples from where the map was started were not perfectly smooth. This introduced an error in the depth profile estimated to be in the order of ± 10 µm. The depth of grafted layers were between 10 µm and 70 µm and were all a mixture of PFA and PS rather than pure PS. The highest proportion of PS was observed when a dose rate of 0.56 kGy hr^{-1} was used for a total dose of 11.1 kGy, where the mole fraction of PS reached 0.95. The profiles are indicative of a grafting process which begins at the surface and progresses into the substrate, increasing in mole fraction of PS with increasing penetration depth, regardless of the dose rate. What is curious is that in every profile, the mole fraction of PS is lower at the surface than just below the surface. This effect may be partially due to the large error in the first few spectra recorded close to the edge of the cross-section where the spectra were very weak and focusing was a problem due to the rough surface. However, the trend appears to be very real in samples such as the one irradiated to 11.1 kGy at 0.56 kGy hr^{-1} where the proportion of PS reaches a maximum approximately 20 µm from the surface. Surface restructuring due to migration of the graft below the surface has been postulated based on XPS,[31] however, this occurs on a nanometer scale, not on the micron scale observed here. A more likely explanation for the increase in the proportion of PS below the surface may be due to crystallinity heterogeneity throughout the sample. It has been shown using Raman mapping

that Mimotopes lanterns made from a blend of poly(propylene), poly(ethylene) and ethylene-propylene rubber have high crystallinity at the surface which was in contact with the mould.[28] The thickness of this highly crystalline layer was approximately 10 – 20 µm. While the samples used for the vapour-phase grafting were in the form of films, and not lanterns, it is possible that a similar crystallinity profile was present. It is known that grafting occurs predominately in the amorphous regions of fluoropolymers which are more accessible to monomer[32] so that any areas with high levels of crystallinity would have low grafting.

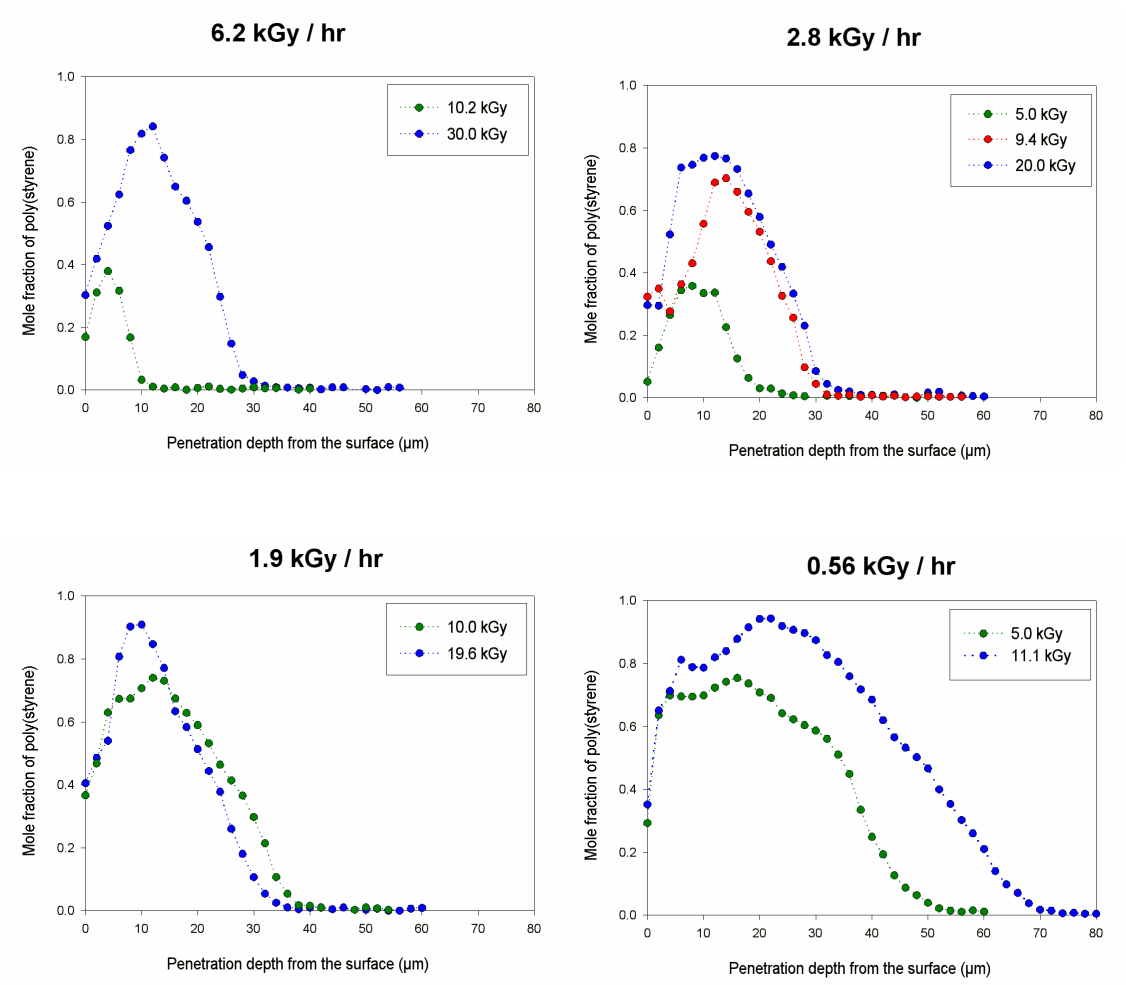

Figure 6.8 Depth penetration profiles of the mole fraction of PS for films grafted with styrene vapour at different dose rates.

To test the validity of the microprobe Raman mapping as a quantitative method, the area under each penetration profile was plotted as a function of the graft yield and is shown in Figure 6.9. While there is a certain amount of scatter, it is evident that the graft yield is

directly proportional to the area under the penetration profile suggesting that the microprobe Raman mapping and calculation of mole fraction of PS does have merit as a quantitative method.

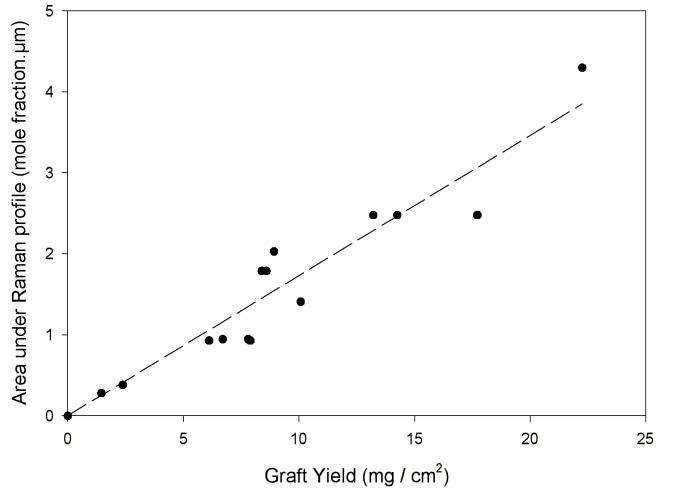

Figure 6.9 The correlation between the area under the Raman profile and the graft yield for vapour-phase grafted PFA.

6.4.3 Effect of Solvents on the Graft Yield

The use of solvents in grafting reactions can determine the specific nature of the graft copolymer.[33] Solvents have been used to aid the swelling of polyolefin substrates or to accelerate the grafting reaction by changing the viscosity of the grafted region to lower termination reactions.[34,35] The influence of solvents on the graft yield of monomers to fluoropolymers, however, has received little attention in the literature. In this section, the effect that a range of solvents have on the grafting of styrene to PFA is examined.

The solvents chosen in this study have a diverse range of polarities and chemical compositions ranging from non-solvents for PS to good solvents for PS; they were: methanol, ethanol, acetonitrile, toluene and dichloromethane. The simultaneous radiation grafting method was used where the polymer substrate, monomer and solvent (if any) were all exposed to the radiation source. As well as graft polymer being formed, this method invariably results in homopolymer formation so that the graft solution becomes a complex

mixture of polymer substrate, monomer, solvent, graft polymer and homopolymer. PFA moulded into Mimotopes lanterns were used as the polymer substrate.

Figure 6.10 shows the effect of styrene concentration in the five different solvents studied on the graft yield to PFA. It is clear that at low monomer concentration the graft yield is low, while the converse is generally true at high monomer concentration. In dilute styrene solutions the rate of termination of the grafted chains is large due to lack of monomer available for propagation and to a lesser extent, high termination via chain transfer to the solvent. Above 50 % styrene concentration the graft yields for reactions in each of the solvents becomes complex.

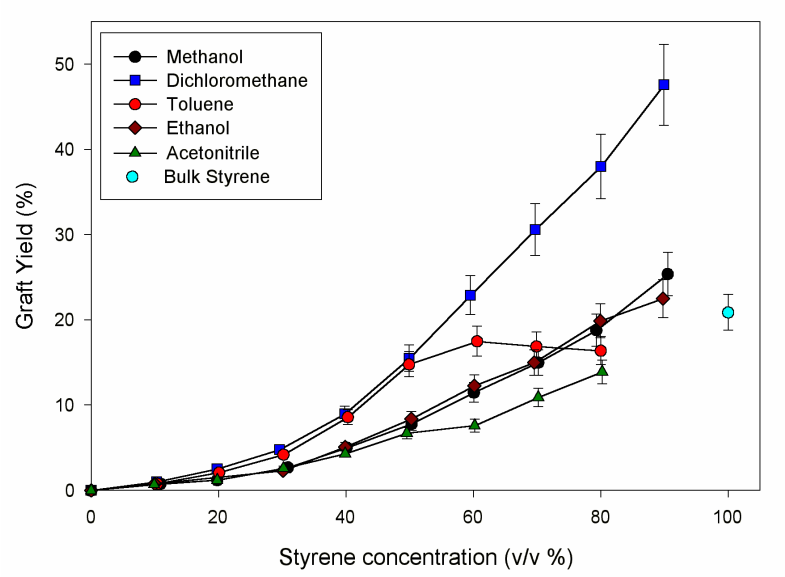

Figure 6.10 Effect of monomer concentration for various solvents. Total dose: 15 kGy, dose rate: 0.69 kGy hr^{-1}.

It was interesting to observe that some of the solutions became heterogeneous during the irradiation process. While the dichloromethane and toluene solutions remained clear, cloudiness and phase-separation was observed in the methanol, ethanol and acetonitrile solutions. The solutions with initial styrene concentration between 10 % and 30 % became cloudy during the irradiation, whereas the solutions with styrene concentration between 40 % and 70 % had a cloudy layer sitting above a viscous clear layer. Above 80 % styrene concentration the solutions remained clear throughout the irradiation. The size of the clear layer in the phase-separated solutions increased with

styrene concentration so it was deduced that the lower clear layer must have been predominately styrene monomer with some PS homopolymer dissolved in it, while the upper layer was predominately solvent with some styrene and PS homopolymer dissolved. Since the PFA lanterns have a density greater than any of the solvents or monomer used, they sunk to the bottom of the solutions and were in contact with the lower clear layer in cases where phase-separation was present. To test whether the phase-separation was impacting on the grafting yields observed, three lanterns were stacked on top of one another, covered in a solution of styrene in methanol (60 % v/v) then irradiated to 15 kGy. When removed from the gamma-cell, the solutions were phase-separated with the bottom lantern half-immersed in the clear layer, while the upper two lanterns were in the cloudy layer. The graft yield for the bottom lantern was 17 %, 14 % for the middle lantern, and 15 % for the upper lantern. While the difference is not great, it may be argued that the lantern in the bottom of the tube has slightly more PS grafted to it as a result of being present in the viscous styrene layer devoid of methanol compared with the upper layer higher in methanol content. It may also be that the phase-separation does not occur until the later stages of the irradiation time used, in which case this would account for the small difference between the graft yields of the lanterns observed. It was also interesting to note that the graft yields of the lanterns in this experiment were greater than when just one lantern was used. This is possibly due to the change in the monomer:polymer substrate ratio which may have caused these different results.

When comparing similar monomer diluents, for example methanol and ethanol, there is little difference in the results over the concentration range used. Using acetonitrile gave similar results to when methanol and ethanol were used possibly due to its similar polarity to the alcohols. Given the similarity in the graft yields when methanol, ethanol and acetonitrile were used, it was decided that of these three solvents, methanol would be representative for further experiments. Using dichloromethane led to a dramatic increase in graft yield over any of the other solvents used above 60 % styrene concentration, while using toluene led to little change in the graft yield when used in concentrations between 50 % and 80 % styrene.

Nasef, Nasef *et al.* and Cardona *et al.* have all examined the effect of solvents (methanol, benzene and dichloromethane) on the grafting of styrene to PFA.[12,13,36] Each

group of workers reported that when dichloromethane was used as a solvent for styrene when grafting to PFA, a maximum in the graft yield – solvent composition plots was observed. Nasef and Nasef *et al.* reported this maximum at 60 % styrene concentration, although as they only had points every 20 % the actual maximum could have been 60 ± 20 %. Cardona *et al.* observed the maximum at 70 ± 10% styrene and also reported a maximum at 50 ± 10 % when benzene was used, although the maximum was much less pronounced than when dichloromethane was used. Neither group reported the effect of monomer composition in methanol on the graft yield. The maximum seen by Cardona *et al.* when benzene was used as a diluent is similar to the trend for toluene in Figure 6.10, however, it was curious why no maximum was seen for dichloromethane in Figure 6.10, despite one being observed by these two other groups of workers. One explanation may be the different conditions used. Nasef and Nasef *et al.* grafted to films of PFA and FEP with thickness of 120 μm and used a dose rate of 1.32 kGy hr^{-1}, approximately double the dose rate used here.[12,13,37] The total dose they used, 20 kGy, is comparable to that used here. Cardona *et al.*, like here, grafted to lanterns, although the total dose of 100 kGy at an unspecified dose rate, is much larger than that used here.

The maxima observed by Nasef *et al.* when dichloromethane was used, and by Cardona *et al.* when dichloromethane and benzene were used, were attributed to viscosity effects, hence, the maxima may be expected to be dose and graft yield dependent. To investigate this, a higher total dose of 30 kGy was used with all other parameters the same as for Figure 6.10. The graft yields when methanol, toluene and dichloromethane were used are presented in Figure 6.11. In this case the graft yield at 90 % styrene concentration is approximately the same or lower than the graft yield at 80 % styrene concentration within the bounds of the error limits. The profiles for when methanol and toluene were used are similar to those for a dose of 15 kGy, only the graft yields were slightly higher.

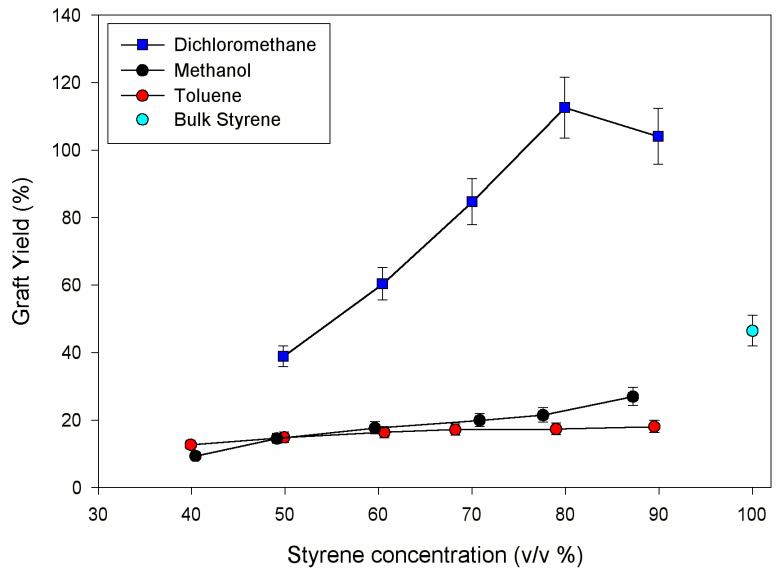

Figure 6.11 Graft yield for higher dose (30 kGy): methanol, toluene and dichloromethane.

The explanation given by Nasef, Nasef *et al.* and Cardona *et al.* for the observed behaviour when dichloromethane was used as the diluent was that styrene diffusion and concentration in the grafting layers increased with increasing styrene concentration to approximately 60 to 70% styrene, above which, the homopolymer formation hindered the diffusion of styrene through the polymer matrix. Nasef and Nasef *et al.* ignored the possibility that if the diffusion of styrene is hindered, the motion of the growing chains ends will be hindered as well, and termination by combination may be lowered, leading to higher molecular weight grafts, hence higher graft yield. Nasef also contradicts himself by saying that *no homopolymer was observed* in the styrene / dichloromethane grafting residue.[13] What is more likely is that homopolymer was formed, but because it was completely soluble in the dichloromethane it was simply not visible to the naked eye. Later in this chapter, in Section 6.4.5, results of measurement of the homopolymer formation is presented.

To investigate the enhancing effect increased viscosity may have on grafting, lanterns were grafted in solutions with artificially high amounts of homopolymer present. To do this, solutions of styrene in solvent were irradiated to a dose of 15 kGy *without* any PFA, then untreated PFA was added to the solutions now containing homopolymer, and irradiated for a further dose of 15 kGy. The results were compared with PFA grafted under

standard conditions to 15 and 30 kGy. A control experiment irradiating PFA with just homopolymer (that is, no monomer) showed that no grafting occurred between the PS homopolymer and the PFA substrate. The results in Table 6.1 show that for both methanol and dichloromethane solutions, the graft yield was higher after 15 kGy in the pre-irradiated solutions compared with the untreated solutions. This would suggest that homopolymer formation, under the right conditions, increases the graft yield for these two solvents. In the case of methanol, the graft yield after 15 kGy in the pre-irradiated solution was actually higher than if PFA was irradiated to 30 kGy in the untreated solution. This may be a consequence of the phase separation and effective lowering of the methanol concentration around the PFA substrate. The same trend was not observed for dichloromethane.

Table 6.1 Graft yield in methanol and dichloromethane solutions irradiated to 15 and 30 kGy and pre-irradiated.

Grafting conditions	Styrene / Methanol (70% v/v)	Styrene / Dichloromethane (70% v/v)
15 kGy (standard conditions)	15	31
15 kGy (in a solution pre-irradiated to 15 kGy)	32	43
30 kGy (standard conditions)	20	85

Nasef, Nasef *et al.* and Cardona *et al.* are no doubt correct in postulating that at higher monomer concentration in dichloromethane or benzene the diffusion of styrene into the substrate is hindered. However, this may not be due to an increase in viscosity due to homopolymer formation, but may rather simply be that at higher monomer concentration, there is less solvent available to swell the substrate. This is based on the observations that increasing the amount of homopolymer increases the graft yield and that no drop in graft yield was observed when methanol was used at high styrene concentration.

To further characterize the grafted copolymers and investigate the mechanism of grafting, the distribution of the graft into the PFA substrate was examined using Raman microprobe mapping.

6.4.4 Raman Microprobe Mapping of Lanterns – Effect of Grafting Solvent

Microprobe Raman spectroscopy was used to map the penetration depth of the graft into PFA after grafting in various solvent/monomer solutions. To do this, cross-sections of the graft copolymer were exposed by physically cutting the grafted lantern (see Figure 6.12), then, using a microprobe Raman spectrometer, spectra were recorded at 2 μm intervals over the cross-sections with the aid of an automated stage controller. A result of the injection moulding during manufacturing of the lanterns, is that there are slight variations in crystallinity throughout the lanterns, presumably due to temperature variations in the mould and shearing effects.[38] To avoid complications with crystallinity heterogeneity, the same ring (the second ring from the top) of the lanterns was used for all Raman mapping with the cross-section pieces being opposite to the injection points.

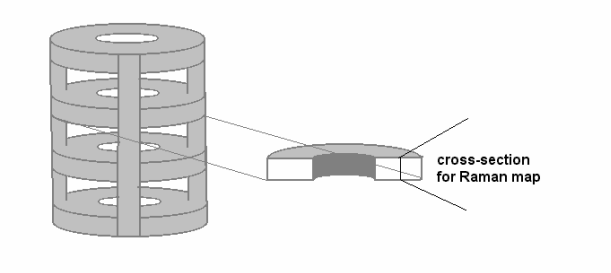

Figure 6.12 Cross-section cut from a lantern for Raman-mapping. A one-dimensional Raman map was produced by collecting spectra along a path perpendicular to the surface.

Examples of spectra obtained from the graft copolymers are shown in stack plots in Figure 6.13. These examples were from lanterns grafted in methanol and dichloromethane, each with 70 % v/v styrene. It is clear from the examples that the PS graft has penetrated the substrate much further when dichloromethane was used as a solvent when compared with methanol. In the stack plot of the copolymer grafted in methanol / styrene in Figure 6.13 it may be noted that there is a decrease, then a subsequent increase in the intensity of the PS peak at 999 cm^{-1} between spectra five and thirteen from the surface. This is believed to be due to slight variations in the focusing of the microscope on the sample due to roughness of the cross-section. The fluctuation of the PS peak over the cross-section is accompanied by a similar but less noticeable change in the PFA peak at 734 cm^{-1}.

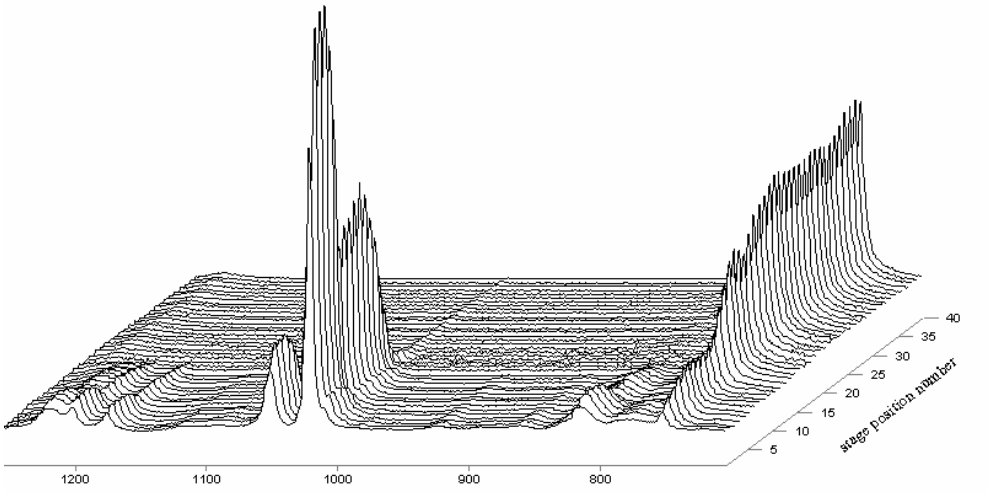

Raman Shift (cm^{-1})

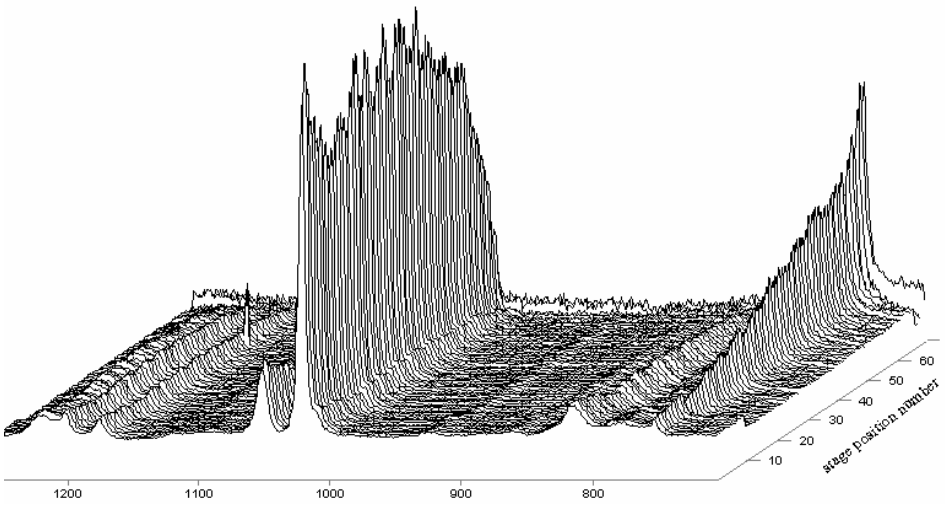

Raman Shift (cm^{-1})

Figure 6.13 Stack plots of Raman spectra obtained by microprobe mapping of cross-sections. Top: PFA grafted in a solution of styrene and methanol (70 % v/v styrene); Bottom: PFA grafted in a solution of styrene and dichloromethane (70 % v/v styrene). Each was irradiated to a dose of 15 kGy.

The mole fraction of PS was calculated from Raman spectra measured over the cross-sections of lanterns grafted in styrene and methanol, toluene or dichloromethane solutions made up to various concentrations in the same way as for the vapour-phase grafted films in Section 6.4.2. The calculated mole fraction of styrene was plotted against the distance into the cross-section and is shown in Figure 6.14.

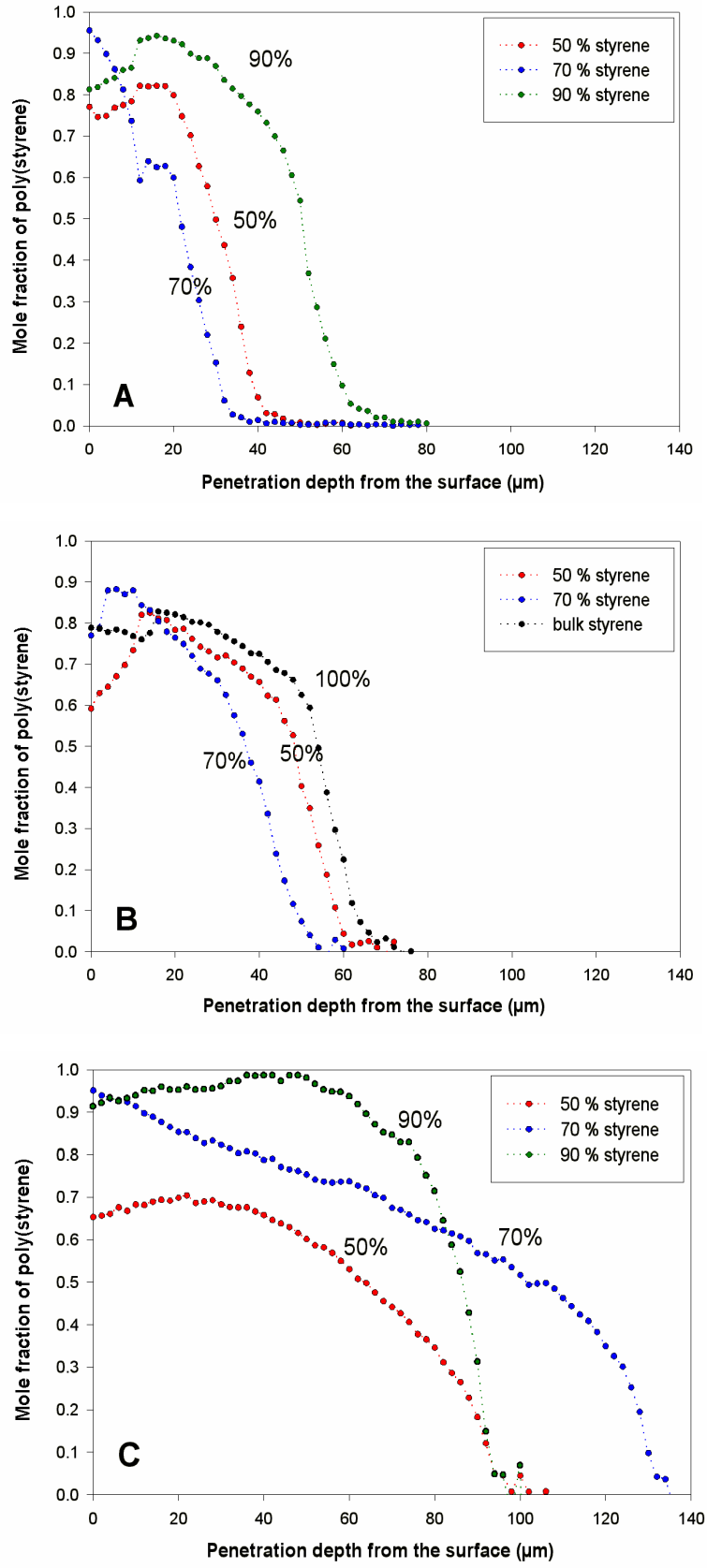

Figure 6.14 Profiles of the mole fraction of PS into graft copolymers prepared by grafting in styrene dissolved in: (A) methanol; (B) toluene (note: bulk styrene is included in this profile); (C) dichloromethane. The total dose for all samples was 15 kGy at a dose rate of 0.69 kGy hr^{-1}.

The profiles in Figure 6.14 show that as with the vapour-phase grafted films, there was not a sharp boundary between the PS graft and the PFA substrate, but rather the grafted layer was a mixture of the two polymers. Even at the edge of the cross-sections the graft never reached a mole fraction of 1.0. This is consistent with the graft growing inwards from the surface forming a PS/PFA boundary, the thickness being dependent on the conditions employed for the grafting reaction.

It is clear from Figure 6.14 that the penetration of the graft into the PFA substrate was greatest when dichloromethane was used as a solvent for styrene across the entire concentration range examined. This result is reflected in the relatively high graft yield as seen earlier in Figure 6.10. Conversely, when methanol was used as the solvent, the penetration was relatively shallow, while when toluene was used it lay somewhere between the penetration depth for when methanol and dichloromethane were used. When styrene was grafted to PFA without using a solvent (this profile is shown in Figure 6.14 B), the penetration was deeper than when methanol or toluene were used, but shallower than when dichloromethane was used. These observations may be explained in terms of the ability of each of the solvent / monomer solutions to swell the grafted layers and PFA substrate. Nasef showed that a mixture of 60 % v/v styrene in methanol, benzene or dichloromethane swelled thin films of ungrafted PFA by 0.17, 0.22 and 0.4 %, respectively.[13] While Nasef did not report the swelling ability of toluene, it may be assumed that it would give a comparable result to that reported for benzene, based on their similar polarity. However, it is not just the swelling of the untreated polymer substrate which is important in the penetration of the graft. The swelling of the grafted layer, which as the Raman maps show is composed of *both* PFA and PS, is also critical. No data is available on the solubility of PFA-PS copolymers in styrene / solvent mixtures, however some predictions may be made based on their individual solvent strengths. Toluene, dichloromethane and styrene are all solvents for PS, while methanol is a non-solvent. A mixture of dichloromethane and styrene may be expected to be a good swelling solvent for PFA / PS grafted layers as long as the styrene content is not too high, while a toluene / styrene mix may swell the graft to a similar extent over a broad concentration range. A methanol / styrene mix conversely would precipitate the graft and force the chains to lie flat on the surface at high methanol concentration, whereas, at high styrene concentration, the swelling properties would be more like that of styrene.

When methanol was used as a grafting solvent, the penetration of the graft was relatively shallow as indicated by the Raman maps in Figure 6.14 A for 50, 70 and 90 % v/v styrene in methanol. The difference in the penetration depth for samples grafted in 50 and 70 % v/v styrene is within the error of the measurements, however, the sample grafted with 90 % v/v styrene obviously had graft penetrating significantly further into the substrate. At this concentration the methanol may be considered to be present in only additive amounts and the resulting graft distribution is similar as if bulk styrene (see Figure 6.14 B) were used.

When toluene was used there was no significant difference in the penetration depths between 50, 70 % v/v styrene and bulk styrene. This is presumably due to the similar polarity of toluene and styrene and is also reflected in the similar graft yields at these concentrations from Figure 6.10 in Section 6.4.3.

The depth profiles of the graft for samples grafted in dichloromethane show that the dichloromethane is very effective in enabling the styrene to penetrate deep into the PFA matrix. From the plots in Figure 6.14 C it is quite clear why the graft yield is so much higher when dichloromethane was used as a solvent compared with any of the other solvents used. When 50 % v/v styrene in dichloromethane was used, the penetration was deep but the mole fraction of PS was less than 0.7 at its maximum. Using 70% v/v styrene resulted in a higher mole fraction of PS in the graft which meant the graft was more “PS-like” and less “PFA-like” and hence swelled more allowing greater penetration of the graft front. Using 90 % v/v styrene something different happened. As mentioned earlier in Section 6.4.3, at high percentage of styrene in the graft solution, there was higher viscosity in the graft layers due to homopolymer formation and a lower percentage of dichloromethane which led to lower swelling of the graft and consequently less penetration. Accompanying the lower penetration was a higher mole fraction of PS in the graft.

6.4.5 Molecular Weight Distribution of the Homopolymer

It is evident that homopolymer formation plays a pivotal role in the grafting reactions. In addition, the molecular weight distribution (MWD) of the grafted chains is of interest for the optimization of the graft copolymer for use in SPOC. Unfortunately, since the graft is formed through a C–C bond between the PFA and the grafted PS it is not possible to selectively cleave the graft as has been done for cellulose-*g*-PS.[39] Instead, the MWD of the homopolymer was measured and used as an estimate of the MWD of the graft. Other workers have done this for grafted polyolefins,[40] however, it is believed that this is the first time the homopolymer formation has been investigated for a range of solvents when grafting to a fluoropolymer.

Since the simultaneous radiation-grafting method was used, homopolymer formed not only in the solutions surrounding the graft copolymer, but in the swollen grafted regions as well. To distinguish between the homopolymer formed in these two regions, the homopolymer formed in the grafted regions will be referred to as occluded homopolymer, while the polymer formed in solution will be referred to as free homopolymer. The latter was isolated by simply decanting the excess solution after grafting followed by precipitation into methanol and isolation by filtration, while the former was isolated by soaking the grafted copolymers in a known volume of tetrahydrofuran (THF) for 48 hours to extract the occluded homopolymer. It should be noted that the MWD of the occluded homopolymer for the vapour-phase grafting was not measured as the amounts of homopolymer formed around the sample was less than is practical for SEC sample preparation.

The conversion of the isolated free homopolymer is presented in Table 6.2 for each of the solvents studied. With the exception of toluene and dilute alcohol solutions, addition of solvents increased the percent conversion compared with bulk styrene. The low conversion values in Table 6.2 reported for dilute alcohol solutions was due to loss of very fine homopolymer particles during the filtration step leading to lower than expected values. The effect of the solvents was to act as additional initiation sources via radical fragments formed as a result of the exposure to radiation.

Table 6.2 Percentage conversion of styrene to PS for each solvent over a concentration range. The total dose was 15 kGy at a dose rate of 0.69 kGy hr^{-1}.

	% Conversion					
Styrene concentration (vol %)	MeOH	EtOH	MeCN	Toluene	CH_2Cl_2	Bulk styrene
20	...	...	...	5.1	...	-
30	2.4	...	6.1	5.1	11.1	-
40	1.4	4.8	6.5	6.0	11.0	-
50	5.8	7.0	7.3	5.1	10.8	-
60	8.0	9.8	7.7	6.1	10.6	-
70	10.1	11.5	8.6	5.1	9.8	-
80	13.3	11.4	8.6	5.6	9.1	-
90	14.3	10.7	-	-	9.1	-
100	-	-	-	-	-	5.1

... indicates that no homopolymer was isolated because it was too fine for the filters used.

THF solutions of occluded and free homopolymer were analyzed by SEC. The concentration of occluded homopolymer in the THF solutions was calculated from lanterns which were grafted in parallel and dried and weighed before and after washing of the occluded homopolymer. Some of the key SEC chromatograms are presented in Figure 6.15.

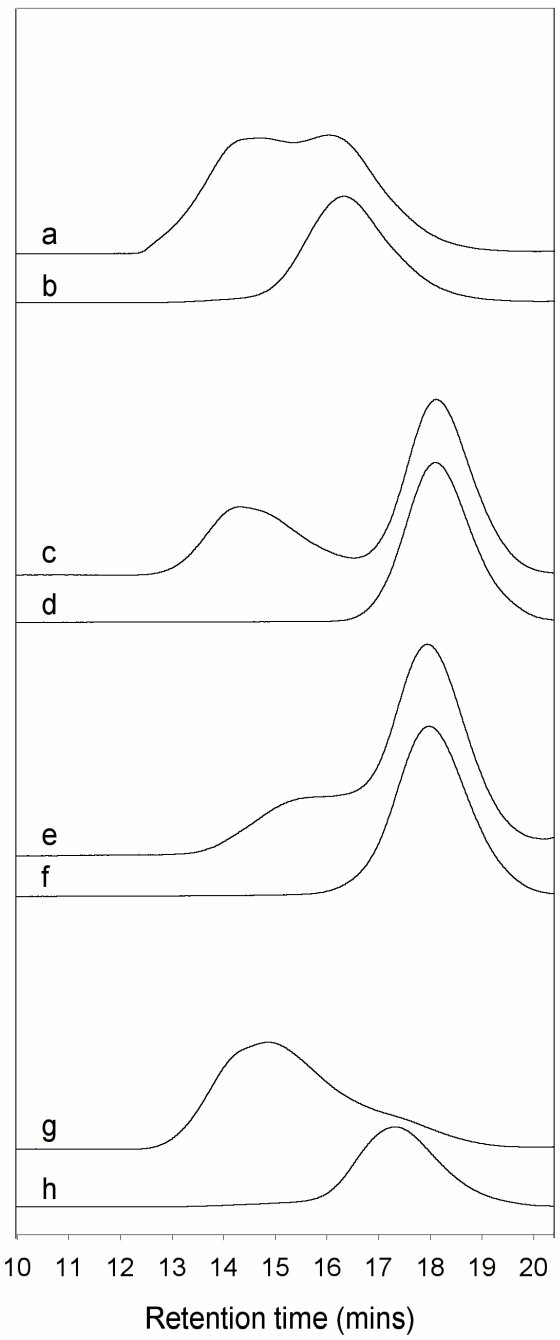

Figure 6.15 SEC traces of homopolymer isolated from the grafting reactions: (a) occluded and (b) free homopolymer from bulk styrene; (c) occluded and (d) free homopolymer from methanol solutions; (e) occluded and (f) free homopolymer from dichloromethane solutions; (g) occluded and (h) free homopolymer from toluene solutions. The concentration except for the bulk styrene experiments was 50 % v/v styrene in each case and the total dose was 15 kGy.

The traces of occluded homopolymer (Figure 6.15 a, c, e, g) show bimodal MWDs consisting of residual free homopolymer (Figure 6.15 b, d, f, h) and a higher molecular weight (earlier retention time) component. The MWD of the occluded homopolymer was

calculated by subtracting the free homopolymer component of the chromatograms b, d, f and h to give a chromatogram approximating the occluded polymer. The number-average (M_n) and weight-average (M_w) molecular weights and the polydispersity (PD) were calculated using Equations 1-3:

Equation 1 $M_n = \sum n_i.M_i / \sum n_i = \sum H_i / \sum H_i / m_i$

Equation 2 $M_w = \sum n_i.M_i^2 / \sum n_i.M_i = \sum M_i.H_i / \sum H_i$

Equation 3 $PD = M_w / M_n$

where M_i is the molecular weight of a molecule and n_i is the number of such molecules. These values were extracted from the chromatograms using H_i as the detector response and m_i as the molecular weight at this detector response, obtained from the calibration curve. In each case the PD was 2.0 – 2.1, consistent with a random MWD.[41] The termination mechanism for conventional free radical polymerization of bulk styrene is mainly by combination (77 %) and to a less extent by disproportionation (23 %) which would lead to PD closer to 1.5.[42] However, in the grafting system the presence of solvents will mean that termination by chain transfer to the solvent or by combination with small radical fragments will play an important role. A feature of radiolysis is that it attacks all components in the system including the solvent which may explain why the PD was higher than for conventional free radical polymerization.

The calculated M_n values of the free and occluded homopolymer for samples grafted with bulk styrene and 50 % v/v solutions are shown in Table 6.3. The lower M_n values of the free homopolymer when solvents were used compared with when bulk styrene was used is consistent with lower monomer availability and additional termination by chain transfer to the respective solvents. The order of the chain transfer constants are: methanol (0.3) > dichloromethane (0.15) > toluene (0.11).[43] This is reflected in the MWD of the free homopolymer where MWD in methanol < dichloromethane < toluene. The same trend was not observed for the occluded homopolymer and obviously the mobility of the growing PS chains is important. The higher molecular weight polymer can be considered to originate in the highly viscous swollen grafted regions where motion of the growing chains

is restricted and the rate of termination by mutual combination is lowered. While it is not certain that the MWD of the graft is the same as that of the occluded homopolymer, given that the two were formed in the same region with the same local viscosity, then it is reasonable to suggest that they have approximately the same MWDs. For bulk styrene and each of the three solvents used, the molecular weight of the occluded homopolymer was significantly higher than the molecular weight of the free homopolymer. Assuming similar MWD for the occluded and graft polymer, the grafts also had higher molecular weight than the free homopolymer. If this is the case then it may be inferred that the MWD of the graft when toluene and methanol were used as solvents for styrene was higher than when dichloromethane was used.

Table 6.3 Number-average molecular weight (M_n) of the free and occluded homopolymer for each of the solvents used. The concentration was 50 % v/v styrene.

	M_n (free)	**M_n (occluded)**
Bulk styrene	5.2×10^4	5.2×10^5
Methanol	9.8×10^3	3.9×10^5
Dichloromethane	1.2×10^4	1.5×10^5
Toluene	2.1×10^4	3.1×10^5

In Chapter 3 the approximate average molecular weight of the PFA chains was calculated as being at least 1.2×10^5 g mol.$^{-1}$, based on the NMR data. This lower limit estimate of the molecular weight is of the same order of magnitude as the molecular weight of the grafted PS, assuming the occluded homopolymer molecular weight is a reasonable estimate of the grafted PS molecular weight. The highest mole fraction of PS in the grafts from the Raman mapping data was approximately 0.97 mole fraction which equates to 97 PS chains for every 3 PFA chains. In most cases, the average mole fraction of PS across the grafted layer was closer to 0.5, or a 1:1 ratio of PS chains to PFA chains. At a molecular weight of 1.2×10^5 g mol.$^{-1}$, each PFA chain has 2.4×10^3 CF_2 units, of which on average only one, or 0.04 % of these units is a graft point if the mole fraction of PS of 0.5. At such low proportion of graft points per average PFA chain, it is unlikely that the graft points could be detected by any analytical method. NMR work (not presented) supported this conclusion.

6.4.6 Loading of Grafted Substrates

Loading tests were performed on the grafted copolymers to determine which are most suitable for SPOC. The loading test is a measure of how much of the grafted PS can be bonded with a linker and functional group. The test is performed by bonding a Fmoc-Rink group to the available PS then cleaving the Fmoc groups.[44] By measuring the intensity of the ultra-violet absorption of the cleaved groups in solution, the amount of Fmoc-Rink which was loaded onto the solid support can be calculated. The mechanism of the Fmoc-Rink test is shown in Scheme 6.1.

To obtain meaningful results from the Fmoc-Rink loading tests, scale-ups of the grafting reactions were done to obtain five lanterns grafted under each of the conditions chosen so that the loading results were an average of five separate experiments. Lanterns were grafted using bulk styrene, styrene vapour and styrene in methanol, toluene and dichloromethane. The concentrations of the solutions used are shown in Table 6.4. The doses used for each condition were chosen so that the graft yield in each case was similar. Apart from the dilute methanol solutions, the graft yield in all cases was between 12 and 16 %. The loading figures in Table 6.4 were expressed in terms of the graft yield so that a direct comparison could be made for all the lanterns prepared using the different grafting conditions. The loading tests show that lanterns grafted in styrene vapour had higher loading than lanterns grafted in bulk styrene for similar graft yields. While a direct comparison was not made using the Raman mapping for lanterns grafted under these two conditions, it may be assumed that the higher surface grafting characteristic of vapour-phase grafting was responsible for the better loading performance of the vapour-phase grafted samples due to better accessibility of the reagents during the loading reactions.

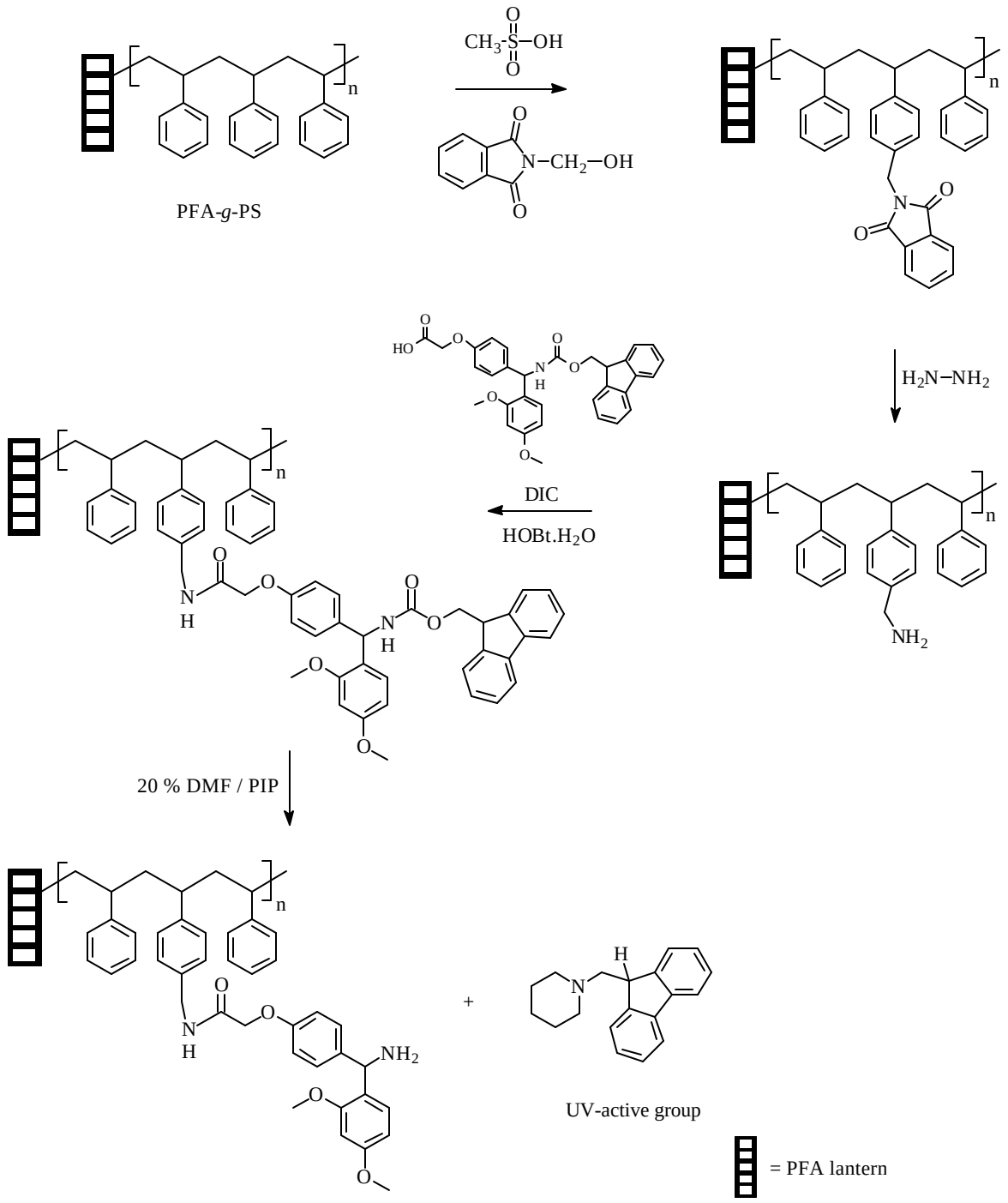

Scheme 6.1 Mechanism of the Fmoc-Rink loading test.

Table 6.4 Results of Fmoc loading tests.

Solvent	% styrene (v/v)	Total dose used (kGy)	Graft Yield (%)	Loading (µmol / lantern)	Loading / mg of graft
Styrene (bulk)	100	12	13	27	2.0
Styrene (vapour)	n.a.	15	16	65	4.0
Methanol	30	30	5	27	5.5
Methanol	50	15	8	46	5.7
Methanol	70	12	12	57	4.8
Toluene	50	15	12	11	1.0
Dichloromethane	50	15	13	3	0.2

When solvents were used in the grafting reactions, the resulting grafted lanterns exhibited a wide range of loading capacities. While the highest graft yield was observed when dichloromethane was used as a solvent, these lanterns had the lowest loading of 0.2 µmol. per mg of PS graft. This result stemmed from the distribution of the graft into the PFA. Since most of the graft was buried below the surface, the reagents used to functionalize the PS would not be able to reach the majority of the graft. Conversely, lanterns grafted in methanol solutions exhibited good loading characteristics. Unfortunately comparison of the loading results of the three different concentrations was difficult because of the variation in graft yield over the concentration range, however there does not appear to be a great difference when the loading is expressed in terms of loading per mass of graft. The high loading of PFA grafted in methanol solutions can be attributed to the graft being limited to the near surface area. The loading for samples grafted in toluene solutions, like the depth profiles from microprobe Raman spectroscopy, was between that of samples grafted using methanol and dichloromethane.

6.5 Conclusions

Grafted solid supports have been prepared which may be used in high temperature SPOC applications. To obtain these supports, a number of different grafting conditions were examined, including vapour-phase grafting and solution-phase grafting. The graft copolymers were characterized in terms of their graft yield and the penetration of the graft into the substrate using microprobe Raman spectroscopy. The vapour-phase grafting was found to be diffusion controlled at low grafting times and at dose rates of 2.8 kGy hr^{-1} or below. At higher grafting times the factors influencing the grafting such as changes in crystallinity, radical-radical recombination reactions and possibly loss of vapour pressure due to homopolymerization of the feed monomer led to deviation from independence on the dose rate.

Solution-phase grafting was shown to be highly dependent on the solvents and the concentrations in which they were used in terms of the graft yield, penetration profile of the graft and loading characteristics. The penetration depth of the grafts decreased in the order: dichloromethane > toluene > methanol. Despite grafting reactions performed in methanol having low graft yield and penetration, the loading tests showed that this was the most successful solvent for preparing supports for SPOC. The molecular weight of the homopolymer formed in the grafted regions was significantly higher than that formed in the surrounding solutions which would suggest the same may be true of the graft.

6.6 References

1. Chapiro, A., *J. Polym. Sci.* **34**, 481-501 (1959).

2. Chapiro, A., Matsumoto, A., *J. Polym. Sci.* **57**, 743-761 (1962).

3. Gupta, B., Scherer, G. G., *Chimia* **48**, 127-137 (1994).

4. Hegazy, E. A., Ishigaki, I., Okamoto, J., *J. Appl. Polym. Sci.* **26**, 3117-3124 (1981).

5. Hegazy, E. A., El-Assy, N. B., Rabie, A. M., Ishigaki, I., Okamoto, J., *J. Polym. Sci.* **22**, 597-604 (1984).

6. Hegazy, E. A., Dessouki, A. M., Rabie, A. M., Ishigaki, I., *J. Polym. Sci. Polymer Chem Ed.* **22**, 3673-3685 (1984).

7. Hegazy, E. A., Taher, N. H., Kamal, H., *J. Appl. Polym. Sci.* **38**, 1229-1242 (1989).

8. Hegazy, E. A., Taher, N. H., Ebaid, A. R., *J. Appl. Polym. Sci.* **41**, 2637-2647 (1990).

9. Hegazy, E. A., Osman, M. B. S., Mokhtar, S. M., Mostafa, A. E. B., *Polymer* **33**, 4230-4235 (1992).

10. El-Sawy, N. M., Hegazy, E. A., Rabie, A. M., Hamed, A., Miligy, G. A., *Polym. Int.* **33**, 285-291 (1994).

11. Gupta, B., Buchi, F., Scherer, G. G., *J. Polym. Sci., A, Polym. Chem.* **32**, 1931-1938 (1994).

12. Nasef, M. M., Saidi, H., Nor, H. M., Dahlan, K. Z. M., Hashim, K., *J. Appl. Polym. Sci.* **73**, 2095-2102 (1999).

13. Nasef, M. M., *Polym. Int.* **50**, 338-346 (2001).

14. Gupta, B. D., Chapiro, A., *Eur. Polym. J.* **25**, 1145-1148 (1989).

15. Walsby, N., Paronen, M., Juhanoja, J., Sundholm, F., *J. Polym. Sci., A, Polym. Chem.* **38**, 1512-1519 (2000).

16. Brack, H., Buhrer, H. G., Bonorand, L., Scherer, G. G., *J. Mater. Chem.* **10**, 1795-1803 (2000).

17. Kamel, I., Machi, S., Silverman, J., *J. Polym. Sci., Part A-1* **10**, 1019-1029 (1972).

18. Smekal, A., *Naturwiss.* **11**, 873 (1923).

19. Raman, C. V., Krishnan, K. S., *Nature* **121**, 501 (1928).

20. Landsberg, G., Mandelstam, L., *Naturwiss.* **16**, 557 (1928).

21. Keen, I., Rintoul, L., Fredericks, P. M., *Macromolecular Symposia* **184**, 287-298 (2002).

22. Imai, M., *J. Polym. Sci., A, Polym. Chem.* **14**, 2887-2894 (1976).

23. Yamamoto, F., Yamakawa, S., Kato, Y., *J. Polym. Sci., A, Polym. Chem.* **16**, 1883-1895 (1978).

24. Yamamoto, F., Yamakawa, S., Kato, Y., *J. Polym. Sci., A, Polym. Chem.* **16**, 1897-1907 (1978).

25. Austin, M. E., Busfield, W. K., Pomery, P. J., *Eur. Polym. J.* **31**, 683-687 (1995).

26. Hegazy, E. A., Dessouki, A. M., El-Assy, N. B., El-Sawy, N. M., El-Ghaffar, M. A. A., *J. Polym. Sci., A, Polym. Chem.* **30**, 1969-1976 (1992).

27. Nasef, M. M., Saidi, H., Dessouki, A. M., El-Nesr, E. M., *Polym. Int.* **49**, 399-406 (2000).

28. Keen, I., Rintoul, L., Fredericks, P. M., *Appl. Spec.* **55**, 984-991 (2001).

29. Legeay, G., Coudreuse, A., Legeais, J.-M., Werner, L., Bulou, A., Buzare, J.-Y., Emery, J., Silly, G., *Eur. Polym. J.* **34**, 1457-1465 (1998).

30. Cutler, D. J., Hendra, P. J., Rahalkar, R. R., Cudby, M. E. A., *Polymer* **22**, 726-730 (1981).

31. Tan, K. L., Woon, L. L., Wong, H. K., Kang, E. T., Neoh, K. G., *Macromolecules* **26**, 2832-2836 (1993).

32. Hietala, S., Holmberg, S., Karjalainen, M., Nasman, J., Paronen, M., Serimaa, R., Sundholm, F., Vahvaselka, S., *J. Mater. Chem.* **7**, 721-726 (1997).

33. Chapiro, A. Radiation Chemistry of Polymeric Systems. In: *High Polymers;* Mark, H.; Marwell, C. S.; Melville, H. W. Eds.; Interscience: New York, 1962; Vol. XV.; p. 598.

34. Odian, G., Henry, R., Koenig, R., Mangaraj, D., Trung, D., Chao, B., Derman, A., *J. Polym. Sci., Polym. Chem.* **13**, 623 (1975).

35. Machi, S., Kamel, I., Silverman, J., *J. Polym. Sci., Part A-1* **8**, 3329-3337 (1970).

36. Cardona, F., George, G. A., Hill, D. J. T., Rasoul, F., Maeji, J., *Macromolecules* **35**, 355-364 (2002).

37. Nasef, M. M., Saidi, H., Nor, H. M., *J. Appl. Polym. Sci.* **76**, 220-227 (2000).

38. Cardona, F. (University of Queensland), Personal Communication

39. Garnett, J. L., Jankiewicz, S. V., Sangster, D. F., *Radiat. Phys. Chem.* **36**, 571-579 (1990).

40. Berg, R. H., Almdal, K., Pedersen, W. B., Holm, A., Tam, J. P., Merrifield, R. B., *J. Am. Chem. Soc.* **111**, 8024-8026 (1989).

41. Rudin, A. Molecular Weight Distributions. In: *Comprehensive Polymer Science;* Allen, G.; Berington, J. C. Eds.; Pergamon Press: Oxford, 1989; Vol. 3; pp. 239-244.

42. Allcock, H. R., Lampe, F. W. *Contemporary Polymer Chemistry*; Prentence Hall, Inc.: New Jersey, 1981.

43. Brankdrup, J., Immergut, E. H. Polymer Handbook; John Wiley and Sons: New York, 1999.

44. Maeji, N. J., Valerio, R. M., Bray, A. M., Campbell, R. A., Geysen, H. M., *React. Polym.* **22**, 203-212 (1994).

Chapter 7

7 Grafting II – Grafting by "Living" Polymerization

7.1 Introduction

Controlled or "living" polymerizations have aroused intense interest from polymer chemists in the past few years due to of the prospect of alleviating many of the limitations of free radical polymerization. Some of these limitations arise from the lack of control of the process, leading to structures with undefined molecular weight distribution, structure and end groups. Controlled polymerizations offer the prospect of narrow polydispersity homopolymers, high purity block copolymers and end functionalized polymers.[1]

The forms of controlled polymerizations available include nitroxide-mediated "living" free radical polymerization,[2] atom transfer radical polymerization (ATRP)[3-5] and reversible addition fragmentation chain transfer (RAFT) polymerization.[6,7] Of these "living" free radical polymerization (LFRP) techniques, this chapter will only be concerned with using nitroxides as the LFRP agent, although all three methods are based on the same premise that the growing chains permanently undergo reversible dissociation of the end groups.

The synthesis of well-defined polymers by "living" free radical methods was first demonstrated by Rizzardo and coworkers in the early 1980s using stable nitroxide free radicals.[2] Nitroxide species, when used in certain polymerizations, act to mediate the reactivity of the growing polymer chains by forming thermally unstable alkoxy amine chain ends. An equilibrium is formed between the dormant alkoxy amine chain ends and active free radical chain ends upon homolysis of the carbon-oxygen bond of the alkoxy amine (Scheme 7.1). In the free radical state, more monomer units can add before the growing chains are reversibly terminated by the nitroxide radical. The reversible reaction between active and dormant chain ends gives the polymerization a "living" character.

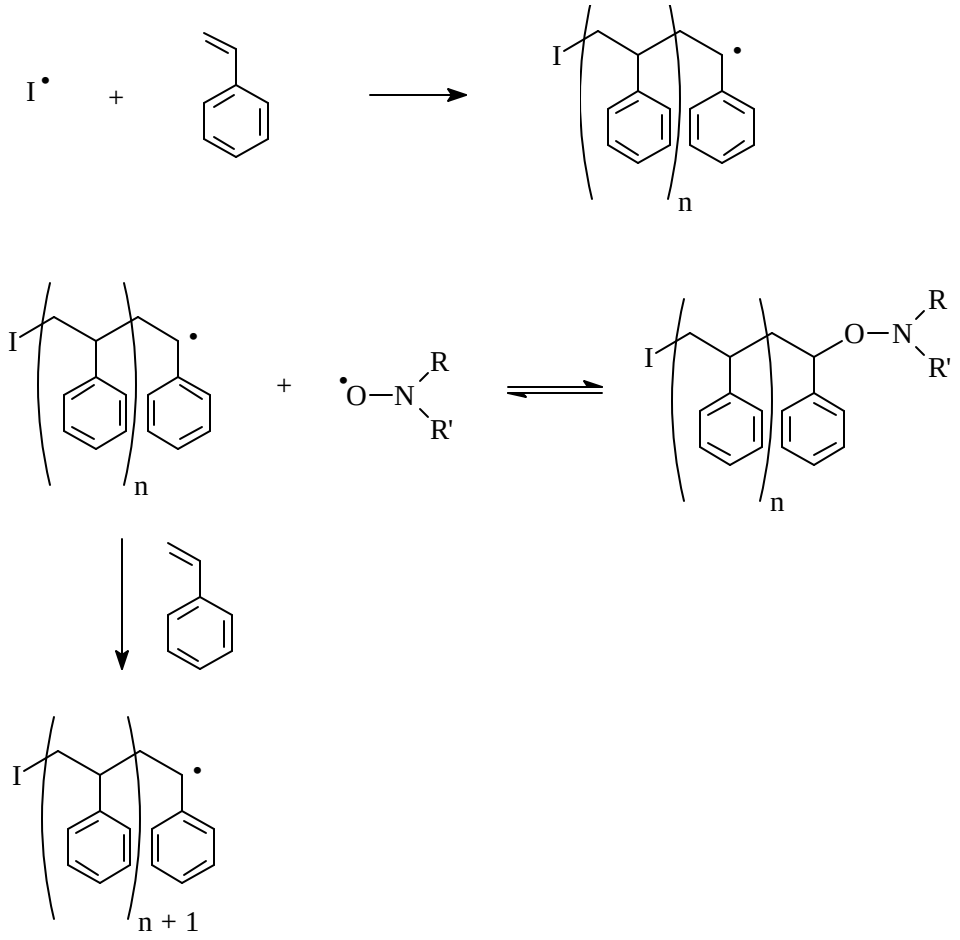

Scheme 7.1 Proposed mechanism for nitroxide-mediated polymerization.

This technique has enabled control of chain ends, molecular weight and macromolecular architecture for the polymerization of a number of monomers.[8-11] The polydispersity attainable with nitroxide-mediated polymerization is typically below 1.5 (conventional radical polymerization with termination by chain transfer or disproportionation will give polydispersity of approximately 2.0, or 1.5 for combination termination).[1,12]

Normally nitroxide-mediated LFRPs are performed by adding an initiator and a nitroxide to bulk monomer and heating between 353 and 408 K. At these temperatures the alkoxy amine will readily dissociate so that additional monomer units can add to the growing chains before being capped by the nitroxide. This process of dissociation, monomer addition, and re-association continues until either all the monomer is consumed or the reaction is stopped by the operator.

The linear, narrow molecular weight distribution polymers attainable using LFRP potentially have an application in SPOC since well-defined, uniform solid supports, in the form of a surface or a bead, may be expected to lead to better loading and reaction kinetics. Recently, workers at the Park-Davis laboratories reported using nitroxide-mediated LFRP to graft what was believed to be long straight chain polymers bearing functional groups to a crosslinked PS core (Merrifield resin).[13] These resins, called "Rasta" resins (Figure 7.1 A), when prepared using styrene and 3-isopropenyl-*a*,*a*-dimethylbenzyl isocyanate (TMI) monomers to incorporate isocyanate functional groups, (Figure 7.1 B) exhibited higher loading than Merrifield resin. Optical analysis experiments bonding fluorescence probes to the isocyanate moieties showed that the isocyanate groups were distributed throughout the entire resin, suggesting that during the LFRP step the reagents are free to diffuse throughout the Merrifield resin.[14] Control of the polymerization allows the customized spacing of the functional groups through judicious choice of comonomers and fine-tuning of solvent affinity.

A B

Figure 7.1 (A) Cartoon picture of "Dreadlocked" "Rasta" resin; (B) TMI / styrene "Rasta" resin (taken from reference [13]).

Other high-loading resins have also been reported using dendrimers bound to a resin core,[15] however, in this case the dendrites were part of the linker groups and not the polymeric substrate and will not be discussed further other than to mention that it demonstrates the potential of well-defined supports for high loading.

Graft copolymers have been prepared using LFRP by including an alkoxy amine in the backbone of the base polymer during the synthesis step.[16] Grafting involves heating the backbone polymer with incorporated alkoxy amine groups in the presence of a monomer to form a graft copolymer with controlled molecular weight. While this chapter of the thesis is mainly concerned with using nitroxide LFRP to form graft copolymers, it should be noted

that other "living" techniques have been used to prepare graft copolymers. Recent examples include the use of ATRP to control grafting of styrene to the fluoropolymer PVDF,[17] and the use of RAFT to graft various monomers to polypropylene.[18]

A novel method for using nitroxide-mediated LFRP to graft a polymer to a pre-existing polymer was recently demonstrated by Miwa *et al.*[19] Using the pre-irradiation peroxy grafting method (outlined in Chapter 1, Section 1.5.1), these workers were able to graft styrene to polypropylene with control of the molecular weight of the graft using the classical nitroxide, 2,2,6,6-tetramethyl-1-piperidinyloxy (TEMPO). Their method involved initially irradiating polypropylene in the presence of air to create hydroperoxy groups. Styrene and TEMPO were then added to the irradiated polypropylene and heated. The hydroperoxy groups decomposed to form oxy radicals, which initiated the graft copolymerization of styrene (Scheme 7.2). A consequence of using oxy radicals as the initiating species was that an ether group was formed between the polymer substrate and the graft. Miwa *et al.* exploited the presence of the acid sensitive ether group by selectively cleaving the graft through the ether bond by treatment with trifluoroacetic acid in toluene. This allowed the measurement of the MWD of the cleaved graft using SEC. Comparison of the MWD of the graft and free homopolymer revealed little difference between the two. It is interesting to note that they were only able to cleave approximately 1 % of the grafted chains by treatment with acid. The end groups of the cleaved PS were identified as hydroxy groups by NMR, thereby proving that the PS isolated was not a product of thermal auto-initiation. Unfortunately, when the hydroperoxy groups on the polypropylene decompose to form oxy radicals during the grafting reactions, they produce $^{\bullet}$OH radicals capable of initiating homopolymerization of styrene.[20] Therefore, while much of the homopolymer may be expected to have end groups resulting from thermal auto-initiation,[21] in this case there may also be some homopolymer formed from reaction of styrene with $^{\bullet}$OH radicals. Hence, it may be possible that Miwa *et al.* may have simply removed occluded homopolymer during their cleavage reaction, which would explain why most of the graft remained bonded to the polypropylene substrate after the cleavage reaction.

The pre-irradiation peroxy method has draw-backs when grafting to PFA where the application is for SPOC supports. Firstly, PFA becomes very brittle when irradiated in air.[22] Secondly, the presence of acid sensitive ether groups is undesirable when the graft

copolymer is used for SPOC as strong acid treatment is regularly used to deprotect groups during synthesis steps. To overcome these problems the vacuum pre-irradiation method was used where PFA is irradiated in vacuum to create carbon-centred radicals before the nitroxide / styrene solution is added.

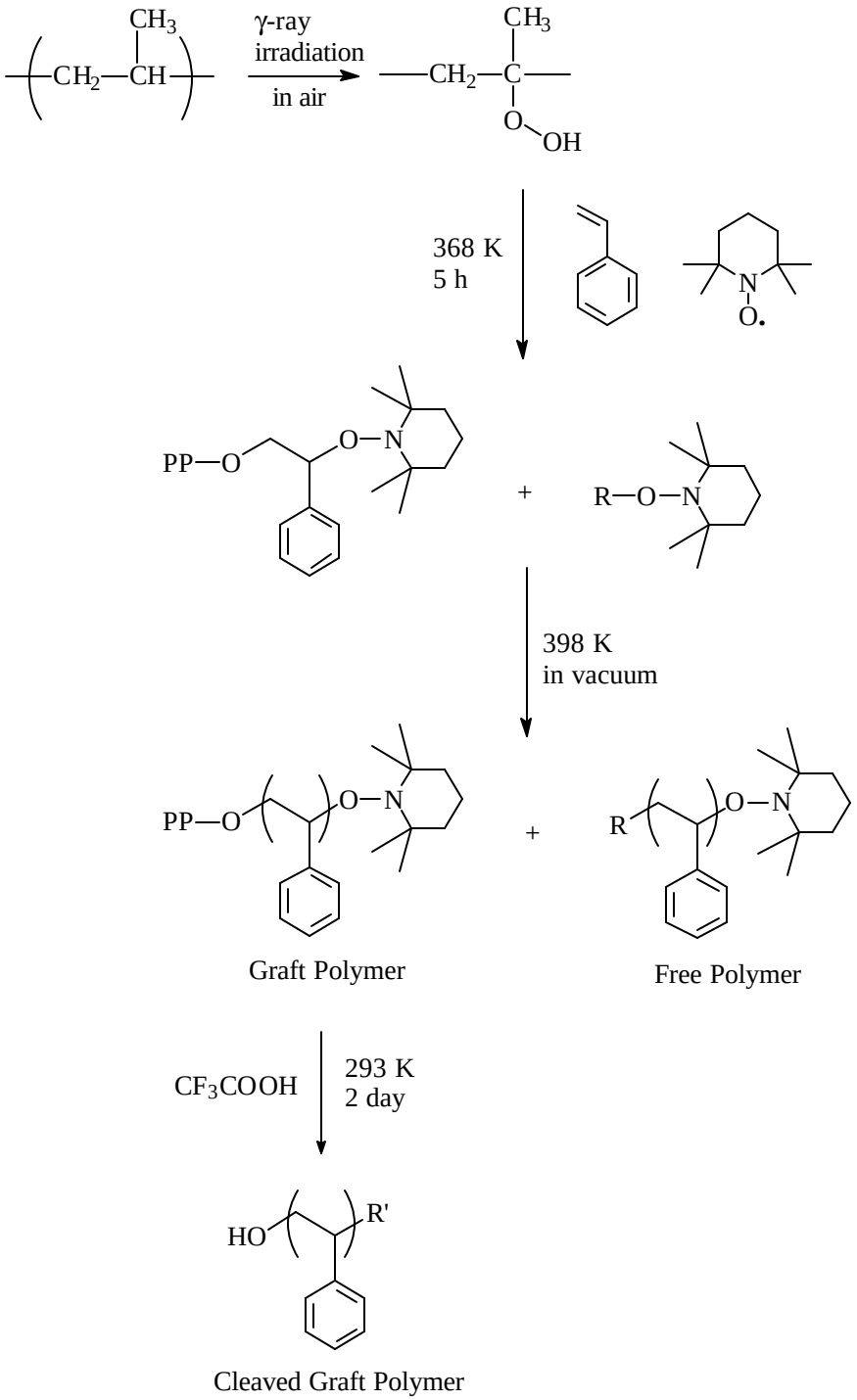

Scheme 7.2 Reaction scheme of graft polymerization of styrene to PP. Taken from Miwa *et al.*[19]

7.2 Experimental

7.2.1 Reagents

Styrene (Fluka) was passed through a column of alumina oxide then distilled under reduced pressure just prior to use. 2,2,6,6-Tetramethyl-1-piperidinyloxy (TEMPO) (Aldrich) was used as received. 1,1,3,3-Tetraethylisoindolin-2-yloxyl (TESIO) was kindly donated by Urs Wermuth from Griffith University and recrystallized from *n*-pentane before use. Dichloromethane used for washing was reagent grade and used as received.

7.2.2 Grafting

Grafting of styrene to PFA was performed using the pre-irradiation method in vacuum. PFA (Du Pont, code TE 7132), injection molded lanterns with rings of 0.5 mm in thickness were evacuated at 1×10^{-2} Pa in glass tubes for 24 hours and sealed. The samples were then irradiated at 300 K in a 220 Nordian Gammacell to a dose of 20 kGy at a dose rate of 4.7 kGy hr^{-1}. Nitroxide solutions were prepared by dissolving either TEMPO or TEISO in styrene (5 mL) to make up to the desired concentration. The nitroxide solutions were added to the irradiated PFA under a stream of nitrogen gas through a tap fitted with rubber o-rings. The tubes were then degassed by three freeze-pump-thaw cycles and sealed under vacuum by melting a narrow neck in the glass. The tubes containing irradiated PFA, styrene and the nitroxide were then heated in an oil bath at 373 ± 2 K for 40 hours. The tubes were then opened and the grafted PFA washed overnight with dichloromethane in a Soxhlet-extractor to remove any non-reacted styrene and occluded homopolymer. The grafted PFA samples were then dried under vacuum. The graft yield was determined as the weight of the graft as a percentage of the initial weight of the PFA.

7.2.3 Differential Scanning Calometry

A Perkin Elmer DSC7 was used to perform DSC on sections of the grafting rings cut using a blade. Samples were heated under a nitrogen atmosphere from 323 to 633 K at 40 K min^{-1}, held at 633 K for one minute, then cooled to 303 K at 40 K min^{-1} using ice as

the coolant. For the ungrafted samples, the heat of fusion was taken from the peak area under the melting endotherm. For grafted samples, where the amorphous PS component dilutes the crystallinity, the heat of fusion for just the PFA component was calculated as:

$$\Delta H_{PFA} = \frac{\Delta H_{total}}{(W_{PFA} / W_{PFA+PS})}$$

where W_{PFA} and W_{PFA+PS} are the weight of the samples before and after grafting, respectively.

7.2.4 Microprobe Raman Spectroscopy

Details of the microprobe Raman are described in Chapter 6, Section 6.3.4.

7.2.5 Loading Tests

Details of the loading tests are described in Chapter 6, Section 6.3.6.

7.3 Results and Discussion

7.3.1 Nitroxide Effect on Graft Yield

The rate determining step in nitroxide LFRPs is the bond dissociation of the alkoxy amine group.[23,24] The rate of homolysis of the NO–C bond of the alkoxy amines is known to depend on a combination of steric compression around the NO–C bond, the stabilities of the radicals formed, and polar factors.[1] By varying the R and R' groups of the nitroxide shown in Scheme 7.1, the reactivity of the nitroxide can be modified.[10,11,21,25] Of the two nitroxides used for this work, the rate of homolysis of the NO–C bond is known to be more rapid for TEISO than for TEMPO (structures are shown in Figure 7.2).[25]

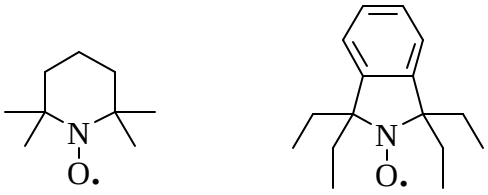

Figure 7.2 Structures of TEMPO (left); and TEISO (right).

The concentration of the nitroxide used in a thermally initiated styrene mixture influences the conversion and molecular weight distribution of the PS formed.[9,26] At low nitroxide concentration the system behaves more like a traditional free radical polymerization giving rise to high conversion, high molecular weight distribution, and wide polydispersity. If excess nitroxide is used there is a definite incubation period where little or no polymer is formed. Once all of the excess nitroxide is consumed the rate of conversion is similar to that observed for normal nitroxide-mediated LFRPs and polymers with narrow polydispersity and low molecular weight distribution are formed.

The effect of nitroxide concentration on the grafting of styrene to pre-irradiated PFA was investigated by using a range of nitroxide concentrations, from neat styrene to styrene with 3.6×10^{-2} M nitroxide. When the reaction was performed at room temperature with 4.6×10^{-3} M TEMPO no grafting or homopolymerization was observed, even after 100 hours, due to the stability of the alkoxy amine at this temperature. By way of

comparison, the same reaction at room temperature without any nitroxide led to a graft yield of 65 % after 40 hours.

By increasing the temperature of the reaction to 373 K the alkoxy amine groups can dissociate and the polymerization becomes "living". The effect of different concentrations of TEMPO and TEISO at 373 K on the graft yield is shown in Figure 7.3. The higher the nitroxide concentration, the lower the graft yield, although above 1×10^{-2} M nitroxide concentration any increase in concentration appeared to have little effect. Clearly the nitroxides lower the rate of polymerization although there was no significant difference in the graft yield when TEISO was used compared to when TEMPO was used.

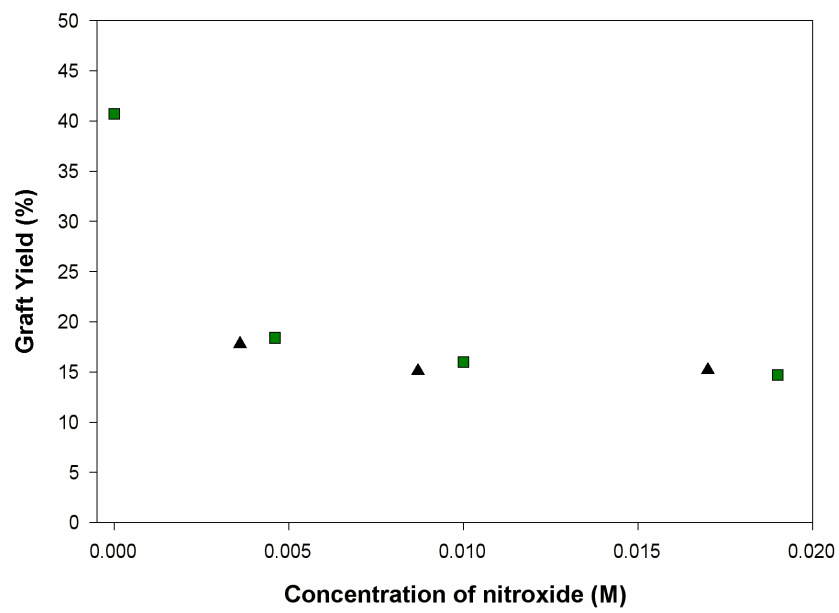

Figure 7.3 Graft yield for different nitroxide concentration when grafting styrene to PFA at 373 K – (|) TEMPO; (?) TEISO. The grafting time was 40 hours.

PFA swollen in styrene represents a highly viscous medium for grafting, which may explain why the degrees of grafting when TEISO was used were not higher than for TEMPO, as may be predicted from the more labile NO–C bond when TEISO forms an alkoxy amine. It is possible that mediation by the nitroxides used in this system is diffusion controlled and independent of the NO–C bond stability. Lutz *et al.* have reported experimental validation of kinetic models for nitroxide-mediated polymerization proposed by Fischer[27,28] and found that at high conversion, the experimental values deviated from

theoretical predictions and suggested that the behavior was due to viscosity effects.[29] When grafting styrene to PFA, the highly viscous grafting regions may be considered to mimic a polymerization which has gone to high conversion. It was therefore not surprising that the graft yield for TEMPO and TEISO did not obey the rules predicted by the NO–C bond strength.

7.3.2 Distribution of the Graft

The distribution of the graft and the accessibility of the graft to reagents are important factors when the grafted supports are to be used for SPOC. To measure the distribution of the graft, microprobe Raman spectroscopy was used to map cross-sections of the grafted supports. The well-resolved Raman shifts at 999 cm^{-1} for PFA and 734 cm^{-1} for PS were used as a measure of the PS distribution in the graft copolymer. The Raman map of a cross-section of PFA-*g*-PS with 4.6×10^{-3} M TEMPO is shown in Figure 7.4. The map for PFA grafted under the same conditions, only without any nitroxide, is shown in Figure 7.5. Without nitroxide added, the peak due to the PS graft was more intense relative to the peak due to PFA, while the opposite was true when nitroxide was used. TEMPO has an intense Raman shift at 847 cm^{-1} (Figure 7.6) which was not observed in the map spectra. This suggested that either the alkoxy amine end-groups were not present in high enough concentration to observe, or that the chain ends were "dead" as a result of termination by combination, disproportionation or chain transfer.

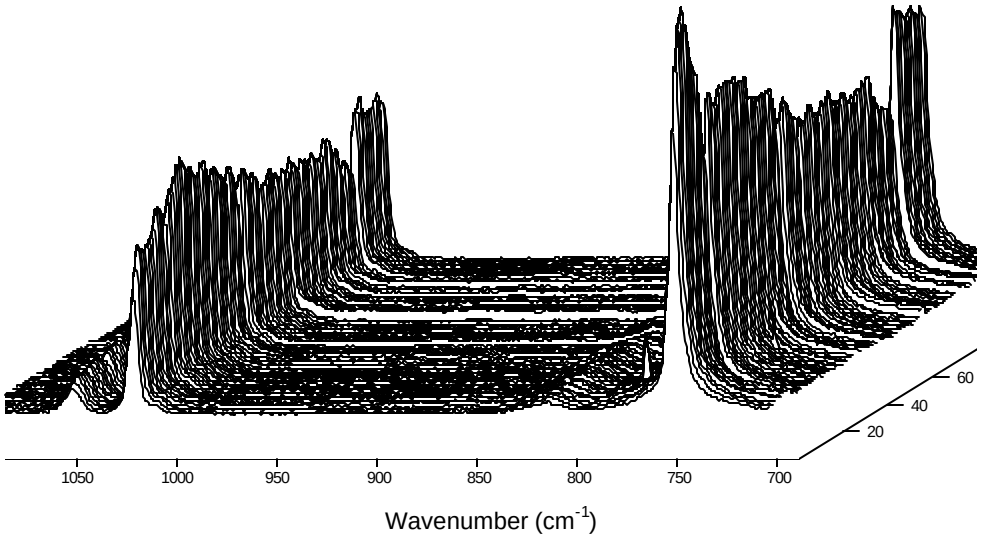

Figure 7.4 Raman map of a cross-section of PFA grafted with styrene with 4.6×10^{-3} M TEMPO.

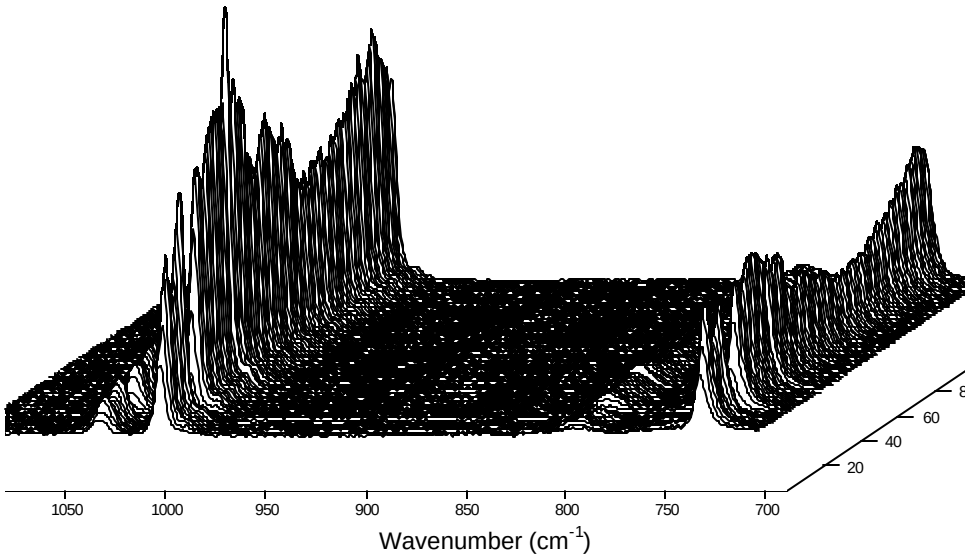

Figure 7.5 Raman map of a cross-section of PFA grafted with neat styrene.

A semi-quantitative measure of the distribution of PS graft in PFA was calculated from the maps and are shown in Figure 7.7. The penetration profiles have been expressed as the distance into the cross-sections as a percentage of the total thickness, since each grafted sample had a different thickness. It was assumed that the cross-sections were symmetrical and the other 50 % of the map was a mirror image to the first 50 %.

Figure 7.7 shows that the mole fraction of PS in the PFA decreased with increasing concentration of nitroxide. At 373 K with no nitroxide, the mole fraction of PS was between 0.5 and 0.65, whereas with TEMPO added the fraction of PS dropped to < 0.2 mole fraction PS. It appears that the TEMPO has an influence on the grafting reactions within the PFA substrates, presumably lowering the molecular weight. Increasing the concentration of TEMPO from 4.6×10^{-3} to 1.9×10^{-2} M resulted in a slight decrease in the mole fraction of PS in the grafted PFA. Grafting performed at 373 K, either with or without nitroxide added, led to the graft penetrating the entire substrate. Grafting performed at room temperature without nitroxide in neat styrene resulted in PS only partially penetrating the substrate. The mechanism at room temperature is most likely to be the *front mechanism* where grafting begins at the surface and progressively moves into the substrate as the grafted layers swell in the styrene. This was confirmed using Raman microprobe mapping in Chapter 6. When the grafting temperature was raised to 373 K the graft penetrated the entire substrate for the same grafting time. At this temperature it is likely that diffusion of styrene is rapid and it may not be the rate determining step.

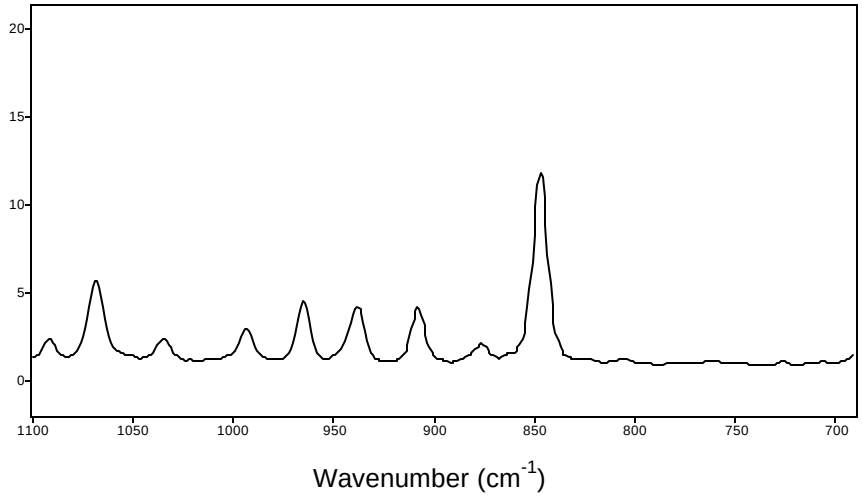

Figure 7.6 Raman spectrum of TEMPO in the range 700 – 1100 cm^{-1}**.**

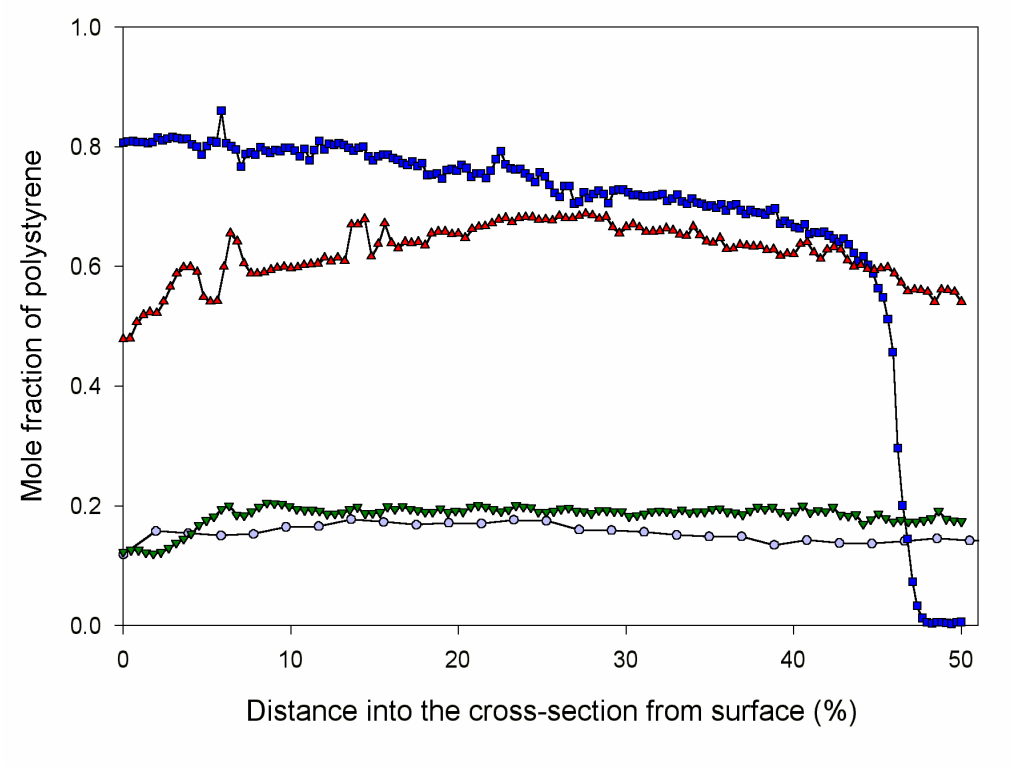

Figure 7.7 Map of PS graft into PFA substrate. (-¦ -) room temperature grafting, no nitroxide; (-? -) no TEMPO, 373 K; (-? -) 4.6×10^{-3} M TEMPO, 373 K; (-•-) 1.9×10^{-2} M TEMPO, 373 K. 0 % indicates the surface of the graft copolymer, while 50 % indicates the mid-point into the cross-section.

7.3.3 Radical Stability and Crystallinity

At the high temperatures needed to force nitroxide-mediated polymerization to proceed, the majority of the radicals created during the irradiation at ambient temperature would have decomposed. Examination of the radicals formed in PFA when irradiated in vacuum at room temperature using ESR spectroscopy, revealed that at approximately 400 K all end-chain (~$C^{\bullet}F_2$) radicals had decomposed leaving just a portion of the main-chain (~CF_2–$C^{\bullet}F$–CF_2~) radicals (Chapter 2). The less thermally stable end-chain radicals are assumed to be present in the amorphous regions, while the long-lived main-chain radicals must reside in the crystallites or at the surface of the crystallites.

To determine whether the grafting process disturbs the crystallites, the heat of fusion of the crystalline melting endotherm of PFA was measured using differential scanning calorimetry (DSC) before and after grafting. Since little difference was observed

between the graft yield when using TEMPO compared with TEISO, this was done only for the samples grafted with TEMPO as the LFRP agent. The heat of fusion from the first DSC runs for untreated, radiation-treated only, and grafted samples are shown in Table 7.1 A. Because of the dilution factor observed for the grafted amorphous PS, a correction factor was used determine the heat of fusion of the PFA component. The corrected heat of fusion of PFA is shown in Table 7.1 B. The corrected data show little change in the crystallinity compared with the untreated or irradiated only samples. This suggests that there was little disruption of the crystallites during grafting. The effect of radiation on the crystallinity of PFA has been explored in Chapter 5. To determine if the low radiation dose used in the grafting experiment leads to a significant change in the heat of fusion, a control sample which had been irradiated to the same dose as the samples grafted in vacuum was used. Little difference is seen between the DSC results of this sample and the untreated and grafted samples. It was thus concluded that for the nitroxide LFRP grafting reaction, the initiating species, I• in Scheme 7.1, are ~CF_2–C•F–CF_2~ radicals on the surface of the crystallites.

Table 7.1 Heat of fusion determined by DSC (first run) for PFA grafted using various conditions.

	(A) Overall Heat of fusion ?H (J g^{-1})	(B) Heat of fusion of PFA ?H (J g^{-1})
Untreated	26 ± 3	26 ± 3
Irradiated only	28 ± 3	28 ± 3
Grafted at RT	17 ± 2	28 ± 3
1.9×10^{-2} M TEMPO	24 ± 3	27 ± 3
1.0×10^{-2} M TEMPO	24 ± 3	27 ± 3
4.6×10^{-3} M TEMPO	24 ± 3	28 ± 3
Neat sty (no TEMPO)	19 ± 2	26 ± 3

7.3.4 Loading Tests

Fmoc loading tests were performed on representative samples of lanterns grafted with LFRP, however, no loading was detected. Despite most of the graft being observed by

Raman mapping to be below the surface due to the high temperature used, it was expected that surface grafting would be sufficient to allow some loading. From the cross-section maps in Figure 7.7 it can be seen that the mole fraction of PS at the surface of the samples grafted with LFRP was less than 0.2. At such high proportions of PFA in the lanterns, the graft substrate would have swelled only slightly in the dichloromethane and dimethylformamide / dichloromethane used as solvents for the loading tests and would not be able to access significant amounts of the "buried" PS, hence leading to the lack of measurable loading.

7.4 Conclusions

Grafting of styrene to PFA pre-irradiated in vacuum using nitroxide-mediated LFRP has been examined. The effect of the nitroxides, TEMPO and TEISO, was to lower the graft yield compared with the system without nitroxide added. Microprobe Raman mapping showed that most of the graft was below the surface presumably due to rapid diffusion of styrene at the high temperatures needed to force the nitroxide mediated LFRP to proceed. After grafting styrene to PFA using the nitroxides, the crystallinity of the substrate did not change appreciably which suggested that the grafting was occurring at the surface of the crystallites. The failure of the loading tests on the grafted samples was a result of the graft not being accessible under the loading conditions, however, such graft copolymers may have promise as conducting membranes since a homogeneous graft across the entire substrate was achieved.

7.5 References

1. Moad, G., Solomon, D. H. *The Chemistry of Free Radical Polymerization*, First ed.; Elsevier Science: Oxford, 1995.

2. Solomon, D. H., Rizzardo, E., Cacioli, P., *US Pat. 4581429*, *Chem. Abstr.* **102** (1985).

3. Patten, T. E., Xia, J., Abernathy, T., Matyjaszewski, K., *Science* **272**, 866-868 (1996).

4. Matyjaszewski, K., Coca, S., Gaynor, S. G., Greszta, D., Patten, T. E., Wang, J.-S., Xia, J., *WO 87/18247*, (1997).

5. Wang, J. S., Matyjaszewski, K., *J. Am. Chem. Soc.* **117**, 5614-5615 (1995).

6. Moad, G., Chiefari, J., Krstina, J., Postma, A., Mayadunne, R. T. A., Rizzardo, E., Thang, S. H., *Polym. Int.* **49**, 993-1001 (2000).

7. Chiefari, J., Chong, Y. K., Ercole, F., Krstina, J., Jeffery, J., Le, T. P. T., Mayadunne, R. T. A., Meijs, G. F., Moad, C. L., Moad, G., Rizzardo, E., Thang, S. H., *Macromolecules* **31**, 5559-5562 (1998).

8. Hawker, C. J., Hedrick, J. L., *Macromolecules* **28**, 2993-2995 (1995).

9. Devonport, W., Michalak, L. M., Malmstrom, E. E., Mate, M., Kurdi, B., Hawker, C. J., *Macromolecules* **30**, 1929-1934 (1997).

10. Harth, E., Van Horn, B., Hawker, C. J., *Chem. Commun.*, 823-824 (2001).

11. Benoit, D., Chaplinski, V., Braslau, R., Hawker, C. J., *J. Am. Chem. Soc.* **121**, 3904-3920 (1999).

12. Billingham, N. C. Molecular Weight Distributions. In: *Comprehensive Polymer Science;* Allen, G.; Berington, J. C. Eds.; Pergamon Press: Oxford, 1989; Vol. 3; pp. 43-57.

13. Hodges, J. C., Harikrishnan, L. S., Ault-Justus, S., *J. Comb. Chem.* **2**, 80-88 (2000).

14. McAlpine, S. R., Lindsley, C. W., Hodges, J. C., Leonard, D. M., Filzen, G. F., *J. Comb. Chem.* **3**, 1-5 (2001).

15. Mahajan, A., Chhabra, S. R., Chan, W. C., *Tett. Lett.* **40**, 4909-4912 (1999).

16. Stehling, U. M., Malmstrom, E. E., Waymouth, R. M., Hawker, C. J., *Macromolecules* **31**, 4396-4398 (1998).

17. Holmberg, S., Holmlund, P., Wilen, C.-E., Kallio, T., Sundholm, G., Sundholm, F., *J. Polym. Sci., A, Polym. Chem.* **40**, 591-600 (2002).

18. Barner, L., Zwaneveld, N., Barner-Kowollik, C., Davis, T. P. "Gamma Radiation Induced Grafting onto Solid Surfaces Using the RAFT Process"; 25th Australasian Polymer Symposium, 2002, Armidale, Australia.

19. Miwa, Y., Yamamoto, K., Sakaguchi, M., Shimada, S., *Macromolecules* **34**, 2089-2094 (2001).

20. Bozzi, A., Chapiro, A., *Radiat. Phys. Chem.* **32**, 193-196 (1988).

21. Moad, G., Rizzardo, E., Solomon, D. H., *Polym. Bull.* **6**, 589-593 (1982).

22. Gangal, S. V. Tetrafluoroethylene-Perfluorovinyl Ether Copolymers. In: *Encyclopedia of Chemical Technology;* Kirk-Othmer Ed.; John Wiley & Sons: New York, 1994; Vol. 11; pp. 671-683.

23. Veregin, R. P. N., Georges, M. K., Kazmaier, P. M., Hamer, G. K., *Macromolecules* **26**, 5316-5320 (1993).

24. Veregin, R. P. N., Georges, M. K., Hamer, G. K., Kazmaier, P. M., *Macromolecules* **28**, 4391-4398 (1995).

25. Moad, G., Rizzardo, E., *Macromolecules* **28**, 8722-8728 (1995).

26. Mardare, D., Matyjaszewski, K., *Polym. Prep.* **35**, 778-779 (1994).

27. Fischer, H., *J. Polym. Sci. Part A: Polym. Chem.* **37**, 1885-1901 (1999).

28. Fischer, H., *J. Am. Chem. Soc.* **108**, 3925-3927 (1986).

29. Lutz, J., Lacroix-Desmazes, P., Boutevin, B., *Macromol. Rapid Commun.* **22**, 189-193 (2001).

Chapter 8

8 Overall Conclusions and Further Work

8.1 Radiolysis of PFA

The radiation chemistry of PFA was examined to identify the radicals responsible for initiating grafting reactions and to understand the chemical and physical changes in radiation-treated PFA.

PFA was shown to be intolerant to radiation across a wide range of irradiation temperatures in terms of the changes in the tensile properties, main-chain and end-chain radical formation, changes in the chemical structures and thermal properties, and the emission of volatile fragments. The damage that radiation exposure caused to PFA was illustrated by the drop in the energy to break and percentage elongation to $^{1}/_{10}$ of their original values after a dose of 20 kGy at 303 K.

Chain scission was identified as the main radiolytic process when PFA was irradiated at 303 K. This was based on the observed increase in crystallinity, drop in the melting temperature, tensile strength and energy to break, increase in rigidity and increase in the number of $\sim C^{\bullet}F_2$ and $\sim CF_3$ chain ends. The lack of branch formation when PFA was irradiated at 303 K was attributed to the glassy-state of the amorphous regions and to the rigid crystalline regions preventing sufficient movement of the macro-radicals to combine to form branches. At 77 K the polymer chains are even more rigid. When irradiated at 77 K the radical yield was 0.16, lower than at 303 K (0.93), suggesting that many of the radicals formed at 77 K immediately recombined. At 303 K, PFA has short chain motion as it is above the γ-relaxation transition, recombination is less prevalent and the radicals formed are able to move far enough apart from each other to prevent instant recombination. The stability of the main-chain radicals in the crystalline regions exceeded two years at 294 K.

Analogous chain mobility arguments were used to explain the formation of branched structures when PFA was irradiated at high temperature. When irradiated above

the T_g but below the T_m, both long and short branches were identified by ^{19}F high-speed MAS NMR. Two types of short perfluormethyl branches were assigned based on comparison of their respective T_2 relaxation times, measured using a Hahn echo pulse experiment. The perfluoromethyl side chains with short T_2 were assigned to side groups incorporated into the crystallites, while the perfluoromethyl side chains with long T_2 were assigned to those in the amorphous regions or at the surface of crystallites. Assignments of small peaks in the range –52 to –64 ppm remain inconclusive. Further work using correlation spectroscopy is required for unequivocal assignment of these peaks.

The formation of long chains was postulated to occur by combination of end-chain and main-chain radicals in the amorphous regions or at the crystallite surfaces. Radiation-induced crystallization was observed in the samples irradiated above and below the T_g at low dose due to lowering of the molecular weight by chain scission and loss of perfluoralkoxy groups allowing crystallization. When irradiated below the T_g the crystallinity increased with increasing dose due to further chain scission, while the samples irradiated above the T_g but below the T_m decreased in crystallinity due to disruption of the crystallites by the newly formed pendant groups.

When irradiated at the T_m the G value of branch points was 1.2 but was exceeded by the number of chain ends (1.8). When PFA was irradiated with electron beams at 633 K (above the T_m) the G value of long branch points (1.6) was greater than that of chain ends (1.4) suggesting that net crosslinking occurred. A decrease in the crystallinity supported this finding.

The loss of perfluoroalkoxy groups from the PPVE units across the irradiation temperature range examined was prevalent. G values calculated from the NMR data for loss of perfluoroalkoxy groups ranged from –0.8 at 303 K to –6.0 at 633 K. The gases evolved from PFA irradiated at 303 K were analysed by FTIR and MS and found to consist of large amounts of oxygen-containing species. Cleavage appeared to occur at the C–O bonds and to a lesser extent at the C–C bond of the CF_3 at the end of the pendent groups. The fragment, CF_3CF_2COF, was identified by FTIR, while ethyl ether and acyl fluoride groups were identified by NMR and FTIR. The major decomposition pathways of the PPVE units of PFA are summarized in Scheme 8.1.

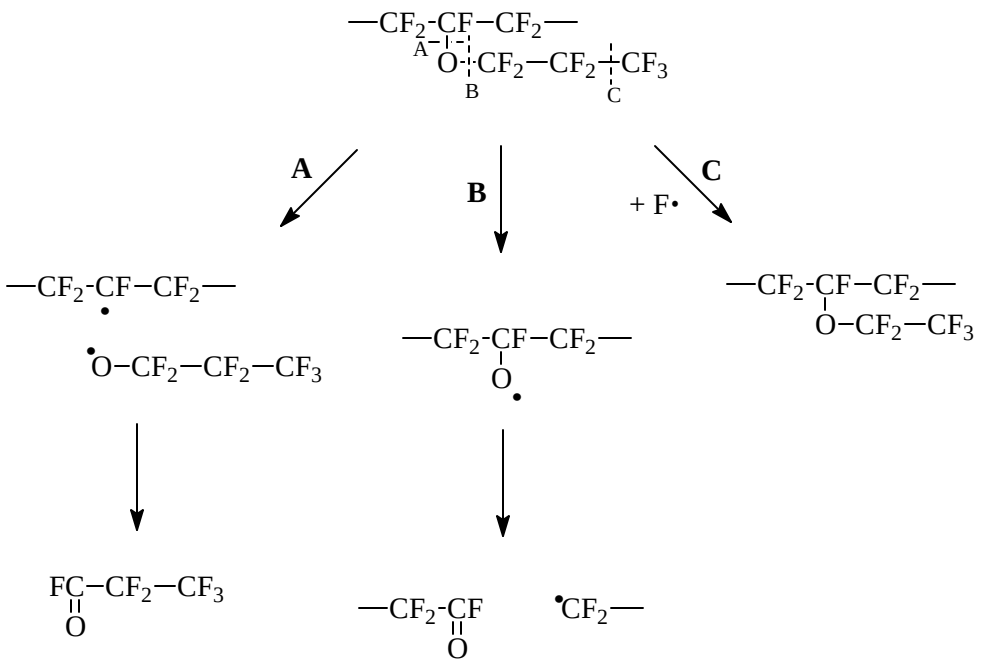

Scheme 8.1 The major decomposition pathways of the PPVE units in PFA when exposed to γ-radiation.

8.2 Grafting to PFA

The effect of monomer phase (vapour / liquid), solvent, and addition of nitroxides were investigated for the preparation of PFA-*g*-PS graft copolymers for use in SPOC.

The distribution of the PS graft in the PFA substrate was a key factor in determining the loading, and hence usefulness, of the grafted copolymer as a SPOC support. In all cases the graft layer was not pure PS, but instead was graded into the PFA substrate as a mixture of PFA and PS. The distribution of the graft was largely dependent on the diffusion of styrene into the substrate, which was aided or hindered by the conditions used, such as solvent selection or temperature.

The solvents used to dilute the styrene for the grafting reactions could be classified into three categories according to swelling ability and resulting graft yield and distribution of the graft:

1) Swells PFA slightly and is a good solvent for PS (dichloromethane) – high graft yield distributed mostly below the surface.
2) Swells PFA very weakly and is a good solvent for PS (toluene) – moderate graft yield with the graft below the surface but not penetrating as far as in (1).
3) Does not swell PFA and is a poor solvent for PS (methanol, ethanol, acetonitrile) – low graft yield restricted to the near-surface region of the substrate.

The viscosity of the grafting medium played an important role in the grafting reactions. Under certain conditions an increase in viscosity of the grafting solution led to a higher graft yield, presumably due to longer graft chains being formed as a result of fewer termination reactions by combination. High viscosity could also lower the graft yield by hindering diffusion of styrene to the graft front.

When styrene vapour was used, transport of styrene into the substrate was independent of dose rate at low graft times and the graft was limited mainly to the surface regions.

The nitroxides TEMPO and TEISO were used to give the grafted chains a "living" character. Unfortunately the high temperature required for the nitroxide-mediated reactions to proceed allowed diffusion of the styrene into the amorphous regions of the PFA such that the resulting graft was below the surface. The resulting graft copolymers were unsuitable for SPOC, but if sulfonated, may have an application in conducting membranes.

In Chapter One the following list of aims was presented:

Aims:

- to understand the radiation chemistry of the base fluoropolymer.
- to understand how grafting conditions affect the extent and rate of grafting so that grafted polymer preparation can be carried out in a rapid and reproducible manner.
- to develop a solid support with thermal and chemical stability to a large range of solvents and conditions.

- to develop a solid support with better loading and kinetics than that of existing solid supports.

The radiation chemistry of PFA has been studied in-depth and is now well understood. A range of grafting conditions were investigated and correlations made between solvents used and their concentration, dose and dose rates and use of "living" polymerization additives. By using PFA as the graft substrate, the thermal and chemical stability of the support made it useful in harsh SPOC conditions. The mechanical properties of the substrate after irradiation were of a concern above 10 kGy and future work may be required to improve these properties. Some preliminary work (not presented) examining the grafting of styrene to crosslinked PFA showed some promise. A relationship between the distribution of the graft and the amount of loading was identified. The best conditions found for preparing a PFA-based solid support were using a non-solvent for PS or styrene in the vapour-phase. Further work is required to test the kinetics of the chemistry on the grafted solid support.